LUCIA FUSCO

EXPERIMENTAL INVESTIGATION OF LUBRICANT FILM THICKNESS IN AN AUTOMOTIVE FINAL DRIVE UNIT

DEPARTMENT OF AUTOMOTIVE ENGINEERING

PhD THESIS

LUCIA FUSCO

EXPERIMENTAL INVESTIGATION OF LUBRICANT FILM THICKNESS IN AN AUTOMOTIVE FINAL DRIVE UNIT

DEPARTMENT OF AUTOMOTIVE ENGINEERING

PhD THESIS

2013

Supervisor: Dr. G. Sherwood

This thesis is submitted in partial fulfilment of the requirements for the degree of Doctor of Philosophy

© Cranfield University, 2013. All rights reserved. No part of this publication may be reproduced without the written permission of the copyright holder.

Abstract

Society has been aware of the environmental impact of vehicles for some time now, with governments trying to control and reduce this impact by introducing emissions standards to control pollutants as well as CO_2 emissions. One way in which total emissions can be reduced is by increasing the efficiency of vehicles as a whole, resulting in greater fuel economy. Related to increased transmission efficiency, lubricant flow within a final drive unit (FDU) was researched, enabling a better understanding of the system through visualisation and laser induced fluorescence (LIF) measurements

A LIF measurement technique has been developed, along with a quantitative wedge calibration method, to measure lubricant thicknesses within a Jaguar Land Rover X150 FDU. The measurements and data recorded in this thesis are taken from an original clear-cased replica FDU, which proved to be suitable for visualisation and LIF measurements.

The results show lubricant thickness trends are dependent on the fill volume and rotational speed of the gear. The measured peak lubricant thickness on the carrier- and cover-side of the crown wheel increased with fill volume. As the fill volume increased, the amount of lubricant entrained by the crown wheel increased, resulting in the increased lubricant thickness.

As the equivalent vehicle road speed increased to approximately 8mph, the measured lubricant thickness increased to its maximum value of 1.75mm for a fill volume of 900ml. From 8mph onwards, the lubricant thickness was found to decrease again to less than 0.1mm at around 10mph. Up to 8mph, gravity appeared to be the overriding influence, pulling the lubricant from the crown wheel. At 8mph, these forces seemed to be in balance, resulting in the greatest measured lubricant thickness. Above 8mph, the force from the gear rotation ejected lubricant from the crown wheel.

Gathered data and relationships provide new quantitative metrics for measurement and enhanced understanding of lubricant movement within the FDU. The methodology and equipment developed here for studying the FDU are suitable for wider use in any geared or lubricated system.

Acknowledgements

There are many people who have supported, guided and encouraged me through my PhD.

I'd like to thank Glenn Sherwood, my supervisor, and Nick Vaughan for your guidance and support throughout.

I would also like to thank Brett Hallam, Russell Osborn and Kevin Allin for their help and encouragement and of course Jaguar Land Rover for sponsoring this work.

I wish to express my sincere thanks to Kevin Stevens and Marko Tirovic, your continued encouragement, guidance and support.

I am especially indebted to my Mum and Dad, for their belief in me, their unfaltering support and love.

Last but by no means least; I must thank Paul for his continued understanding and patience.

"Every accomplishment starts with the decision to try"

Gail Devers

Table of Contents

Table of Figures

List of Tables

List of Equations

Notation

A	Absorption
b	Path length
c	Speed of sound
C	Molar concentration
f	frequency
h	Height
I_o	Intensity of the incident light
I_t	Intensity of transmitted light
K	Stiffness
m	Frequency mode
n	Number
R	Reflection coefficient
t	Thickness
x	Path length
α	Absorption coefficient
Δ	Phase difference
δ	Film thickness
ε	Molar absorptivity
λ	Wavelength
μ	Kinematic viscosity
ρ	Density
ψ	Polarisation change amplitude ratio

Acronyms

AFM	Atomic force microscopy
CW	Continuous wave
EHD	Elastohydrodynamic
EHL	Elastohydrodynamic lubrication
FDU	Final drive unit
GS/s	Giga samples per second
HeCd	Helium cadmium
ICCD	Intensified charge-coupled device
ISE	Image scanning ellipsometry
LIF	Laser induced fluorescence
MS/s	Mega samples per second
Nd:YAG	Neodymium-doped yttrium aluminium garnet
PIV	Particle image velocimetry
PM	Photomultiplier
TEHD	Thermo-elastohydrodynamic
ToF	Time of flight
VI	Virtual instrument

CHAPTER 1
INTRODUCTION

Chapter 1 introduces the possibility for increased efficiency and fuel economy through alterations to the automotive driveline. The Jaguar Land Rover X150 final drive unit is highlighted as an area in which little is known about the lubricant movement and interactions, and yet has the potential to be improved. The intention is to find out more about the lubricant movement by measuring the lubricant thickness in selected areas within the unit. This will provide a metric for analysis which has thus far not been recorded. The final section of this chapter outlines the aims and objectives for this research.

1 Introduction

1.1 Environmental Impact

While for some, global warming and our impact on the planet is an on-going debate (Brahic, 2007), it is generally accepted that steps need to be taken to reduce the impact of our transport on the environment through reductions in emissions such as CO_2. According to the IMechE, (IMechE, 2009), transport in the UK accounts for almost a quarter of the country's CO_2 emissions. This was approximately between 135M and 157M tonnes in 2006, 80% of which was due to road vehicles alone. At the moment there are no viable alternatives to our road use, so modification and optimisation of road vehicles is suggested to be the only way forward (King, 2007).

One way in which governments have tried to control and reduce the impact of CO_2 is through the introduction of emissions standards such as Euro 5, which restrict the emissions of hydrocarbons and toxic gases (European Parliament, 2007). From 2015, the required average fleet emissions becomes 130g CO_2/km for cars (175g CO_2/km for vans in 2017), moving to 95g CO_2/km by 2020 (147g CO_2/km for vans). The fuel consumption target for 2015 is equivalent to 5.6L/100km for petrol vehicles and 4.9L/100km for diesel, moving to 4.1L/100km and 3.6L/100km by 2020 respectively (European Commission, 30/07/2012). At the moment, US CO_2 emissions are being reduced through Corporate Average Fuel Economy (CAFE) legislation, which stipulates that vehicle manufacturers have to achieve a combined fleet average of 34.1mpg for passenger cars and light trucks by 2016 (NHTSA).

While low carbon vehicle options are being explored and developed to address the issue, there is still much that needs to be done to make them practical and affordable. Currently, low carbon vehicles such as electric vehicles, are still ultimately powered by fossil fuels as they depend on electricity from power stations for charging. This is unlikely to change until more suitable renewable energy sources are developed. The short-term result from hybrids and electric vehicles may be fewer emissions from road vehicles, but more from power stations. In the end there is a very small reduction in CO_2, with most simply transferred from one area to another. In an EC Joint Research Centre report, a well-to-wheel analysis is given which explains that while low carbon fuels or renewable energies can reduce greenhouse gasses, they generally require more total energy (Edwards,R. Larivé,J.F. Beziat,J.C., 2011). The advantage with centralising the energy supply for vehicles is that as efficiency at the source (electricity generation) improves; this has an impact on all vehicles, no matter the age, resulting in a massive saving. The same is not true of combustion powered vehicles. In the

meantime, there is continuing pressure on the motor industry to reduce overall emissions, reduce energy consumption and hence improve fuel economy by looking at improving all areas of a vehicle.

Fuel economy can be improved by increasing the efficiency of a vehicle as a whole. Greater efficiency can be achieved through reduction of losses, for example aerodynamic losses, rolling resistance from tyres, braking and powertrain losses. The powertrain losses are associated with the engine, the transmission and the final drive unit (FDU). Typically, geared systems such as the transmission and FDU, can reach 95% efficiency and higher, but opportunities exist to improve this further through reduction of churning losses and improved heat dissipation. Recent developments in engine efficiency, such as reducing friction of pistons in cylinders (Ryk and Etsion, 2006; Tateishi, 1994; Wakuri et al., 1992), have shown that there are still improvements to be made to fuel consumption. In the King Report (King, 2007), details are given of the potential efficiency savings to be had from different technologies. A summary of these technologies can be found in Table 1-1.

Table 1-1 - Percentage efficiency savings from new technology (King, 2007)

Technology	**Efficiency Saving**
Lightweighting	10%
Low rolling resistance tyres	2-4%
Improved aerodynamics	2-4%
Direct injection and lean burn	10-13%
Variable valve actuation	5-7%
Downsizing engine capacity with turbocharging or supercharging	10-15%
Dual clutch transmission	4-5%
Stop-start	3-4%
Stop-start with regenerative braking	7%
Electric motor assist	7%
Reduced mechanical friction components	3-5%

Improvements in stop-start technology are well known, as it is an area that is being advertised by vehicle companies as an economical addition to their products, as well as a selling point of their vehicles. Other areas, such as transmission and driveline efficiency improvements are less well known to the general public, but still have potential to increase efficiency, and as such are of interest to companies such as Jaguar Land Rover, who are the generous sponsors of this work. Jaguar Land Rover are interested in optimising their systems where possible to increase overall efficiency through improvements in multiple areas, particularly the FDU.

1.2 Final Drive Unit

One area of interest highlighted by Jaguar Land Rover is the final drive unit, FDU, (also called the rear drive unit) found in the rear axle of their vehicles. The FDU is the final system in the driveline before the rear wheels. A diagram of the external profile and location of the X150 FDU is shown in Figure 1.1. Drive from the engine is transmitted through the drive shaft to the rear axle via the final drive unit. From the FDU, drive is transferred to the wheels via the half shafts. The FDU housing is made up of 2 parts; a cover and a carrier. The unit contains a hypoid crown wheel drive gear (attached to the differential case) and pinion, and a set of differential gears, which allows independent drive to the rear wheels as necessary, such as when cornering (Hillier, 1991). These components are shown in more detail in Figure 1.2.

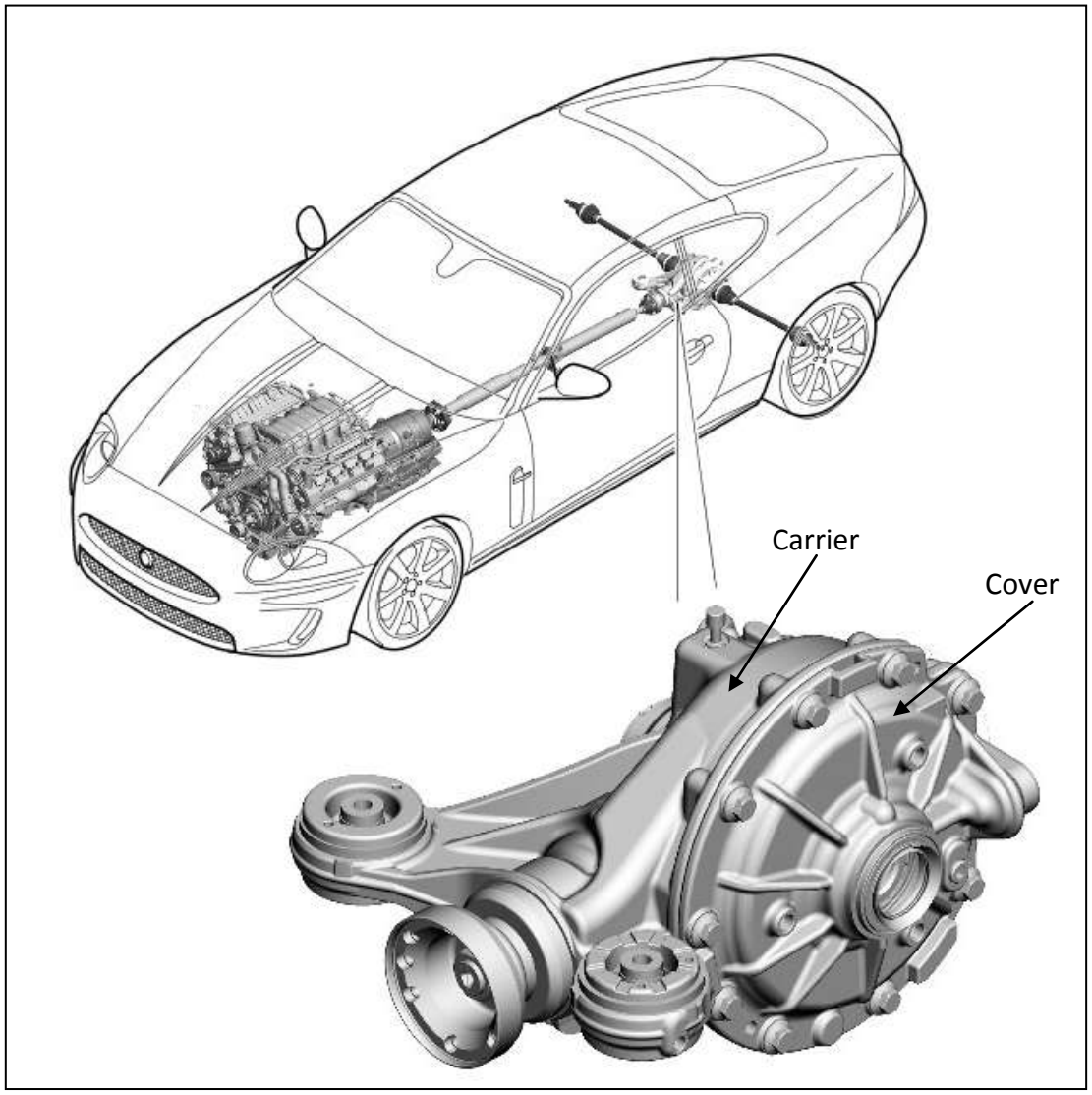

Figure 1.1 - X150 final drive unit

The differential case sits on bearings, situated in the carrier and cover. Through these bearings and the differential, there is a bore for the two rear drive half shafts that drive the rear wheels.

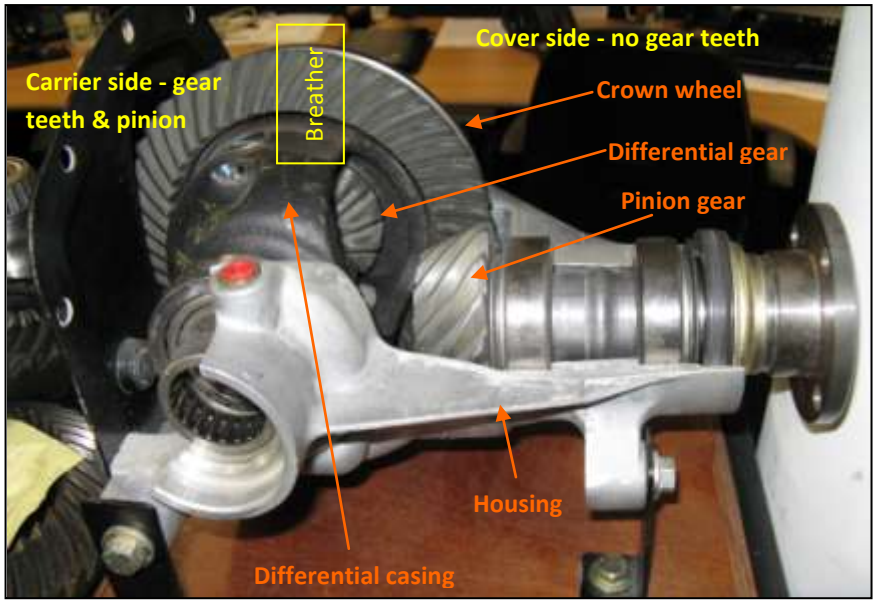

Figure 1.2 - Jaguar X150 FDU main components

The rotation from the drive shaft is transferred through the pinion shaft to the pinion gear before transfer to the crown wheel, where the direction of rotation is changed by 90°. As the crown wheel and differential casing are joined, the rotation is also passed through to the planet gears (2 of the 4 differential gears). At this point, the sun and planet gears behave differently depending on the driving condition. If the vehicle moves in a straight, forward direction, equal torque is passed to both left-hand and right-hand sun gears. This results in equal rotational speed of both half shafts. The planet gears rotate with the differential casing and so behave as a lock. If the vehicle corners, the torque to the sun gears is not equal. The outermost wheel rotates at a faster speed than the inner and so the planet gears rotate to compensate for the difference in wheel speeds. This is shown diagrammatically in
Figure 1.3.

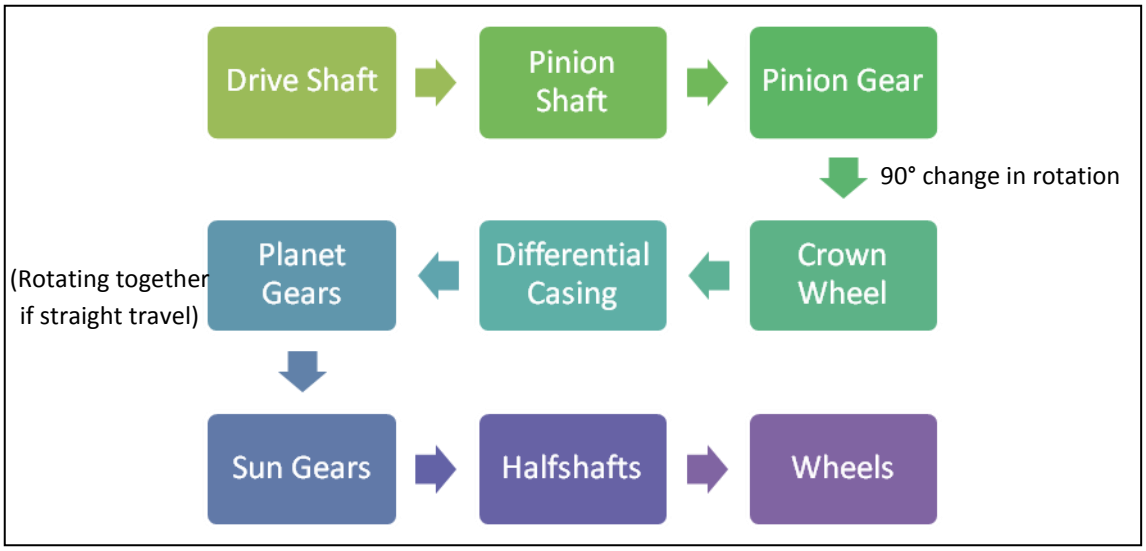

Figure 1.3 - FDU differential rotation path

1.3 Final Drive Unit Efficiency

From section 1.1, it was stated that transmission gears can reach an efficiency of up to 95%, and while 95% is reasonably high, Jaguar Land Rover have identified this as an area in which improvements can be made. Efficiency improvements from many small areas combine to produce more significant energy savings, and this is where developments in the FDU come in. The majority of FDU losses come from the gears and lubricants and how they interact, particularly churning, heat dissipation, heat transfer, and lubricant expulsion from the breather. The link between these and any potential efficiency savings in the system is the lubricant. At the moment, relatively little is known about the behaviour of lubricants within hypoid gear systems and unless the systems are better understood, no further efficiency savings can be made. Once understood, investigation into the effect of lubricant fill volume, lubricant type, gear geometry and surface finish can be carried out and the associated efficiency improvements can be assessed.

Movement of the bulk lubricant flow within the FDU has been investigated by Burlison (Burlison and Sherwood, 2010) and Pigenel (Pigenel, 2009) using particle image velocimetry (PIV). Pigenel studied the effects of Castrol SAF-XO within the FDU, while Burlison used a clear Castrol flow-test lubricant with a lower viscosity than that of SAF-XO. The flow-test lubricant viscosity at room temperature was comparable to that of SAF-XO at 100°C, allowing tests to be carried out at ambient temperature. Comparing the data from both lubricants at room temperature showed that the lower viscosity lubricant resulted in faster flowing lubricant and an increase in the amount of lubricant in motion within the FDU. Burlison states that eddies were visible within the lubricant around the crown wheel, and that the speed of motion of these eddies increased with

rotational speed of the crown wheel. It is suggested that by introducing baffles or deflectors, the eddies (which form part of the churning losses) could be decreased.

Further to internal lubricant flow analysis, Castberg (Castberg, 2010) investigated the heat transfer from the FDU housing. Increased air flow around the FDU is required to increase heat transfer from the housing to the surroundings. The difficulty with this is that the package space allowed is limited, which restricts the air flow. Ideally, the heat generation would be minimised, removing the heat production at the source, instead of increasing heat dissipation. As it is not possible to prevent heat generation altogether due to churning and friction within the housing, improvements to heat dissipation are necessary. Castberg analysed heat dissipation of the unit through FE and CFD simulations and found that consideration of the internal thermal behaviour was needed in order to gain a meaningful solution that resembles reality as the system interactions are complex. Measurements of lubricant thicknesses on the housing may help in understanding and improving heat dissipation.

At present, data on the behaviour of a lubricant within a FDU is limited. For example, there is no quantitative information on the lubricant distribution as the road speed changes, which is important when considering heat and churning losses over a range of speeds as experienced in a drive cycle. This information would assist in the understanding of the system so that energy and cost saving changes can be made. If oil distribution, channelling, redirection data are of interest, such as during the design phase for optimisation of lubricant feed to bearings or prevention of excess lubricant churning around gears, a surface measurement to work from is an advantageous starting point.

A logical place to start for investigations into lubricant behaviour is visualisation. If the lubricant flow patterns and movement can be seen, a picture of what happens within dip-lubricated geared systems can be created so that it is better understood. Furthermore, a way to measure the lubricant within the system would be beneficial in understanding areas of high and low flow rates as well as lubricant thicknesses and distribution.

In summary, improving the efficiency of the final drive unit contributes to the overall drivetrain efficiency. To achieve this, research into the interaction between lubricant, gears and casing is necessary to identify critical areas in need of improvement. While flow visualisation can show the bulk flow patterns, another tool is required for quantitative measurement of lubricant thicknesses. Measurement of lubricant thicknesses in areas of high or low flow or temperature could help to identify areas within the FDU that could be improved.

1.4 Aims & Objectives

Development and expansion of the current understanding on lubricant behaviour within geared systems is the core motivation for this thesis. A lubricant thickness measurement technique would enable future geared system designs to be based on measured data. In addition, if it can be established that there is an efficiency saving to be had through increased or reduced lubricant feed to a certain area or a lubricant saving through a reduction in lubricant fill volume, then there could be a cost and time saving associated. Subsequently, the research aims of this project are:

1. To successfully implement a lubricant thickness measurement technique
2. To develop and implement a suitable quantitative calibration method for use with the lubricant thickness measurement technique
3. To increase understanding of lubricant behaviour in an FDU

To achieve these aims, a number of objectives have to be realised; they are:

1. To identify suitable lubricant thickness measurement techniques
2. To produce a functional calibration technique
3. To understand the effects of lubricant fill volume on lubricant thickness
4. To investigate the effects of gear speed on lubricant thickness
5. To measure lubricant thicknesses from an FDU

Although film thicknesses between contacting surfaces, such as meshing gear teeth, is a well-researched area and is an important part of gear-lubricant interactions, it is not the focus of this research. Instead, lubricant coatings on surfaces such as casings and non-contacting gear surfaces (for example before or after meshing of gear teeth) will be the focal point. The term lubricant film will be used throughout this thesis to mean surface coatings of lubricant. Changes in the thickness of lubricant coatings or films give an indication of the lubricant movement, and by measuring this, a greater understanding can be achieved. Knowledge of the methods used to ascertain lubricant thicknesses between contacting surfaces provide a foundation for a new lubricant measurement technique described herein. The measurement technique developed has been successfully applied within an optical final drive unit for the first time to quantitatively measure lubricant thicknesses.

1.5 Thesis outline

This thesis is organised into 6 further chapters. In Chapter 2, a review of gear and lubrication basics is given along with an overview of the final drive unit and its place within a vehicle. A description of a number of lubricant thickness measurement techniques is provided, with particular attention paid to laser induced fluorescence techniques, applications and calibration.

Chapter 3 covers the development of the experiment set-up, which includes the equipment used in laser based thickness measurement, with the advantages and limitations of each item discussed. In chapter 4, the evolution of the laser induced fluorescence thickness measurement technique is presented, from initial validation through to the initial stages of calibration. Although Chapters 3 and 4 have been separated in this text, the works described therein were carried out in parallel and therefore the chapters should be considered together.

Chapter 5 discusses the calibration technique which is vital to the thickness measurement. It includes discussion of the effects of temperature and absorption on fluorescence. Chapter 6 contains a flow visualisation summary from the FDU as well as the lubricant thickness measurements and analysis from the crown wheel at varying speeds and fill volumes. And finally, Chapter 7 brings this thesis to a close with achievements, final conclusions and possibilities for further work.

CHAPTER 2
A REVIEW OF GEARS AND LUBRICATION RESEARCH

The behaviour of a system such as an FDU requires knowledge of gears, lubricants and how the two interact. In this chapter, an overview of gears, lubricants and lubrication is given. These are areas in which valuable research and development have already been carried out, so are included here for reference. Also in this chapter, a summary of techniques used for measurement of liquid film thicknesses across a number of different applications is given. Laser Induced Fluorescence (LIF) is highlighted as a potentially suitable and effective thickness measurement tool. Several applications of LIF measurement and calibration methods are discussed, including limitations of LIF and a review of the calibration techniques used in previous research.

2 A Review of Gears and Lubrication Research

In the introduction, the need for lubricant thickness measurement was explained. Before a suitable thickness measurement technique can be chosen, a greater understanding of the FDU is required. Gears, lubricants and their interaction will form the first three sections of this chapter. In the fourth section of the chapter, previously used lubricant thickness measurement techniques and their application will be discussed. The final section of this chapter will look in more detail at the chosen technique for lubricant thickness measurement; laser induced fluorescence.

2.1 Gears

Gears have been used to transmit power for hundreds of years, but the biggest leaps in understanding have occurred within the last 150 years[1]. Developments in gear understanding have resulted in multiple different possibilities for gear configuration. Examples of some of these configurations are shown in Figure 2.1.

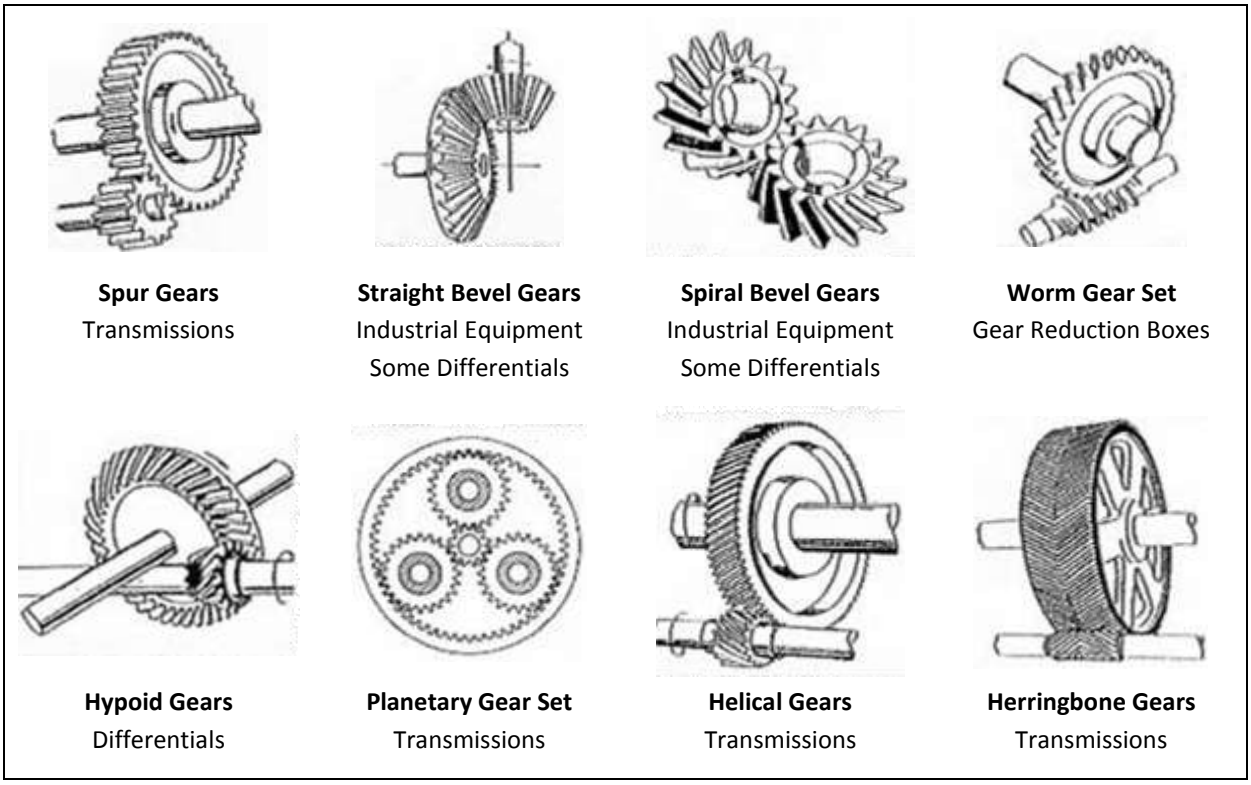

Figure 2.1 - Examples of gears and applications (Amsoil, 2006)

[1] A brief history of gear developments is given by Kolivand (Kolivand, 2009)

The differential in the automotive FDU is a bevel gear set within a hypoid gear system. Hypoid gears are a type of spiral bevel gear in which the pinion is offset from the centre line. Examples of the different gear off-sets are shown in Figure 2.2. This off-set allows the pinion to be larger in diameter and have a greater contact area. This creates a stronger gear set by up to 30% compared with a bevel gear set. Much like bevel gears, hypoid gears allow the drive direction to be shifted through 90°, making them ideal for use in drive units where drive needs to be transmitted from the propshaft to the halfshafts. In addition to providing torque transfer, the X150 FDU hypoid gears provide a final speed reduction and torque increase of 3.31. A ratio of between 3 and 4 is typical for a final drive applications.

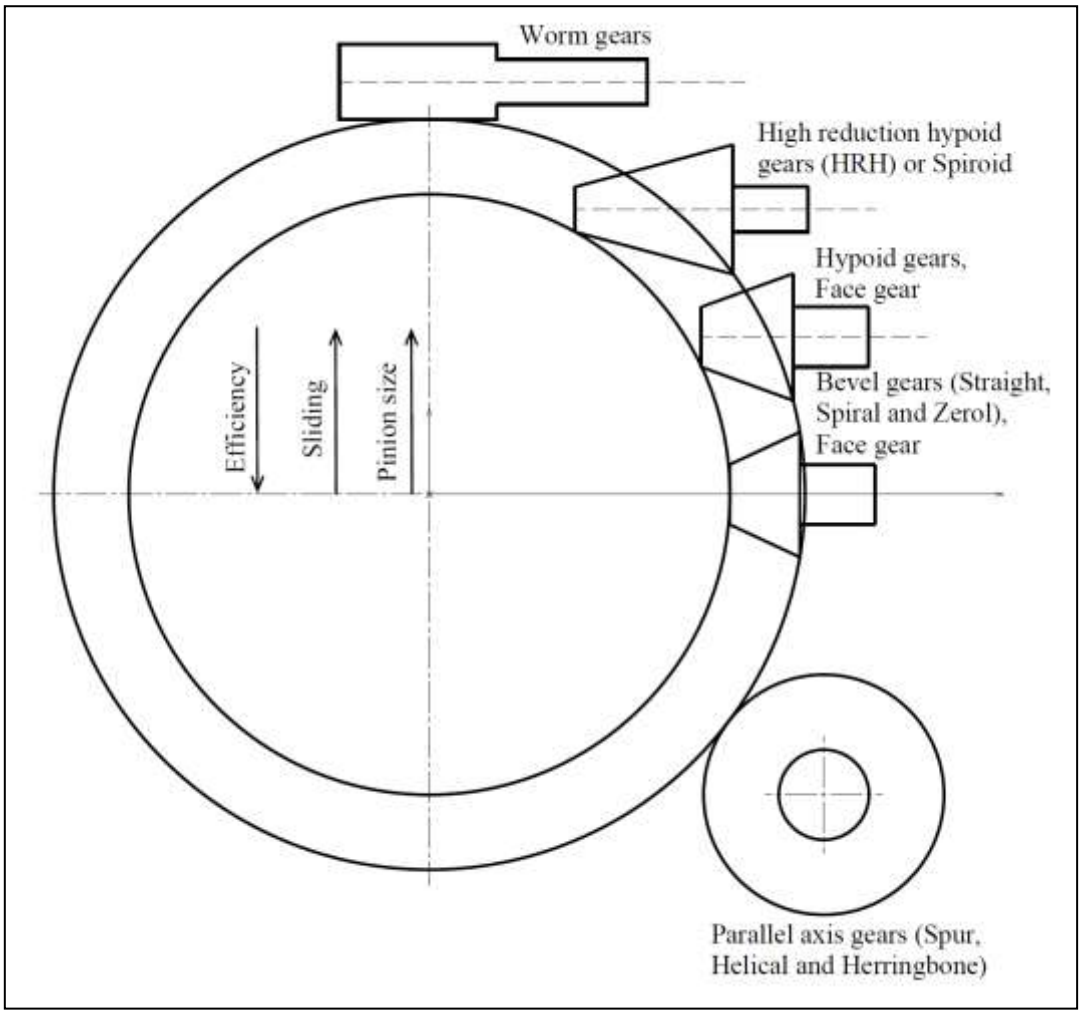

Figure 2.2 - Gear types based on pinion location (Kolivand, 2009)

During hypoid gear meshing, there is an increase in sliding compared with bevel gears where rolling is prominent. As a result, there is additional heat generated through friction leading to a reduction in efficiency from up to 99% for bevel gears to 96% for hypoid gears. This efficiency is load dependent, and the higher the load the more

efficient the gear. (Gleason). Furthermore, hypoid gears are categorised by the method with which they are manufactured; continuous indexing face hobbing (FH) or single indexing face milling (FM) as shown in Figure 2.3.

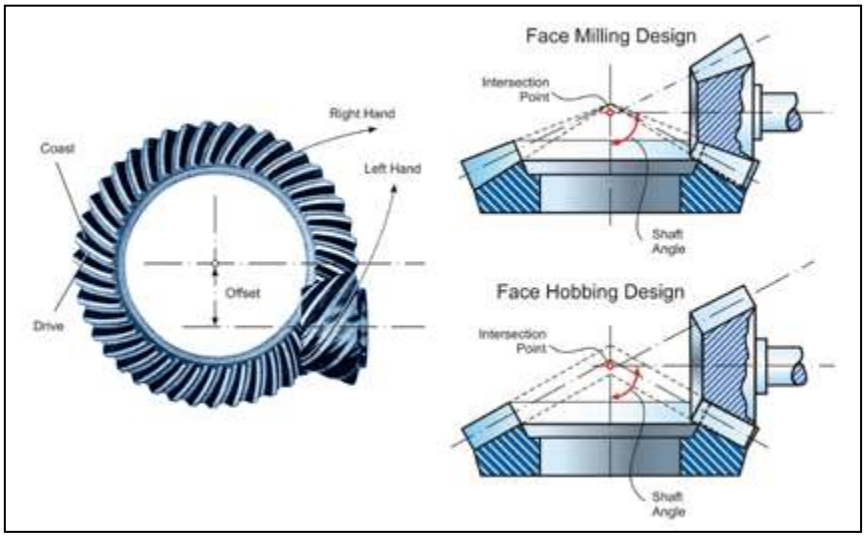

Figure 2.3 - Face milling and face hobbing (Stadtfeld, 2011)

For many years, FM was the preferred method for gear manufacture, but more recently, FH has taken over in axle applications. This transition is due to the increase in productivity presented by continuous indexing; however this technology is still behind that of FM. Further information and more detailed descriptions of gear design can be found from Gleason, Stadtfeld and Wang (Gleason Works (Rochester, 1947; Stadtfeld, 1993; Wang, 1994).

2.1.1 Gear lubrication

The need for lubrication is a shared characteristic of all gears. Lubricants are used to reduce friction between contacting surfaces, to reduce wear and to protect metals from corrosion (Hatton, 2008). Lubricants are also used to dissipate heat from localised zones of high temperature, such as contacts between mating gear teeth.

Most research carried out on lubrication of gears to date is concerned primarily with spur gears and therefore has only limited relevance for FDUs, as they contain hypoid gears which differ in kinematics and geometry. In a paper by Simon (Simon, 1981), a thermoelastohydrodynamic mathematical model of a hypoid gear pair was developed. The model included analysis of temperature and friction variations across gear teeth as well as viscosity and pressure variations. Simon determined film thickness profiles numerically for the duration of a contact event and found that maximum lubricant film temperature and friction factor (the ratio of frictional force to load) increased with speed and lubricant film thickness respectively.

2.2 Losses

Understanding the behaviour of lubricants in geared systems is important because lubricants affect the overall efficiency of geared systems. If there is insufficient lubricant within the system, surface contact occurs, resulting in wear, rubbing, scuffing and overheating. With too much lubricant, churning losses are introduced through the movement of the excess lubricant by the gears.

Churning is the term given to describe the unnecessary movement of lubricant in dip-lubricated geared systems, which significantly affects efficiency and heating of gears and gear systems (Luke and Olver, 1999; Iritani et al., 1999). Churning causes splashing which is an inefficient use of the energy being put into the system. Windage is similar to churning in that it affects the efficiency and heating of the system, but it is related to air movement around the gears rather than a lubricant. It has been found that power loss through windage can be reduced by reducing the volume surrounding the rotating gear, but there is a point beyond which reducing the gear clearance and volume actually increases power loss (Dawson, 1984). This suggests that there is an optimal casing volume and clearance to be found for each system to reduce windage.

The effect of volume reduction on churning losses in the X150 final drive unit has been investigated by Jeon (Jeon, 2010). As with windage, reducing the volume in which a gear rotates results in fewer churning losses, however the relationship is somewhat complex due to the addition of a lubricant. From Jeon's work, it appears that there are optimum radial and axial clearances between gears and housings, which result in the least churning losses. Too great or too small a clearance results in an increase in churning. In addition, the immersion depth of gears in a lubricant is significant and must be optimised along with the axial and radial clearances for the system in question. Churning losses are not discussed further in this work as it falls outside the scope of this study however, further details can be found in the thesis of Jeon. In addition to the clearance measurements and immersion depths, lubricant properties must also be taken into account as this too affects churning.

Although the use of lubricants in dip-lubricated systems can result in churning losses, they remain an essential part of geared systems, and the lubricants are often modified to suit a particular application. Most lubricants contain modifiers or additives to enhance their suitability for different situations, such as high pressure modifiers for use with gears or viscosity improvers for systems that encounter a range of temperatures. Fluid lubricants can be either synthetic or mineral oil based. Mineral fluid lubricants are products of refining crude oil, while synthetic liquid lubricants are manufactured by polymerisation (Kopeliovich, 2009). Lubricants contain additives

which are designed to help the system work more efficiently, as well as extend system life. A summary of these additives can be found in Table 2-1.

Table 2-1 - Lubricant additive summary (Kopeliovich, 2009)

Additive	Description	Examples of substances used
Friction modifiers	Reduce the coefficient of friction. Most consist of molecular platelets or layers which easily slide over each other.	• Graphite; • Molybdenum disulfide; • Boron nitride (BN); • Tungsten disulfide (WS_2); • Polytetrafluoroethylene (PTFE)
Anti-wear	Prevent direct metal-to-metal contact when the oil film is broken down, which results in longer machine life due to higher wear and score resistance of the components. The mechanism of anti-wear additives: the additive reacts with the metal surface and forms a film, which may slide over the surface.	• Zinc dithiophosphate (ZDP); • Zinc dialkyldithiophosphate (ZDDP); • Tricresylphosphate (TCP).
Extreme pressure (EP)	Prevent seizure conditions caused by direct metal-to-metal contact between the parts under high loads. The mechanism of EP additives is similar to that of anti-wear additive: the additive substance form a coating on the part surface. This coating protects the part surface from a direct contact with other part, decreasing wear and scoring.	• Chlorinated paraffins; • Sulphurized fats; • Esters; • Zinc dialkyldithiophosphate (ZDDP); • Molybdenum disulfide
Rust & corrosion inhibitors	Form a barrier film on the substrate surface reducing the corrosion rate. The inhibitors also absorb oxygen, water and other chemically active substances on the metal surface forming a film protecting the part from attack.	• Alkaline compounds; • Organic acids; • Esters; • Amino-acid derivatives.
Anti-oxidants	Inhibit the oxidation process of oils. Mineral oils react with oxygen of air forming organic acids. The oxidation reaction products cause increase of the oil viscosity, formation of sludge and varnish, corrosion of metallic parts and foaming. Most of lubricants contain anti-oxidants.	• Zinc dithiophosphate (ZDP); • Alkyl sulfides; • Aromatic sulfides; • Aromatic amines; • Hindered phenols
Detergents (Commonly added to Engine oils.)	Neutralize strong acids present in the lubricant (for example sulfuric and nitric acid produced in internal combustion engines as a result of combustion process) and remove the neutralisation products from the metal surface. Detergents also form a film on the part surface preventing high temperature deposition of sludge and varnish.	• Phenolates, • Sulphonates and • phosphonates of alkaline and alkaline-earth elements, such as calcium (Ca), magnesium (Mg), sodium (Na) or Ba (barium)
Dispersants	Keep foreign particles present in a lubricant in a dispersed form (finely divided and uniformly dispersed throughout the oil). The foreign particles are sludge and varnish, dirt, products of oxidation, water etc.	• Long chain hydrocarbons • succinimides, such as polyisobutylene succinimides
Pour point depressants	Pour point is the lowest temperature, at which the oil may flow. Wax crystals formed in mineral oils at low temperatures reduce their fluidity. Pour point depressants inhibit formation and agglomeration of wax particles keeping the lubricant fluid at low temperatures.	• Co-polymers of polyalkyl methacrylates

Additive	Description	Examples of substances used
Viscosity index improvers	Viscosity of oils sharply decreases at high temperatures. Low viscosity causes decrease of the oil lubrication ability. Viscosity index improvers keep the viscosity at acceptable levels, which provide stable oil film even at increased temperatures. Viscosity improvers are widely used in multigrade oils, viscosity of which is specified at both high and low temperature.	• Acrylate polymers
Anti-foaming agents (Engine oils & Gear oils)	Agitation and aeration of a lubricant may result in formation of air bubbles in the oil - foaming. Foaming not only enhances oil oxidation but also decreases lubrication effect causing oil starvation.	• Dimethylsilicones

Even with viscosity index improvers, which are added to enhance lubrication at high temperatures, the viscosity of lubricants changes significantly with temperature. Viscosity can be expressed in two forms, dynamic and kinematic. Both forms are measurements of a fluids resistance to flow, and are dependent on temperature and pressure. In addition, kinematic viscosity is inversely proportional to the density of a fluid; as the density of a fluid is increased, its kinematic viscosity decreases.

Castrol SAF-XO is the lubricant used by Jaguar Land Rover in their X150 FDU, and contains improvers for high and low temperatures as well as wear and extreme pressures for a range of temperatures and loads. These additives all contribute to making a more efficient and longer life system, which ultimately result in better performance and reduced maintenance costs.

The viscosity index (or VI) of a lubricant is a way to identify how much a lubricant's viscosity changes with temperature. The viscosity of a lubricant with a low VI will vary greatly at temperature extremes, whereas the viscosity of a lubricant with a high VI will undergo little change with temperature. A higher VI indicates a more stable viscosity.

Table 2-2 - Viscosity Index (Engineers Edge, 2010)

	Viscosity Index (VI)
Low	<35
Medium	35-80
High	80-110
Very High	>110

From the material safety data sheet, the VI of Castrol SAF-XO can be found to be 162. In Table 2-2, the classifications of viscosity index are given and from this it can be seen

that the VI of Castrol SAF-XO is very high. Even though at this level the VI is considered to be stable with temperature, a change in viscosity will still occur. A diagram of the change in viscosity of Castrol SAF-XO with increasing temperature can be found in Figure 2.4.

The temperature range in which this lubricant is expected to function is from -40°C up to 160°C, but for the most part, the working temperature is between 40° and 100°C. The temperature within the FDU is highly dependent on the airflow around the housing (Castberg, 2010) and the drive cycle. Fast speed and high load result in increasing lubricant temperatures, but increasing air flow around the unit also assists in heat dissipation from the casing. From Figure 2.4, it can be seen that between 40°C and 100°C the viscosity decreases from 100 mm^2/s to 15 mm^2/s respectively. This is of interest as changes in viscosity ultimately affect the thickness of the lubricant films that adhere to gears and casings. When the temperature increases, thinner films would be expected due to the decrease in viscosity, resulting in a variation of lubricant circulation within the FDU, which will affect the heat transfer and system lubrication.

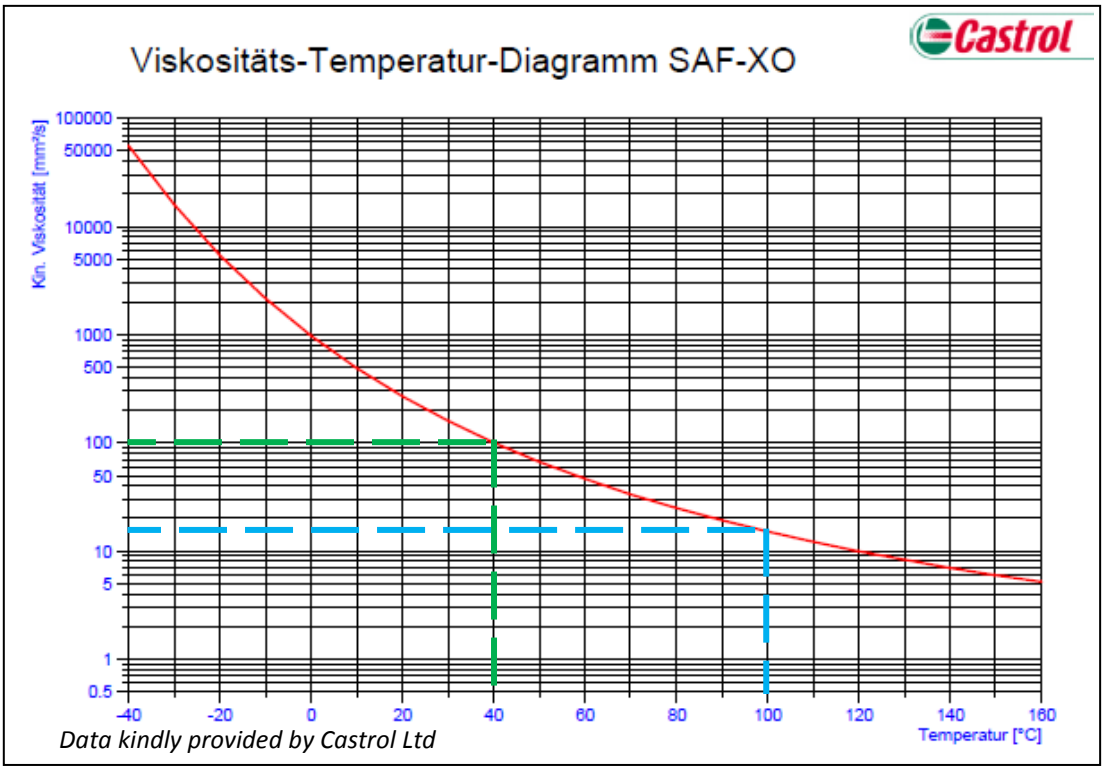

Figure 2.4 - Viscosity vs. temperature diagram for Castrol SAF-XO

From this section it can be seen that matching a suitable lubricant to an application is important for the efficiency and lifetime of a system such as a FDU. The significance of lubricant behaviour, in particular viscosity, has been noted. In terms of lubricant thickness measurements, it is important to take into account any changes in

temperature, and therefore viscosity, as this will affect the range of lubricant thicknesses observed. The higher the lubricant viscosity, the greater the lubricant thickness will be on casings and gear surfaces. This means that any calibration technique has to cover a sufficiently large range of lubricant thicknesses to account for the thicknesses likely at relative high and low viscosities during typical operation.

2.3 An Overview of Lubrication

Due to their benefits, lubricants are used in most mechanical devices. Lubrication generally takes the form of a fluid film between contacting surfaces and it is the thickness of this film determines the type of lubrication. There are four basic types of lubrication; boundary, mixed, hydrodynamic and elastohydrodynamic. These types of lubrication have been studied extensively and described fully in many texts, including Dowson and Higginson (Dowson and Higginson, 1977) and Hamrock (Hamrock et al., 2004).

The Stribeck curve, Figure 2.5, shows the relationship between friction and sliding speed of surfaces. Boundary lubrication is achieved through the combination of low speed, low viscosity and high load, resulting in high friction. Mixed lubrication occurs when the speed and viscosity are increased or the load decreased, resulting in a thin film which can support some of the load. This is shown as a sharp drop in friction on the Stribeck curve. Once the separation of surfaces is complete and the load is fully supported by the lubricant, the lubricant type is termed hydrodynamic. There is low friction and no wear as there is no solid boundary contact. If the thickness of the lubricant continues, fluid drag is introduced to the system resulting in higher friction, which is shown on the far right of the Stribeck curve. The Stribeck number is a non-dimensional number where μ is dynamic viscosity, N is speed and P is pressure.

$$St = \mu \frac{N}{P} \tag{2.1}$$

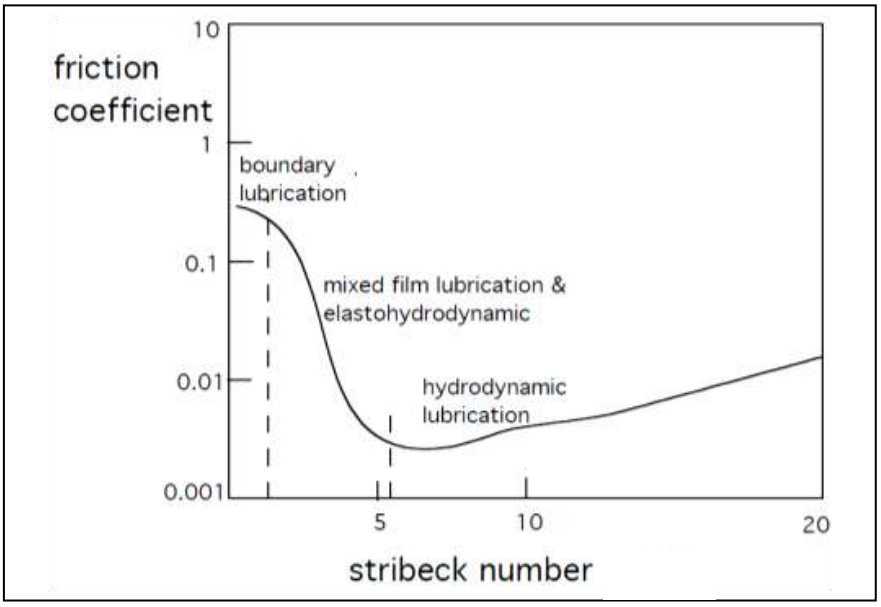

Figure 2.5 - Stribeck curve (Bryant, 2005)

When two bodies, such as mating gear teeth, contact either side of a lubricant film, there is a point of high localised pressure at the point of contact. If at this point, there is also elastic deformation of the contacting surfaces, then the type of lubrication may be termed elastohydrodynamic (EHD). In general, EHD theory considers only Newtonian fluids in isothermal conditions which, in the case of gears, is unrealistic as lubricants behave in a non-Newtonian fashion and are subject to temperature changes between meshing gear teeth (Habchi et al., 2008). The term for the lubrication mode that also takes into consideration the thermal effects of contacting gear teeth, is thermo-elastohydrodynamic (TEHD) (Wang et al., 2004).

The majority of experimental work on EHD lubrication has been carried out since 1950, as it was during the early 1950s that film thicknesses began to attract greater interest. Methods including electrical resistance (Lane and Hughes, 1952), capacitance (Dowson and Higginson, 1977) and volume flow rate (Crook, 1958) were used to measure film thicknesses both qualitatively and quantitatively. There have been a number of studies carried out and mathematical models created to assess the thickness of lubricant films in geared systems. However, due to the many variables, each of the models simplifies the complex system by omitting or making assumptions about certain factors such as temperature, viscosity and deformation.

The basis of many equations for calculating fluid film thickness is the assumption that the contacts are isothermal and fully flooded (Hamrock et al., 2004). Ideally, there should be a full film of lubricant between contacting metal surfaces. However, many factors prevent the development of full-film lubrication, these include: friction, debris contamination, lubricant starvation, unsteady loading and surface roughness. Surface roughness can be thought of as any variation of the actual surface height from a reference level (Hamrock et al., 2004). The surface roughness is controlled by the forming and surface finishing processes. A summary of the typical surface finishes associated with the different processes can be found in Figure 2.6. In general, the smoother the surface finish, the more expensive it is to achieve so a balance is found between the required gear behaviour (noise and vibration) and the cost of the finishing process.

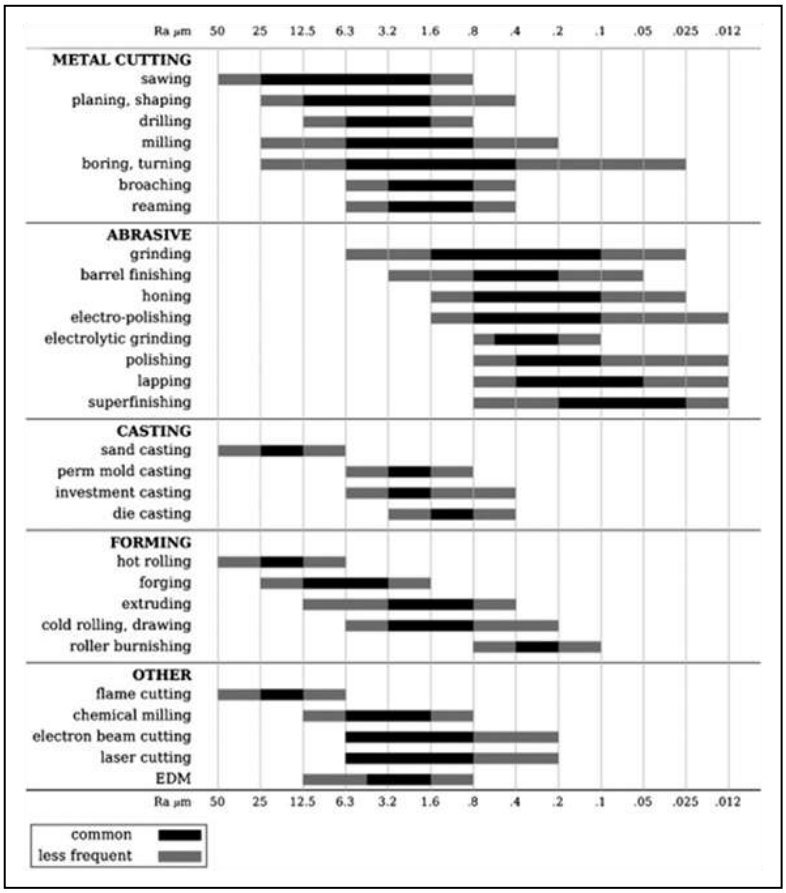

Figure 2.6 - Typical surface finish processes (Degarmo, 2003)

At a microscopic level, metal surfaces are not flat; they are covered in asperities due to their microstructure and finishing processes, as previously discussed. If a lubricant film thickness between two surfaces is greater than the height of the asperities, i.e. thick enough to completely separate the contacting surfaces, the fatigue life of the components is increased and the wear on the surfaces is decreased. On the other hand, if the lubricant film thickness is less than the height of the asperities, the asperities collide and introduce high shear stresses as a result. Although the peaks of the asperities come into contact, the valleys of the asperities can hold lubricant so that it is present during contact. According to Olver (Olver, 2002), failure of lubricant films to significantly exceed the asperities, or surface roughness, is one of the main problems in gear lubrication. Asperities not only affect the film thickness, they also affect the pressure distribution and friction within the contact (Dowson and Ehret, 1999). It is proposed by Simon (Simon, 1981), that the minimum film thickness should be two to three times greater than the surface roughness to ensure full EHD lubrication. To be certain that the calculation of lubricant film thickness is accurate; all of the above factors need to be taken into consideration, which is not currently possible via modelling.

In a high speed, high load geared system, such as a FDU, a great deal of heat is generated, and as a result, temperature effects should be considered. An increase in temperature causes a decrease in viscosity, which in turn causes a reduction in film thickness (Herschel, 1922). Large rises in temperature are detrimental to lubricant durability, so as a response to this, a model for prediction of lubricant oil temperature was developed by Iritani *et al* (Iritani et al., 1999) as a tool to be used to reduce the time taken during the design process. In their paper, Iritani *et al* explain that heat generation within a manual transaxle is due to lubricant stirring (churning), friction and gear meshing. The heat generated by these methods is transferred through the lubricant to the housing, where it is then transferred through the outer wall to the surrounding air. A method of predicting the lubricant temperature using their understanding of the heat transfer within the system was described in the paper and ultimately showed that if the lubricant fill volume was reduced, so was the lubricant temperature. According to the data, a reduction from a fill volume of 2.7 litres to approximately 1.3 litres resulted in a temperature reduction of 12°C at a vehicle running speed of 100km/h. Most of the cooling is thought to be from areas where lubricant is in direct contact with the casing as opposed to areas of splash or mist. This contradicts the findings by Wang and Cheng (Wang and Cheng, 1981) that say that in gears meshing at high speeds, the main source of cooling is the oil mist surrounding the gears. Although there is no evidence given to confirm the cooling effect of oil mist, a substantial improvement to lubricant performance was noted when the ambient temperature around the gears was decreased.

The role of lubrication has been clearly described, but ensuring that lubricant reaches the right places at the right time is not always simple. Dip lubrication is the term given to describe a system in which the gears pass through, or dip into, a reservoir (sump) of lubricant which sits at the bottom of a housing. Dip lubrication is often used in geared systems as it is reliable compared with, say, spray lubrication. The advantage with spray lubrication over dip lubrication is that less lubricant is needed and the lubricant used can be directed precisely to where it is needed. The disadvantage however is that if the spray lubrication fails, there may be no fall back and the geared system may fail. With dip lubrication, the lubricant is entrained by the gears and dispersed through splashing around the casing. It is important to consider the lubricant movement after entrainment. Churning losses have already been discussed as a disadvantage and are part of all dip lubricated systems, but nonetheless, dip lubrication is a tried and tested, and perhaps more importantly trusted method of lubrication, therefore optimisation of such a system is beneficial for obtaining higher efficiency for a reliable system.

At low speeds there is a small amount of lubricant splash, but at high speed this increases significantly. It is possible to use the casings to direct and control lubricant

flow direction to ensure the lubricant reaches the areas where it is needed, such as bearings and also is limited in areas where it may cause excess churning.

In this section, an overview of the interaction between lubricants and surfaces has been given. The effect of temperature changes on lubrication and importance of viscosity and fill volume have been discussed. In the following section, a number of the techniques used for measuring EHD lubricant film thicknesses will be summarised. The suitability of these techniques for measurement of lubricant thickness within the FDU will be explored.

2.4 Film Thickness Measurement Techniques

It has been established that lubricant thickness is a widely used quantity to describe and understand geared systems, so it is a valuable quantity to measure. In this section some of the numerous fluid thickness measurement techniques will be discussed.

There are many ways to measure thicknesses of fluids; some techniques are applicable over multiple orders of magnitude, while others are limited to narrow ranges of thicknesses. A short summary of several thickness measurement techniques that have been used to measure thin films, including EHD films, can be found in Table 2-3.

From the table, it is clear that while there are a number of techniques available for measuring lubricant thicknesses, not all of them are suitable as they are limited to low vibration or static systems. For the purposes of measuring lubricant thicknesses in a FDU, the technique used should be applicable to a noisy, high vibration system and be able to measure a suitable lubricant film thickness, which will be assumed to be of the order of 0.5mm to 2mm. Although LIF had initially been favoured as a suitable technique, the ultrasonic, laser absorption and LIF techniques will all be discussed in more detail in the next section.

Table 2-3 - Summary of film thickness measurement techniques

Measurement Technique	Measurement Range	Description of Method
Ultrasound	From 2nm upwards	Ultrasonic pulses in a liquid layer between two solid boundaries reflect from the solid boundaries. The reflection depends on the ultrasonic frequency, acoustic properties of the solid and liquids and liquid thickness. Liquid thickness can be calculated if the other variables are known.
Optical Interferometry	From 5nm	Light from a single source is split into two separate beams, and when recombined, a series of light and dark bands, or fringes, can be seen from which the film thickness of the oil can be calculated. The light fringes are due to constructive interference and the dark due to deconstructive interference.
Image Scanning Ellipsometry	From 0.1nm to several micrometers	Ellipsometry measures a change in polarization as light reflects or transmits from a material structure. The polarization change is represented as an amplitude ratio and the phase difference. The measured response depends on optical properties and thickness of individual materials. Thus, ellipsometry is primarily used to determine film thickness and optical constants.
Conductivity (Parallel wire)	From order of 10^{-6}m	This technique relies on the fact that conductance between two parallel wires is related to the liquid level between them.
Laser Absorption	0.5mm-12mm	Absorption is described by the Beer-Lambert law, from which liquid film thicknesses can be calculated: $A = \log\frac{I_0}{I} = ahC$, where A is absorbance, I_0 is the intensity of incident light, I is the light intensity after passing through a liquid layer, a is a constant determined by calibration, C is the dye concentration and h is the liquid film thickness.
Optical Interferometry/ Fringe method	From 5nm upwards	Using interference patterns of light from the surfaces of liquids, thicknesses of films can be measured down to a minimum of 5nm
Laser Induced Fluorescence (LIF)	From 5µm upwards	Fluorescence is an emission of light from atoms or molecules that have been excited to higher energy levels by absorption of electromagnetic radiation. The fluorescence from a liquid film is proportional to its thickness.

2.4.1 Ultrasonic Techniques

Ultrasound is frequently used as a non-destructive testing technique to find defects in solid bodies. Its success relies on the difference in acoustic properties between a defect and the surrounding material. Much work has been carried out in the area of ultrasonic thickness measurement between contacting bearing surfaces (Dwyer-Joyce et al., 2003; Dwyer-Joyce et al., 2004; Kasolang and Dwyer-Joyce, 2008; Reddyhoff et al., 2008; White et al., 1998) and, to a lesser extent, real-time laser-based ultrasonic measurement of automotive paint thicknesses (White et al., 1998). The remainder of this section will focus primarily on the work carried out by Dwyer-Joyce *et al*. (Dwyer-Joyce et al., 2003) as it encapsulates much of the work carried out in ultrasonic film thickness measurement.

Reflection of ultrasonic pulses in a lubricant between metal surfaces depends on the ultrasonic frequency, the acoustic properties of the lubricant and metals, and the layer thickness. The thickness of the film depends on the lubricant properties, geometry of the metal surfaces (in this case bearing geometry) and operating conditions. When an ultrasonic pulse reaches a boundary between two different media, such as a lubricant and bearing metal, some of the energy is reflected and some transmitted. In the paper by Dwyer-Joyce three ways in which the ultrasonic signal can be used to measure lubricant film thickness are described, they are; time of flight, through-thickness resonance and spring interface modelling. If the lubricant layer to be investigated is sufficiently thick (usually greater than 50μm), the thickness of the lubricant layer can be measured via a time of flight (ToF) technique. ToF is the time taken for reflections to reflect from top and bottom boundaries, and can be calculated if the speed of sound in the lubricant is known. Although ToF is the simplest technique for measuring film thicknesses and has no upper limit for thickness measurement, for very thin films the ToF technique is flawed as it is impossible to distinguish between multiple reflections that may occur. Based on the assumption that the lubricant thicknesses within the FDU will be in the region of 0.5 to 2mm, the ToF technique could potentially suit this range.

The through-thickness resonance is measured and interpreted with a continuum model. The resonant frequency of a layer and its thickness h, are related by:

$$h = \frac{cm}{2f_m} \tag{2.2}$$

where c is the speed of sound in the lubricant layer, m is the mode number of the resonant frequency, and f is the resonant frequency (in Hz) of the mth mode (Pialucha et al., 1989). Higher resonant frequencies correspond to thinner films. There is however a limit: at 10μm and below, the resonant frequency is above the measurable range. Theoretically, the smallest film measurable with this technique is 2nm, based on a 60MHz measuring frequency and assuming the reflected pulse is approximately 20 times that of the noise level (60dB is typical for a conventional UT ND testing system).

The spring modelling technique is based on the similarity between the dependence of spring deflection on spring stiffness and dependence of the interaction of ultrasound on the layer stiffness. For films with a resonant frequency above the measurable range, the stiffness of the layer can be used to calculate film thickness. The interaction of ultrasound with a thin layer is governed by the stiffness per unit area, K, of that layer,

$$K = \frac{\rho c^2}{h} \tag{2.3}$$

where ρ is the density of the layer and c the speed of sound in the layer (Hosten, 1991). This spring stiffness can then be used in a model of the interaction of the ultrasound and the lubricant layer. Dwyer-Joyce goes on to incorporate the reflection coefficient, R, and acoustic impedance of the material either side of the lubricant film, z, to give an equation that relates film thickness to the reflection coefficient.

$$h = \frac{\rho c^2}{\pi f z'}\left(\frac{R^2}{1-R^2}\right)\ldots \tag{2.4}$$

From this, it can be seen that h approaches infinity as R approaches unity. To calculate the lubricant-film thickness using equation 2.3, knowledge of layer density and speed of sound through the lubricant film are necessary, but density changes as the pressure increases. A correction factor, taken from Jacobson and Vinet (Jacobson and Vinet, 1987), was used to allow for the variation in pressure and therefore density.

In addition to the measurement of films in bearings ultrasound has also been used to measure paint thicknesses. The principle behind the laser-based ultrasonic measurement of paint thicknesses studied by White *et al* (White et al., 1998), is that a short pulse (10ns) from a laser can cause an increase in temperature (<5ºC) in the paint surface, which produces a density gradient, which in turn produces ultrasound. The laser pulse can be thought of as equivalent to a hammer striking a bell. In addition to the pulsed laser, a continuous wave (CW) laser is used to detect the movement of the fluid surface as a result of the ultrasonic energy induced by the laser. Light is transmitted to and from the lasers via fibre optics so as to keep the sensitive equipment out of the spray booth. The authors claim that the liquid film thickness can be measured to an accuracy of ±1.5µm.

If ultrasound were to be used to measure film thicknesses between the gear teeth, it is hard to see how a transducer could be embedded into a gear tooth without significantly altering the structural integrity of the gear, the micro geometry of the gear and the film to be measured. While ultrasonic thickness measurement has proven valuable for the measurement of lubricant films between contacting surfaces, for measurement on surfaces with only one boundary, there seems to be very limited possibilities for application. One such example is the measurement of paint film thickness carried out by White (White et al., 1998). In this example, a laser is used to

induce ultrasonic waves in the paint surface. This set-up would require a calm and still environment in which to work, unlike the FDU.

2.4.2 Laser Absorption Techniques

In order to illustrate the use of laser absorption for the measurement of film thicknesses, a summary of the work carried out by Mouza *et al*. (Mouza et al., 2000) will be discussed in this section. In an attempt to find an alternative verification method, a film thickness measurement technique using laser absorption in tandem with a parallel wire conductance technique, was developed. It is important to note that the parallel wire conductance technique is a calibration device for the absorption technique but is not suited to geared machinery.

Mouza identified a need for a reliable and easily calibrated system for the measurement of flowing liquid films. The parallel wire conductance probe method used by Mouza, is based on the inverse proportionality between electrical resistance and layer thickness. While parallel wire conductance was used successfully, there were difficulties when attempting to measure films less than 0.5mm. The source of the difficulty was the meniscus formation on the parallel wires. The exact details of the meniscus effects are not given, but it is assumed here that a false thickness could be measured due to the way in which a meniscus alters with increasing or decreasing liquid level. As the thickness increases, the meniscus would fall below the mean thickness level, while a thickness decrease results in a higher meniscus than the mean, thus giving a reading indicating a thicker film than is actually present. Details regarding the thickness at which the meniscus began to affect the measurements were not given. The meniscus of a liquid depends on the liquid used and the contact material which in this case is the wire.

The principle behind the laser absorption technique is that the thickness of a liquid layer is proportional to the amount of light absorbed by that layer. A similar method was used by Lilleleht and Hanratty (Lilleleht and Hanratty, 1961) and by Portalski and Clegg (Portalski and Clegg, 1972). Light absorption is described by the Beer-Lambert Law:

$$A = \log_{10} \frac{I_0}{I_t} \tag{2.5}$$

where A is the absorbance, I_0 is the intensity of incident light and I_t is the light intensity after passing through the layer, or transmitted light. Absorbance can also be calculated via another equation:

$$A = \varepsilon C d \tag{2.6}$$

where ε is molar absorptivity, d is the path length (which in this case is the layer thickness) and C is the molar concentration of the fluid. In the paper by Mouza, absorptivity is given as the product of the layer thickness, dye concentration and a constant to be calculated during calibration, which suggests that perhaps the molar absorptivity was unknown.

The test liquid used was water containing methylene blue dye flowing inside an inclined 24mm inner diameter tube and re-circulated. Three different flow rates were tested; 3, 5 and 7.5cm^3/s. Downstream from the liquid entry point, a Plexiglas section was incorporated into the tube at a point where the film was considered fully developed. Within this Plexiglas section, the laser absorption and parallel wire conductance technique apparatus were set up 10cm apart. Both techniques were carried out simultaneously.

The layer thickness was determined by measuring the laser light intensity after it had passed through the liquid layer. A 635nm diode laser beam with a diameter of 0.25mm was used for its stable light intensity. A photodiode with an amplifier was used to collect the transmitted light. The voltage from the photodiode was then output to a 12-bit A/D converter before being recorded by a PC. Data were collected for 15 seconds at a sampling frequency of 200Hz for statistical analysis. The sampling rate and size were checked and found to be satisfactory with respect to previous film thickness experiments however, there appears to be no evidence to support this.

To calibrate the system, a stagnant liquid layer of known thickness was measured with both the conductance and absorption techniques. The film height varied linearly with conductance and also with absorbance over the range of thicknesses assessed, from 0.5, to 5mm. For film thicknesses below 0.5mm, the thickness data was extrapolated to zero. The absorbance data was checked for repeatability and stability of the laser. A 3% maximum deviation was noted for the absorbance technique, so the technique was considered repeatable and stable.

The thickness measurement data was analysed in both instantaneous and time averaged forms. Both the conductance and absorption techniques showed agreement within 5% of the time averaged data. For the RMS values, a greater variation was noted with the capacitance technique than the absorption technique. The variation

was put down to the response time of the photo diode, but the value of variation was not given.

From this paper, it is apparent that both the parallel wire conductance and the laser absorption techniques were successful in measuring static and dynamic films down to 0.5mm. Below 0.5mm, film thicknesses were extrapolated, which could result in erroneous film thickness calculation.

2.4.3 Optical Interferometry Techniques

Optical interferometry has been used to measure lubricant films between contacting surfaces (Ciulli et al.; Johnston et al., 1991) and also for analysing droplets (Kariyasaki et al., 2009). A brief overview of the work carried out by Johnston *et al*. is included here. The basic principle behind interferometry is that light waves from two sources can interact to create an interference pattern through constructive and destructive interference as first demonstrated by Young in 1801.

In a study carried out by Johnston *et al*. (Johnston et al., 1991), optical interferometry was investigated as a tool for measuring elastohydrodynamic films in rolling contacts at low speeds. The principle of the technique is shown in Figure 2.7. Light enters the oil through a glass disc where some of the light is reflected from the base of the glass. The remaining light passes through the oil to the surface of the steel ball where it is reflected. The light that passed through the oil travelled two oil thicknesses further than the light that was reflected at the base of the glass and so the two are out of phase. The light reflected back out through the glass combines to form constructive and destructive interference, and from this, the oil film thickness can be calculated. The disadvantage with optical interferometry is the need for one surface to be made of glass or sapphire and therefore this particular method is not suitable for application to the FDU.

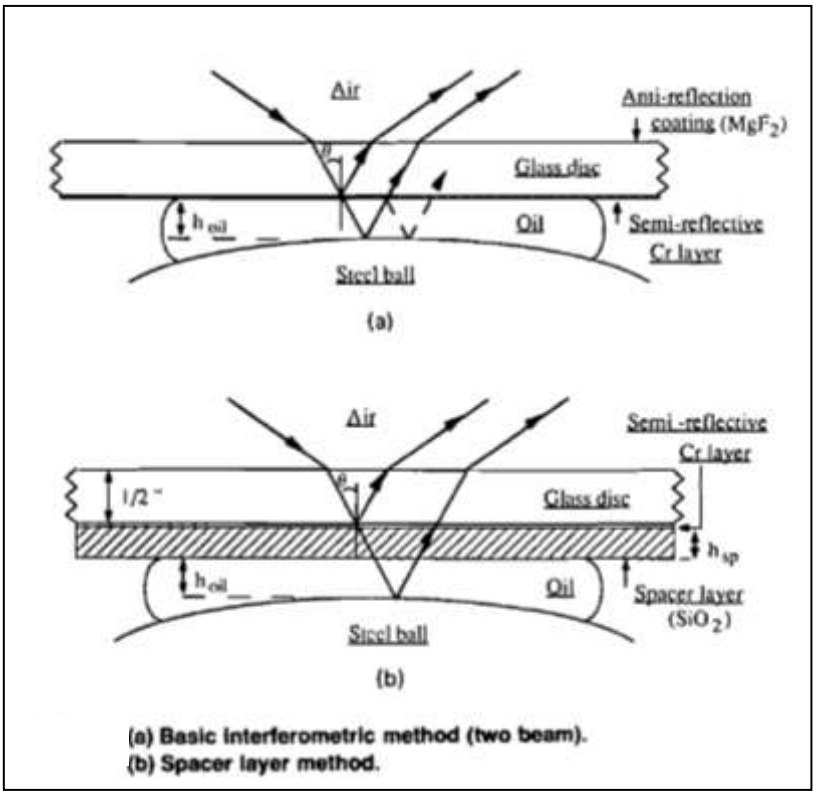

Figure 2.7 - Optical interferometry study set-up by Johnston et al.

The minimum measureable film thickness with this method was limited to a quarter of the wavelength of light, but through the introduction of a spacer by Johnston, it was possible to measure thinner films.

In their study, Johnston *et al*. found that they were able to reliably measure films down to 5nm when the rotational speed of the rig was sufficiently slow. As the speed increased up to a maximum of 1m/s, the film thickness of mineral oil increased up to approximately 1µm. Ciulli *et al*. used interferometry to measure and assess 3D film thickness profiles of lubricants between a ball and disc for varying amounts of sliding and rolling. Their results showed that there was a reduction in film thickness with an increase in sliding compared to rolling, and that central film thicknesses were smallest when the ball was running faster than the disc.

From these papers, it appears that optical interferometry is used for easily controlled and relatively small features. The use of glass makes the technique unsuitable for the FDU, although it would be interesting to apply this method to the housing to see if lubricant thickness data could be acquired from there.

2.5 Laser Induced Fluorescence

The basic principles and uses of laser induced fluorescence (LIF) have been covered comprehensively in a number of key texts, such as Eckbreth (Eckbreth, 1988), Lakowicz (Lakowicz, 2006) and Lange (Lange, 2005). A synopsis of the key points is covered in this section. In addition, an overview of the key components of the LIF method; lasers and fluorophores, will be given to show that there is a link between the two. Some practical applications of LIF will be described to illustrate the applicability of the technique to film thickness measurement and a drawback of the LIF technique, bleaching, will be considered. Finally, the importance of a suitable calibration technique will be discussed.

Fluorescence is an emission of light from atoms or molecules that have been excited to higher energy levels by absorption of electromagnetic radiation, often (but not always) in the form of visible light. The intensity of fluorescence emitted is proportional to the quanta of light absorbed. LIF uses the fluorescence phenomenon with laser light to excite a selected area of interest so that the magnitude of fluorescence intensity may be studied.

Uses of LIF include the detection and study of small particles. More specifically, LIF has been used to detect particles in combustion and to study flow visualisation. Its uses are not limited to engineering and chemistry; LIF is also used in biomedical applications, such as classification of colonic polyps and the LIF-guided resection of brain tumours (Schomacker et al., 1992). This shows that LIF is useful for measurement of particulates as well as film thicknesses, which will be discussed further in a later section.

2.5.1 Practical Applications of LIF Film Measurement

LIF can be used to take precise measurements in many locations simultaneously without disturbing the subject matter. A few examples of this are the use of LIF to study lubricant starvation (Smart and Ford, 1974; Ford and Foord, 1978), flowing films (Driscoll et al., 1992), and liquid film thicknesses. LIF has been used by several researchers to measure liquid film thicknesses in a number of areas. One area in which research has been carried out is the measurement of fuel film thicknesses on combustion chamber surfaces of gasoline engines, to better understand and reduce hydrocarbon emissions (Cho and Min, 2003; Jermy et al., 2004; Richardson and Borman, 1991; Shaw et al., 1992; Hoult et al., 1988). The obvious restriction with LIF is the need for optical access. To overcome this, fibre optics and LIF have been used simultaneously in the engine to gain access to an area which would otherwise be inaccessible (Richardson and Borman, 1991; Shaw et al., 1992). Another area of research involves the use of LIF and a fluorescence microscope to study pure sliding in

what are called compliant contacts (Myant et al., 2010). Summaries of the applications mentioned here are given in the remainder of this section.

Cho and Min (Cho and Min, 2003) used a pulsed Nitrogen,N_2, laser operating at 337.1nm (ultraviolet light), along with fibre optics and an ICCD (intensified charge-coupled device) camera to visualise fuel film thicknesses on cylinder liners, through a quartz cylinder liner. The laser pulse width of 5ns is significant because it allows temporal measurements to be made. The results showed a linear relationship between fluorescence intensity and fuel film thickness, with a standard deviation of less than 10%. Corrections were made for image magnification by the quartz liner, and the test area dimensions were specifically selected to minimise distortion and magnification, caused by the quartz liner.

Jermy (Jermy et al., 2004) also used a LIF technique to measure fuel film thicknesses. A pulsed Nd:YAG laser, operating at 532nm wavelength (green light) was used. A Nd:YAG laser, with its high power and capacity for temporal measurements, lends itself to LIF methods. A LaVision SprayMaster 3 CCD camera with IRO image intensifier was used to visualise the fluorescence from the fuel film through a fused silica window to allow optical access. One problem that was encountered was noise on the intensity signal, which was thought to be partially due to imperfect mixing of the dye (disodium fluorescein) and the fuel. This resulted in an uncertainty of ±16µm film thickness, which is a variation of 1.6% at thicknesses of 1000µm, and a variation of 8% at 200µm. Other possible sources of noise were thought to be fluctuations in the laser power. Despite the uncertainty and inaccuracy, Jermy describes LIF as being one of the most successful techniques for measuring fuel wall film thicknesses within the dirty environment of a piston engine as it is robust and nonintrusive.

Richardson and Borman (Richardson and Borman, 1991) developed a LIF technique for measuring oil films on cylinder walls using fibre optics with a Helium-Cadmium (HeCd) laser, operating at a wavelength of 442nm (blue light). A fibre optic was mounted flush with the piston surface, through which it carried the light from the laser to the oil and the fluorescence from the oil to a photomultiplier. A series of three tests were carried out, static and dynamic, to verify the system's capability for measuring thin films. In each of the 3 systems, the set-up of the fibre optics was altered to suit. The first set-up used a single static fibre optic, while the second moved with a ring relative to a stationary liner. The third set-up incorporated four fibre optics in to a real engine cylinder. One fibre optic was placed at TDC, two in the mid region and the final one just above BDC. Overall, the use of LIF with fibre optics was considered a success as measurements were made in both static and dynamic cases. However, a number of the problems were encountered. The dye used was affected by temperature, so

accurate calibration was impossible, yet it is unclear what the exact problem was with the dye. The end of the fibre exposed to the combustion gasses became covered in soot and therefore unusable. From this it seems fibre optics should only be used in areas where they cannot be covered, thus preventing them from transmitting and receiving signals.

In a paper by Driscoll *et al* (Driscoll et al., 1992), a LIF fuel film thickness measurement technique is described which is applied to steady and unsteady variations in film thickness, using a continuous wave, Argon ion laser operating at 514.5nm wavelength (green light). The experimental set-up comprises a laser, which is focused on to a surface of an air-blast fuel atomiser, as well as collection optics to direct and focus the fluorescence to a photomultiplier. The intensity of fluorescent light collected by the photomultiplier is a measure of the thickness of the liquid film. Film thicknesses from 300µm up to 1mm were measured during calibration, and a linear relationship was noted between the absolute film thickness and scaled photomultiplier output voltage. Correction for absorption of light through the film is taken into consideration using the Beer-Lambert law, $I_t = I_0 e^{-\alpha x}$, where I_t is the intensity of transmitted light, $I_0$is the intensity of the incident light, α is the absorption coefficient and x is the path length. In addition, a geometrical correction coefficient was used to account for the angle of incidence at the air/liquid boundary. If the incident beam is perpendicular to the fluid (and surface), no correction is required. The authors acknowledge that the main limitation with this method is that the system used is not capable of temporal resolution, which would be necessary for time-varying thickness measurements.

Dual emission laser induced fluorescence (DELIF) is a two-dimensional method that has been used by Hidrovo and Hart (Hidrovo and Hart, 2000) to measure oil film thicknesses and temperatures using two fluorescent dyes. A plane of observation in a system containing two dyes is illuminated using a laser. The fluorescence signal from dye one contains the information required on the scalar of interest and information on the exciting light intensity. The fluorescence signal from the dye two contains the same information but behaves differently than the first dye to the scalar of interest. By ratioing the fluorescence from dye one with dye two, the information regarding excitation light is cancelled out leaving only the scalar information sought. Normalisation is necessary as there is an irregularity of the illumination light intensity from lasers. A notable observation from Hidrovo's work is that fluorescence dependence on film thickness is linear, but only for optically thin systems. For optically thick systems, the dependence is exponential. Whether a system is thick or thin is dependent on the product of the molar absorption, molar concentration and laser wavelength used. At this stage, it is useful to mention that not all wavelengths of light pass through all materials. A good example of this is infrared wavelengths and glass.

Although visible light can pass through glass, infrared cannot. In this case, the glass can be described as optically thick to infrared wavelengths. Bearing in mind the success had using this method, it may be possible to develop this and apply it to film thicknesses measurement within the FDU to extend the LIF technique already favoured.

One factor that is known to affect fluorescence emission is reabsorption as acknowledged by Hidrovo. Reabsorption occurs when the emission and absorption spectra of dyes or fluorescent markers overlap. In his paper, Crosby (Crosby and Demas, 1971) explained that reabsorption is most significant when the overlap is large, although it is not clear what is meant by large. As a result of the aforementioned reabsorption, reemission can occur which leads to an artificially high fluorescence intensity result or reemission error. Crosby goes on to explain that qualitatively, reabsorption will be smallest if the detector views the emission on the excitation side instead of the back side of the system.

In Hidrovo's method, oil film thickness information is found in the reabsorption of fluorescence measurements, so an optically thick arrangement is used in order for the reabsorption signal to be great enough to measure. The results contained data for thicknesses between 10 and 110 microns. Interestingly, the temperature data showed that only one of the dyes produced less fluorescence with increasing temperature, which is the relationship that had been recorded by Bowen. The other dye showed an increase in fluorescence with increasing temperature.

In a separate paper by Hidrovo (Hidrovo and Hart, 2001), which discusses the method in greater detail, an investigation into the effect of different back surface reflectivities was carried out. It was found that for high reflectivity materials, such as a polished steel block, the LIF signal was approximately twice that of a low reflectivity material such as matt rubber. This is not surprising as a polished surface can act as a mirror so that the laser can excite on both entry and exit. This may be significant if film thickness measurements are to be taken from any gear surfaces, such as the edge of the crown wheel or on gear teeth.

In a more recent study, Myant (Myant et al., 2010) used LIF to measure fluid film thicknesses in compliant, pure sliding contacts. Compliant contacts are contacts in which significant elastic deformation occurs in one or both contacting surfaces, but where there is no significant change to the lubricant viscosity. This type of contact is associated with "soft" materials, low load and low pressure. Examples given include windscreen wipers and rubber o-ring seals.

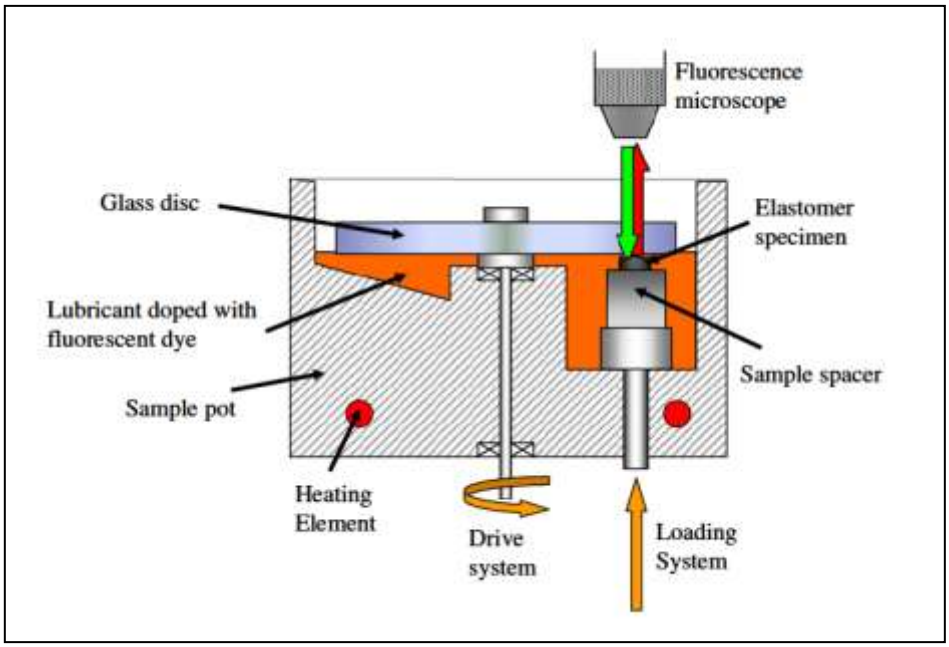

Figure 2.8 - Set-up of experiment by Myant

Myant's investigation comprised a sliding contact, made from a disc and hemisphere and a fluorescence microscope. A diagram of experimental layout is shown in Figure 2.8. A PDMS (polydimethylsiloxane) elastomer hemisphere was submerged below the surface of the lubricant, with the glass disc positioned horizontally on the surface of the lubricant. This set-up allowed lubricant to be entrained as the disc rotated, thus replicating pure sliding conditions.

Glycerol, distilled water and a glycerol-distilled water solution were used as the lubricants with dynamic viscosities of 1.16, 0.0055 and 0.00089Pa·s respectively. As no other temperature is specified in the paper, it is assumed that the viscosities stated were measured at room temperature. The three lubricants contained the fluorescent dye, Eosin, which was chosen for its compatibility with the excitation wavelength. A Laser 2000 Ltd solid-state, diode-pumped pulsed 532nm laser was used to excite the dye. Myant *et al*. refer to a separate paper for further details on the optical set-up; however, the reference details are incorrect, so the additional details of the set-up are unknown.

A Zeiss Axiotech Vario Microscope, together with a QImaging Rolera MGi B/W EMCCD camera (controlled via PC) were used to observe and capture the fluorescence intensity images for a range of entrainment speeds from 1mm/s up to 100mm/s. As fluorescence intensity is proportional to lubricant thickness, the intensity images were used to create film thickness maps of the lubricant in the contact zone. Myant gives the range of the technique as between 200nm and 25µm, although it is suggested that

this could be extended through alteration of the fluorescent dye concentration in the lubricants.

Analysis of fully flooded contacts was carried out using the camera images captured for the range of entrainment speeds. The data from the images were compared with theoretical data. The equations used to obtain the theoretical data were taken from a paper by Hamrock and Dowson (Hamrock et al., 2004),

$$h_c = 3.3\bar{U}^{0.64}\bar{W}^{-0.22}R' \quad (2.7)$$

$$h_m = 2.8\bar{U}^{0.65}\bar{W}^{-0.21}R' \quad (2.8)$$

Where h_c and h_m are the central and minimum film thickness respectively, $\bar{U}$ is a dimensionless speed parameter, $\bar{W}$ is a dimensionless load parameter and R' is the reduced radius of curvature.

A close relationship was noted between the theoretical and experimental values for increased entrainment speed for water and glycerol-water at entrainment speeds greater than 10mm/s. Below 10mm/s, there appeared to be no correlation with the theoretical data at all, suggesting that 300nm was the minimum thickness detectable for the set-up described. For glycerol, the experimental measurements were much lower than the theoretical data; however, by adjusting the dynamic viscosity value in one of the initial calculations, a good agreement was noted between measurements and calculations.

2.5.2 Fluorophores

A fluorophore is a substance that will fluoresce if suitably excited. Fluorophores follow a cycle of absorption, excitation and emission before returning to their ground state where the process can begin again (Figure 2.9). The ability to re-use fluorophores is one of the aspects that makes them so useful.

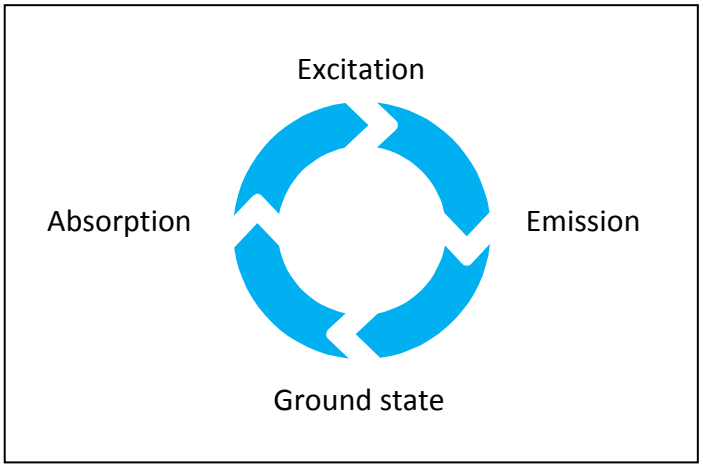

Figure 2.9 - Fluorescence Cycle

Typically, fluorescence arises as a result of the excitation of and emission from conjugated bonds in functional groups such as alkenes, esters, benzene derivatives and toluene derivatives. These functional groups are often found in lubricant additives, so at the right wavelength of light, lubricants can be made to fluoresce. As not all substances fluoresce, and the substances that do are not necessarily excited by the same wavelengths of light, it is important to find a compatible wavelength of light for the substance under investigation. Alternatively, if the wavelength cannot be made to suit the substance under investigation, a fluorescent marker or dye can be added to enable fluorescence at the wavelength of light available. There are many commercially available dyes available, each with a unique excitation and emission spectrum. Rhodamine is one such dye that can be used with a 532nm wavelength to produce red fluorescence.

By altering either the laser wavelength, the substance under review or adding a dye to the substance under review, fluorescence can be produced in many ways at various emission wavelengths.

2.5.3 Laser Bleaching of Oil Films

When using a fluorescence based system, it is important to note that there is limit to the amount of light that can be absorbed and emitted. In Figure 2.9, it was shown that fluorescence follows a repeating cycle but, if too high an intensity of light is used, the structure of the fluorophore changes so that it can no longer fluoresce (Figure 2.10 (Invitrogen, 2010)).

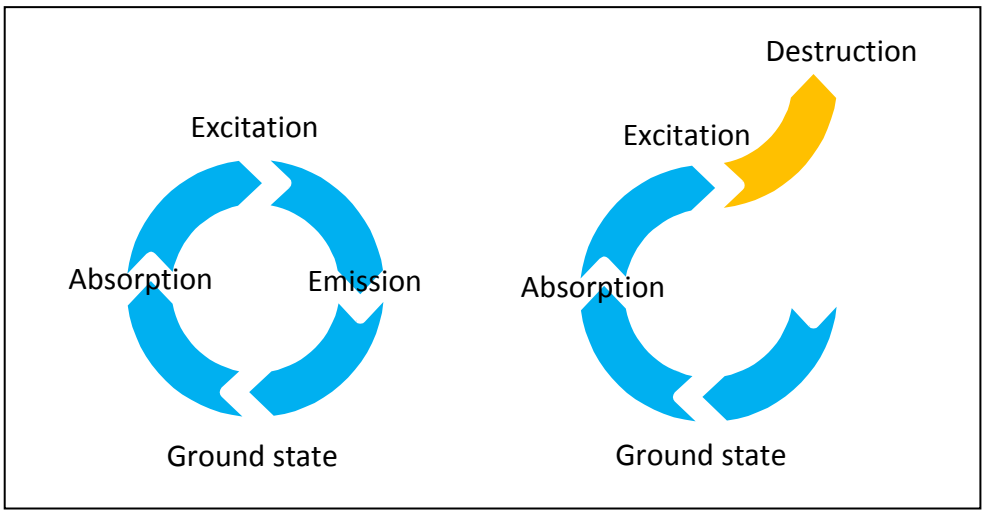

Figure 2.10 - Bleaching

During their static tests Richardson and Borman (Richardson and Borman, 1991) noted a bleaching effect, which is a decrease in fluorescence, as the oil was exposed to laser light. When the laser was turned off after exposure, the oil remained bleached, which meant that fresh oil was required for each new measurement. Decreasing the power of the laser, or increasing the temperature of the oil were found to decrease the effects of bleaching; however, fluorescence can be greater at lower temperatures (Bowen, 1959) so increasing the temperature too far could reduce the amount of fluorescence to begin with. Richardson and Borman found that if movement was introduced to the oil so that the oil under the laser light is being constantly refreshed, the effects of bleaching became negligible(Richardson and Borman, 1991)(Richardson and Borman, 1991) (Richardson and Borman, 1991).

For film thickness measurements of stagnant films, bleaching is a real concern. However, for moving fluids it would seem that bleaching has less of an effect and may even be negligible. While films within the FDU are dynamic, films during calibration may be stationary or slow moving, so it is important to consider bleaching at that stage.

In addition to bleaching, there are other processes, known as quenching processes, that reduce fluorescence emission (Eckbreth, 1988). For an excited molecule, fluorescence is not the only option for energy loss. Other possibilities for energy loss include (but are not limited to) dislocation, energy transfer to another molecule and chemical reaction. These quenching processes can be calculated if the data is available, or they can be experimentally determined and corrected for where required.

2.5.4 Calibration Techniques

Calibration is an essential part of LIF techniques. Without suitable and reliable calibration, only qualitative data can be acquired. In this section, the calibration techniques of the aforementioned methods will be discussed.

To calibrate their system, Cho and Min (Cho and Min, 2003) used thickness gauges placed between the quartz liner and a calibration device, which has the same radius as that of the inner radius of the quartz liner. Fuel was introduced through a hole in the calibration device via a syringe, and the film thickness was measured with a thickness gauge with an accuracy of 1µm. A total of five thickness gauges were used for calibration; 10µm, 20µm, 30µm, 40µm and 60µm. The fluorescence intensities at each point were measured with an ICCD camera ten times, and then averaged. The results showed a linear relationship between fluorescence and fuel film thickness; the greater the fuel thickness, the greater the fluorescence. The standard deviation of each point was less than 10%.

Jermy (Jermy et al., 2004) calibrated his system using a tray of fuel of varied depth, which was illuminated with the laser, then imaged using a LaVision SprayMaster 3 CCD camera with IRO image intensifier. Intensity verses depth data showed a general upward trend from 200µm to 1000µm, but the relationship was only linear when the camera was ‘nearer’ to the imaged region. It is unclear what is meant by ‘nearer’ as there are no dimensions or scales given.

Richardson and Borman (Richardson and Borman, 1991) made use of a metal plate to simulate a cylinder wall and a piece of metal to simulate a piston ring, with oil in between. The piston ring was attached to a micro-translator which was able to move the piston ring closer to the metal wall face with micron accuracy. The film thickness data from the static test showed a linear relationship between photomultiplier voltage and film thicknesses between 10µm and 30µm, with slight deviations from a perfectly straight line due to laser power fluctuations.

Driscoll (Driscoll et al., 1992) used a dynamic calibration nozzle, which allowed measurement of different thicknesses. The test fluid used was a mixture of water and

fluorescein, and was kept in motion due to a build-up of long-lived phosphorescence and dye decomposition caused by laser light, or bleaching. The calibration nozzle consisted of a steel base with an inclined glass cover plate through which the fluid is allowed to flow, and is vital to this system as it provides quantified thickness data. The relationship between photomultiplier output voltage and absolute film thickness was found to be linear over the measured range between 300µm and 1200µm. The results were shown to be repeatable, with a standard deviation of less than 5µm, and a maximum deviation of less than 10µm. As this calibration method is taken at an angle to the film, it is an apparent film thickness that is measured, not the actual film thickness. The angle of incidence was known, so a correction was made to attain actual film thickness.

Hidrovo and Hart (Hidrovo and Hart, 2000; Hidrovo and Hart, 2001) used two optical flats placed on top of each other with a shim at one end to produce a wedge-type arrangement. Two 12-bit cameras were used to capture the fluorescence intensities simultaneously before normalisation. Two dichroic mirrors were placed in front of the mirrors to separate the fluorescence and laser emissions. For the dye combination used, it was possible to measure film thicknesses from 5 to 400 microns with 1% accuracy, and it is thought possible to improve on this accuracy over a select range with an adjustment of the dye selection and concentrations.

Myant's calibration technique used optical interferometry measurement of the contact area and radius of the hemisphere on the glass disc. These were then used to calculate the applied and static loads necessary to mathematically calculate lubricant thickness from the Hertz theory and JKR model of elastic contact. This calibration assumes that Hertz theory alone is sufficient to measure the gap thickness of the contact and that no other forces, such as adhesion, are significant. In addition, normalisation of the fluorescence data was carried out to overcome any irregularities in light intensity or from filters. This was achieved by normalising all images with a background, non-contact, image. Exact details of the normalisation method were not given in the paper, but from the examples given, it appears that the fluorescence data image was divided by the background image to give the normalised fluorescence intensity. This in turn was converted into a lubricant thickness through data acquired via calibration.

Calibration plays a vital role in LIF applications; without it data may not be able to produce important quantitative data or may include errors or irregularities that can be removed. A robust calibration method is essential for reliable LIF data.

2.6 Summary of Chapter 2

In this chapter, gears, lubricants and their interactions have been discussed and a lack of information on hypoid gear and lubricant interactions has been identified. Lubricant thickness measurements have been highlighted as a useful metric for the analysis of lubricant flows in complex geared systems, such as a FDU. Quantitative lubricant measurements are also valuable where modelling is not possible, or is not able to produce satisfactory results due to the many variables and complexities of the system.

The need to understand lubricant movement has been established and measurement of lubricant thicknesses from gears and casing surfaces would work towards that understanding. LIF has been established as a potentially suitable tool for the measurement of lubricant thicknesses within a FDU and past applications of LIF have been discussed. Calibration has been identified as being important to obtaining useful, meaningful data, and will be considered further in Chapter 5.

A brief overview of a number of film thickness measurements was presented in this chapter, with more detailed information given on the ultrasonic, laser absorption and laser induced fluorescence techniques. LIF was described in detail, and the importance of calibration was reiterated. With the right combination of complimentary laser and fluorescent substance, together with suitably sensitive imaging or capturing apparatus, LIF is an effective technique for the measurement of dynamic film thicknesses. Pulsed lasers are essential for temporal measurement of dynamic or transient measurements. For the aims identified in the introduction, and the range of film thicknesses likely to be encountered in a FDU, LIF seems to be a suitable technique to investigate further.

To date, there have been no studies into film thickness measurement in a FDU. Research into this is advantageous because better understanding of lubricant flow patterns and movement through measurement of lubricant thicknesses, provides data that up to now has not been available. With a tool that can measure the amount of lubricant in key areas within a geared system housing, redirection and redistribution of lubricant can be investigated to create a more efficient system.

It is expected that as the fill volume rotational speed of the crown wheel increases, the measured lubricant thickness will decrease. It is also expected that as the fill volume increases, the measured lubricant thickness will also increase.

CHAPTER 3
INSTRUMENTATION

In this chapter each of the key instruments required for calibration and FDU lubricant thickness measurement are described. Their function and behaviour affect the output results and so it is necessary to analyse and better understand each component and its role within the system. As the laser has a direct impact on the emitted fluorescence, it is important to understand how it works and which features have the potential to affect fluorescence. The photomultiplier and data collection instruments have an impact on the way in which the fluorescence data is received and in turn interpreted, so it is crucial to understand their strengths, weaknesses and potential anomalies that may affect the output data.

3 Instrumentation

The instruments used in this work will affect the final output data and results, so it is important to consider their strengths and limitations, and to have a basic understanding of how they work. In this chapter the key instrumentation used for calibration and lubricant thickness measurement are described. The aim is to identify and highlight any significant characteristics that may affect the precision or accuracy of the final thickness measurements. Castrol SAF-XO is used as the lubricant in the FDU, and so all calibration and measurements are based on this fluid.

3.1 Laser fundamentals

The principles of lasers have been explained in many texts, including Yariv (Yariv, 1989) Wilson and Hawkes (Wilson and Hawkes, 1987), Silfvast (Silfvast, 2004.), Chartier (Chartier, 2005) and Das (Das, c1991.). A brief overview of how lasers work is taken from these texts.

3.1.1 Energy Levels & Population Inversion

To understand and visualise the complexity of a laser, assume an atom has 2 energy levels; E_1, the ground state and E_2, the upper energy level (Figure 3.1a). An atom generally exists in the ground state unless an external force acts upon it. If an atom absorbs a photon[2] through exposure to radiation (Figure 3.1b), the atom will become excited and will shift to the upper energy level E_2. After a certain amount of time, the atom may emit a photon and return to its ground state spontaneously (Figure 3.1c). This is known as spontaneous emission.

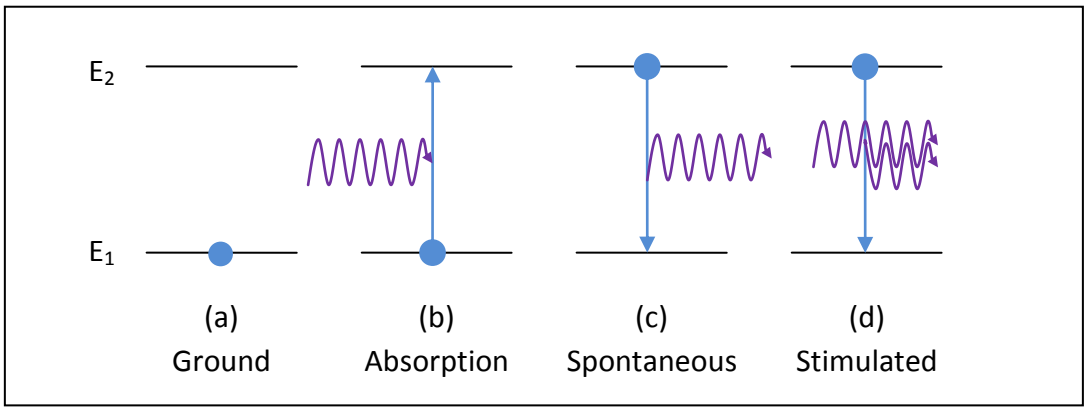

Figure 3.1 - 2-level energy diagram

[2] Often referred to as a packet or quantum of light, a photon is the smallest quantity in which electromagnetic radiation can be transmitted. Photons have no mass or charge.

If however, the emitted photon has the same energy (and therefore frequency) and polarisation as the stimulating photon, the emitted photon adds constructively to the incident photon and therefore increases its amplitude. This is known as stimulated emission, and is used in lasers to achieve light amplification by stimulated emission of radiation.

There is a far lower probability of achieving stimulated emission than spontaneous emission, but stimulated emission can be made more likely through the introduction of population inversion, which is a greater number of atoms in the upper energy level than in the ground state. To achieve this, the 2-level model is unsuitable because the probability for absorption and spontaneous emission is the same. Therefore multiple discrete energy levels are required to permit the inversion to occur. Consider a 3-level system as shown in Figure 3.2.

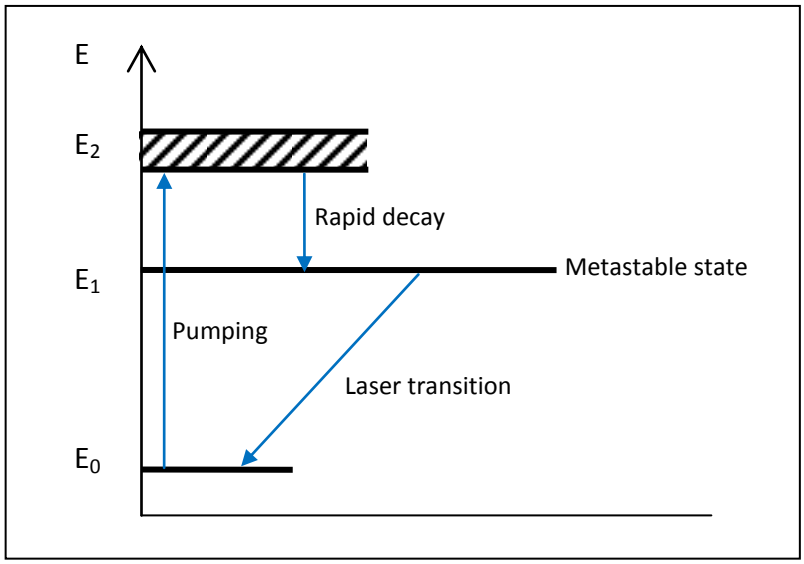

Figure 3.2 - 3-level energy diagram

Atoms in the ground state, E_0, are excited or pumped to the upper energy level, E_2, by absorption of radiation from an external source, such as a flash lamp. At the upper energy level, the atoms decay (dissipate energy) to an intermediate energy level E_1. If the number of atoms in the intermediate level is greater than the number in the ground state, population inversion has been reached. This is achieved through the rapid and usually non-radiative decay from the upper to the intermediate energy level and a metastable or long life time, intermediate energy level. As the atoms decay back to the ground state from E_1, photons are emitted. The photons emitted are coherent and in phase. This process forms the basis for laser emission.

3.1.2 Laser Types

Once photons are emitted within a laser medium, amplification occurs as the coherent light passes repeatedly through the gain medium between a mirror and a partially transmitting output coupler. Some of the light passes through the partially transmitting coupler to produce the output beam. The output beam of a laser is coherent, which means it consists of light of the same wavelength (monochromatic), direction and phase. However, lasers are not limited to emitting visible light: they can emit from deep infrared to ultraviolet (methanol lasers λ = 37-1224µm and F_2 excimer laser λ = 157nm (Weber, 1999)), as shown in Figure 3.3. In terms of fluorescence, this is useful as different substances are excited by different wavelengths of light. While there is generally a range of wavelengths that will excite a substance, there will be one that the molecules are more receptive to.

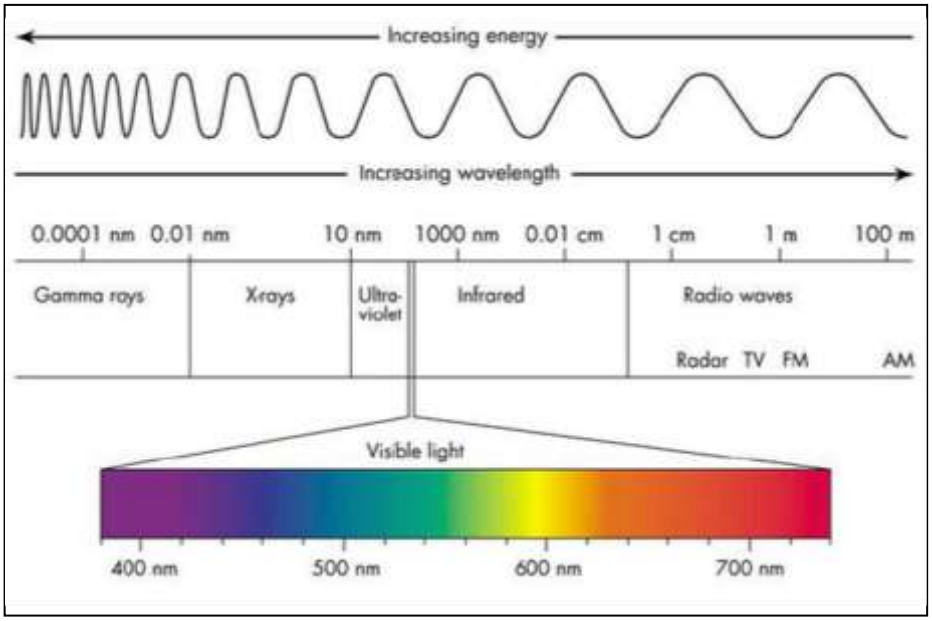

Figure 3.3 - Electromagnetic spectrum
(Kollewin Technology, 2003)

Lasers can be classified in a number of ways, for example, by mode of operation (pulsed or continuous wave, CW) or by element responsible for light amplification (gas, liquid or solid state). As the name suggests, a pulsed laser produces light in pulses while a CW laser produces a continuous beam. One advantage of a pulsed laser over a CW laser is that the pulses allow temporal measurements to be made of high speed activities, such as high speed flows. It is often possible to alter the pulse rate of the laser to suit the application. In addition, the energy within a pulsed laser is higher than a CW laser due to the short duration of the pulse. This can be particularly advantageous for LIF applications.

3.2 Nd:YAG Laser

The laser used for the experiments performed and described in this thesis was a Continuum Surelite II Nd:YAG laser, which is optically and thermally designed to pulse at 10Hz, with a pulse width of approximately 7ns (FWHM), and energy stability of ±3.5% pulse to pulse (Continuum, 2010). The laser is able to operate at other pulse rates, from 5Hz up to 12Hz, in 1Hz increments and can be externally triggered. The power had a tendency to shift over long periods, ±6% over an average of 8 hours with ΔT_{room} <±3°C according to manufacturer specification (Appendix 1).

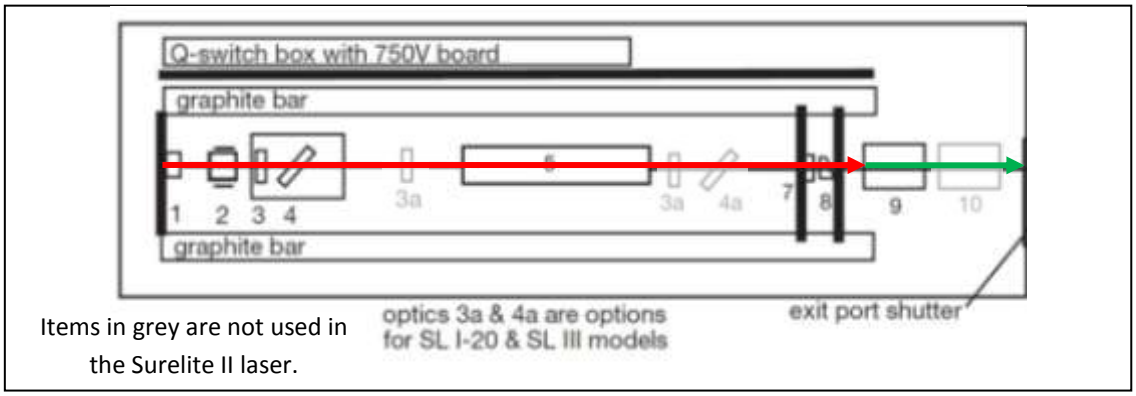

Figure 3.4 - Continuum Surelite II Nd:YAG laser layout (Continuum, 2002)

Table 3-1- Continuum Surelite II Nd:YAG laser components (Continuum, 2002)

No.	Name	Description
1	Rear mirror	Reflects light back towards the head
2	Pockels cell	The Pockels cell forms part of the Q-switch. The cell contains an opaque crystal which becomes optically clear once a voltage is applied.
3	Quarter wave (λ/4) plate	The λ/4 plate also forms part of the Q-switch. The plate rotates the polarisation of the incoming light and prevents laser fire until the Q-switch fires.
4	Dielectric polariser	The polariser forms the final optical component of the Q-switch. The polariser controls the polarisation of the transmitted light.
5	Head	The head houses a xenon flashlamp and a 115mm long, 6mm diameter YAG rod in close proximity. These are surrounded by a high brilliance diffuser. The flashlamp pulse has a FWHM duration of 200 microseconds.
6	Intra cavity shutter	Prevents the beam from exiting the housing
7	Gaussian mirror	The surface of these mirrors has a variable reflection coating to produce a low beam divergence.
8	Output coupler	Allows a portion of the light to pass out of the cavity to form the laser beam and reflects the remaining light back into the cavity.
9	Frequency doubler	The fundamental 1064nm beam passes through the harmonic generator and the resultant output beam has a wavelength of 532nm. The doubler unit is found at the end of the laser assembly, just before the beam leaves the laser housing.

The short pulses provide the possibility of temporal resolution of fast events such as high speed motion and fluorescence (Spectra-Physics, 2002)(Spectra-Physics, 2002)(Spectra-Physics, 2002)(Spectra-Physics, 2002)(Spectra-Physics, 2002), which is clearly significant for this research. The layout of the laser is shown in Figure 3.4, and Table 3-1 lists the laser components with a brief description of their function.

The laser power is controlled by the flashlamp. The higher the flashlamp discharge voltage, the greater the beam intensity. Control of the laser power is via the flashlamp setting on the laser control panel. It is important to point out at this stage that from this section and in the following chapters, reference will be made to the laser power however the value given in kilovolts is actually the flashlamp discharge voltage. This is discussed further in section 4.4.2.

The Q-switch is an electro-optic device which is used to control the laser pulse. Its optical part comprises a Pockels cell, λ/4 plate and a polariser. The electrical components comprise a timed pulse from the power unit, separate power for operation of the Pockels cell (Marx bank) and a 750V power board. The Q-switch allows the energy build up through maximum population inversion to be stored and released quickly in the form of a short, high intensity laser pulse.

Through frequency doubling, or second harmonic generation, the output wavelength of the Nd:YAG can be changed from 1064nm (infrared) to 532nm (green). The frequency doubling process for the Surelite II requires the fundamental 1064nm beam to pass through a potassium dideuterium phosphate (KD*P) crystal. The crystal's birefringence allows circularly polarised photon pairs to enter the crystal and combine. This is a non-linear effect. The results of the combinations are photons with double the input frequency, horizontal polarisation and a velocity equal to the initial photon pair. The frequency, polarisation and velocity of the combined photons ensure the conservation of energy, angular momentum and linear momentum respectively. The input photons must enter the crystal at a particular angle (known as the phase matched angle) in order for the photon combination to occur (Continuum, 2002).

Nd:YAG lasers are versatile tools that can be tuned to suit many situations through adjustment of the pulse rate or wavelength as described. This flexibility is desirable for many techniques, including LIF. If, however, the laser operates just above the lasing threshold, the output intensity fluctuates due to a lower population inversion. With fewer occupied high energy states the laser power becomes less stable. This can be overcome by designing a system that accepts the higher laser powers. With respect to LIF, a stable laser power is desirable because an unstable laser power can lead to instability in the fluorescence intensity.

3.2.1 Nd:YAG Energy Levels

In section 3.1.1, the principles of a 3-level energy system were discussed. Because 3-level systems require more than half of the atoms to be excited to achieve population inversion, the pumping must be very strong, making 3-level systems rather inefficient. Subsequently, the Nd:YAG uses the more efficient 4-level system.

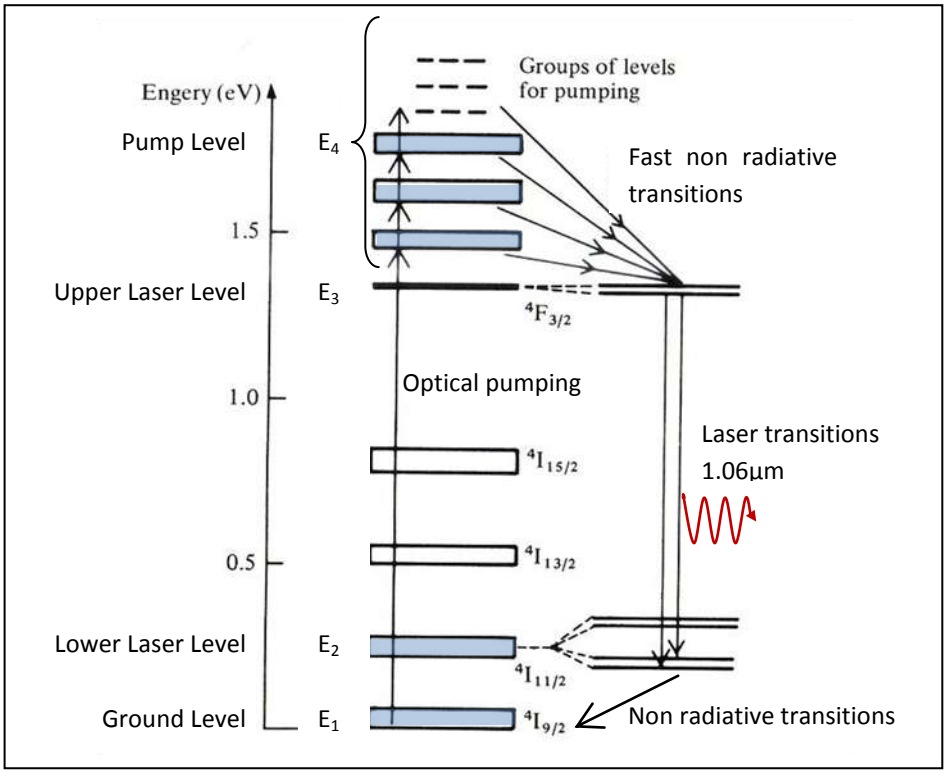

Figure 3.5 - Nd:YAG 4-level energy diagram (Willingale, 2007)

As with the 3-level system, an external source is required to pump the atoms from their ground state, E_1. However in a 4-level system (Figure 3.5), the atoms are excited to a pump level, E_4, where they decay rapidly to the upper laser level, E_3, via non-radiative decay. If the lifetime of the laser transition to the lower laser level, E_2, is long compared with the decay between levels E_4 and E_3, population inversion occurs. From E_2, the system decays rapidly back to the ground state, E_1, via non-radiative decay. The rapid decay from E_4 to E_3 and E_2 to E_1 results in a negligible population in levels E_4 and E_2, and a population inversion between E_3 and E_2. Compared with the 3-level system where half the atoms had to be excited, only a few atoms must be excited to achieve population inversion in a 4-level system, making them much more efficient.

3.2.2 Laser Modes and Bandwidth

Although we categorise lasers by their output wavelength, this is not entirely accurate as the light emitted is made up of many discrete wavelengths, which fall within a narrow band. This band is known as the frequency distribution or spectral density of a laser, and can be characterised in terms of its linewidth[3], which is the width (FWHM) of the frequency distribution (Figure 3.6). The discrete wavelengths or modes produced are a function of the laser cavity and through the use of a seeded laser, the range of frequency distribution can be reduced. The linewidths for an unseeded and seeded Nd:YAG are $1cm^{-1}$ and $0.005cm^{-1}$ respectively.

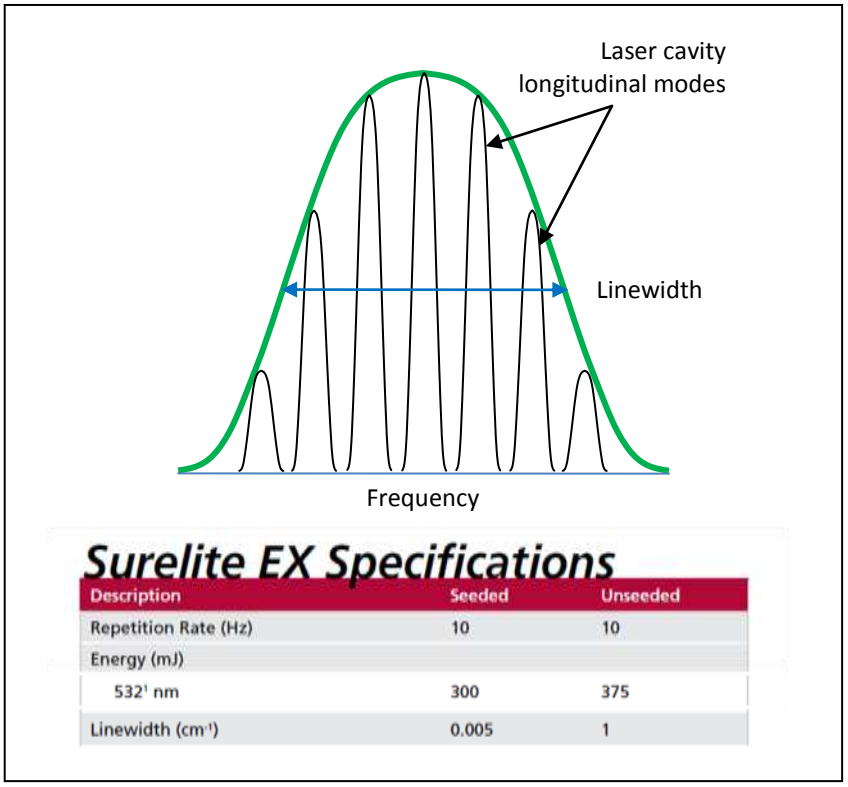

Surelite EX Specifications

Description	Seeded	Unseeded
Repetition Rate (Hz)	10	10
Energy (mJ)		
532[1] nm	300	375
Linewidth (cm^{-1})	0.005	1

Figure 3.6 – Linewidth
(Continuum, 2010; Continuum, 2002)

Seeded lasers achieve narrower frequency distributions through injection of another laser, a seed laser, into the resonator, which is then amplified. The seed laser is often a lower power continuous wave laser as it is easier to control features such as narrow linewidth by precise control of temperature (Paschotta, 10/12).

[3] Laser coherence falls into two parts; spatial and spectral. Spatial coherence is connected to beam divergence, while spectral coherence is linked with linewidth.

If the fluorophore within a substance is particularly sensitive to one specific mode within the linewidth on a laser, it stands to reason that as the modes shift within the laser linewidth that the energy to excite at the required wavelength will change, resulting in varying amounts of fluorescence from pulse to pulse. Although no literature has been found to support or disagree with this idea, it could be tested through the use of a seeded laser. If this theory is correct, comparison of a standard Nd:YAG laser and a seeded Nd:YAG laser would show that the results from the seeded Nd:YAG are more consistent. Attempts were made to source a seeded Nd:YAG for this experiment, but none were available. – See Section 4.4.4

3.3 Detectors

Light detectors are available for various applications and as such they vary greatly. In this research, photomultipliers were chosen for detecting the fluorescence from the lubricant due to their ability to detect low light levels. In this section, the principles behind photomultipliers will be discussed as well as some findings from data processing of the photomultiplier data.

3.3.1 Photomultipliers

Photomultipliers, or Photomultiplier Tubes, are optical devices which are used to detect photons, using the photoelectric effect. A photomultiplier is made up of a vacuum tube containing a photocathode, dynodes and an anode (Figure 3.7). When light enters a photomultiplier, electrons in the photocathode become excited and photoelectrons are ejected via the photoelectric effect. These ejected photoelectrons are focused towards the first dynode where a chain reaction of secondary emission begins, multiplying the number of photoelectrons at each dynode. The anode collects the photoelectrons at the end of the multiplication, and outputs a current. It is the multiplication of photoelectrons that allows even low light levels to be measured.

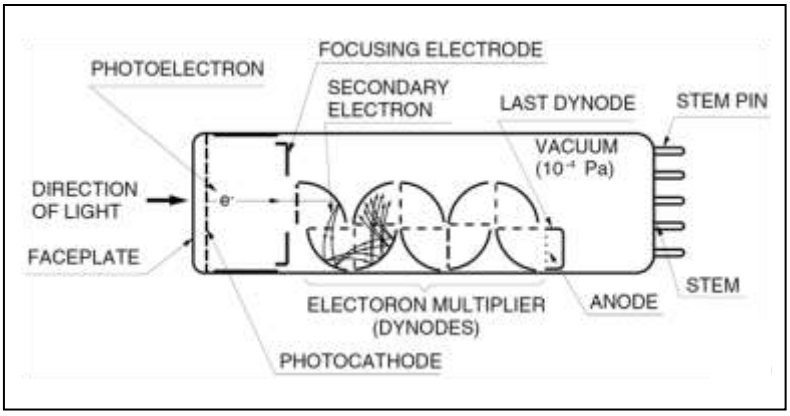

Figure 3.7 - Photomultiplier Tube (Hamamatsu Photonics, 2007)

For work described here, two Hamamatsu H6780-20 photomultipliers were used for monitoring of the laser power, and fluorescence measurement. This particular model was chosen as it has a spectral response from 300nm to 900nm, which covers both the 532nm of the laser and 650nm of the fluorescence, and is particularly sensitive to wavelengths between 500nm and 700nm. In addition, the H6780-20, metal channel photomultipliers have a high speed response, with a rise time of between 0.65ns and 1.5ns, and a fall time of 1-3ns.

In this research, two photomultipliers have been used during data collection. The first has been used to monitor the laser power fluctuations as any change in laser power

will have an effect on the fluorescence. This photomultiplier is referred to as the laser power photomultiplier from here on. The second photomultiplier has been used to measure the fluorescence intensity from the lubricant and is referred to as the fluorescence photomultiplier. The signals from both photomultipliers were required for data analysis and normalisation, which will be discussed in more detail later in this thesis.

3.3.2 High Speed Camera Imaging

A LaVision FlowMaster camera was used to visualise flow patterns and areas of interest within a clear-cased replica final drive unit. This replica contained the exact internal profile and details of the X150 FDU, but an idealised outer. By looking at the lubricant and gears together, it was possible to identify areas of high and low flow which could indicate areas where too much lubricant is present, thus causing excess churning; or areas where there is insufficient lubricant resulting in starvation. In addition to its use alone, the LaVision FlowMaster camera can be added to a number of systems, such as a spectrograph for measurement of electromagnetic radiation wavelengths. Both the flow visualisation and spectrograph measurements are discussed in more detail later in this thesis.

3.3.3 Fluorescence Wavelength Measurement Using Spectroscopy

When excited with 532nm light, the molecules of the fluorophore within Castrol SAF-XO emit light in the red portion of the visible spectrum. It is useful to know the exact wavelength of the emitted light was so that filters and other optical equipment, such as photomultipliers, could be chosen to suit. This section describes how the fluorescence wavelength from SAF-XO was identified.

One way to measure the wavelength of the emitted light is to use a spectrograph. A spectrograph (also known as a spectrometer, spectrophotometer or spectroscope) is a tool used to measure wavelengths from the electromagnetic spectrum. The components of a spectrograph include mirrors and a diffraction grating enclosed in a spectrometer housing with a small thin opening. A sensor or camera is usually found attached to analyse the received data. The spectrograph works by allowing a small amount of light into the housing, where it is passes through a diffraction grating. The diffraction grating separates the wavelengths of the incoming light in a similar way to a prism that separates the wavelengths of light into the visible spectrum. Certain spectrometers can be used to measure the discrete wavelengths or modes within a laser beam.

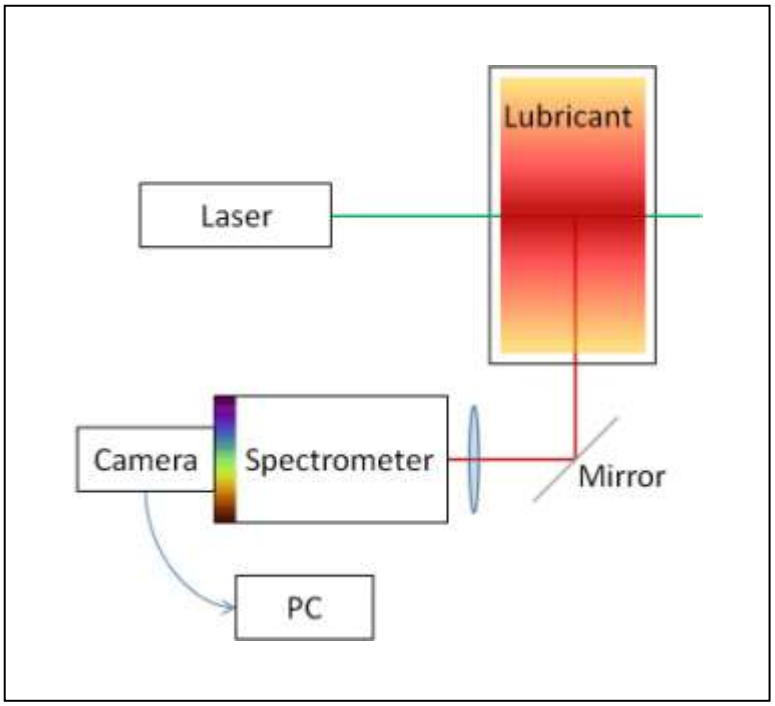

Figure 3.8 - Fluorescence wavelength measurement set-up

An Acton Research Corporation SpectraPro 275 (Figure 3.9) together with a FlowMaster camera, were used to measure the wavelength of the fluorescence emission from SAF-XO. A diagram of the set-up is shown in Figure 3.8. At any one time, the SpectraPro utilises 1 of 3 different gratings that are calibrated to measure different ranges of wavelength. For measurement of the fluorescence from SAF-XO, grating 3 with a groove density of 300g/mm (grooves per millimetre) was used as it allowed suitable coverage of the range taken up by the He-Ne lasers. The fluorescent light was captured by a 300mm focal length convex lens and directed into the spectrometer. The resultant image formed at the exit plane was captured by the FlowMaster camera.

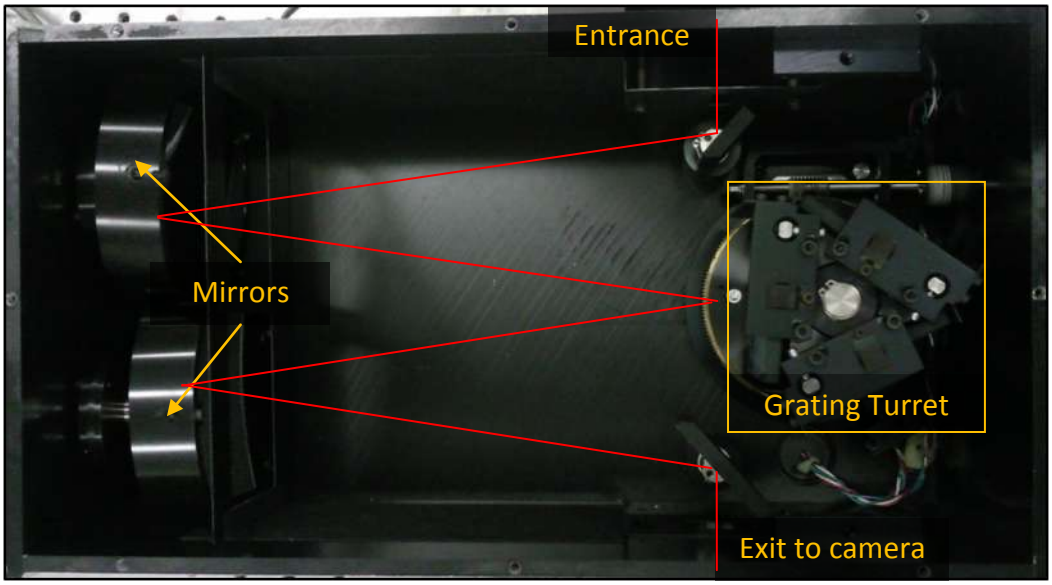

Figure 3.9 - Acton Research Corporation SpectraPro 275

The data from the collected light was transferred to a PC from the FlowMaster camera. These data were then analysed on a PC by pixel binning, which will be explained more in section 3.3.3.1. The option to use pixel binning is one of the advantages to using an ICCD camera, and can be used to increase the sensitivity of cameras by increasing the signal to noise.

3.3.3.1 Pixel Binning

The light received by the ICCD from two He-Ne lasers (543nm and 632.8nm) was spread across the camera chip, resulting in the spectral response shown inset in Figure 3.10. The two lines in the inset image clearly show the two different He-Ne wavelengths on a pixel scale. These data were binned, so that the data from each pixel in a column was transferred to a one pixel to give a single value, which was then plotted. The binned data, shown in Figure 3.10, were then used to calculate a nanometer scale for the fluorescence data. This will be discussed further in the next section. The 543nm and 632.8nm beams were directed along the same path as the Nd:YAG beam, serving as calibration wavelengths.

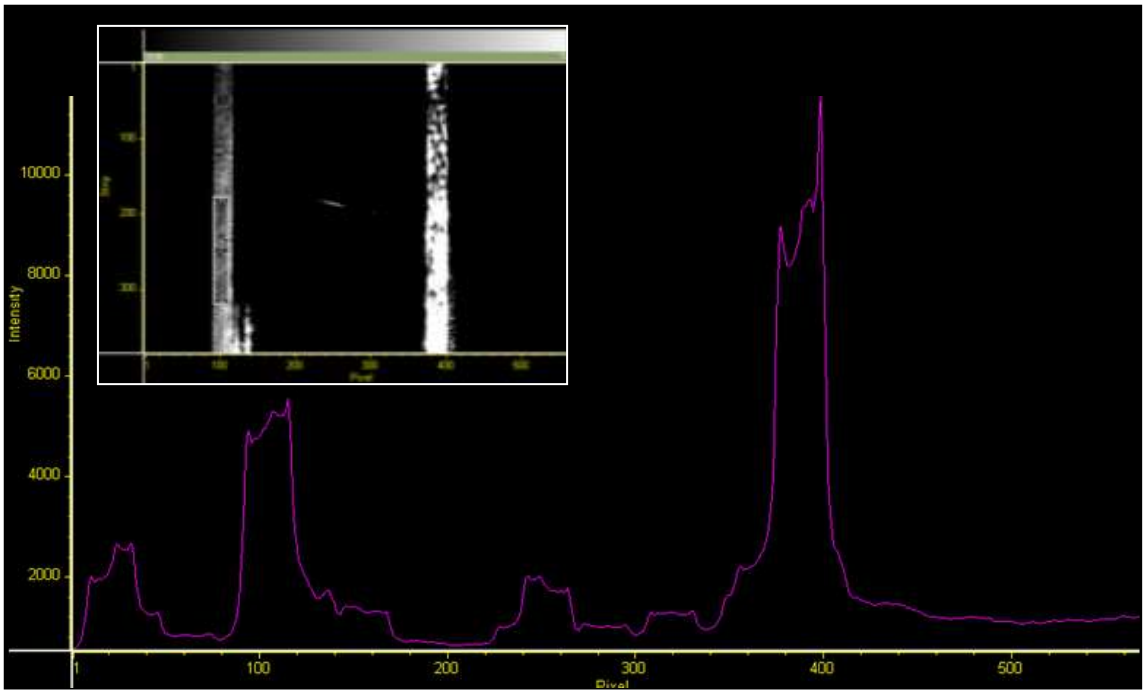

Figure 3.10 - PC view of spectrograph data (inset) and binned calibration data

Pixel binning was also carried out on the fluorescence data as shown in Figure 3.11. The obvious difference between the He-Ne lasers and fluorescence data is that the He-Ne lasers produced sharp spectral lines where the difference between the two wavelengths is clear. The fluorescence data has a broader distribution, suggesting the fluorescence emission is not at one discrete wavelength.

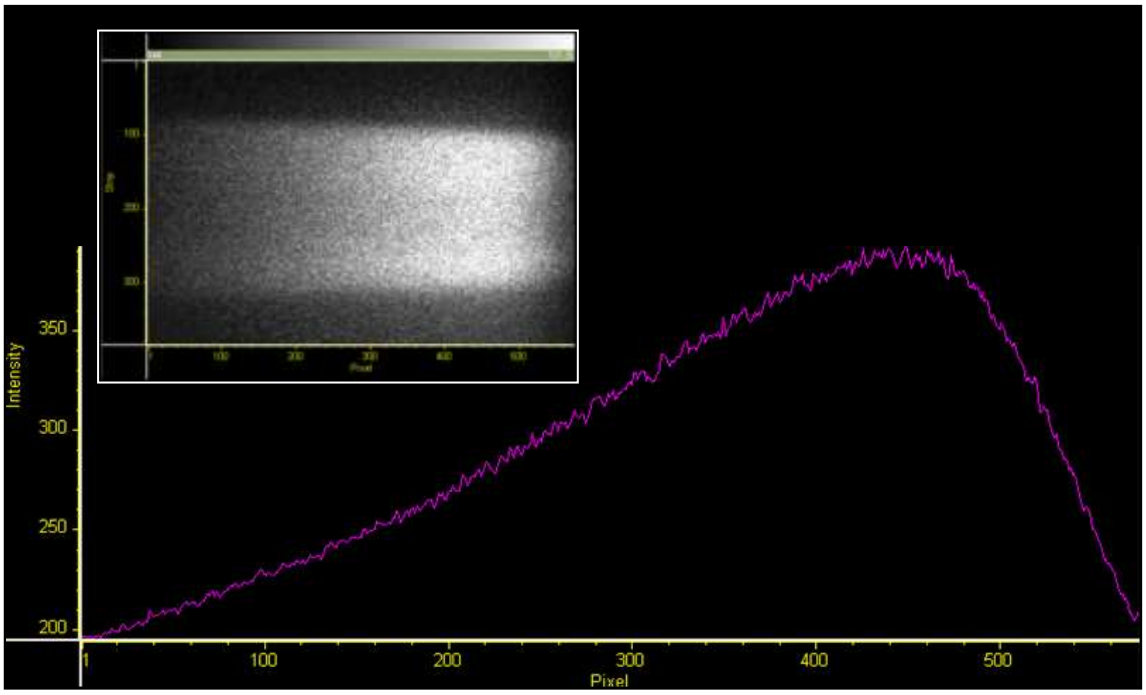

Figure 3.11 - PC view of spectrograph data (inset) and binned fluorescence data

3.3.3.2 Spectrometer Calibration Results

Using the binned data acquired from the He-Ne lasers of known wavelengths 543nm and 632.8nm, the pixel scale used for pixel binning was converted to a nanometre scale (Figure 3.12).

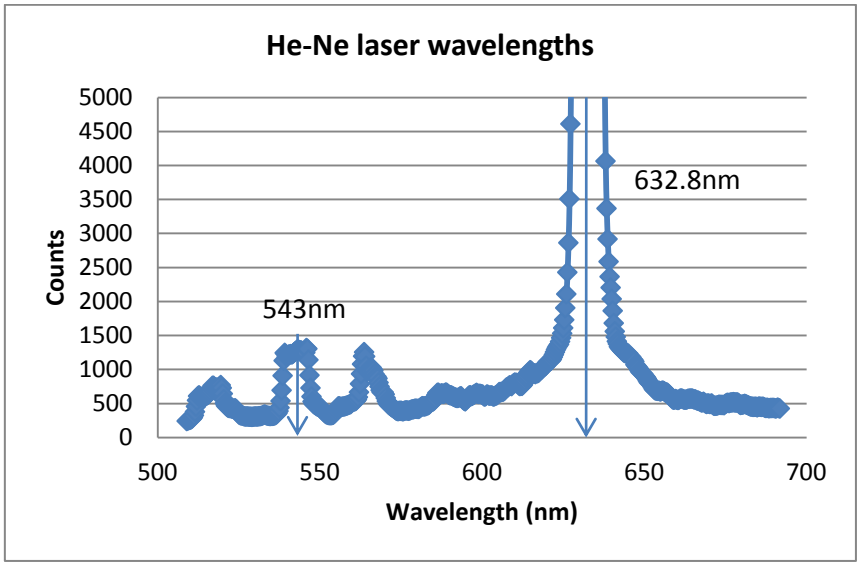

Figure 3.12 - He-Ne calibration wavelengths

Conversion of the fluorescence data from pixel to nanometre scale allowed the accurate determination of fluorescence wavelength from SAF-XO. The measured fluorescence wavelength from SAF-XO was found to cover a range of wavelengths, with the peak occurring at 650nm (Figure 3.13).

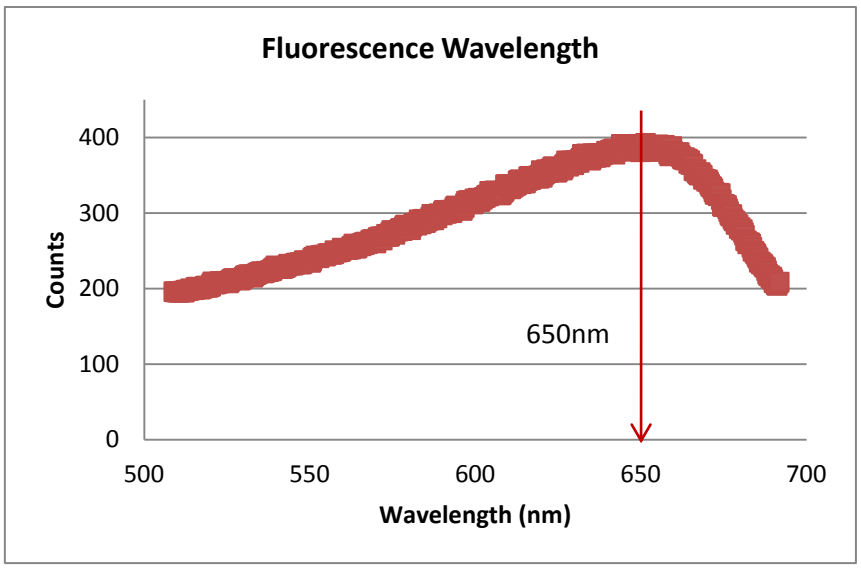

Figure 3.13 - Measured fluorescence wavelength

3.4 Data Collection Instrumentation

In this section, the data acquisition instrumentation will be discussed further and some calibration results will be given. The limitations of the instrumentation will be discussed in terms of sampling rate and resolution used, and how this will affect the final results.

3.4.1 High Resolution Data Collection

The National Instruments PXI5124 unit is a 12-bit analogue to digital converter; capable of taking data at a rate of 200MS/s. The number of samples per second and resolution are vital to attaining accurate and reliable results. (The number of samples taken depends on the amount of data required).

The fluorescence from four pulse events, recorded using 4000 samples at 200MS/s, are shown in Figure 3.14. The first thing to point out is that the peak voltage, which indicates peak fluorescence, is negative. This does not mean that the fluorescence is negative but simply that the instrument is set up to read the photomultiplier voltage as negative. All fluorescence and laser power data are measured this way and are referred to as positive in the text as it is the amplitude of the signal that is significant.

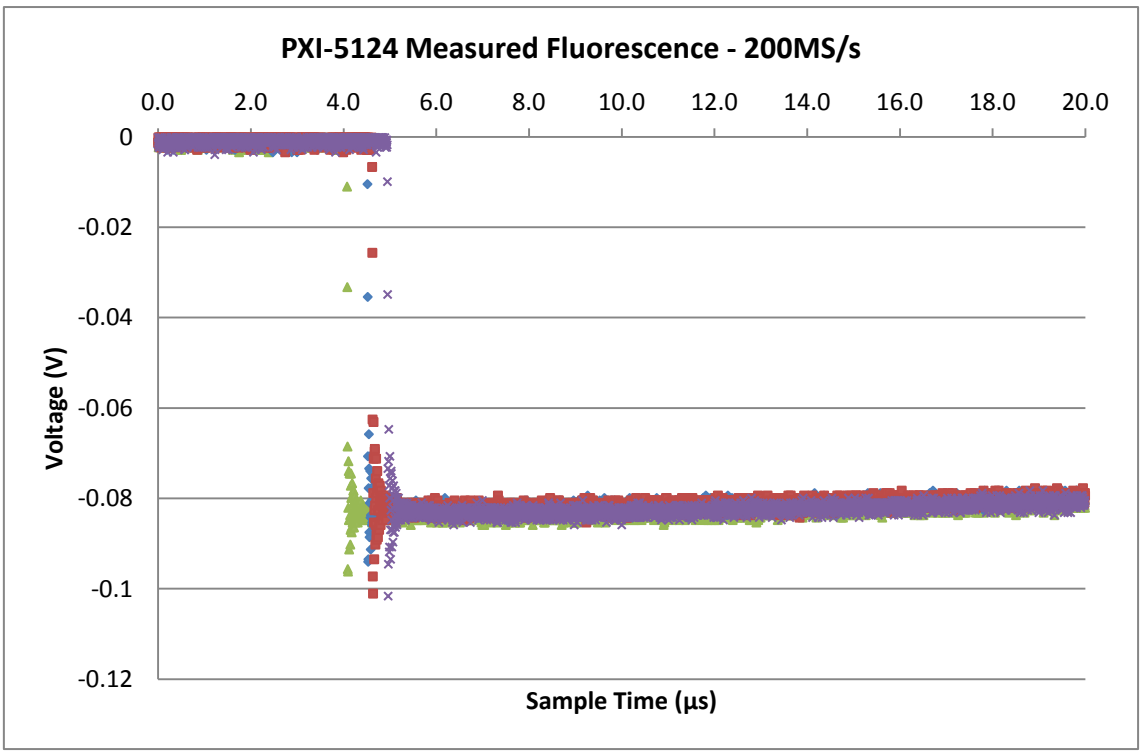

Figure 3.14 - PXI5124 Four Measured Fluorescence Traces at 200MS/s

The four recorded traces appear to oscillate around the peak amplitude of the signal before appearing to settle at approximately 0.08V. The signal oscillations are similar in

appearance to the response curve of an under-damped system as previously described. This response is the same for both the fluorescence and laser power photomultipliers. The signal does in fact tend back to zero, as shown in Figure 3.15, and does not settle at -0.082V. The tendency towards zero is not visible in Figure 3.14 due to the relatively small snapshot of time displayed.

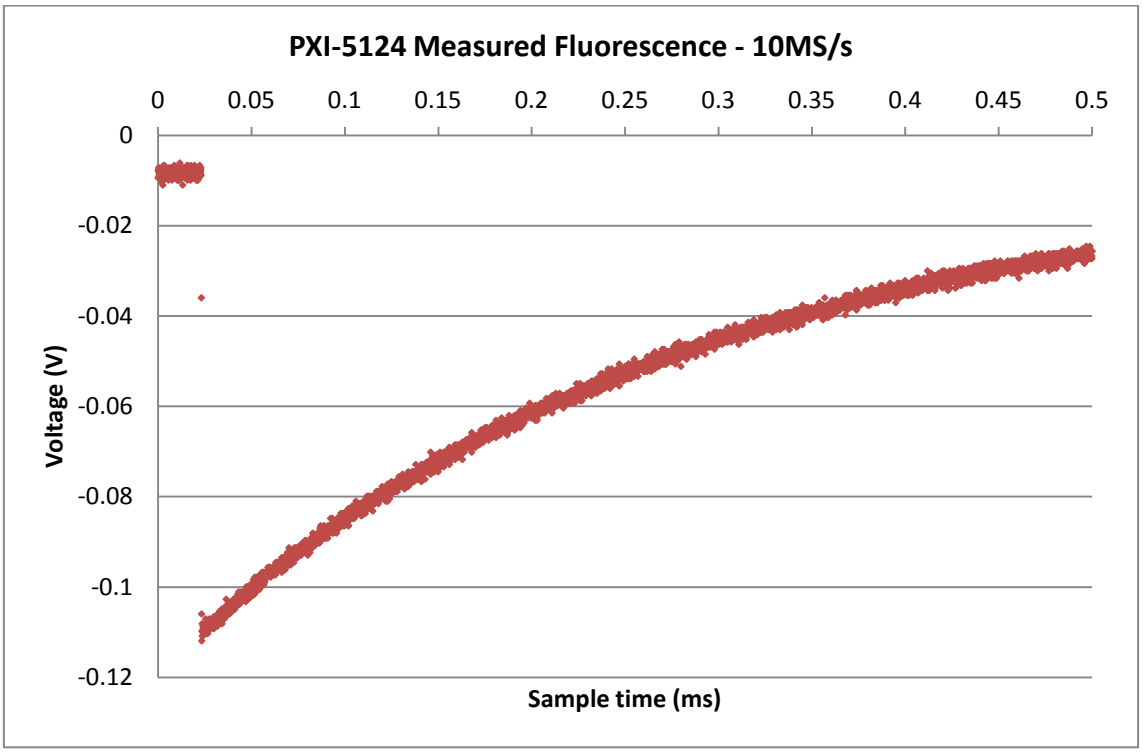

Figure 3.15 - PXI5124 Four Measured Fluorescence Trace at 10MS/s

On closer inspection of the oscillations (Figure 3.16), it can be seen that the peak amplitude of each curve is formed by only 6 sample points at 5ns apart. In order to be sure that the peak value was recorded, a higher sampling rate was necessary. At the 200MS/s sampling rate, there was the potential for the peak value to occur between the 5ns-spaced sample points. Missing the peak would give a false fluorescence magnitude. Increasing the number of data points collected would increase the chances of capturing the true peak fluorescence magnitude.

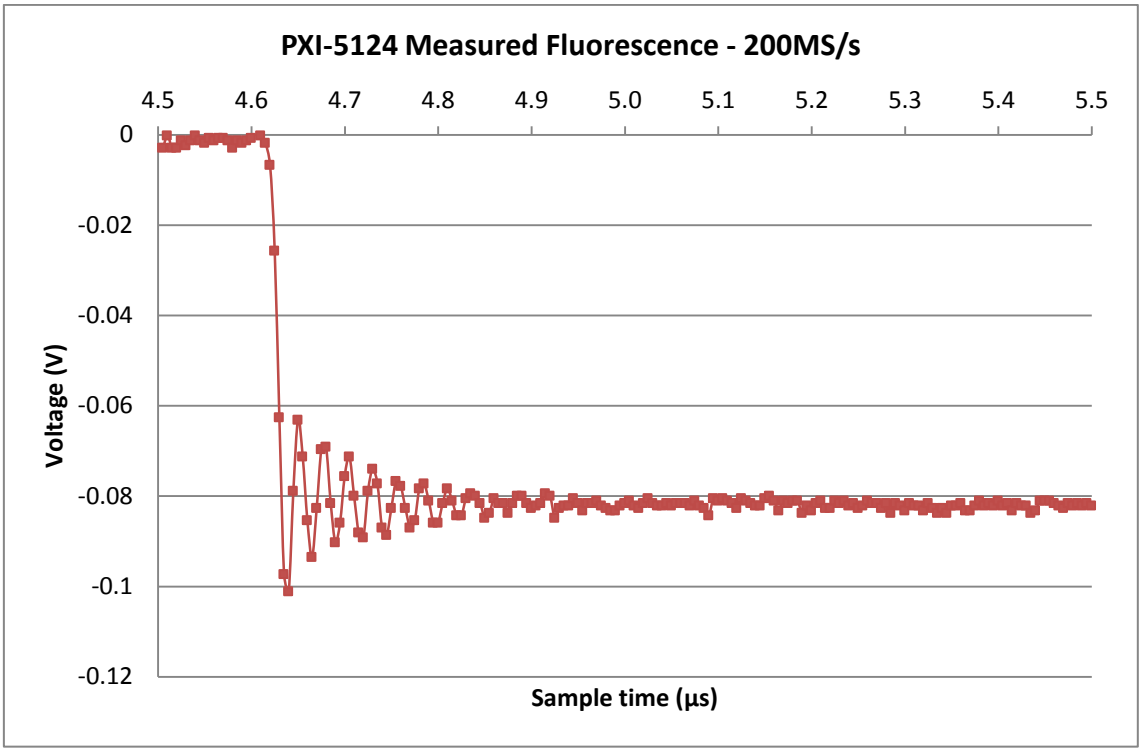

Figure 3.16 - PXI5124 Single Measured Fluorescence Trace at 200MS/s

Using the 200MS/s data for a range of lubricant thicknesses, a relationship between fluorescence and lubricant thickness can be seen. Figure 3.17 shows a plot of normalised fluorescence (fluorescence/laser power) against a range of lubricant thicknesses from 0.7mm up to 3.3mm. The amount of fluorescence measured increased with lubricant thickness; however the relationship was not strictly linear. If a straight line of best fit was forced through the data points, the line would not pass through the origin, implying that fluorescence occurs without lubricant present.

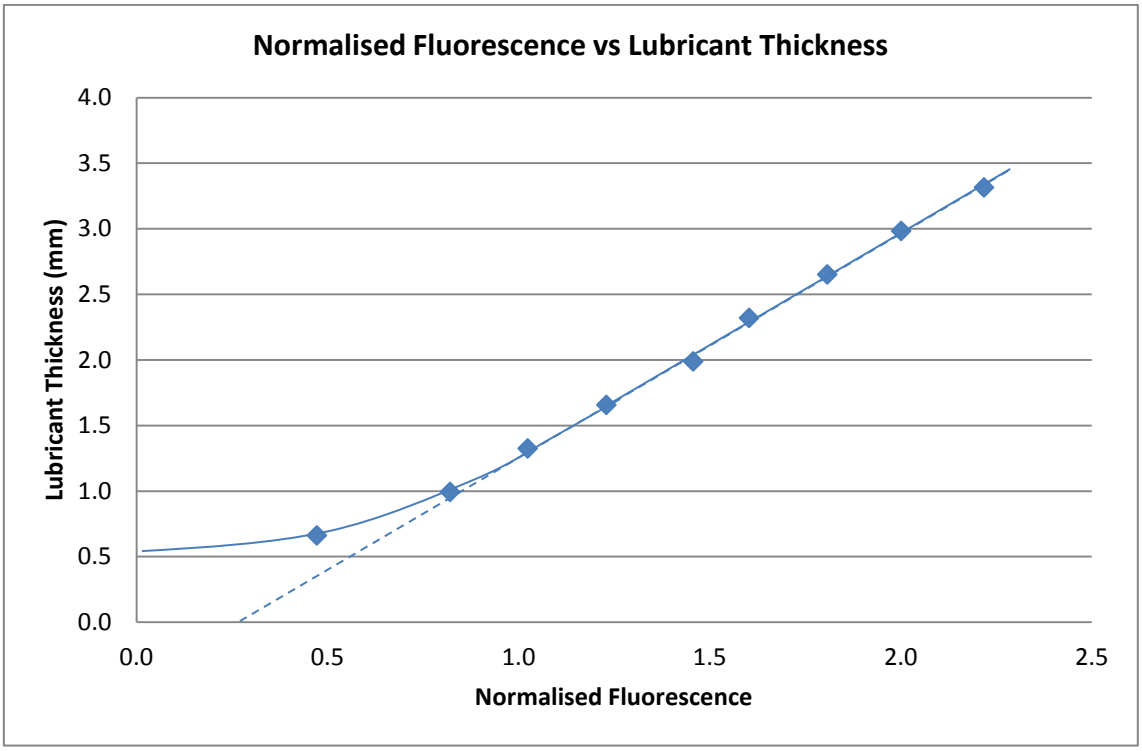

Figure 3.17 - 200MS/s Calibration Curve

As a precaution, tests were carried out to verify that there was no fluorescence from the glass that encased the lubricant. The results showed that the glass used did not fluoresce and so a linear relationship between fluorescence and lubricant thickness is not suitable. A curve however, would enable the relationship to show no fluorescence with no lubricant which is what was found experimentally, and still follow the measured data shown.

Testing for background fluorescence from casings, housings and surroundings in general was an important part of the experimental process to ensure that no external sources skewed data.

In summary, the 12-bit high resolution data acquisition hardware has shown that fluorescence measurements from a range of controlled lubricant thicknesses can be measured and shows a clear relationship between the two. The collected data however shows that the signal oscillates, and that these oscillations appear to be short in duration To be sure that the peak signal is measured, a higher sampling rate system was required. In the following section a higher speed acquisition system will be discussed; PXI5152.

3.4.2 High Speed Data Collection

PXI5152 is an 8-bit resolution, high speed acquisition card capable of taking data at 2GS/s from a single channel or 1GS/s from two channels simultaneously. This system is better suited to looking in depth at the oscillations seen in the data collected from PXI5124 due to the higher sampling rate.

In Figure 3.18 and Figure 3.19, a single measured signal response from the laser power and fluorescence photomultipliers are shown respectively. From these figures it is clear that the oscillations are much more clearly defined. Approximately 30 points are used to make up the first oscillation curve as compared with the 7 from the 200MS/s unit. Aside from the additional resolution, the curve shape is very similar to that from PXI5124.

While the first oscillation from the laser power response data repeatedly has the greatest magnitude, the same cannot be said for the fluorescence response data. When each set of fluorescence response data is examined individually, the magnitude of the second oscillation in the set is sometimes greater than the first. If the data is to be normalised to account for any laser power fluctuations, it is necessary to be consistent with the data analysis and therefore, only the magnitude of the first oscillation was considered from both the laser power and fluorescence photomultipliers.

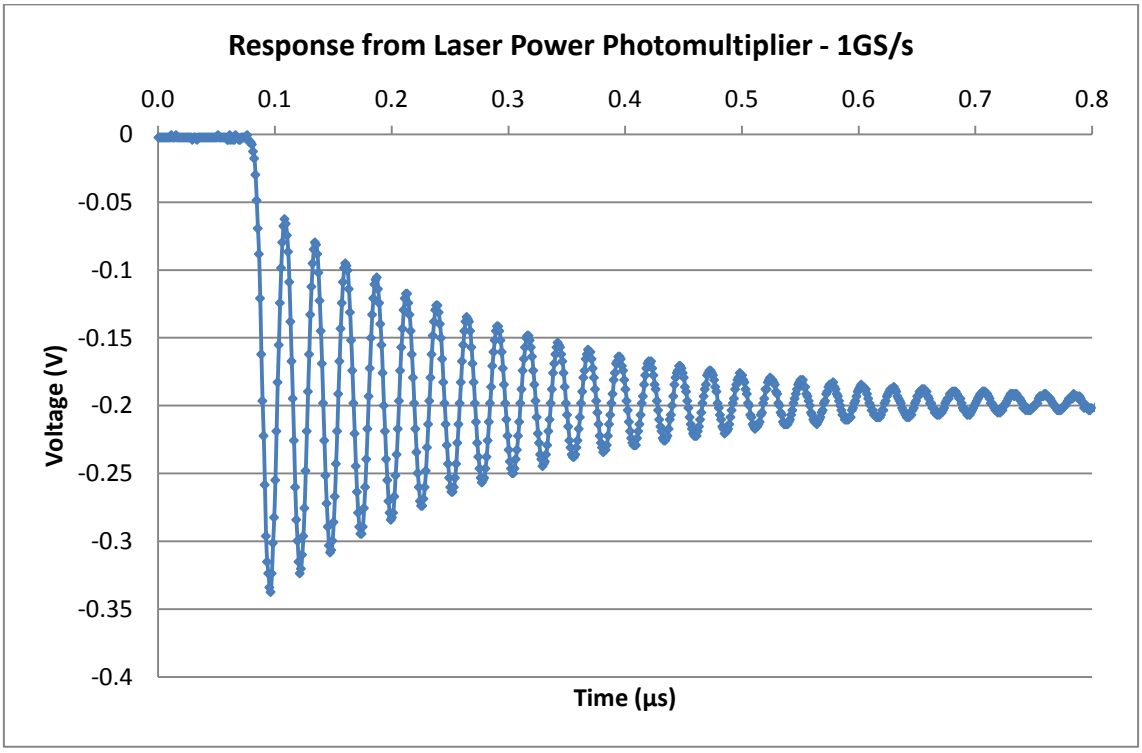

Figure 3.18 - Single pulse response curve from laser power PM at 1GS/s

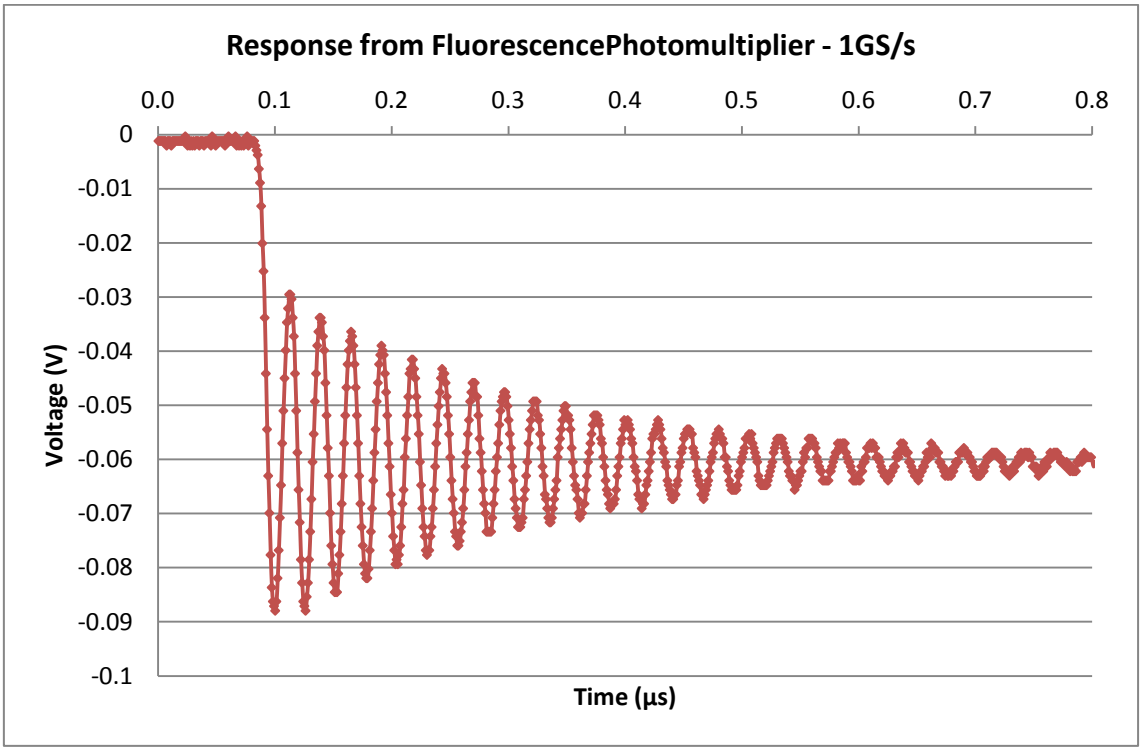

Figure 3.19 - Single pulse response curve from fluorescence PM at 1GS/s

In the same way as described before, 60 pulses of data were recorded and the peaks from the first oscillation were normalised before averaging the normalised data. This again gives a calibration curve that is intended to convert the fluorescence measurements from the FDU into lubricant thicknesses. Normalisation is discussed in more detail in a later chapter.

3.4.3 Resolution vs. Sampling Rate

Ideally for this research, a high speed (above 2GS/s) and high resolution (above 12-bit) system would be used. However, at the time of data collection, no such system was available. A choice had to be made between the sampling rate and resolution. The difference between an 8-bit and 12-bit resolution is not insignificant. Clearly the 4069 levels of a 12-bit system are favourable over the 256 of an 8-bit, but unless there is confidence that the correct point is captured, the high resolution is meaningless. It was felt that obtaining greater confidence in capturing the peak maximum was of higher importance than the resolution of that point. This is why the data collected and presented in the final chapters is acquired via PXI5152.

Table 3-2 - Sampling rate break-down

Sampling Rate	Time between samples (ns)	No. samples in 10ns
200MS/s	5	2
400MS/s	2.5	4
1GS/s	1	10
2GS/s	0.5	20

A breakdown of the significance of sampling rate is given in Table 3-2. The important thing to note is the number of samples in 10ns as this shows how many data points there were to capture the first oscillation from the photomultiplier. If there were insufficient data points to capture the first oscillation, the peak magnitude of the curve may be missed, resulting in inaccurate measurement of the lubricant thickness.

3.5 Summary of Chapter 3

In this chapter, description and discussion of the key equipment used for calibration and FDU lubricant thickness measurement has been carried out. Lasers have been discussed as adaptable, versatile tools that can be chosen to suit a wide variety of systems and applications. For the LIF technique used during the research discussed herein, the Nd:YAG laser was chosen for its pulse capability (from 5Hz up to 12Hz) and ability to excite the fluorophore within the SAF-XO lubricant.

Photomultipliers have been described as useful tools for detection of low level light, such as fluorescence, however preliminary data shows that the responses measured from both fluorescent and laser light are not as expected. The responses oscillate and are to be attributed to an instrument function. The key part of the signal is considered to be the peak of the first oscillation, which was found to increase with increasing lubricant thickness.

The wavelength of the fluorescence from the experimental lubricant, SAF-XO has been identified through spectroscopy as being a broadband fluorescence with a peak at 650nm. Knowledge of this allows selection of suitable optics for calibration and experimentation.

In the final section of this chapter, the advantages and disadvantages of two different data collection options have been considered. In the choice between high resolution and high sampling rate, it was decided that in this case, a higher sampling rate was preferred. As a result, National Instruments PXI-5124 was selected for its ability to capture data at a rate of 2GS/s, or 1GS/s per channel.

In the following chapter, the evolution of the experimental facility will be described in detail and will introduce the calibration wedge which is central to the calibration technique.

CHAPTER 4
METHODOLOGY

In this chapter, the development and evolution of the LIF lubricant thickness measurement technique and method are reviewed. The variability in the acquired data is discussed in terms of laser variability and the impact on the fluorescence data gathered. This chapter also discusses possible causes for the fluorescence variability and introduces the normalisation technique employed in an effort to reduce the fluorescence data dependence on laser power variability.

4 Methodology

In Chapter 2, LIF was identified as a suitable technique for measurement of film thicknesses due to the flexibility of the technique and ability for application without interrupting lubricant movement. Before applying the LIF based measurement technique to a geared system, the method and tools used need to be considered and tested. In this chapter, the validation experiment carried out to confirm the feasibility of the technique will be described, along with the development of the LIF calibration technique. While the instruments used during calibration and measurement of lubricant thicknesses have been discussed in the previous chapter, it is important to understand how the technique developed to incorporate these instruments. With each development, an increased understanding of the complexity of the task was achieved as well as improving accuracy of the data. Use of LIF thickness measurement for lubricants within geared systems is a novel application and so development and evolution of the method was a vital part of the process to achieve the measurements.

4.1 Calculation of Fluid Thicknesses

One of the aims of this research is to measure lubricant thicknesses. In a simplified situation, the thickness of a fluid running down a surface can be calculated using Middleman's equations below (4.1) and (4.2) (Middleman, 1998).

$$Q = \frac{\rho g W \delta^3}{3\mu} \tag{4.1}$$

Rearranging gives:

$$\delta = \sqrt[3]{\frac{3\mu Q}{\rho g W}} \tag{4.2}$$

Where:

Q	Volume flow rate	m^3/s
W	Width of plate covered with oil	m
δ	Film thickness	m
μ	Viscosity of oil	kg/m s
ρ	Density of oil	kg/m^3
g	Acceleration due to gravity	m/s^2

From these equations, it can be seen that film thickness is a function of volume flow rate, viscosity and density of the fluid. These equations hold for steady state laminar flows with incompressible, isothermal Newtonian fluids. The assumption is made that the flow path is down a vertical surface and the surface finish is omitted.

Middleman's equation is unsuitable for calculating lubricant thicknesses in geared systems due to the complexity of the flow. However, this equation indicates that the faster the lubricant (or surface) is moving and the lower the viscosity, the thinner the lubricant will become. This is clearly a simplified situation, but the matter of speeds and viscosities still holds in more complex systems such as a FDU. In these more complex systems, the surfaces are non-uniform and the fluids are non-Newtonian. In addition, there can be multiple surfaces involved. At this point, it becomes increasingly difficult, and computationally expensive, to calculate thicknesses, so experimental observations and techniques for measuring the areas of interest are needed.

In 2009, the current author (Fusco et al., 2009) began investigations into the behaviour of lubricants in geared systems. As a starting point to ascertain the feasibility of measuring lubricant thicknesses using LIF, a preliminary investigation was carried out. It was found that observations of fluorescence were noticeably different between relatively thick and thin films produced by running oil down a vertical surface. An overview of this research is given in section 4.2. The research by Fusco *et al.* was presented at the Magna 4X4 Conference 2009 in Graz, and marks the beginning of the experimental development of LIF based lubricant thickness measurements within the automotive final drive unit.

4.2 Validation of Measurement Concept

As a way to initiate lubricant measurements, a simple experiment was devised to demonstrate fluorescence from gear lubricants, which involved flowing Castrol EPX 75W-80 gear oil down a vertical plate and exciting the flow using a 532nm pulsed Nd:YAG laser. This simple method served as a way to begin assessing fluorescence from oil films, and showed qualitatively that there was a noticeable increase in fluorescence with increasing film thickness. The variation in fluorescence was observed between full flow and the remaining residue on the plate. Although this method was not able to produce quantitative results, it confirmed that the lubricant was naturally fluorescent after laser excitation and that a relationship between oil film thickness and fluorescence exists. Initially, the observations made were visual only, but the method was then expanded to incorporate quantitative measurement.

Figure 4.1 - Validation experiment set-up

Figure 4.1 shows the set-up of the preliminary experiment. Castrol EPX 75W-80 differential oil was pumped to the top section of a mild steel plate and allowed to flow from the top section, down the vertical section, and into a reservoir for recirculation. A mild steel plate was used as it was an inexpensive and uncomplicated way of assessing the feasibility of measuring the fluorescence of the differential oil. The oil was excited on the vertical section with a pulsed 532nm Continuum Surelite Nd:YAG laser and the fluorescence was imaged by a Princeton Instruments 576G/RB-E ICCD (intensified

charge-coupled device) camera, which was set at approximately 10 degrees to the beam. A 600nm long pass filter, placed between the camera and oil, ensured that the light captured by the camera was that of the fluorescence and not the incident 532nm laser.

The camera gate width and delay relative to the laser trigger were optimised and controlled using a Princeton Instruments Pg200 Pulse Generator so that the peak fluorescence intensity of each pulse was captured. A series of gate widths and delays were tested. A gate width of 1µs, with a delay of 180µs after the flash lamp trigger, was found to be most suitable. This suggests that the fluorescence lifetime is approximately 1µs. The fluorescence intensity data were then fed to a PC where an image of the fluorescence intensity was viewed and recorded. As there was a clear fluorescence signal from the oil, it was considered unnecessary to add a fluorescent marker at this stage, and it was assumed that the fluorophore was well mixed within the lubricant.

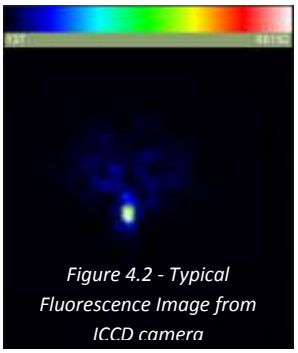

Figure 4.2 - Typical Fluorescence Image from ICCD camera

An example of the typical image created using the ICCD camera data can be seen in Figure 4.2. The intensity scale is shown at the top of the image, with white being the most intense. Viewing the excited region using Nd:YAG laser safety glasses allowed the fluorescence to be seen by eye.

Although it was possible to gather data from the lubricant on the plate using the camera, there was no way to relate the intensity counts back to a known thickness. One option was to use a travelling microscope to measure the thickness of the lubricant, but this was considered impractical. Another technique or solution was needed so that the thickness under observation could be measured or calculated separately. In order to verify the fluorescence noted, an alternative method based on a glass wedge was developed.

4.3 Development of Quantitative Thickness Measurement

A glass wedge was introduced to the experimental set up previously described to replace the vertical mild steel plate. This allowed control over the thickness of the observed lubricant. The thickness of lubricant at any point within the wedge could be calculated using simple geometry. The data for calculating the wedge dimensions can be found in Appendix 2. A diagram of the experiment lay out is shown in Figure 4.3.

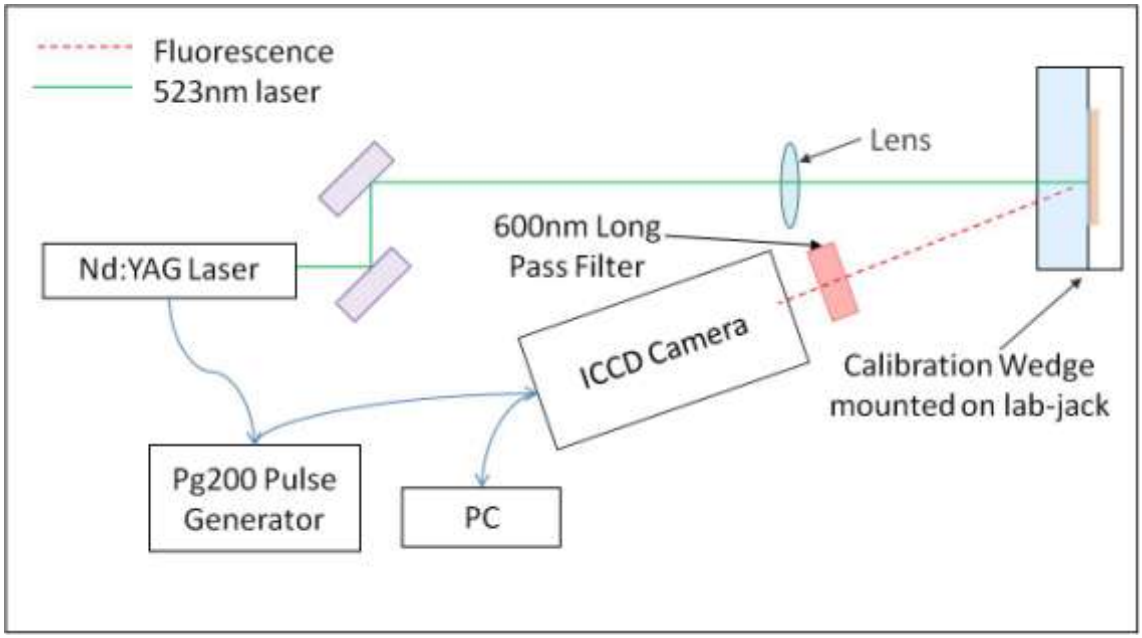

Figure 4.3 - Preliminary experiment set-up

Initially, the wedge was filled with lubricant and allowed to run empty while the maximum number of fluorescence counts were measured using the Princeton Instruments 576G/RB-E ICCD camera. This enabled a qualitative comparison to be made between the mild steel plate and glass wedge. Fluorescence intensity counts were measured at a fixed height in the wedge over 25 minutes in 5 minute intervals to assess the lubricant thickness change. The recorded data are presented in Figure 4.4, which shows that there is a reduction in fluorescence as the lubricant thickness reduced over time, as expected.

During the first 15 minutes, the lubricant thickness decreased steadily, showing that the lubricant was running off of the surface of the glass. After 15 minutes, the lubricant appeared to have reached a stable thickness, which would be consistent with a residual lubricant film on the surface of the glass. Although Figure 4.4 shows the trend of the lubricant thickness change, it does not give quantitative lubricant thickness measurements. To get real thickness data, a conversion between the counts of

fluorescence intensity and lubricant thickness must be obtained, and the wedge is the key to this conversion.

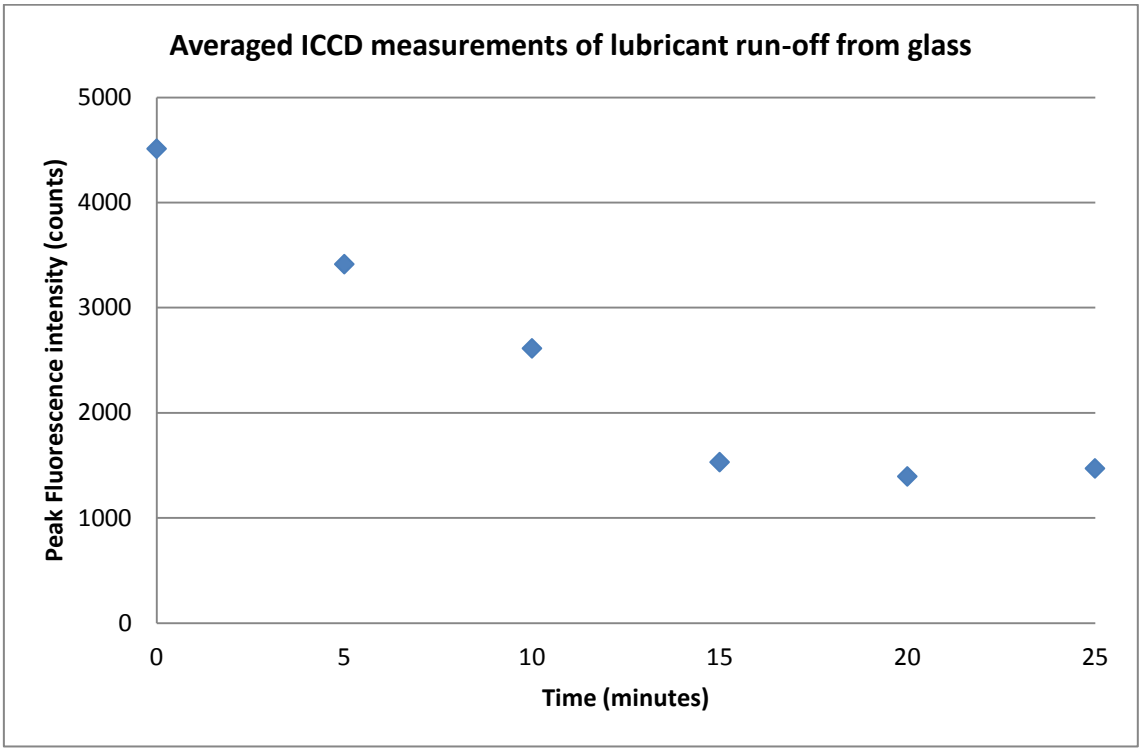

Figure 4.4 - Validation experiment results

By taking fluorescence measurements at 10mm intervals from the bottom to the top of the lubricant filled wedge, a conversion or calibration graph was produced (Figure 4.5). The data gathered at each increment gave a fluorescence that could be related back to a known lubricant thickness. The data from each of the points was combined to produce the graph, which was then used to translate the fluorescence intensity data into lubricant thickness. This forms the basis of the calibration method which will be described in more detail later in this thesis.

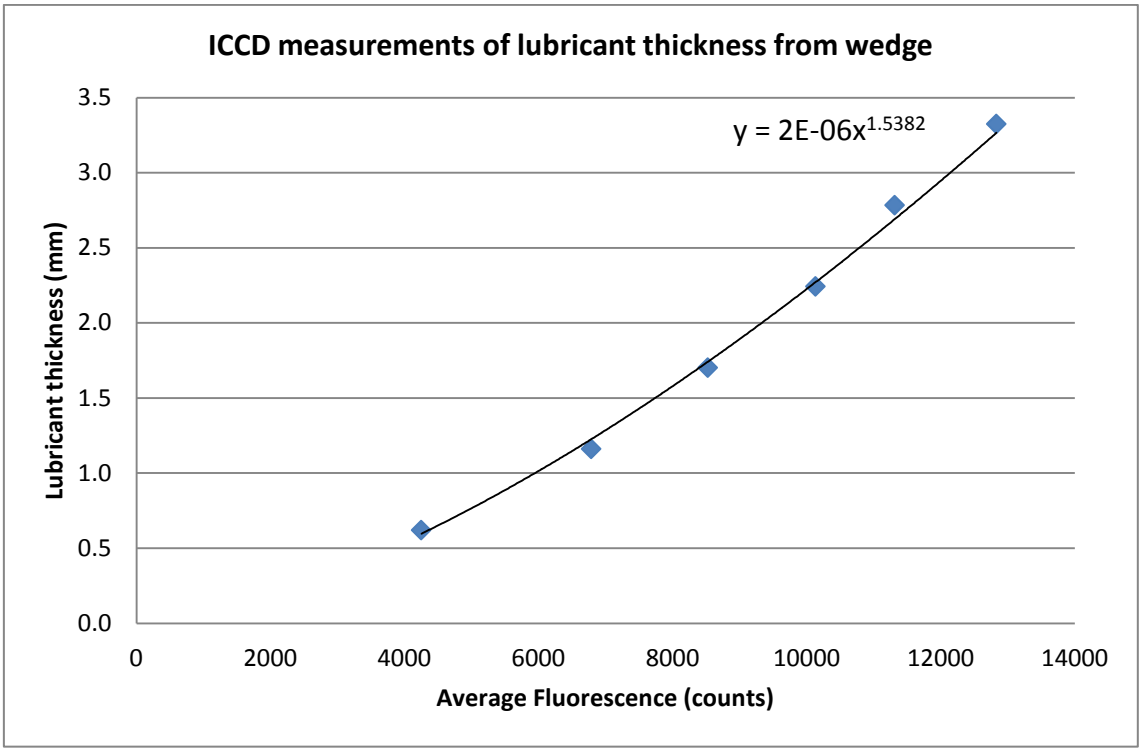

Figure 4.5 - ICCD counts to lubricant thickness conversion

4.3.1 An Overview of Experimental Developments

Up to this point, the peak intensity data from the 576G/RB-E camera were taken manually from the intensity image on the PC. While this was acceptable for proof of concept, this was considered unacceptable and impractical for measurement of lubricant thicknesses within geared systems. As a result, it was decided that the ICCD camera should be replaced with photomultipliers as they are known to have a linear response to light intensity where ICCDs do not, and multiple sets of data could be recorded at once. As discussed in Section 3.3.1, the additional benefit with photomultipliers is their ability to measure very low intensity light which would be expected from thin films.

To begin with, a single photomultiplier was used to measure the fluorescence. This was connected to a Tektronix TDS1012 oscilloscope where the fluorescence intensity was captured and recorded. It quickly became apparent through variation in the signal that there were variations in the laser power, and so an additional photomultiplier was introduced to monitor the laser power fluctuations. Any increase in laser power for a given thickness could result in an increased amount of fluorescence, suggesting a thicker lubricant film than actually present. The data from both photomultipliers were transferred via the oscilloscope on-board SD memory card to the PC for analysis.

To automate data capture and recording, the Tektronix oscilloscope was replaced with a National Instruments (NI) USB5133 (8-bit, 100MS/s) unit, which translated and transferred the signal from the photomultipliers directly to a PC. The USB5133 could be controlled via National Instruments LabVIEW, where the number of data samples, resolution and post processing of the data could be pre-programmed. A comparison of the data collected from the Tektronix oscilloscope and USB5133 was made and the results showed that over the same range of thicknesses, the two different units produced very similar results (Figure 4.6).

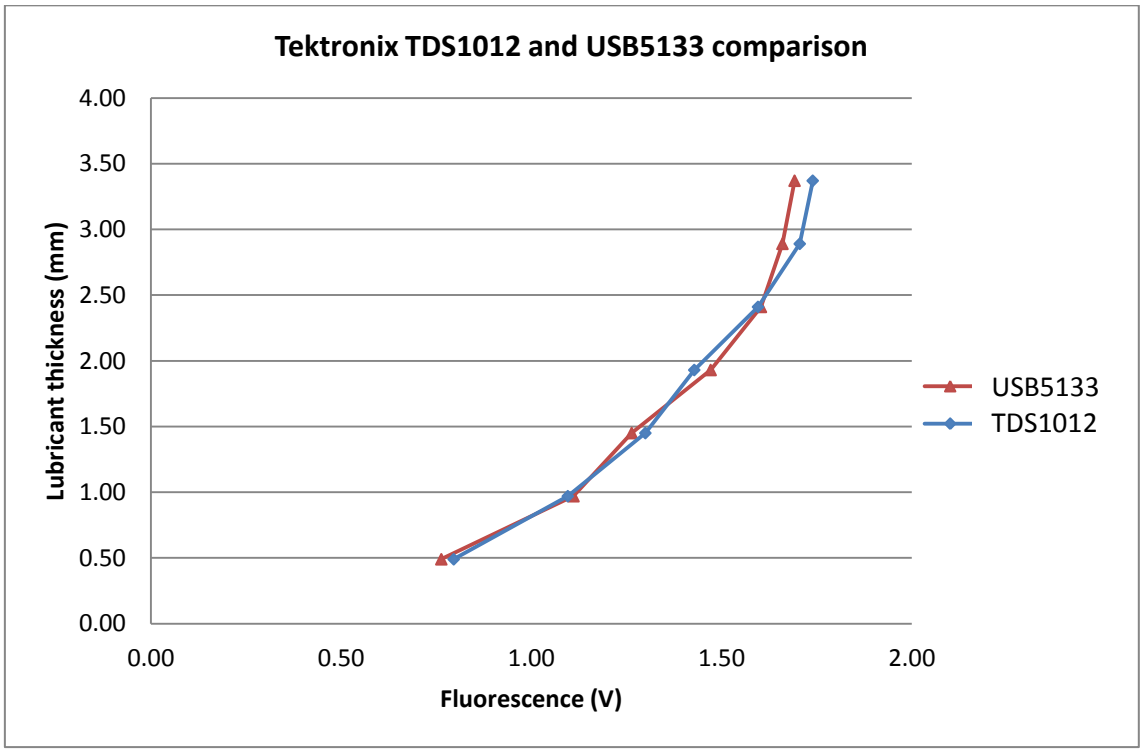

Figure 4.6 - Tektronix TDS1012 and USB5133 comparison

Subsequent changes to the data gathering equipment included the upgrade from NI USB5133 to NI PXI5124 and from NI PXI5124 to NI PXI 5152, resulting in a more accurate measurement of the peak fluorescence intensity as discussed in Section 3.4.

4.3.1.1 Instrument Function

During set-up of the photomultipliers, it was noted that the recorded fluorescence response duration was the same as that of the laser power, which was unexpected. The duration of the laser pulse, approximately 7ns, should be obviously different from the measured fluorescence response of the order of 1µs. As the chosen photomultipliers have a fast rise and fall time, measurement of the laser power and fluorescence signals should be well within their capability. Assuming the response from

both the laser power and fluorescence photomultipliers is a Gaussian curve[4], the expected response times (not signal amplitudes) should resemble the plot in Figure 4.7. A 10ns laser pulse is shown in green, and a 1µs fluorescence response shown in red.

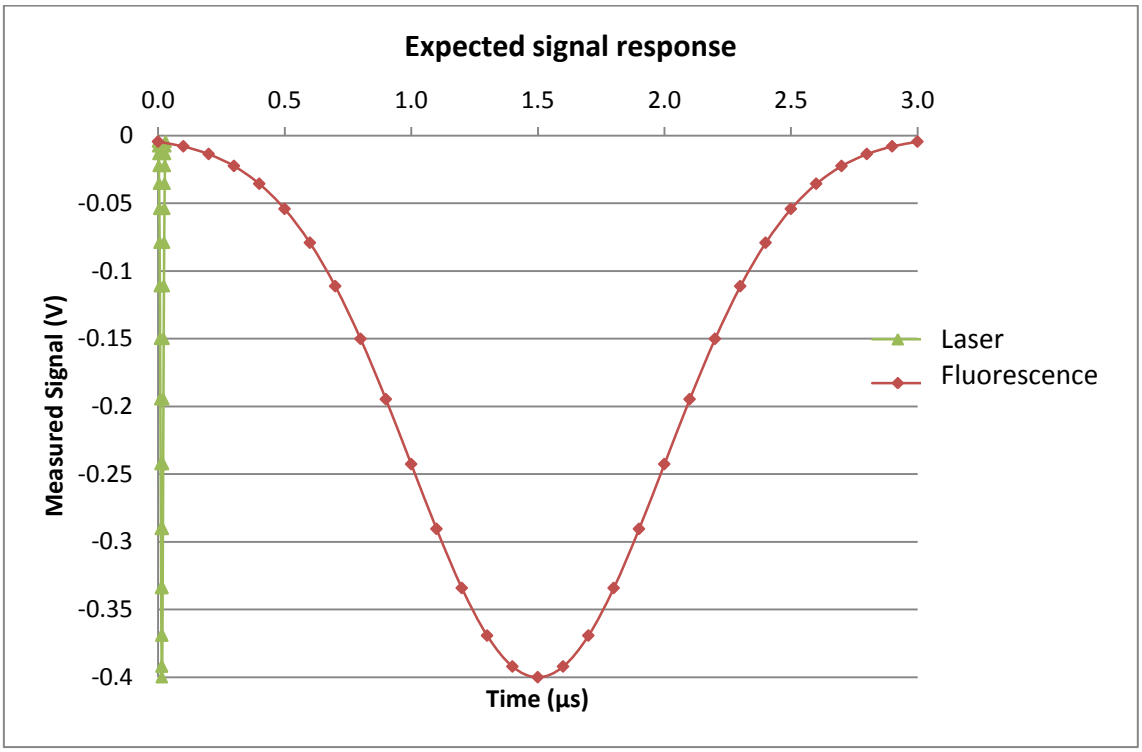

Figure 4.7 - Expected signal responses

However, the actual measured response would not be instantaneous due to the photomultiplier rise, fall and electron transit times (ETT), which must also be taken into account. The ETT is the time taken for the emitted photoelectrons to reach the anode and generally forms the largest delay between input photons and output data. A schematic of these timings are shown in Figure 4.8.

[4] The LIF signal will have a longer fall time (or tail) compared with the rise time, and the Gaussian curve is used for illustration purposes only.

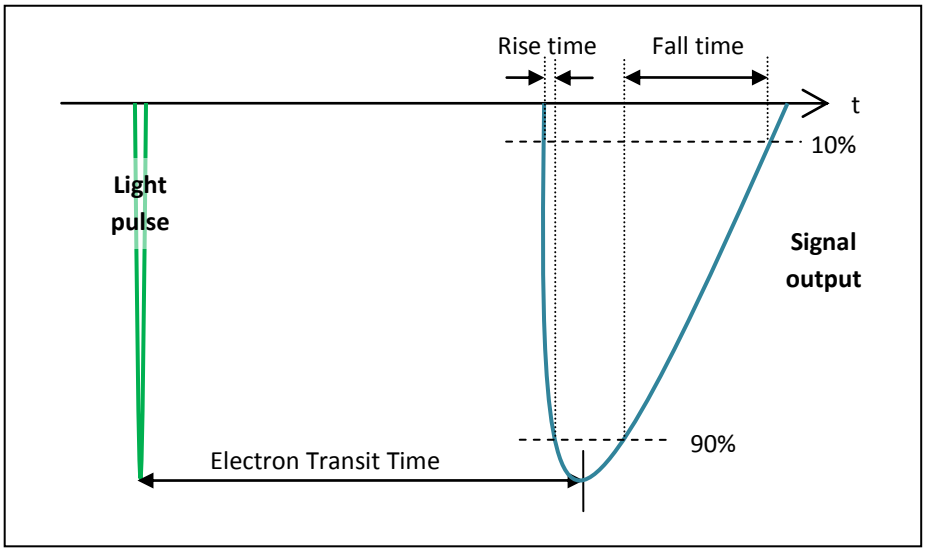

Figure 4.8 - Photomultiplier rise, fall and electron transit time schematic

For metal channel photomultipliers such as the H6780-20, the ETT is 4-9ns, and the rise and fall times are 0.65-1.5ns and 1-3ns respectively. So, at worst, the delay between input photons and output data would be approximately 13.5ns, which is longer than a single pulse from the Nd:YAG laser. This means that the laser pulse has finished before the signal from the photomultiplier can be output. The output signal for the fluorescence data however will overlap with the fluorescence photons being received as it is a much longer lived phenomenon, so the expected signal responses from both the laser power and fluorescence photomultipliers should still resemble those in Figure 4.7.

On examination of the real measured data however, the response curves look very different to what was anticipated (Figure 4.9). The response curves from both photomultipliers show oscillations which are similar in appearance to the response curve of an under-damped system. The FWHM value of the oscillations is approximately 12ns, which may be the sum of the laser pulse at 7ns (FWHM) and the ETT of 5ns, although this does not hold for the fluorescence which is longer lived. One hypothesis is that as both photomultiplier signals respond in a similar way, it suggests that some sort of instrument function is affecting the results. It is thought that as the oscillations repeat regularly up until they diminish, they may be attributed to electrons within the photomultiplier which bounce back and forth between the dynodes.

In order to identify the photomultipliers as the cause of the data oscillations, instead of a laser phenomenon which was carried through to the fluorescence, an alternate light source was used with the same photomultipliers. An EG&G Optoelectronics Machine Vision Strobe, capable of 50-60Hz and 100W, was used to produce a repeated pulse at

a frequency of 5Hz. 5Hz was selected to allow the photomultipliers additional settling time owing to the increase in pulse length of the flashlamp compared with the laser. (Increasing the pulse rate to 10Hz was later found to have no effect on the measured response.)

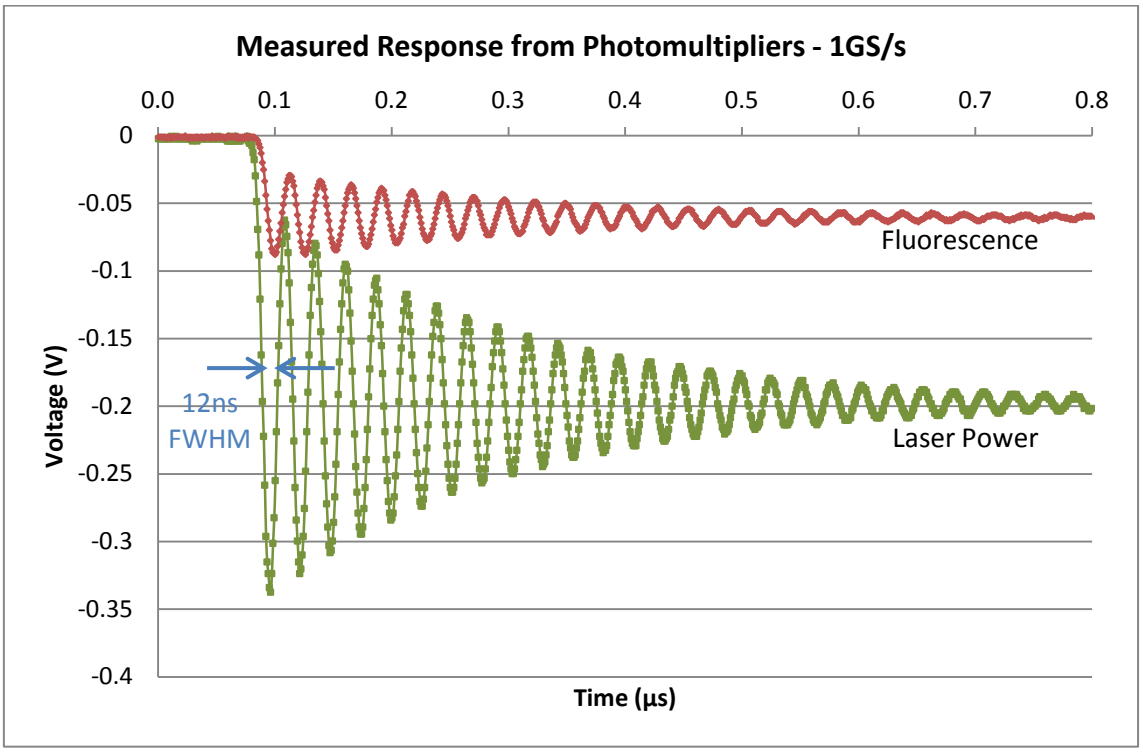

Figure 4.9 - Photomultiplier measured signal responses

This strobe, or flashlamp, produced broadband white light at an approximate pulse width of 2µs to 4µs, which is much longer than a laser pulse at 7ns. Data from 60 pulses was analysed and showed no sign of the oscillation, but a substantial difference between the flashlamp expected response in Figure 4.8 and the measured response was noted. An example of the measured data can be seen in Figure 4.10, where five consecutive pulse peaks are shown. Aside from a small amount of timing jitter, all five light pulses appear to show the same trace.

Instead of the expected 2-4µs FWHM curve, the measured response was greater than 60µs, with a relatively long fall time compared with its rise time. Due to the large amount of data necessary to view the full photomultiplier response from start to finish (from 0 intensity, through the peak and back to 0), enough data to show only the peak amplitude of the signal was captured at a sampling rate of 100MS/s. A higher sampling rate was preferred, however the massive increase in the amount of data produced at a higher sampling rate could not be stored in the processor memory. At 100MS/s, data were taken at 10ns intervals, so 50000 samples would capture 500µs of data. At 2GS/s,

data is taken at 0.5ns intervals, so 50000 samples would capture 25µs of data. A compromise between the number of samples, sampling rate, processor speed and memory capability was required.

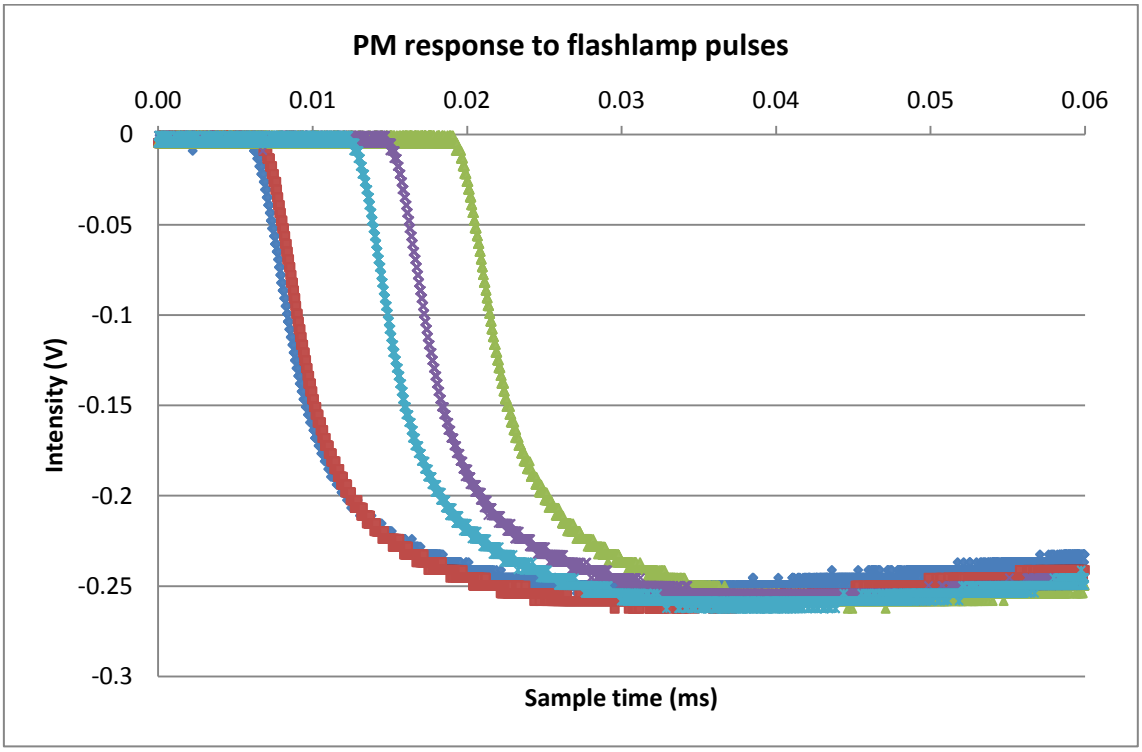

Figure 4.10 - Photomultiplier response to flashlamp pulses

Following an investigation by the manufacturer, the exact cause of the signal oscillations remained unknown. A number of tests were carried out to try to identify a fault with the photomultiplier or the system. The first test involved checking for 1064nm light bleeding through into the 532nm beam, but the 532nm beam was found to be clear of 1064nm radiation. The second test entailed operating the photomultipliers via alternative power supplies to see if the supply was faulty. With all three power supplies tested the oscillations from the laser were clear.

The third test involved removing all optics to identify if any of the lenses or filters were the cause of the oscillatory response, and again, the same response was noted with and without the optics. Finally, the system was checked for laser electrical interference which required running the laser without light emission and running the flashlamp instead. This also resulted in the same oscillatory response. All tests carried out indicated that the photomultipliers were working correctly.

Assuming both the photomultipliers and laser were all working correctly, and that none of the optics, filters or power supplies had an effect on the photomultiplier

response to the laser light, it is assumed that the oscillations visible in the data are a function of the system response to the short pulses of the laser (of the order of 7ns), as the oscillations are not present for pulses of the order of 2µs. Furthermore it is assumed that the fluorophore is evenly distributed through the lubricant.

Further to establishing the cause of the signal oscillation, an investigation into the elements within the signal was conducted to identify which would best show the relationship between lubricant thickness and fluorescence. There were two points within the data that seemed most suitable for using as the lubricant thickness measurement due to their repeatable presence within the measured signal. The first was the magnitude of the first oscillation and the second was the value at which the oscillations appeared to diminish, or settle to (Figure 4.11).

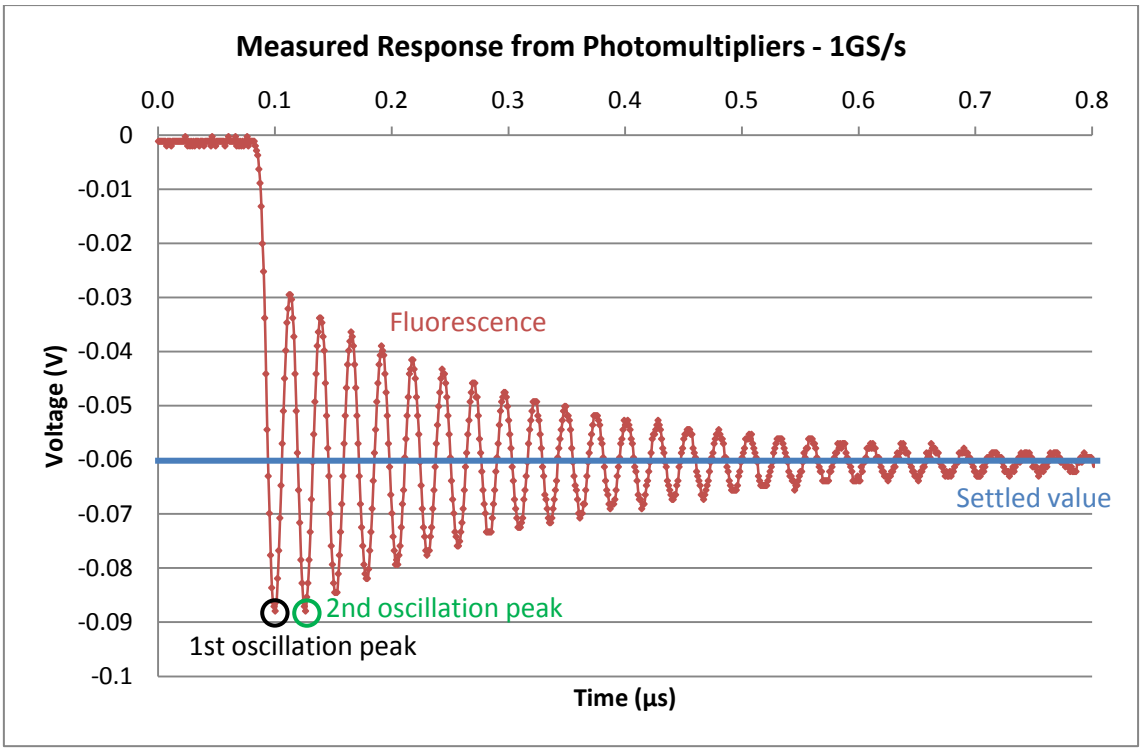

Figure 4.11 - Photomultiplier signal oscillations

Both the peak and settled values were measured and plotted against known lubricant thickness and it was found that the magnitude of the first oscillation increased with increasing lubricant thickness and tended towards zero with decreasing lubricant. The settled value also increased with lubricant thickness, but it was more difficult to distinguish between the different thicknesses measured due to the shallower gradient of the best-fit line. As a result of this, it was decided that the magnitude of the signal first peak oscillation would be used as the lubricant thickness indicator. Although the instrument function was convolved over the whole signal, the remainder of the trace

data after the peak was ignored. This was advantageous as it reduced the data that needed to be stored, and so enabled a faster data collection process.

4.3.2 On Axis Back Scatter Fluorescence Measurement

With the data acquisition hardware upgraded, the focus of the system amendments became the layout and optimisation of the optics used. All the data collected from use of the ICCD camera up to the photomultipliers, involved an off-axis layout of optics where the fluorescent light was received along a different path to the input light. The advantage of this was that expensive, specialised optics were not necessary. The disadvantage was that to switch the set-up between calibration and thickness measurement within the replica FDU, involved many changes in position and alignment, which had the potential to introduce errors.

To overcome this, an alternative alignment of optics was adopted in which the input 532nm and fluorescent 650nm light were able to follow the same path. A custom made broadband mirror with a central 8mm diameter clear glass opening was required. This new layout, shown in Figure 4.12, allowed measurements to be taken within the wedge for calibration and the replica FDU without rearranging the optics. All this could be achieved by simply inserting and removing a plain mirror at 45° to divert the laser towards the wedge rather than the replica FDU.

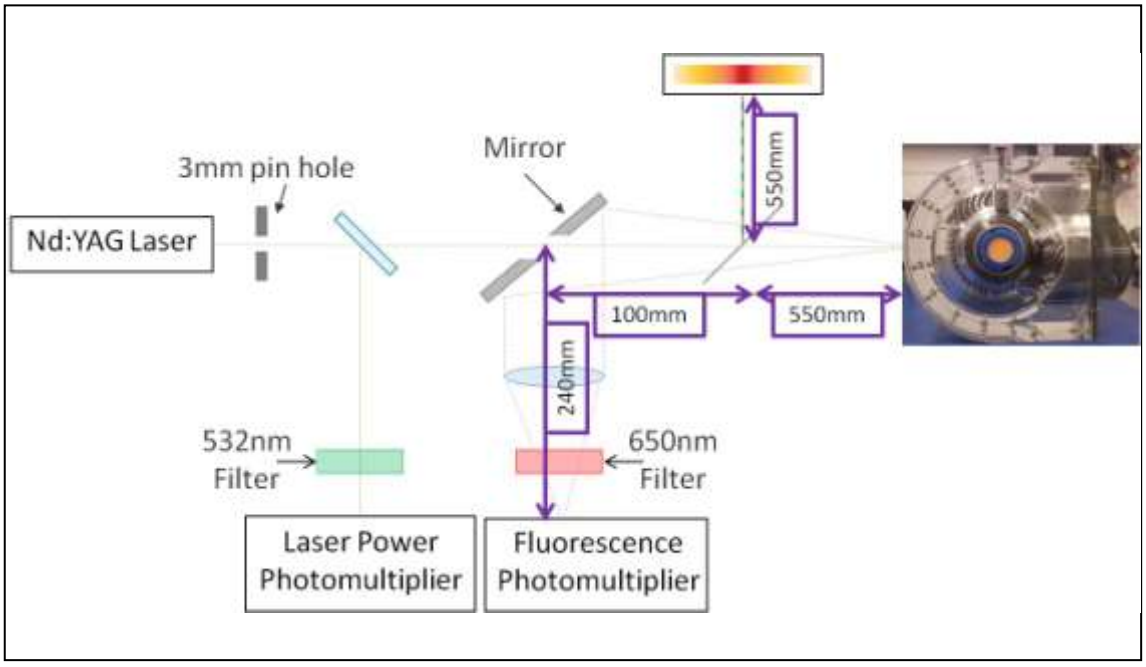

Figure 4.12 - Inline optical arrangement

While this layout should have produced a good optical set-up, and was the preferred way to deal with both the wedge and FDU with minimal changes, it was noted that the

substrate at the centre of the specialist mirror fluoresced as the laser passed through. Furthermore, the clear replica FDU casing was also found to fluoresce. Steps were taken to create a background fluorescence reading and an attempt was made to simply remove this from the measured fluorescence data. However, the intensity of the fluorescence from the housing was too great in comparison with that from the lubricant.

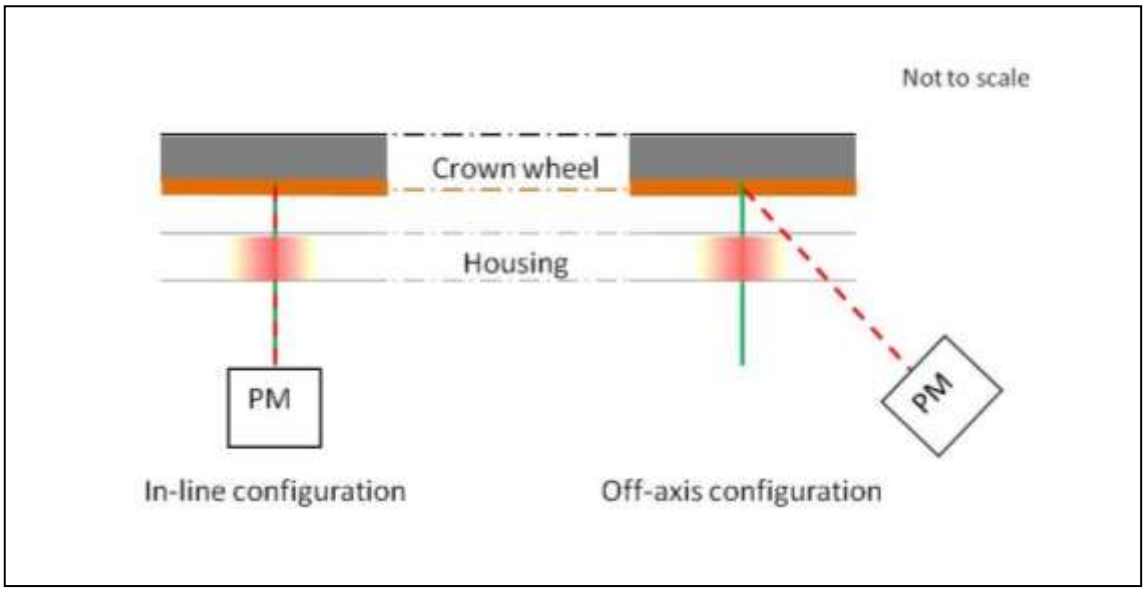

Figure 4.13 - In-line vs. off- axis apparatus layout

As a result of this, the optical layout was returned to the original off-axis configuration as it removed the requirement for a specialist mirror altogether and avoided the fluorescence from the casing. Figure 4.13 shows a schematic of the light paths, housing and photomultipliers in the in-line and off-axis layouts. From this it can be seen that in the off-axis configuration, the fluorescent light bypasses the majority of the fluorescence from the casing, the remainder of which can then be removed using a background correction factor.

4.4 Fluorescence Signal Variation

The irregularity of the fluorescence signal, and its dependence on the laser power, has been referred to a number of times in this thesis. There is a need to understand and correct for this irregular behaviour. In this section, the possible causes of the fluorescence irregularity are discussed and potential corrections are considered.

4.4.1 Laser Power Variability

It is crucial to understand the relationship between laser power and fluorescence; if the laser power increases or fluctuates, the fluorescence increases or fluctuates. Awareness of the connection between the two is vital for the fluorescence measurements covered here. There needs to be confidence that the fluorescence data obtained is an accurate and reliable measure of the lubricant thickness. Essentially, laser power variations will result in fluorescence variations, so consideration of laser power alone is a useful starting point.

4.4.2 Preliminary Nd:YAG Testing

In the manufacturer's handbook, it states that the Surelite II laser requires approximately 20 minutes to warm-up before use to allow the frequency doubling crystals to thermally stabilise. The laser power was monitored for the first 30 minutes to assess the power fluctuations during warm-up. The light from 60 laser pulses was recorded via a photomultiplier every 2 minutes from start-up. These 60 pulses were then averaged to give an indication of the average laser power change or fluctuation with time. The results from this assessment are shown in Figure 4.14.

From this data it can be seen that the laser power fluctuates initially, but settles after the manufacturer's suggested warm-up period. There is still some fluctuation in the laser power after the warm-up time, but considerably less than before.

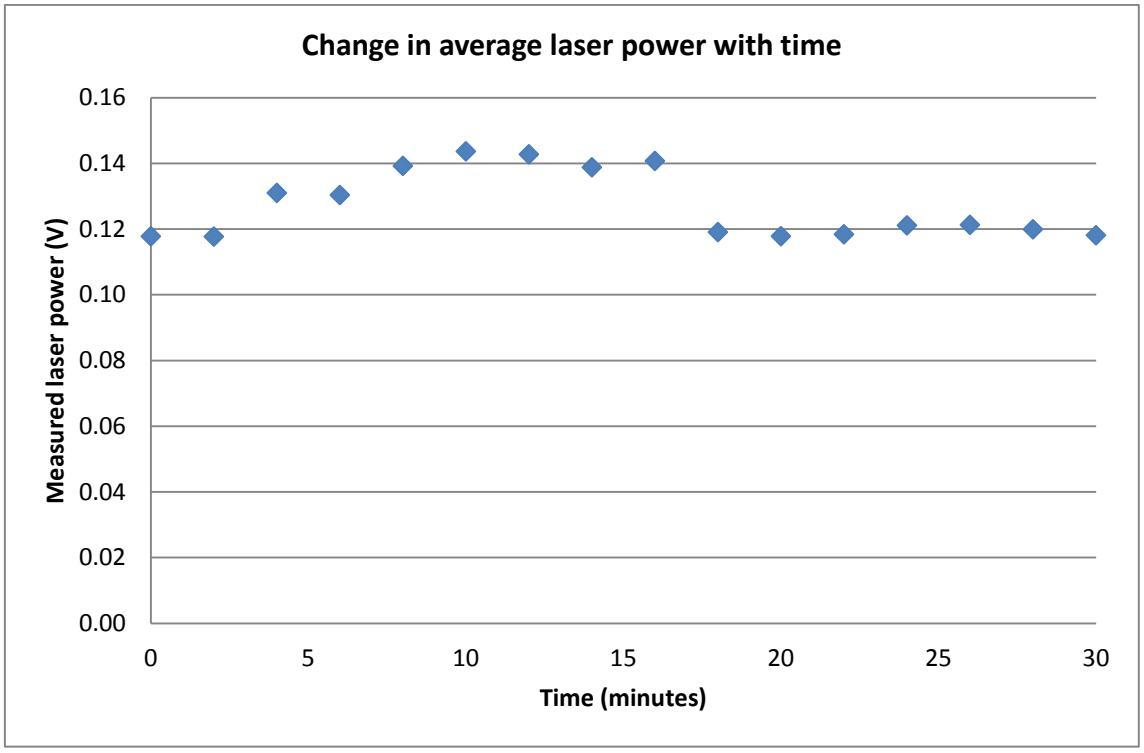

Figure 4.14 - Laser power fluctuation during warm-up (1.09kV flashlamp voltage)

4.4.3 Laser Pulse Rate

The Continuum Surelite II Nd:YAG laser is designed to pulse at 10Hz, with a pulse width of approximately 7ns (FWHM), and energy stability of ±3.5% pulse to pulse (Continuum, 2010). The laser is able to operate at other pulse rates, from 5Hz up to 12Hz. Ideally, the laser power should be stable so that the resulting fluorescence from each pulse is the same for a given lubricant thickness. This, however, is not the case for the set-up used in this research.

A 10Hz pulse rate was used during the development stages, but 5Hz was found to be less jittery when recorded. Although the laser design is optimised to run at 10Hz from a thermal stability perspective, the second harmonic generation crystal was tuned to optimise the energy output for 5Hz due to the reduction in jitter.

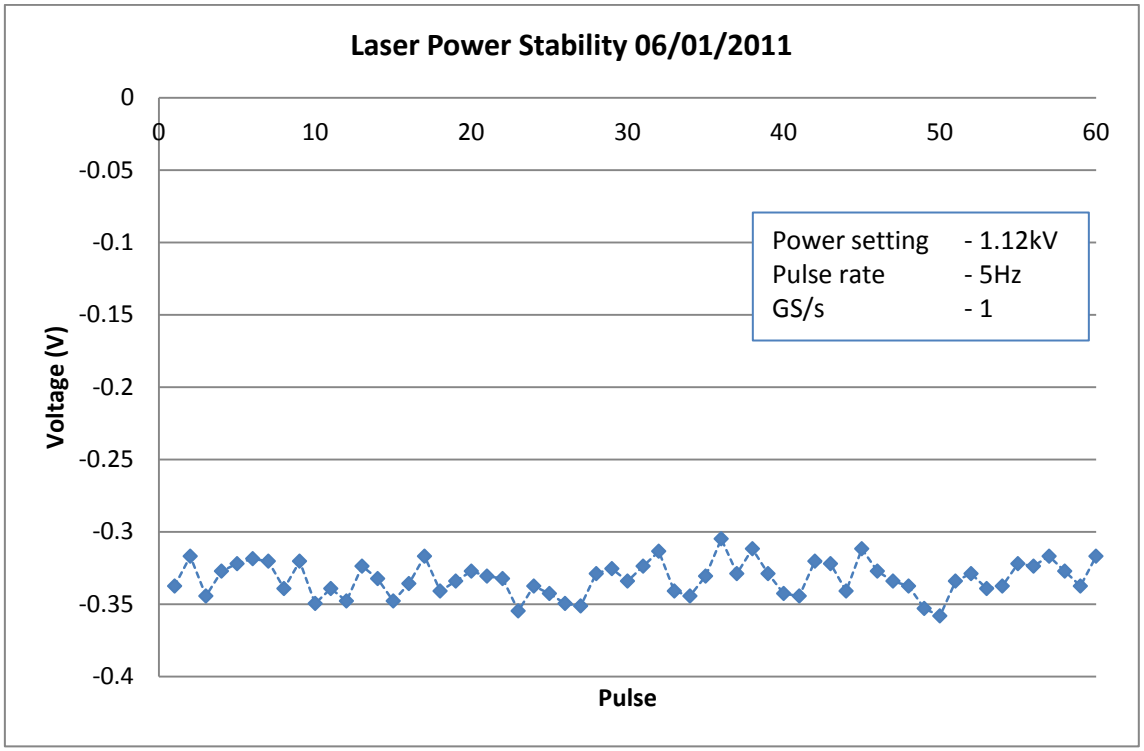

Figure 4.15 - Laser Power Fluctuations 06/01/11

In Figure 4.15, the peak voltage value from the first oscillation (as discussed in Section 3.4.2) is plotted for 60 pulses at 5Hz. The variation in the laser power is clear. This variation is visible for different pulse rates, and leads to the conclusion that the laser power is not constant.

4.4.4 Laser Modes

One possible explanation for the fluorescence variability is the laser mode variation. The discrete mode wavelengths present within a laser have been discussed in section 0. Consider the individual modes within two consecutive laser pulses (Figure 4.16). The modes within example pulse 2 are shifted with respect to those in example pulse 1. The photons from each mode will have a slightly different amount of energy, but combined over the linewidth of the output beam, the sum of the energy emitted is constant (within the stated tolerance), so a power meter would not identify any changes or discrepancies.

If the fluorophore (or fluorophores) within the lubricant is sensitive to an individual mode wavelength, it follows that the resultant fluorescence would vary with the mode shift. This means that the resultant fluorescence from pulse to pulse for the same thickness of lubricant may vary due to the variation of the modes within the laser itself.

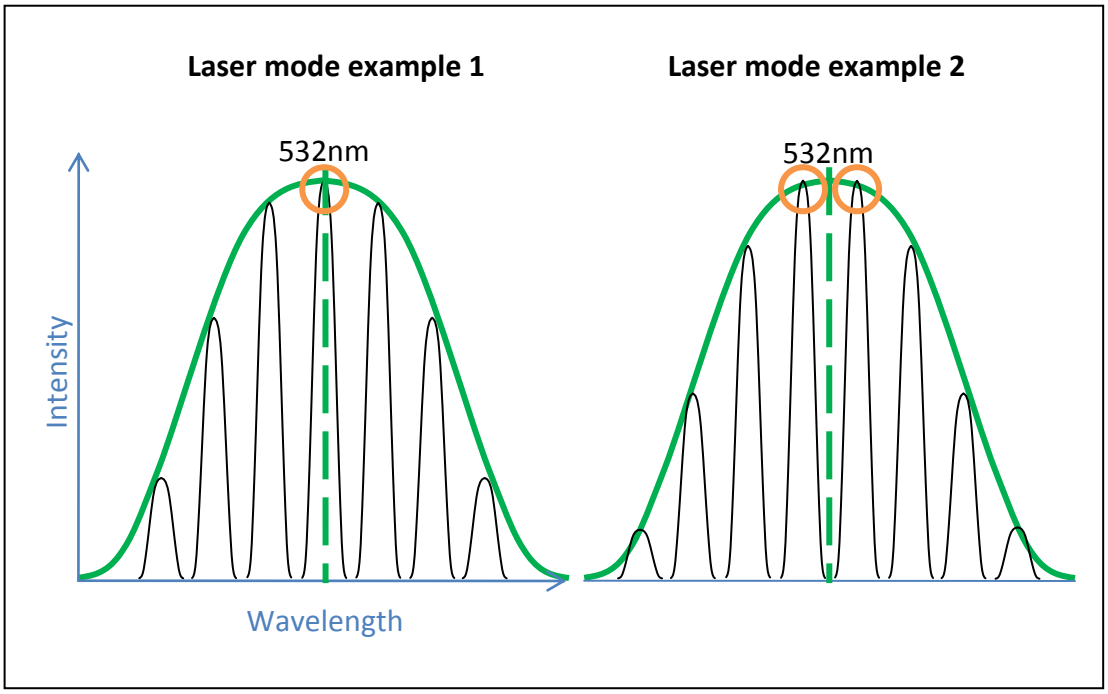

Figure 4.16 - Laser mode variation

One way to establish if this has an effect on the fluorescence measurement is to replace the standard laser with an injection seeded laser. Seeded lasers produce a much narrower linewidth and so would show if this is the cause of the fluorescence variation seen. Due to limited availability, it was not possible to obtain a seeded laser to test this theory, but it is suggested that a seeded laser would be better suited to the technique due to the reduced linewidth of the excitation.

4.5 *Fluorescence Fluctuations*

While laser power fluctuations are clearly a significant part of fluorescence fluctuations, there are additional non laser power based factors which may contribute to the overall variability. This section is concerned with these non-laser power based factors.

4.5.1 Fluorescence Saturation

When using a fluorescence based technique, it is essential to ensure that the fluorophore is not saturated. Saturation occurs when increasing the excitation intensity results in no additional emission. If the fluorophore in the lubricant becomes saturated, it is possible that changes in the thickness of the lubricant could be missed.

A test was carried out to ascertain if the laser power being used resulted in saturation. It is better to work well below the saturation limit to minimise the risk of saturation occurring. Fluorescence and laser power measurements were taken at pulse rates of 1, 3, 5, 7 and 9Hz in 0.02kV increments from 1.08kV to 1.16kV. The intention was to cover a range of possible laser powers and pulse rates that could potentially occur during measurement gathering within the FDU.

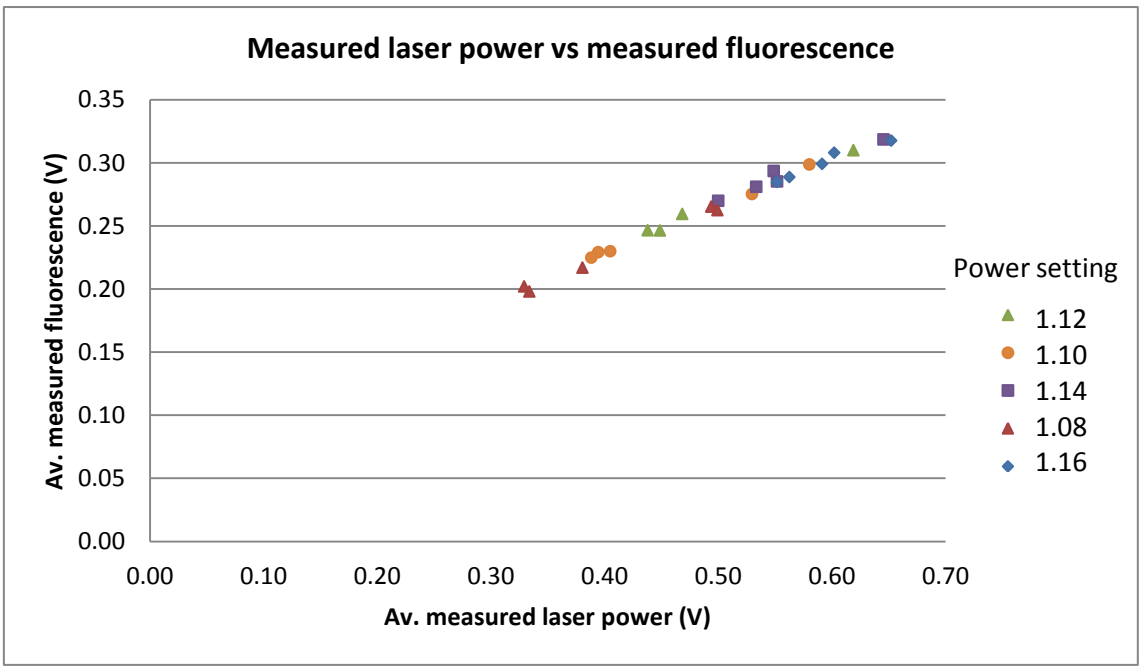

Figure 4.17 - Measured laser power vs. measured fluorescence

The results from the saturation test, displayed in Figure 4.17, show a straight line of measured fluorescence against measured laser power for the range of settings tested. If saturation of the lubricant had occurred, or was approached, the results may have shown a linear relationship with low laser power, followed by a flattening curve as the

laser power increased. This relationship was clearly not shown, so saturation was not encountered during the test and is therefore not a concern for this research.

4.5.2 Effect of Pulse Rate on Laser Power

In addition to the saturation test, the effect of the pulse rate on the fluorescence was investigated to find out the potential impact on the FDU.

When measurements are taken from a rotating surface, it is preferred that the measurements are taken from the same location. As the rotational speed increases, the pulse rate of the laser will be required to increase to match the speed of the rotating surface. If there are any deviations or variations in the laser power due to the increase (or decrease) in pulse rate, then clearly this will need to be corrected for.

An investigation was carried out into pulse rates from 1Hz to 5Hz, to ascertain if there were any variations in laser power. The results from three repeats are shown in Figure 4.18.

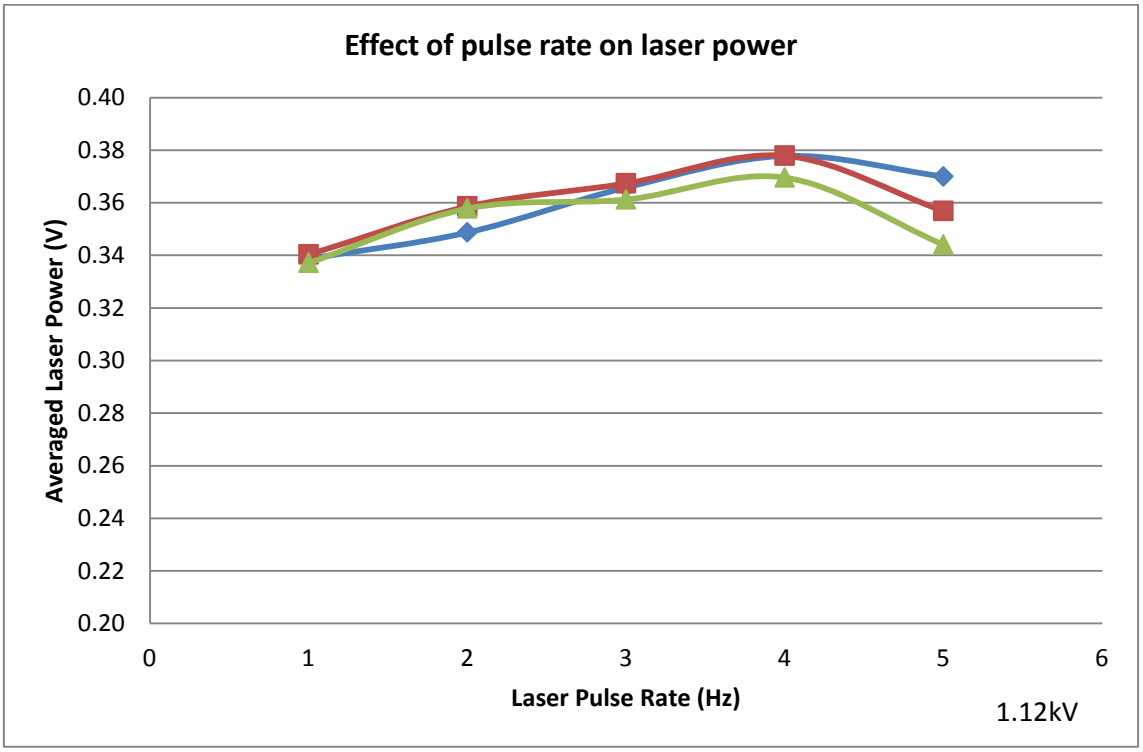

Figure 4.18 - Effect of pulse rate on laser power

While the data shows that there is a variation in the laser power as the pulse rate increases, this variation will be taken into consideration through normalisation which will be discussed in the following section.

4.6 Normalisation

Thus far, it has been established that the laser power cannot be considered constant. As the fluorescence is dependent on laser power and an increase in power results in an increase in fluorescence (even if there is no increase in lubricant thickness), there is a need for some form of correction.

To prove beyond doubt that the laser power fluctuations are the cause of the fluorescence fluctuations, the peak fluorescence and laser power measurements for 60 pulses were measured and compared. The results are shown in Figure 4.19. Four lines have been added to the graph to highlight the shared trend between both the fluorescence and laser power data, confirming that they are related. The peaks and troughs in the measured laser power and measured fluorescence are directly related.

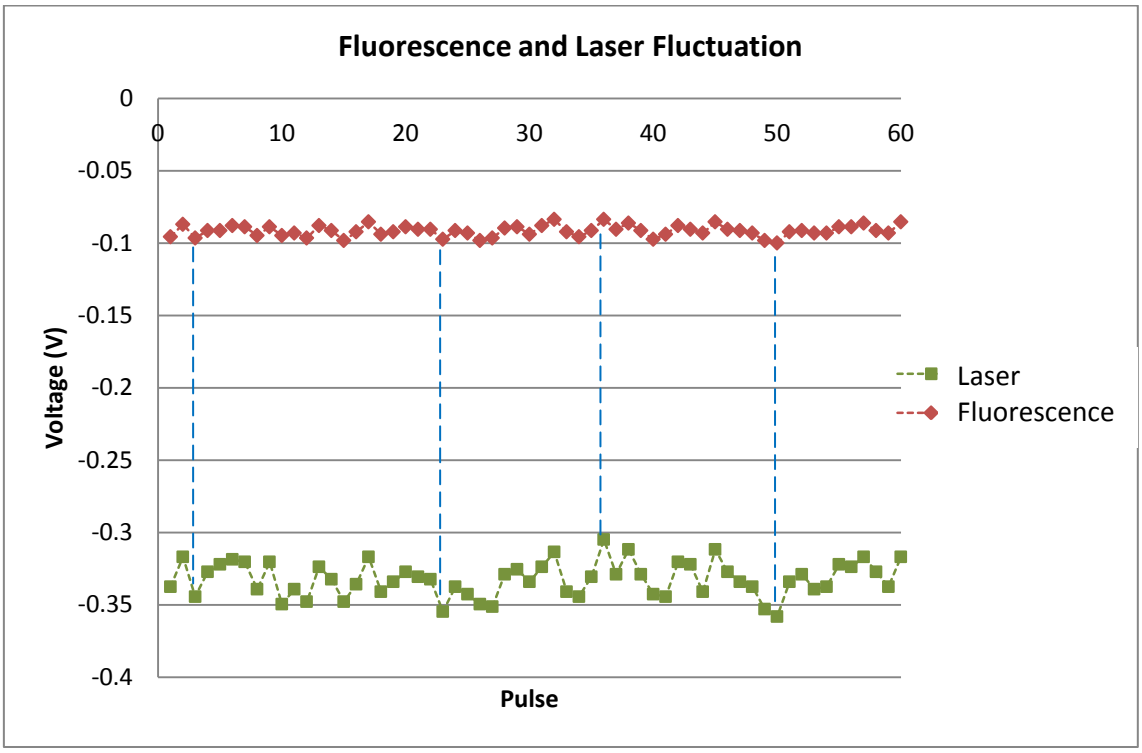

Figure 4.19 - Fluorescence and laser power fluctuations

To correct for this fluctuation in laser power, the peak fluorescence voltage was divided by the peak laser power, making the fluorescence data independent of the laser power fluctuations.

$$\frac{V_{fluorescence}}{V_{laser}} = V_{normalised} \tag{4.3}$$

The normalise fluorescence data is presented in Figure 4.20. This normalisation was carried out for all the fluorescence data gathered.

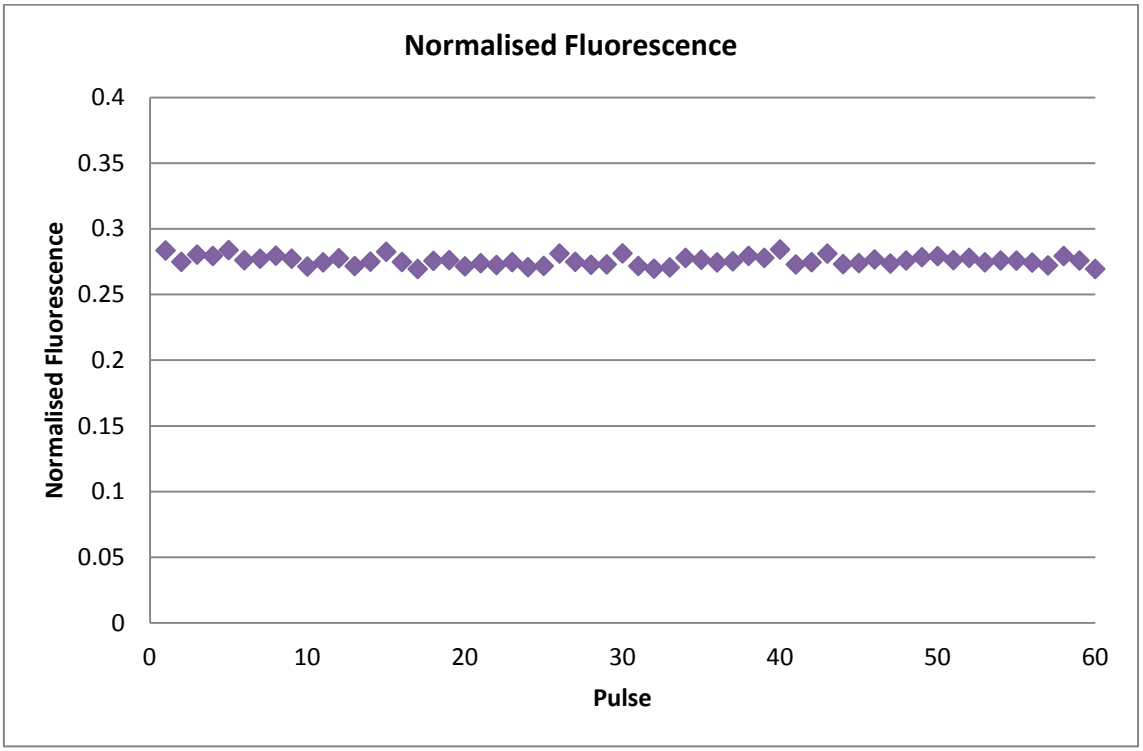

Figure 4.20 - Normalised fluorescence

It is thought that the standard deviation of the normalised fluorescence (0.0037 in this case) is the laser mode noise.

4.7 Summary of Chapter 4

In this chapter, the evolution of the LIF measurement technique from initial proof of concept, through to viable calibration technique has been discussed. The calibration wedge is a vital component of the LIF technique; without it, there is no quantitative measurement of the lubricant.

Initial assessment of fluorescence measurements from the lubricant filled wedge showed that as the lubricant thickness increases, so does the measured fluorescence. In addition, recorded measurements were translated back to lubricant thickness due to the known and calculated geometry of the wedge.

Development of the experiment layout has been described and through investigations into in-line and off-axis equipment configurations, it is understood that the off-axis option is currently the most suitable option because of LIF from the replica housing.

Fluctuations in laser power have been identified as a potential source of error for measured fluorescence data. As a result of this variability, the laser was tested during warm up and also over a range of laser power setting to establish if there was a pattern or obvious solution through selection of optimum settings. Reducing the laser pulse rate from 10Hz to 5Hz showed an improvement in jitter.

The outcome of these investigations is that the laser power is not as stable as first assumed and therefore a correction of the fluorescence data is required. One theory is that the modes within the laser are contributing to the fluorescence variations as each mode has a discrete wavelength that may change between pulses.

As a way to correct for the laser fluctuations a normalisation process was introduced and carried out on all data. This approach enables correction of pulse to pulse laser power variations by dividing the fluorescence by the laser power from the corresponding pulse. A similar technique was used by Myant (Myant et al., 2010).

CHAPTER 5
SYSTEM CALIBRATION

Chapter 5 describes the development of the calibration technique used for LIF lubricant thickness measurement. More specifically, this chapter covers the corrections and additional considerations, such as temperature and absorption, which affect the fluorescence measurement having already considered the role of laser power fluctuations.

5 System Calibration

The importance of creating a repeatable and a reliable calibration technique has been discussed in the previous chapter and a brief overview of the wedge calibration was given. As the calibration is a critical part of the lubricant thickness measurement technique, it will be covered in greater depth this chapter.

5.1 Calibration Development

Quantitative calibration is a vital part of a LIF measurement technique. Once fluorescence from the lubricant has been established, quantification of the fluorescence becomes the next logical step. In this section, the development of a wedge-based calibration technique will be described, which allows measured fluorescence to be converted into a lubricant thickness.

5.1.1 Calibration Wedge

As described briefly in the previous chapter, a glass wedge was used for the basis of the calibration technique. The major advantage with using a wedge is that the oil thickness at any given point can be calculated, so quantitative calibration is incorporated into the system. If the height at which the laser strikes the glass wedge is known, the oil thickness can be calculated using simple geometry (Appendix 2).

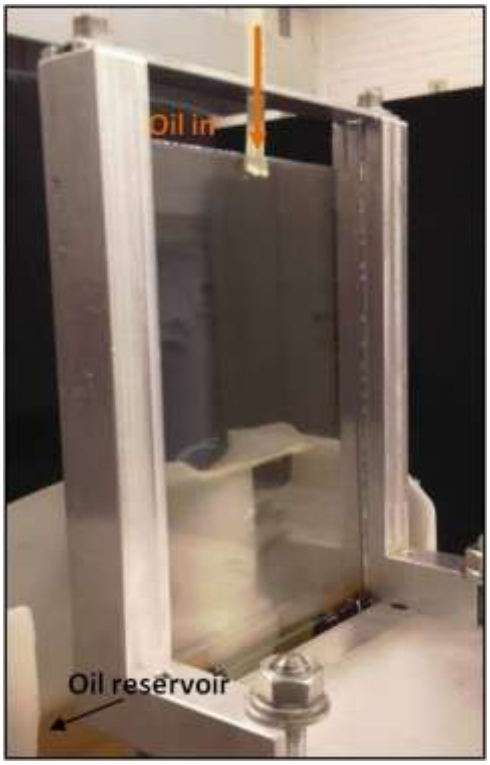

Figure 5.1 - Glass Wedge set-up

The wedge was formed from two sheets of glass, which were set into grooves in two aluminium sides forming a central channel for the oil to flow through (Figure 5.1). The wedge was mounted on a lab-jack, which allowed fine vertical adjustment. As with the validation experiment, oil was pumped from a reservoir to the top of the wedge, and allowed to flow through, before recollection in the reservoir. Fluorescence measurements were taken incrementally in 10mm steps from the bottom of the wedge, and showed an increase in measured fluorescence with an increase in oil thickness.

5.1.2 Calibration Optics and Instrument Layout

Initially, fluorescence intensity data were gathered from the wedge using an ICCD camera, but the data repeatability was poor. The ICCD camera was replaced with two photomultipliers (PM); one to measure the fluorescence intensity and the other to monitor the power of the laser. The incoming light to both photomultipliers was filtered to ensure that only the correct wavelengths of light reached the corresponding photomultiplier; 532nm for the laser power monitor and 650nm for fluorescence. Both photomultipliers were connected to a digital oscilloscope, which received the light intensity data before passing it to a PC (Figure 5.2).

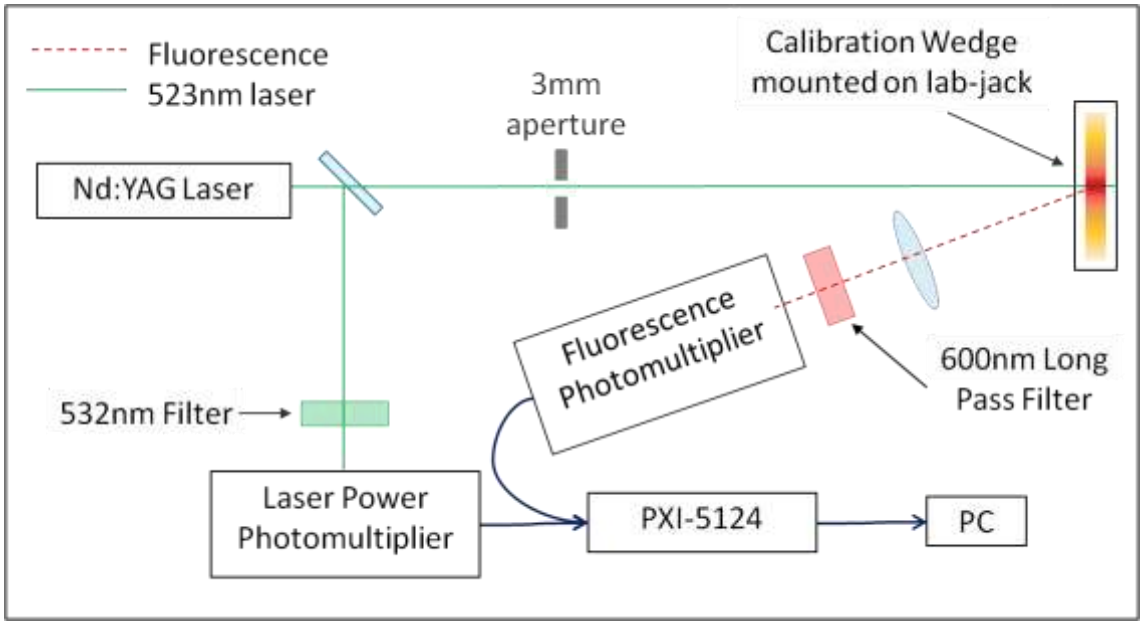

Figure 5.2 - Glass Wedge and Photomultiplier set-up

A Tektronix TDS1012 storage oscilloscope was used initially to capture the photomultiplier signals before upgrading to National Instruments PXI5124, which was discussed in detail in section 3.4. The upgrade allowed greater flexibility and speed of data transfer.

5.1.3 Data Collection Method

In this section, a description of the data collection stages will be given, with an overview of the series of optical events that occur during one laser pulse. Understanding the timings of the laser, fluorescence and data acquisition is important to be sure that data from each pulse is collected.

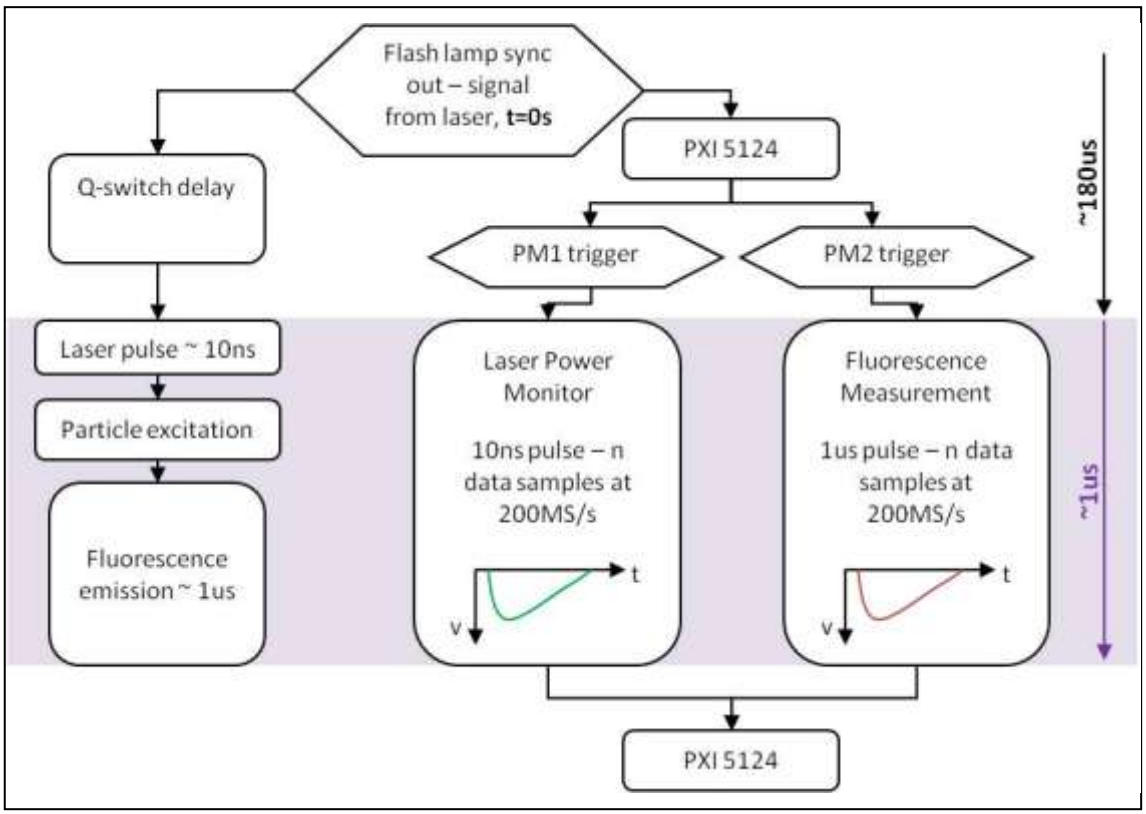

Figure 5.3 - Fluorescence and Acquisition Timing Schematic

In Figure 5.3, the stages in data collection are illustrated. The laser and fluorescence timings form the left branch of the schematic, with the data collection branch on the right. Both the fluorescence generation and data collection have the same start point, which is the signal produced by the laser as the flash lamp prepares to fire. For the purposes of this explanation, this signal occurs at t=0s. The flash lamp out signal triggers the data acquisition unit PXI5124 where a delay before data collection was set to match that of the laser. Approximately 180us after the flash lamp signal, t=0s, LabVIEW was triggered to begin receiving the laser and fluorescent light, and the laser fired. At a sample rate of 200MS/s, the data points for each channel were collected and stored on board PXI5124 before they were transferred to a PC. The number of data points collected, n, was set within the virtual instrument or VI. Each set of data points made up a graph which showed a minimum voltage, corresponding inversely to a measured light intensity. The minimum recorded voltage value per pulse was taken

as the fluorescence measurement. This process was repeated for each laser pulse. The measurements could have been inverted to give a positive value for fluorescence intensity, but as only the magnitude was important, it was decided to leave the measurements as negative values.

60 pulses of data were taken at each measurement thickness on the wedge, and then averaged. The relationship between the averaged fluorescence data and the oil thickness were then analysed. The total time taken from t=0s to data acquisition and processing had to be less than the 0.1 seconds to fit between the laser pulses. If the time taken for collection and processing exceeded 0.1 seconds data may have been lost or incomplete. To ensure all the necessary processes occurred within the allowed time frame, a timing loop was added to the VI to monitor the time taken to collect, manipulate and store the data. From this study, it was shown that most time was spent waiting for the next pulse to commence and that the data from each pulse was being collected. The pulse rate of the laser was then altered to test the system further, and it was noted that the data collection system was more than capable of dealing with pulse rates from 5Hz up to 12Hz without encroaching on the data collection from the subsequent pulse. A diagram of the timing loop can be found in Figure 5.4.

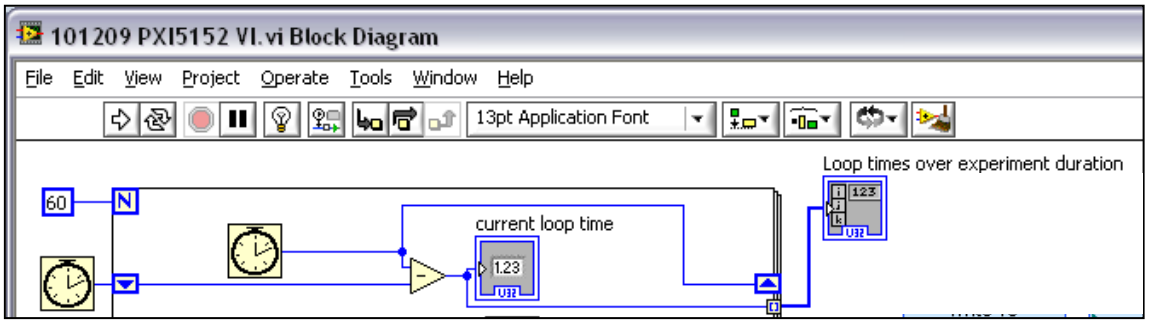

Figure 5.4 - VI Timing Loop

Initially LabVIEW recorded the minimum value only; however it became apparent that the minimum (peak) value did not always occur in the same position – not always on the 1st oscillation. This meant that the values from the first oscillations had to be gathered by searching through the data manually or via DIAdem. DIAdem is a National Instruments alternative to Excel, which is able to manage greater volumes of data and is also able to read the data files directly from the VI. The LabVIEW VI was set up to record the full data set from each pulse and in addition the peak intensity value from each pulse.

5.2 The Effect of Temperature on Fluorescence

According to Bowen (Bowen, 1959), fluorescence generally decreases as temperature increases. It is therefore possible that over the operating temperature range of a FDU, where the temperature of the lubricant can reach up to 90°C (depending on drive cycle), the measured fluorescence intensity may change due to temperature effects rather than changes in lubricant thickness. It is important to know the degree to which the fluorescence is affected so it can be corrected for. In this section, an investigation into the affect of temperature on fluorescence will be carried out.

In addition to the affect on fluorescence intensity, changes in temperature also affect the viscosity and movement of the lubricant within the FDU. This change in behaviour is useful to understand as it will have an impact on the thickness of lubricant found in the FDU.

5.2.1 Temperature Investigation Method

In order to maintain a constant lubricant thickness, the wedge was positioned to keep the thickness of lubricant at 2.32mm, while the temperature of the lubricant was increased. The experimental set up was kept the same as with the previously calibration experiments, but with the addition of a copper heating coil into the lubricant recirculation system. The coil was inserted before the wedge to heat the lubricant, as shown in Figure 5.5.

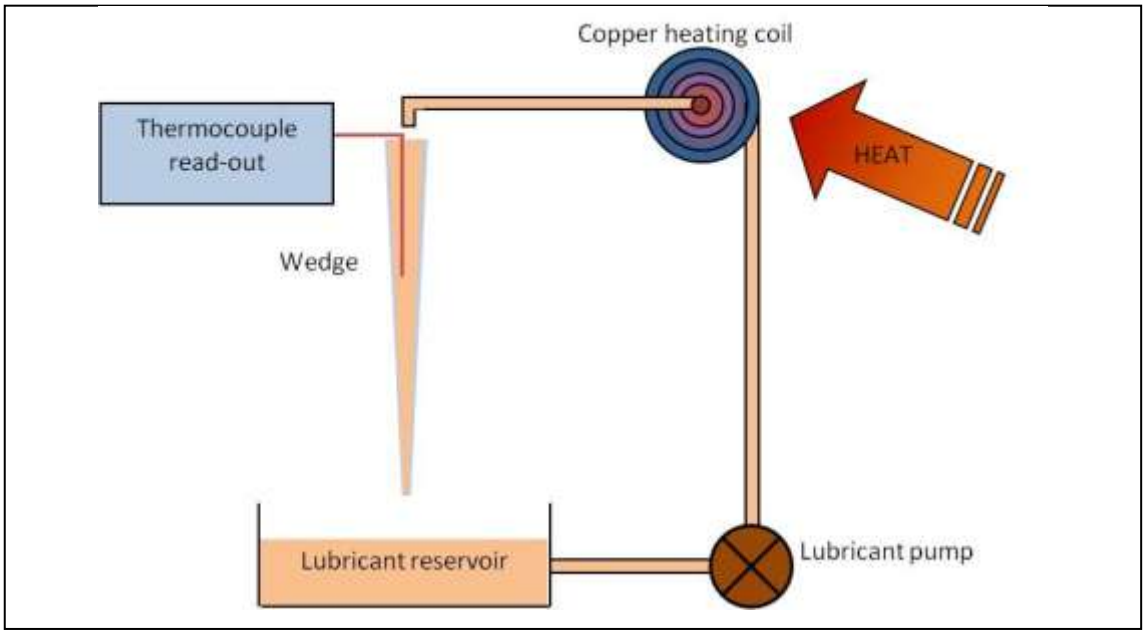

Figure 5.5 - Temperature study set-up

A k-type thermocouple was inserted into the wedge to monitor the lubricant temperature. The thermocouple was placed as close to the beam as possible without obstructing the laser or fluorescence signals.

5.2.2 Temperature Investigation Results

Data was collected using PX5152 (8-bit, 1GS/s) in 5°C increments from 30°C to 65°C. This range was chosen as it covers and extends beyond the lubricant operational temperature of the replica FDU. As the replica FDU is not loaded, the temperature of the lubricant will not be as high as for the real unit. Maximum temperatures of around 35-40°C are expected in the replica FDU.

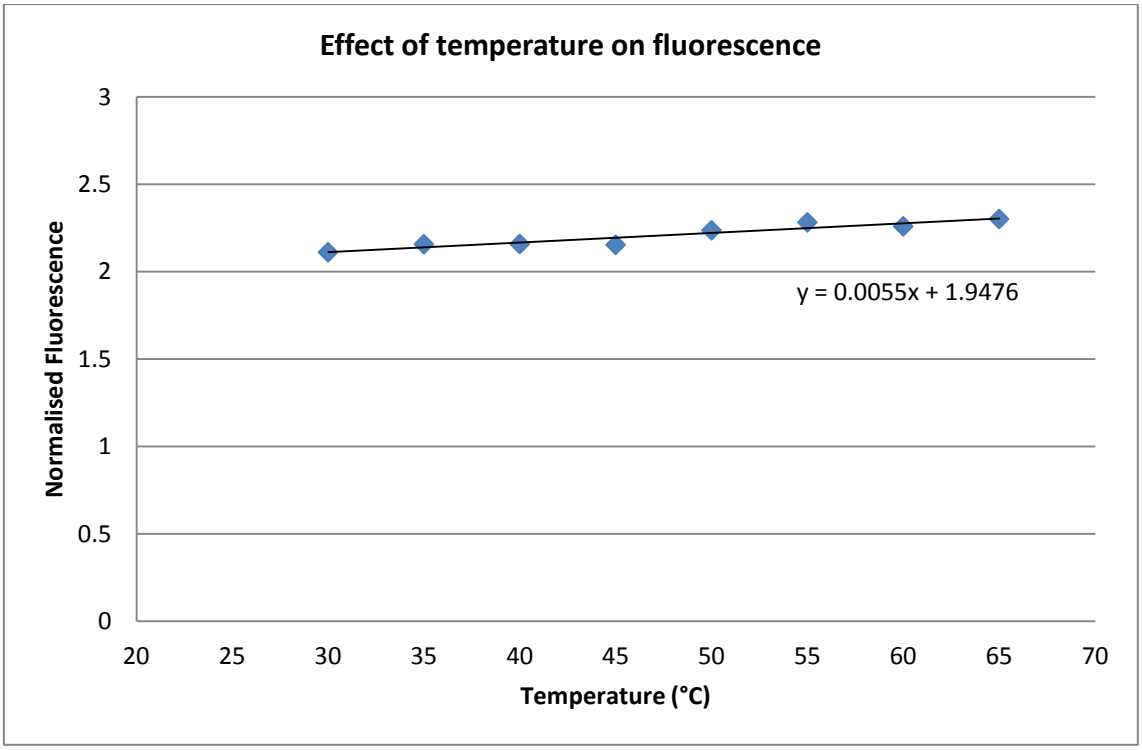

Figure 5.6 - Effect of temperature on fluorescence 100728

In Figure 5.6, the measured relationship between temperature and normalised fluorescence is shown. Between 30°C and 65°C, there is a small increase in fluorescence intensity of approximately 8%. This contradicts the initial comment by Bowen that fluorescence decreases as temperature increases. Repeated data showed a similar trend. If the fluorescence increase over the temperature range expected in the replica FDU is considered (between 30° and 40°), the increase in fluorescence is much lower, only around 2% (based on the data show in Figure 5.6). As this change is so small, the effect of temperature on fluorescence in the FDU will be considered negligible. When studying systems where temperature increase is large, then a correction factor would need to be employed.

5.3 Absorption Study

Absorption of electromagnetic radiation is a process in which energy is transferred from the electromagnetic radiation to the absorbing species (Wayne, 1988). As shown in section 2.4.2, the amount of light absorbed can be calculated using the Beer-Lambert Law (defined in Section 2), where A is the measured absorbance, ε is the molar absorptivity, d is the path length (or layer thickness) and C is the concentration of the solution. This equation is often found in the logarithmic form, where I_0 and I_t are the incident and transmitted light intensities (Figure 5.7).

$$A = \log_{10} \frac{I_0}{I_t} = \varepsilon C d$$

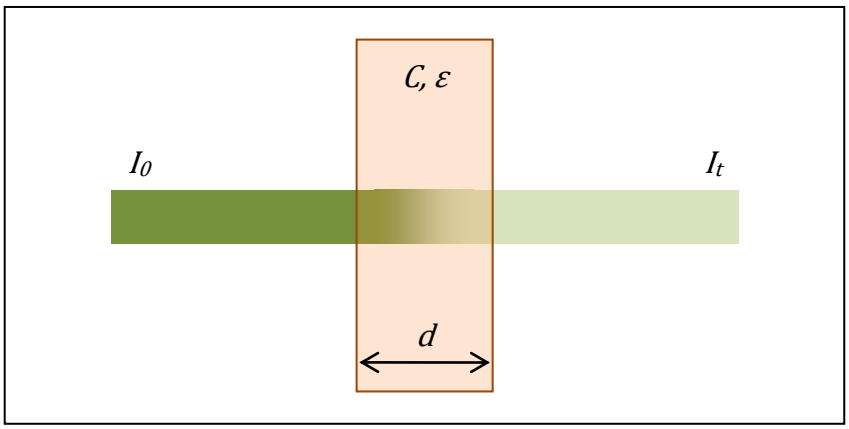

Figure 5.7 - Diagram of Beer-Lambert absorption through a fluid

While in some cases (as described in 2.4.2) absorption is a desired and useful process it is possible that for LIF, absorption could prevent the laser signal from fully penetrating and exiting the lubricant layer. This could result in erroneous lubricant thickness measurements. If the laser beam does not fully penetrate the layer, not all the molecules through the thickness of the lubricant can be excited to emit fluorescence, so the measured thickness would be less than the actual thickness.

Described in the remainder of this chapter is a study which was carried out to investigate the effect of absorption on Castrol SAF-XO. The purpose of this study is to ascertain if a correction factor is needed in the analysis of the lubricant thickness data.

5.3.1 The Effect of a Focused Beam on Absorption

In order to assess the absorption of light through the FDU lubricant, a simple perspex box was filled with Castrol SAF-XO and positioned in the path of the 532nm Nd:YAG laser beam set to 1.09kV at 10Hz (Figure 5.8). In the base of the box was a tap that was used to drain the lubricant during data collection to maintain lubricant movement. By taking measurements while the lubricant was moving, bleaching was prevented and a closer similarity to a real system was achieved. A LaVision FlowMaster camera and intensifier were used to record the intensity of the fluorescence and reflected 532nm light through the 70mm lubricant thickness. Taking images with the FlowMaster camera allowed the profile of the fluorescence through the lubricant to be seen, and monitored along the beam path.

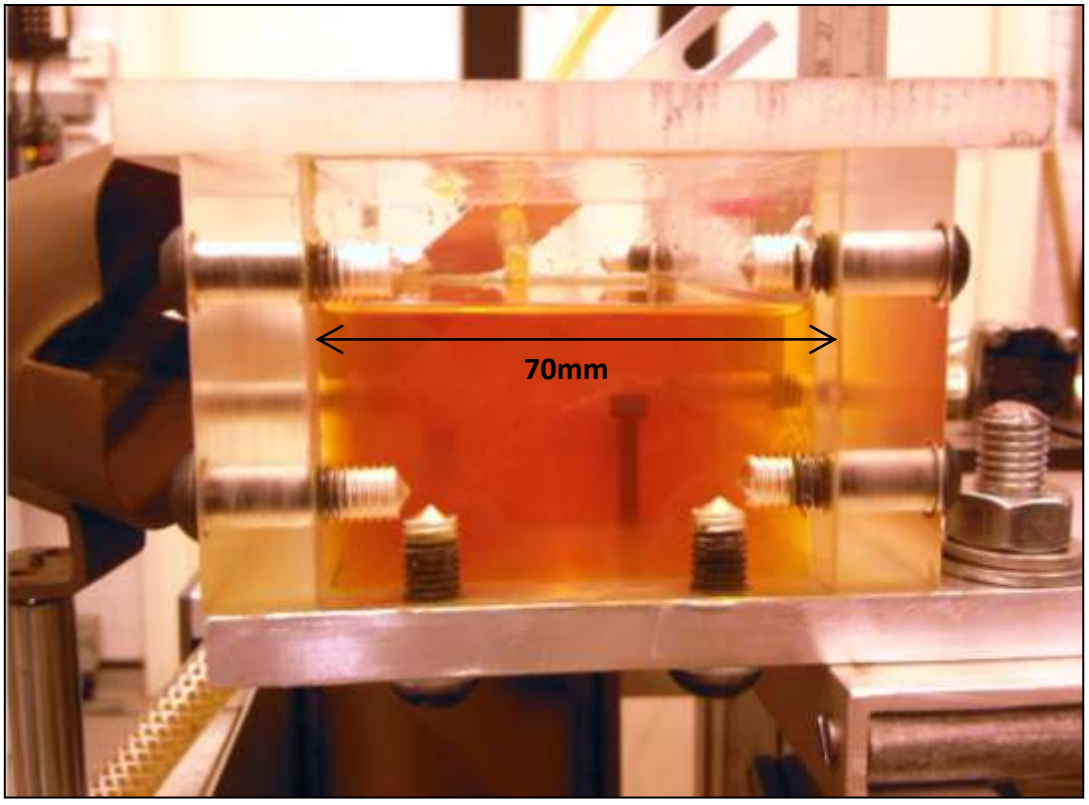

Figure 5.8 - Absorption study - simple perspex box

The image capture was synchronised with the laser pulse as it passed through the oil. A 600nm long-pass (red) and a 532nm (green) filter were alternately placed on the camera lens to allow the laser signal or the fluorescence signal to be seen by the camera. The images from the camera were automatically transferred to a PC where camera control and image analysis took place via LaVison DaVis 7. Fifty images (one per laser pulse) were taken and an average of these was produced to minimise any shot-to-shot differences in light intensity. A schematic of the set-up is shown in Figure 5.9.

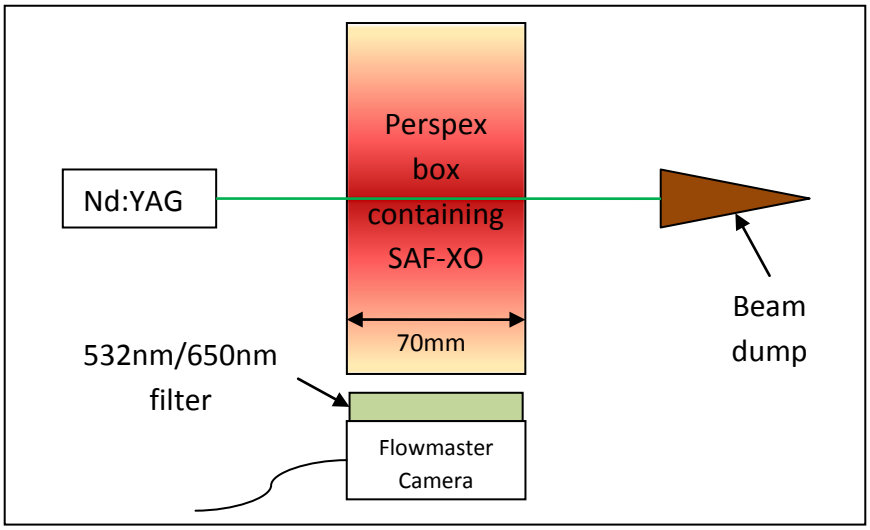

Figure 5.9 - Absorption study set-up

Both the 532nm laser and 650nm fluorescence light were measured separately in case the lubricant absorbed different wavelengths by different amounts. In Figure 5.10 the averaged image captured 532nm laser beam is shown.

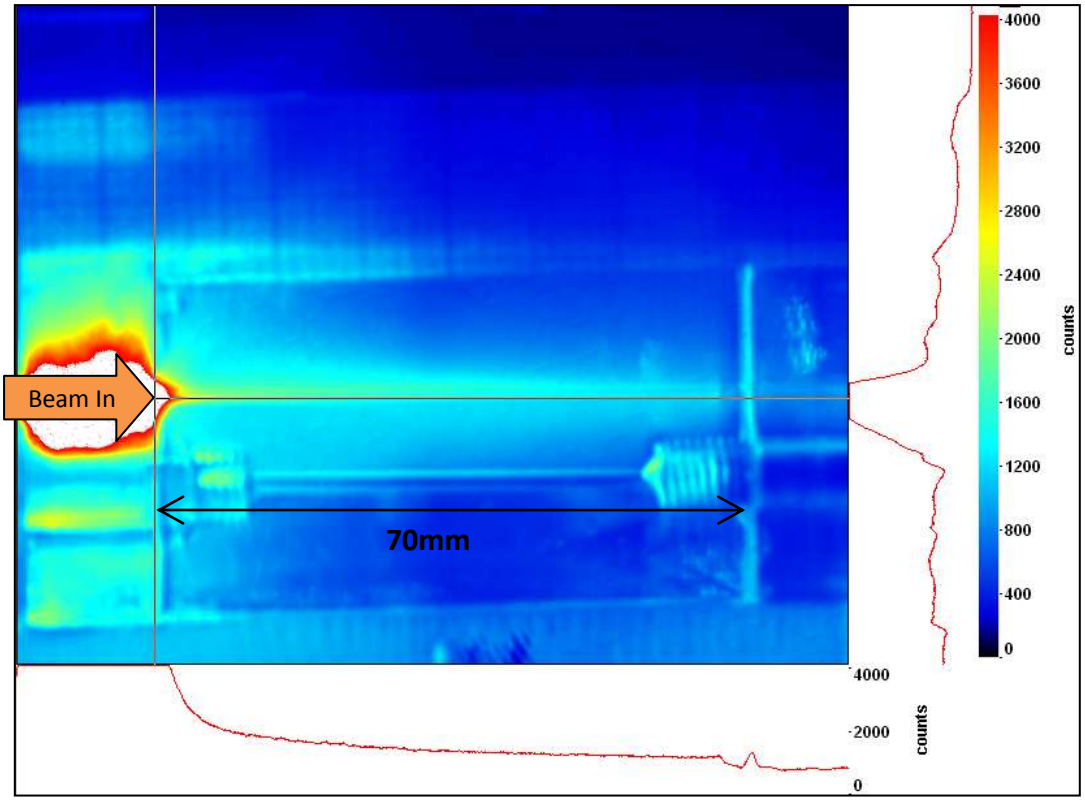

Figure 5.10 - Focused beam through 532nm filter (091022 2 - 1.09kV)

The red line under the false-colour image shows the intensity profile of the 532nm laser beam passing through the lubricant. From the profile, it can be seen that the

532nm light has a penetration depth of approximately 2mm before the intensity decays sharply. After approximately 5mm, the measured intensity dropped to half of its initial value.

The averaged captured image of the fluorescence through the lubricant is shown in Figure 5.11. The intensity profile from this data shows that the fluorescence intensity remains almost constant for the first 20mm of penetration. This plateau demonstrates that while the 532nm light is being absorbed, the 532nm light that is penetrating the lubricant is sufficient to excite the fluorophore through the full 70mm of lubricant. This shows that a focused 1.09kV laser beam is sufficient to penetrate the thicknesses within the wedge and the plateau suggests that the absorption over the range of thicknesses in the wedge is negligible.

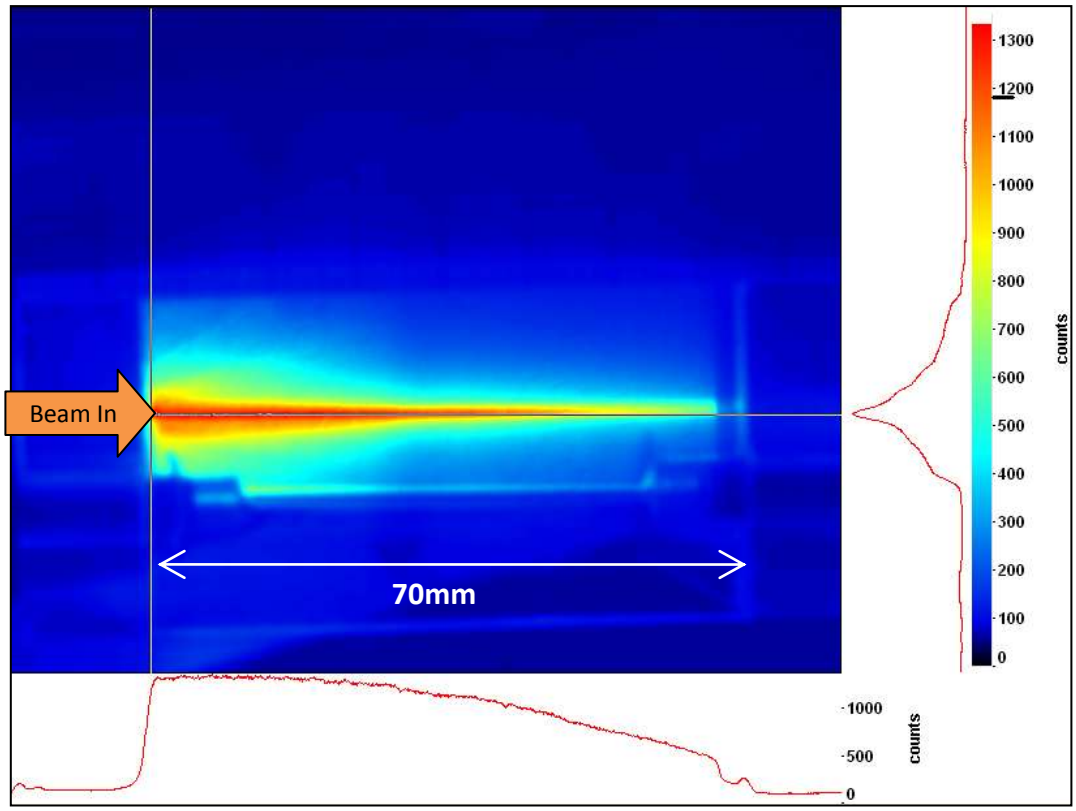

Figure 5.11 - Focused beam through 600nm long-pass filter

The laser was focused on the inside of the perspex casing, but due to the high energy density, was found to damage the perspex. As a result of this, a parallel beam was deemed more suitable as the FDU is also made of perspex. The beam diameter was restricted by placing a 3mm diameter aperture in the path of the beam. The parallel beam prevented damage occurring to the perspex, and the 3mm aperture reduced the area which could be excited by the laser, making it spatially more accurate. Further details on the parallel beam configuration are given in section 5.3.3.

5.3.2 Absorbance of Castrol SAF-XO

Using the measured absorption profiles through the SAF-XO lubricant, the absorbance of the laser and fluorescent light can be calculated. The profiles of the absorption of 532nm and 650nm light are shown in Figure 5.12. Using the entry intensity and exit intensity, the absorbance for both wavelengths were calculated ((5.1)(5.2)).

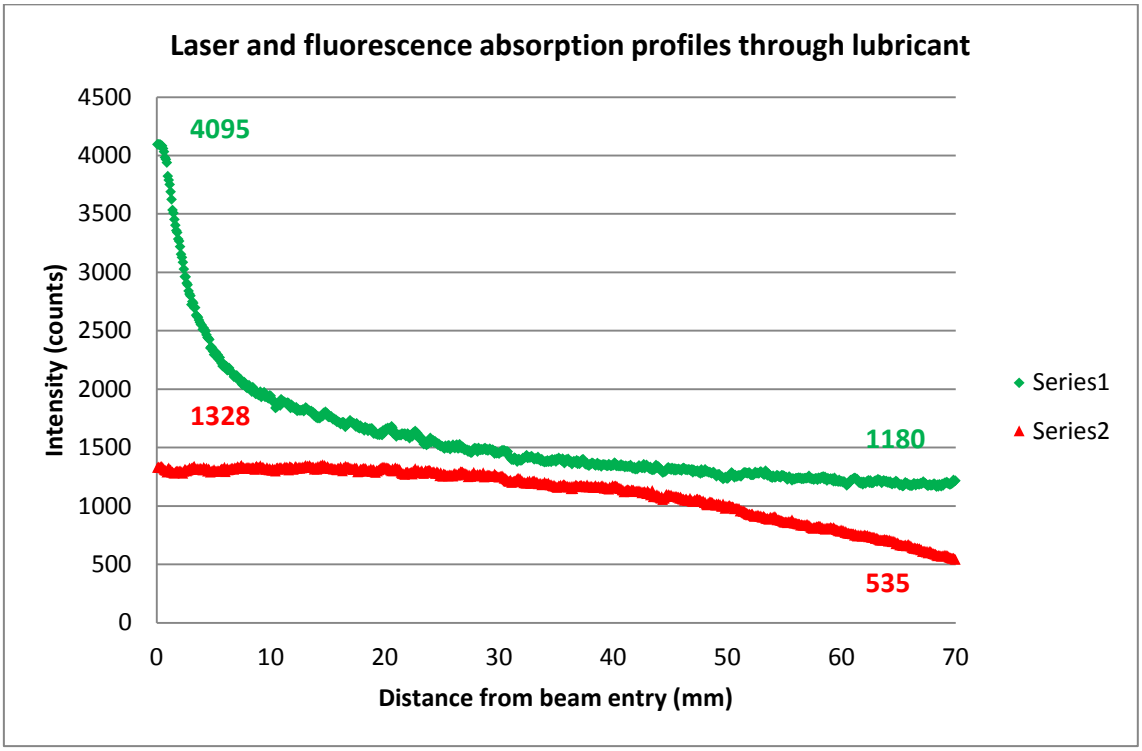

Figure 5.12 - Absorption of 532nm and 650nm light through lubricant

Absorbance 532nm→

$$A_{laser} = \log_{10}\frac{4095}{1180} = 0.54 \tag{5.1}$$

Absorbance 650nm→

$$A_{fluo} = \log_{10}\frac{1328}{535} = 0.39 \tag{5.2}$$

The absorbance of the 532nm laser was found to be 0.54, which is greater than that of the 650nm fluorescence at 0.39. This shows that the SAF-XO lubricant used absorbed green light more effectively than red. In terms of film thickness measurements, this means that provided the laser is able to penetrate through the thickness of the lubricant (which has been shown to be possible with minimal absorption up to 5mm), the fluorescent light will be able to escape essentially unimpeded to the detector.

These values can also be used as a correction factor if considering thicker lubricant layers.

5.3.3 The Effect of a Parallel Beam on Absorption

As the energy density of the beam was reduced, the penetration depth of light also reduced. An investigation into the effect of laser power on penetration depth through the lubricant was carried out and is described in this section.

The fluorescence profile from three different laser powers was assessed. The aim was to find a laser power which was able to sufficiently penetrate the lubricant and yet not cause damage to the perspex case. As the energy density is lower when the beam is parallel, it is possible to use a higher laser power to increase the depth of penetration into the oil. In addition, using a higher laser power should help to reduce the laser power fluctuations caused when low power is used.

The three laser power settings investigated were 1.09kV, 1.11kV and 1.13kV. As with the focused beam, 50 images were taken and an average image created. The average fluorescence beam profiles for the laser powers can be seen in Figure 5.13, Figure 5.14 and Figure 5.15. With each increase in laser power, the depth of penetration of 532nm light into the lubricant can be seen to increase. This is shown through the plateau in the profile under the images, and is highlighted in the figures with the yellow line.

The first thing to note is that although the fluorescence is visible through the full 70mm of the box, the depth of constant intensity penetration is much smaller than for a focused beam, and is reduced to approximately 5mm for each of the laser powers assessed. The intensity profiles for each image appear to be of a similar shape, with the value of peak intensity increasing with laser power, as expected. As the shape of the intensity profiles appear to remain unchanged, and the initial depth of constant intensity are all of approximately equal value, it can be concluded that over the range of laser powers tested, increasing the laser power does not extend the constant intensity region of the fluorescence profile. Furthermore, as the constant intensity region extends to 5mm, it can be assumed that for up to 5mm, absorption does not affect fluorescence, which is sufficient for measurements made from the wedge.

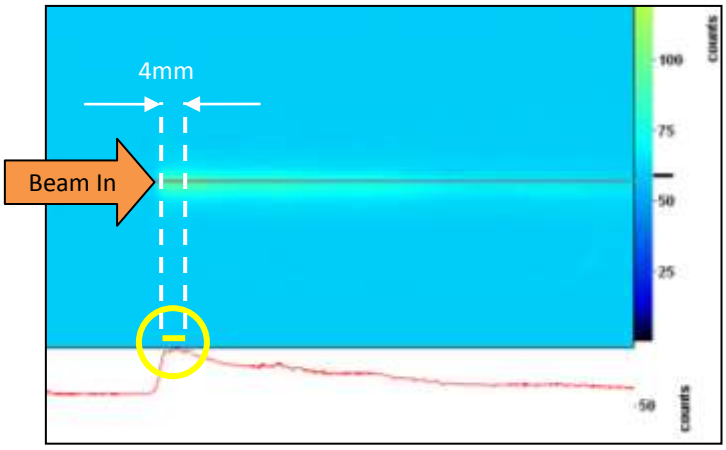

Figure 5.13 - 1.09kV laser, 3mm parallel beam through 600nm long-pass filter

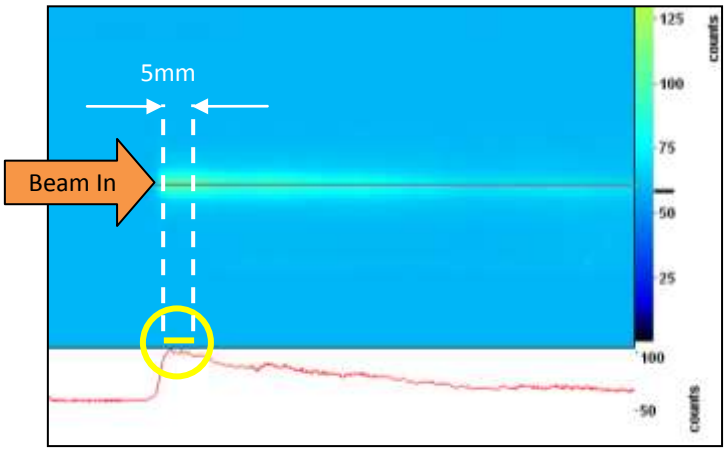

Figure 5.14 - 1.11kV laser, 3mm parallel beam through 600nm long-pass filter

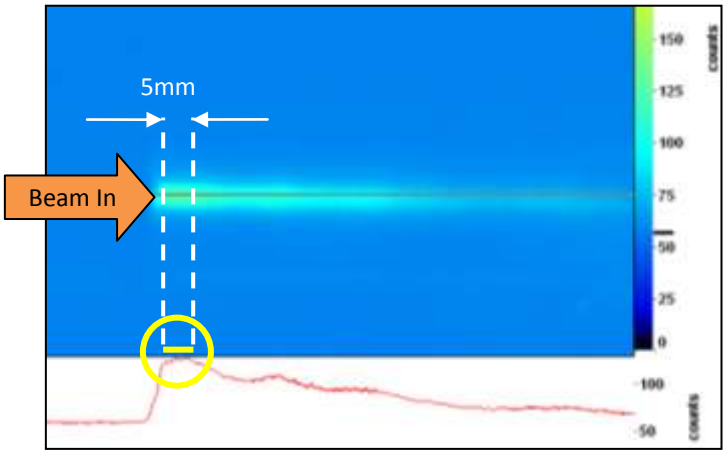

Figure 5.15 - 1.13kV laser, 3mm parallel beam through 600nm long-pass filter

5.3.4 Absorption of Fluorescence (PXI-5124)

Up to now, the focus has been on ensuring that the laser light is able to sufficiently penetrate the lubricant to excite the fluorophore. While this is clearly crucial to the LIF technique, it is also important to consider the ability of the emitted light to escape the lubricant for detection. An experiment was set up to test the ability of the fluorescence to escape through different thicknesses of lubricant. The findings of this experiment are discussed in this section.

The laser was set up to pass through the perspex box as previously described, with the box mounted on a table to allow lateral movement. This lateral movement enabled the thickness of lubricant between the laser beam and the photomultipliers, x, to be changed. The photomultipliers were set-up in a fixed position perpendicular to the laser beam to monitor the 532nm and fluorescent 650nm light able to pass through the different thicknesses of lubricant. A plan view of this set up is shown in Figure 5.16.

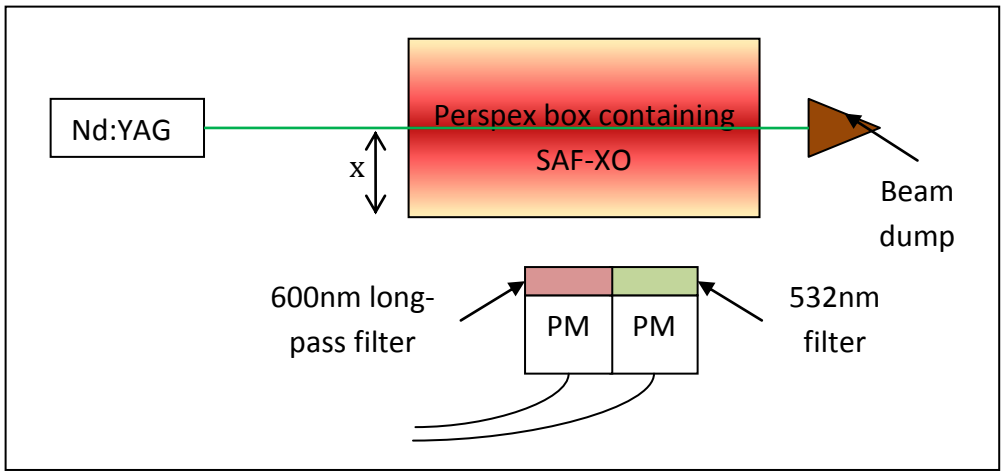

Figure 5.16 - Absorption of fluorescence experiment set-up

Measurements of the fluorescence and laser light were taken in 5mm increments from 0mm thickness of lubricant, where the laser beam skimmed the side of the perspex box just inside the lubricant, up to 80mm.

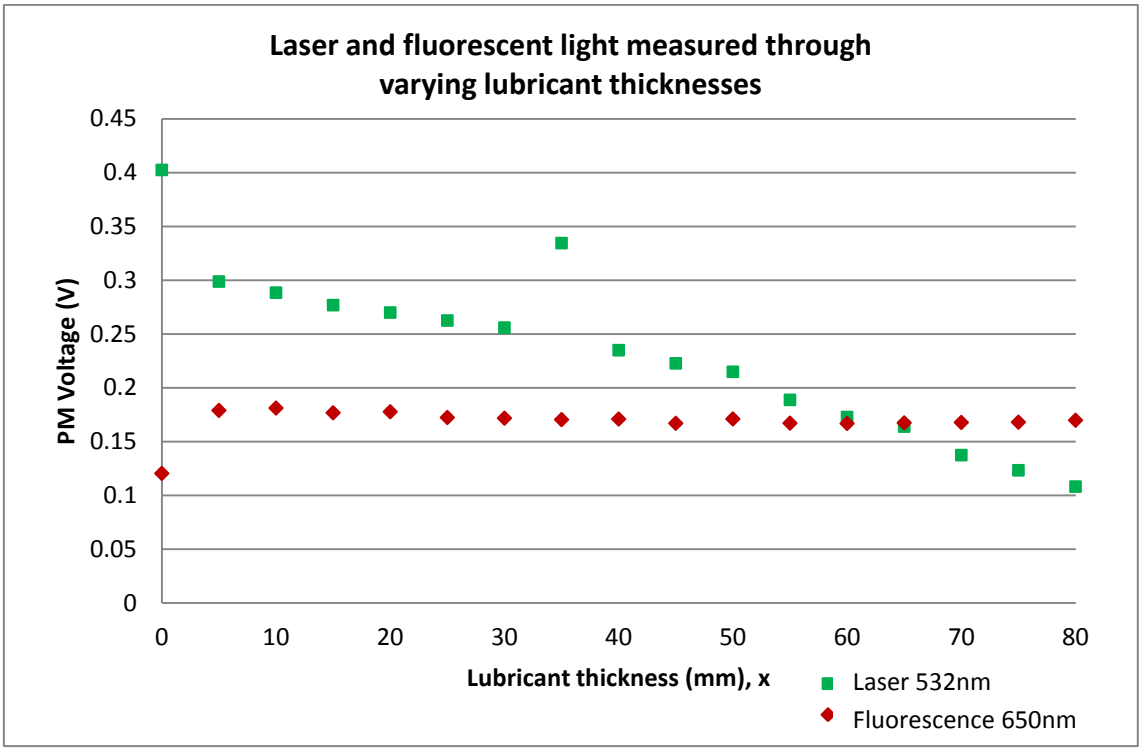

Figure 5.17 - Change in light intensity through increasing lubricant thickness

The results in Figure 5.17 showed that for the 532nm light, the greater the thickness of lubricant between the laser path and the photomultiplier, the more light was absorbed. For the fluorescent 650nm light, there appeared to be very little change as the thickness of lubricant increased after the initial jump. This confirms that the lubricant absorbs green light more readily than red light. From this it will be assumed that fluorescent light is not being absorbed by the lubricant in the wedge and that the fluorescent signal is not prevented from reaching the photomultiplier.

5.4 Summary of Chapter 5

The wedge calibration set-up has been discussed in detail in this chapter. The wedge is crucial to this technique as it allows quantitative thickness measurements to be made.

Temperature has been found to have an effect on fluorescence intensity, however further investigation over the range of temperatures expected in the replica FDU showed that the affect is negligible.

A 1.12kV, 3mm diameter parallel 532nm beam will penetrate the lubricant up to 5mm with negligible absorption. 532nm light was found to be absorbed more readily by SAF-XO than 650nm fluorescent light. This is significant as it confirms that no absorption correction factors were required during calibration. For thicker films (greater than 5mm) a correction factor would be necessary to take into account absorption. Furthermore, the parallel beam will not damage the replica FDU housing.

The investigations explained in this chapter have lead to the creation of a calibration technique, which has shown that temperature and absorption over the thicknesses of lubricant expected can be neglected. A typical calibration curve is shown in Figure 5.18.

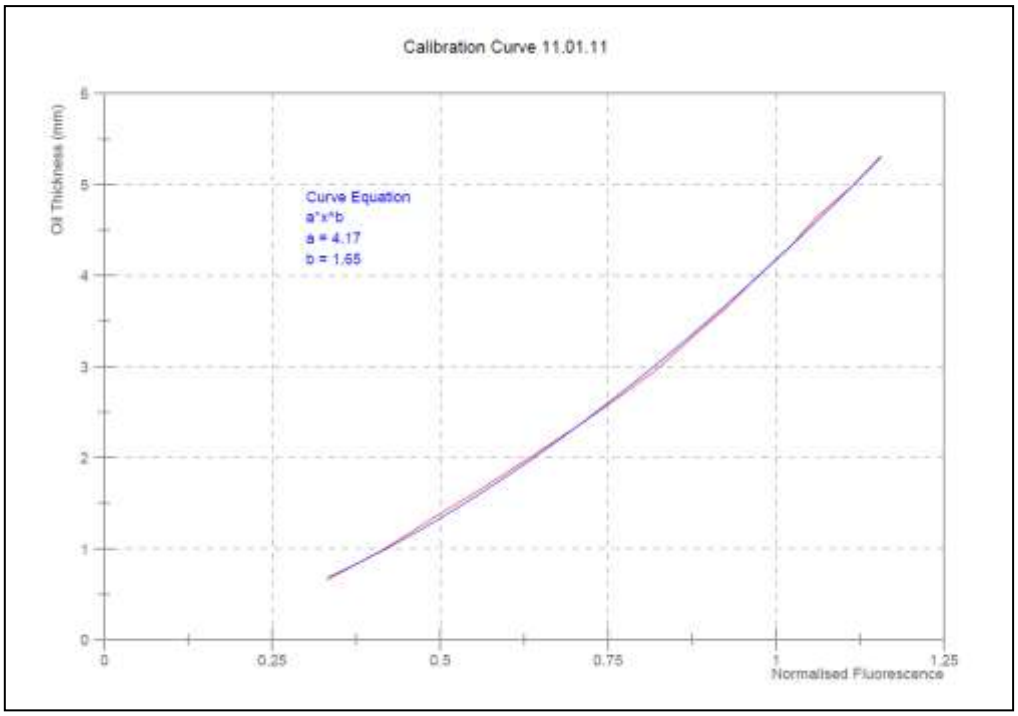

Figure 5.18 - Calibration curve example

CHAPTER 6
FDU LUBRICANT THICKNESS MEASUREMENTS

Chapter 6 describes the lubricant flow behaviour within the FDU through flow visualisation and discusses suitable locations for lubricant thickness measurement. Also discussed in this chapter are the uncertainties and errors that are part of the experiment, and how to capture these uncertainties within the results. The main body of this chapter is focused on the lubricant thickness data acquired from within the FDU at different rotational speeds and fill volumes.

6 FDU Lubricant Thickness Measurements

In the previous chapters, the focus has been on the understanding and optimisation of the LIF lubricant thickness measurement. This chapter will focus on the application of the LIF technique to the replica FDU and resultant LIF data.

Before thickness measurements were taken inside the replica FDU, flow visualisation was carried out to identify areas of interest within the housing, for example at the breather where lubricant expulsion is an on-going issue. In addition, areas where LIF could be applied with minimal interference from splashing lubricant and distortions from the profile of the housing, needed to be identified; this work is also presented in this chapter. Once suitable areas for lubricant thickness measurement were identified, wedge calibration was carried out as previously described and fluorescence data were taken from the crown wheel. The methodology and results are presented in the final sections of this chapter.

6.1 Flow Visualisation

LIF is a valuable tool for the measurement of film thicknesses provided the path to the location of the film is not obscured. Flow visualisation is a useful way to identify areas of interest by studying flow patterns directly, and helps to show clear paths to these areas. High speed imaging has been used widely in the assessment of fast moving bodies, and so is a useful way to observe flow structure in the clear FDU housing. An additional benefit of high speed imaging is that the playback speed can be altered, providing the possibility to capture details which would normally be missed in real-time.

Observations of the lubricant movement within the FDU were made at a number of different equivalent road speeds to see how the flow structure and splashing changed with increasing rotational speed of the gears. The findings from the 4000 frames per second imaging footage, from a Photron Fastcam camera, will be discussed in this section.

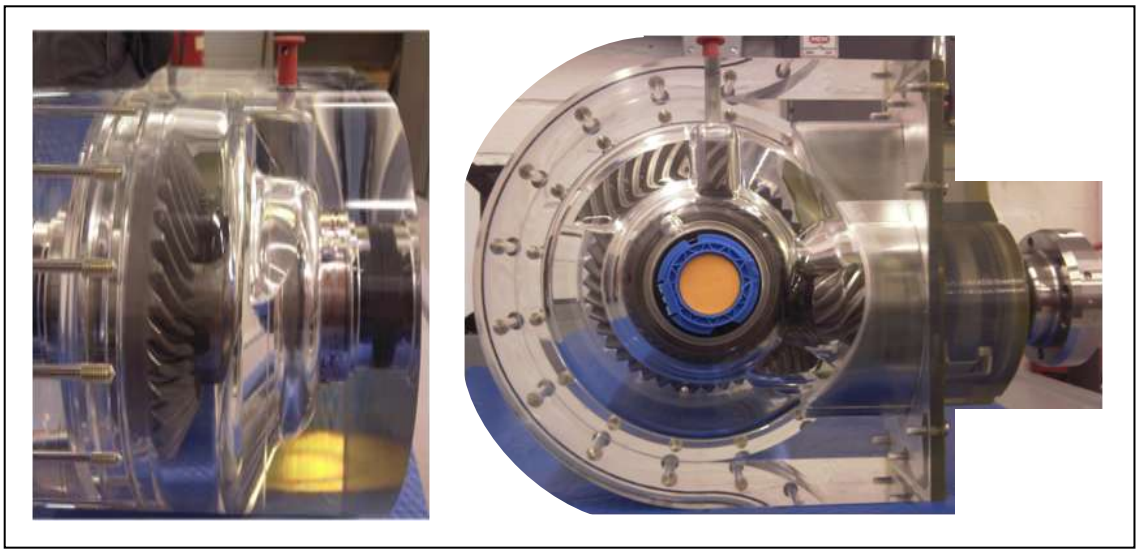

Figure 6.1 - FDU Housing

Even before lubricant was added to the replica FDU, it was apparent that careful selection of optical access points was necessary. In Figure 6.1, the effects of the non-uniform housing profile were seen clearly, where the crown wheel looked as if it was not circular. This effect was most noticeable at the bottom of the housing, whereas the crown wheel looked normal through the top section. The wall of the housing that surrounded the breather was the thinnest and so little distortion was noted. The housing at the curved side where the crown wheel was visible side-on showed no sign of optical distortion at the crown wheel.

Table 6-1 – Crown wheel to road speed conversions

Crown Wheel Speed (rpm)	Road Speed (km/h)	Road Speed (mph)
50	6.51	4.04
75	9.76	6.06
99	12.88	8.00
100	13.01	8.08
200	26.02	16.16
300	39.04	24.24
322	41.90	26.02
371	48.27	29.98
400	52.05	32.32
500	65.06	40.40
510	66.36	41.21
550	71.57	44.44
600	78.07	48.48
700	91.08	56.56
743	96.68	60.04
800	104.09	64.64
900	117.11	72.72
1000	130.12	80.80

At speeds approaching 10km/h equivalent road speed (please refer to Table 6-1 for more crown wheel to road speed conversions), noticeable aeration of the oil was visible, with splashing around the pinion increasing with speed. In addition, the lubricant formed a narrow channel (Figure 6.2(a) & (c)), parallel to the crown wheel on the housing. The length of the channel of lubricant increased with speed and followed the rotational direction of the crown wheel.

At approximately 17-20km/h, the oil sump level formed a series of steps, with the highest beneath the pinion (Figure 6.2 (b) & (d)). This may have been partially due to the internal profile of the housing.

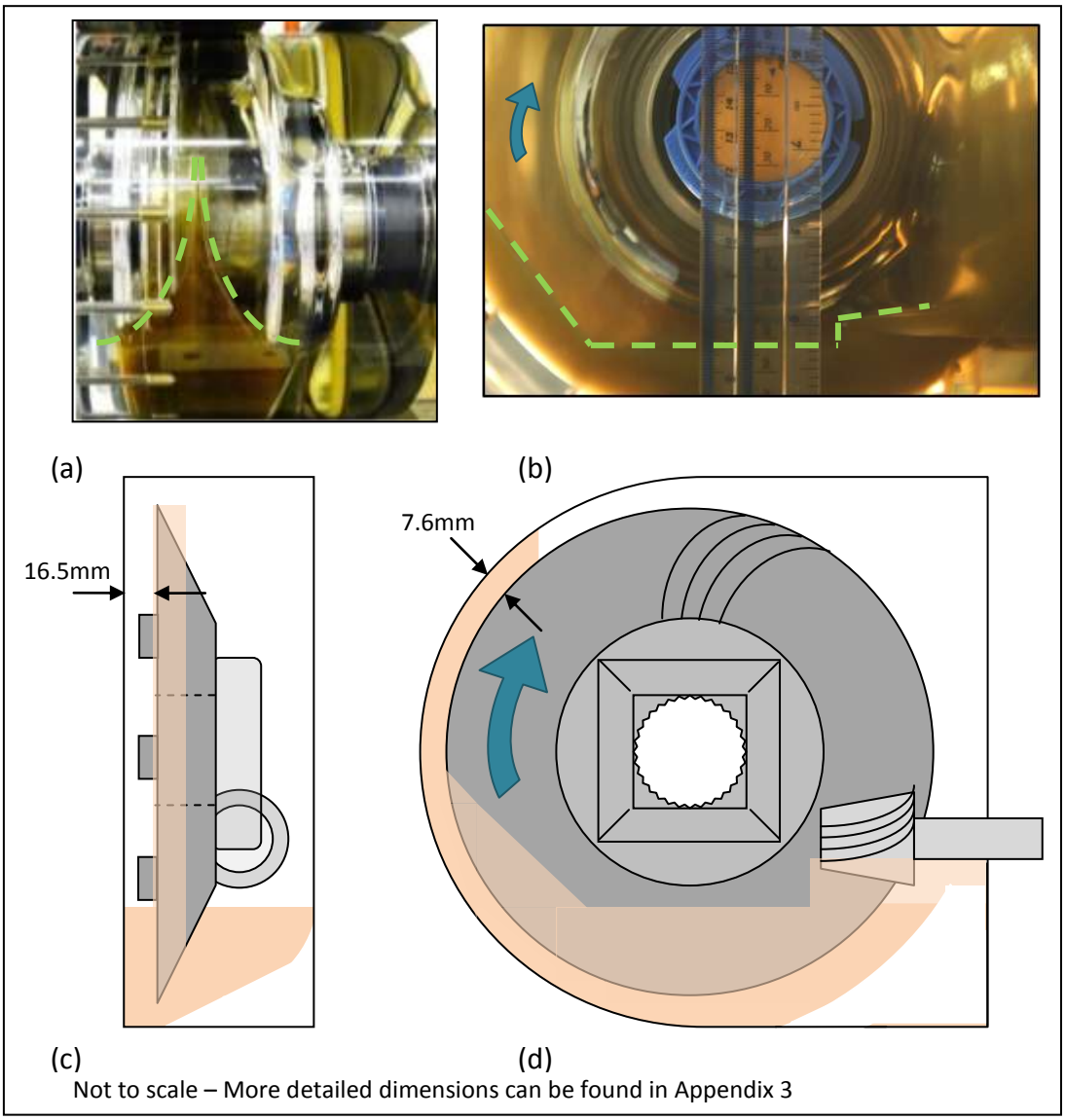

Figure 6.2 - Replica FDU dimensions

In Figure 6.3, the gears on the crown wheel are clearly visible as there is very little lubricant flow on the housing. This is particularly useful, in terms of optical access for LIF measurements, as lubricant on the housing fluoresces and prevents the laser reaching the crown wheel.

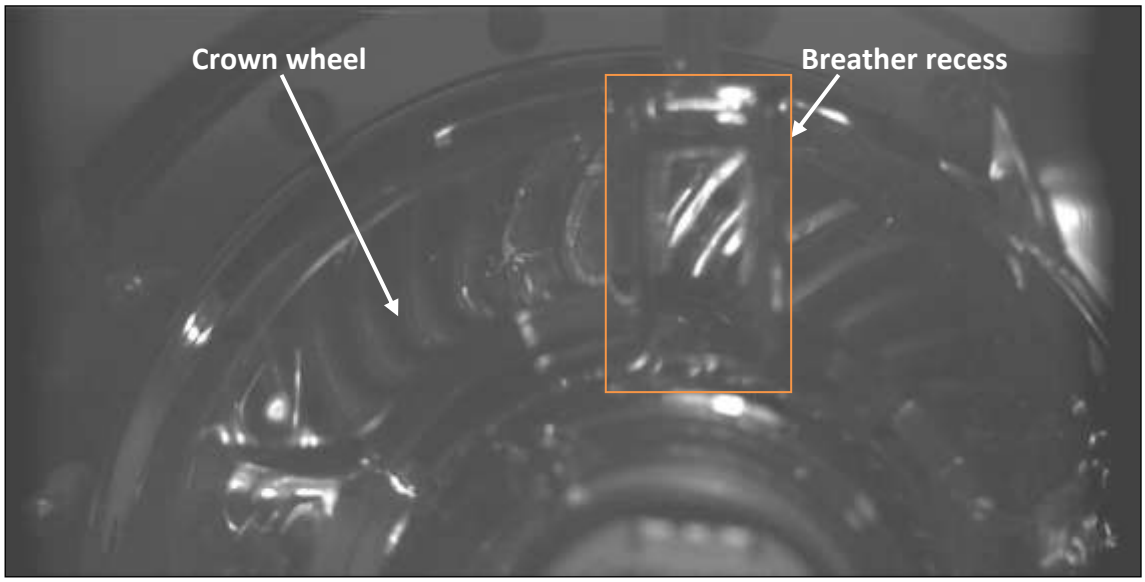

Figure 6.3 - Replica FDU top section at 19km/h

At around 38km/h, stagnant lubricant boundaries with eddies appeared parallel to the crown wheel, which indicated the lubricant was being re-circulated within the sump. Also at this speed, the sump appeared to remain at a constant same level (no step in level beneath the pinion gear); no further changes in the level were noted. Approaching 48km/h, significant flow around the crown wheel was observed (Figure 6.4), with the lubricant channel which ran up the wall of the casing, now encircling the casing completely. Bubbles began to grow, disperse and grow again near the stagnant regions. Obtaining LIF measurements on the crown wheel at this speed and above would not be possible due to the amount of lubricant both on the housing, and in motion between the housing at the crown wheel. However, the breather recess provided a break in the lubricant flow over the housing as shown in Figure 6.4. This break in the cascading lubricant was sufficient to allow the laser beam to reach the crown wheel and also to retrieve a fluorescent signal, provided the rotational speed was not high enough to cause lubricant splash between the housing and gear.

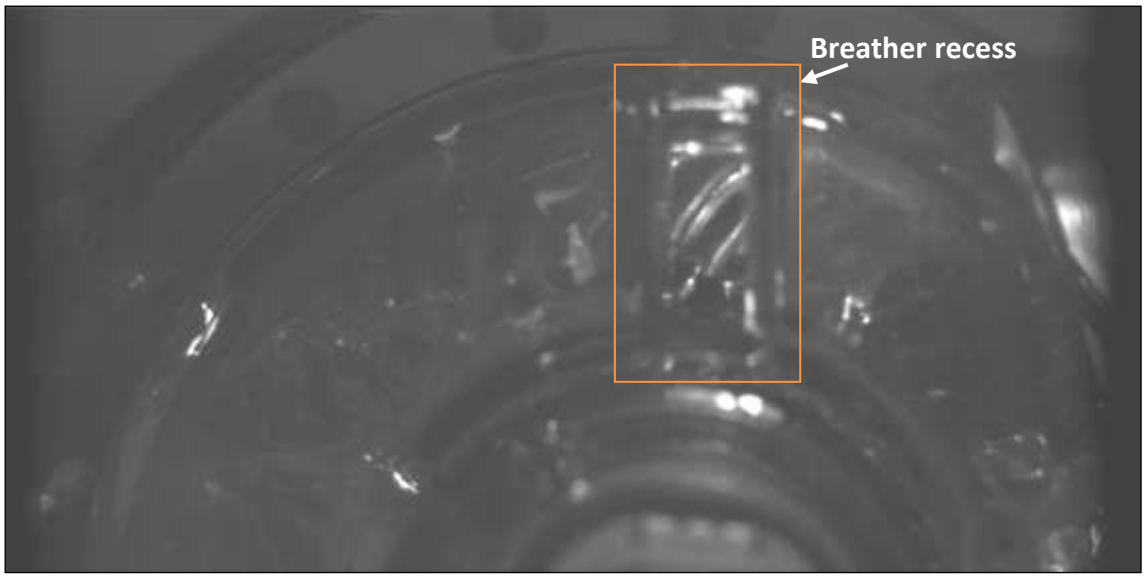

Figure 6.4 - Replica FDU top section at 42km/h

At 66km/h, a constant cascade of lubricant down the breather-side of the housing had developed and appeared to have a wave action. The waves were not limited to the wall opposite the crown wheel teeth as shown in Figure 6.5, but also included waves of oil entering the breather recess. The waves in the breather recess at different rotational speeds can be seen more clearly in Figure 6.6, where the images were taken at 90° to the breather face through the curved side of the housing.

At a road speed of 42km/h, the waves of lubricant did not lap across the breather recess. The curved edge of the wave front at this speed is highlighted in Figure 6.6 with an orange line. When compared with the position of the wave front at a road speed of 66km/h, it can be seen that the lubricant moves further into the breather recess as road speed increases. This behaviour has not been documented before now and suggests that the lapping of lubricant into the breather may be a contributing factor in breather expulsion. In general, much recirculation of oil and churning was observed. By 77km/h, waves were splashing from the breather side of the casing, over the top of the crown wheel, to the cover-side.

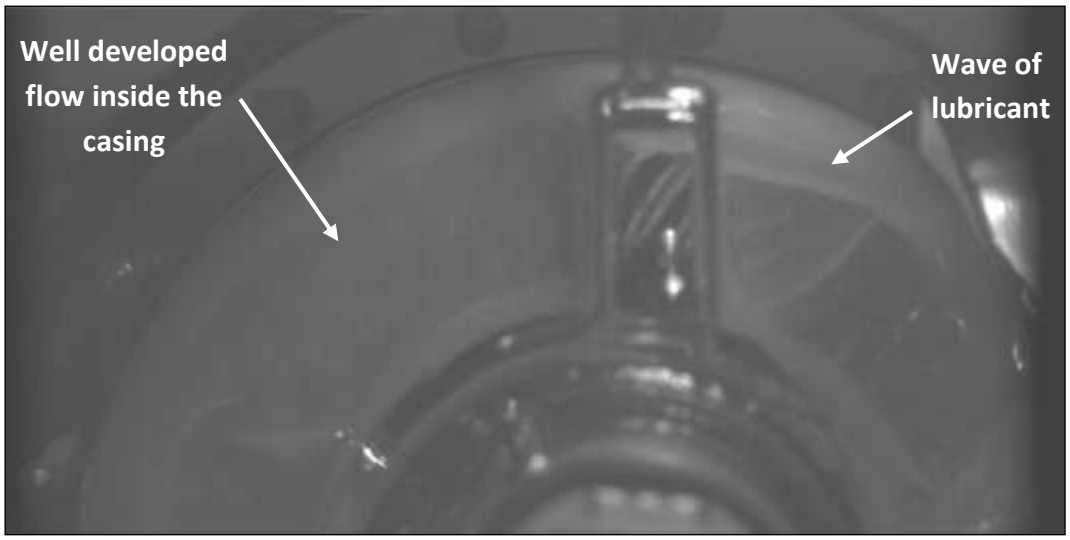

Figure 6.5 - Replica FDU top section at 66km/h

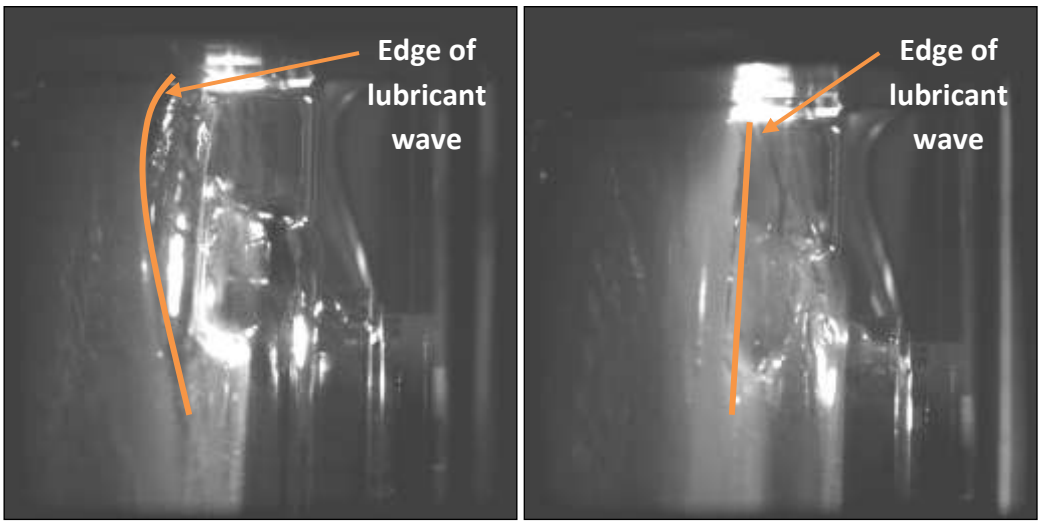

Figure 6.6 - Replica FDU breather section at 42km/h (left) and 66km/h (right)

From this high speed imaging footage, the highly chaotic movement of a lubricant in a FDU can be seen. From very low speeds, approximately 15km/h, the lubricant forms a channel encircling the crown wheel. The formation of this makes it impossible to take laser measurements on the edge of the crown wheel.

Observations from the rear of the crown wheel showed that there appeared to be very little splash and no lubricant covering the FDU housing until speeds exceeded approximately 50km/h. Coupling this with the uniform thickness of the FDU housing made the rear of the crown wheel an ideal location for measurements of lubricant thickness to be taken.

Lubricant thickness measurements from the edge of the crown wheel were not possible above a few revolutions per minute with the LIF technique, due to the channel of entrained lubricant that filled the clearance gap between the housing and crown wheel (approximately 7.6mm).

Both sides of the crown wheel have been identified as areas where LIF measurements of the lubricant thickness can be carried out as a result of this qualitative visualisation. Measurements up to the equivalent of approximately 50km/h road speed were possible, above which the splashing of the lubricant began to interfere with the incoming laser beam and resultant data.

6.1.1 Temperature Effect on Lubricant Behaviour

As the temperature of the lubricant increases, the viscosity decreases. This change in viscosity has an effect on the overall behaviour of the lubricant. In section **Error! Reference source not found.**, the change in viscosity with temperature was described. To assess the behavioural differences of low and high viscosity lubricant inside the FDU, a clear base oil from Castrol was used in place of the usual Castrol SAF-XO lubricant. The low viscosity Castrol lubricant has the same viscosity at room temperature as SAF-XO at 100°C, enabling simulation of high temperature, low viscosity behaviour at room temperature. A summary of the viscosities can be found in Table 6-2.

Table 6-2 - Castrol lubricant kinematic viscosities (Burlison and Sherwood, 2010)

Lubricant	Kinematic Viscosity
Castrol SAF-XO 75W-90	103.7 mm^2/s (103.7 cSt) at 40°C
	15.7 mm^2/s (15.7 cSt) at 100°C
2010 Clear Lubricant	15 mm^2/s (15 cSt) at 40°C
	3.4 mm^2/s (3.4 cSt) at 100°C

The result of this change in viscosity was a large amount of splashing and more lubricant in motion at lower rotational speeds. Compared with SAF-XO at room temperature, the behaviour of the low viscosity Castrol lubricant shared similarities with SAF-XO with regard to flow patterns. However, the flow patterns and splash seen at an equivalent road speed of 60km/h for SAF-XO were seen at a much slower road speed in the low viscosity lubricant, showing an apparent shift in the lubricant movement to rotational speed. An example of the SAF-XO splash within the FDU is given in Figure 6.7.

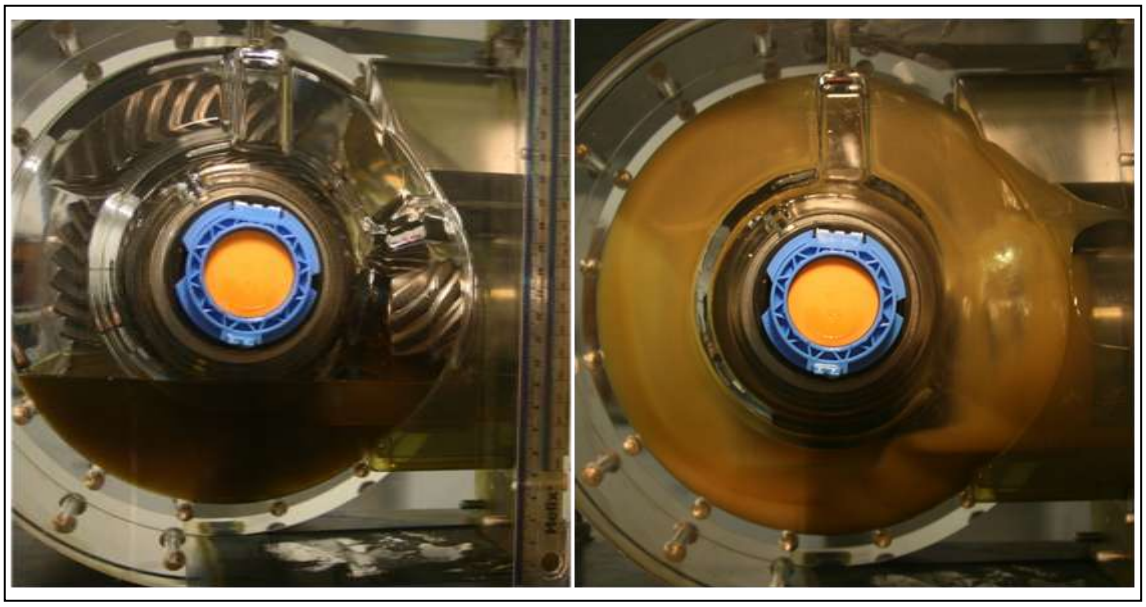

Figure 6.7 - Example of lubricant splash within the FDU

While the SAF-XO in the replica FDU will not reach 100°C, it is possible for the lubricant to reach this temperature in the vehicle X150 FDU. It is therefore useful to bear in mind that the behaviour of the lubricant does change with temperature. Further studies on the low viscosity Castrol lubricant and SAF-XO have been carried out by Burlison (Burlison and Sherwood, 2010) and Pigenel.(Pigenel, 2009).

6.2 Discussion of Uncertainties and Errors

Throughout this research, assumptions and limitations with the experimental set-up and methodology occur, resulting in uncertainties and potential errors. These are a normal part of experimentation, and it is essential that the extent of the errors are known. In this section, the errors and uncertainties encountered during calibration and measurement of lubricant film thicknesses will be discussed.

Any question of uncertainty during research and experimentation leads to doubt in the quality of the results. Up to this point, the uncertainties and errors have been largely overlooked. The aim of this section is to consider them in more detail and discuss the impact these errors have on the results given.

Uncertainty and error analysis has been covered in a number of texts. The summary presented here is taken from a number of sources, namely Taylor (Taylor, 1997; Mendenhall and Sincich, 2007), Moffat (Moffat, 1988) and Mendenhall (Mendenhall and Sincich, 2007).

6.2.1 Identification of True Value

During experimentation, errors and uncertainties prevent measurement of the "true" value. The "true" value of the desired measurement can be stated mathematically as:

$$X_{true} = X_{measured} \pm \delta X \tag{6.1}$$

Where $X_{measured}$is the best estimate of X_{true}, and δX is a known error (Moffat, 1988). Solution of Equation (**6.1** is based on a known value of δX, however in practice, this error is often unknown as it is dependent on a combination of errors and uncertainties. Applying this logic to fluorescence, "true" fluorescence can be expressed as:

$$F_{true} = F_{measured} \pm \left(\delta F_{laser} + \delta F_{temp} + \delta F_{abs} + \delta F_{background} + \delta F_{PM}\right) \tag{6.2}$$

Where δF_{laser}, δF_{temp}, δF_{abs}, $\delta F_{background}$ and δF_{PM} are uncertainties relating to the laser, temperature effects, absorption, background fluorescence and photomultiplier respectively.

In chapter 4, laser power variability was discussed and normalisation was carried out to correct the variability that occurred. In chapter 5, temperature and absorption were investigated and it was concluded that these could be considered negligible over the range of lubricant thicknesses and temperatures expected in the replica FDU. The

background fluorescence was recorded and corrected for during post processing. This leaves the photomultiplier as the main outstanding error within the system.

The errors within the photomultiplier measurements can be thought of as a combination of the uncertainties between the photomultiplier and received light, the connection between the photomultiplier and the cable, the connection between the cable and the NI-PXI5124 acquisition system and also between the acquisition system and computer.

$$\delta F_{PM} = \delta F_{PM\ error} + \delta F_{PX5124\ error} \delta F_{PM} = 1\% + 0.78\% \tag{6.3}$$

For the intrinsic photomultiplier uncertainty, $\delta F_{PM\ error}$, a conservative estimate of 1% is given as it is unclear from the manufacturers documentation what the exact value should be. The uncertainty for PXI5152 has been calculated at 0.78% based on NI data sheet values of maximum volt range sensitivity of 39mV and a maximum voltage of 5V. In the following section a number of uncertainties, specific to the application of LIF to the FDU, will be considered.

6.2.2 LIF Technique Uncertainties

Errors and uncertainties fall in to two distinct categories; systematic and random. Systematic uncertainties affect the accuracy, while random errors affect the precision (Pengra, 2009). The difference between precision and accuracy is shown in Figure 6.8.

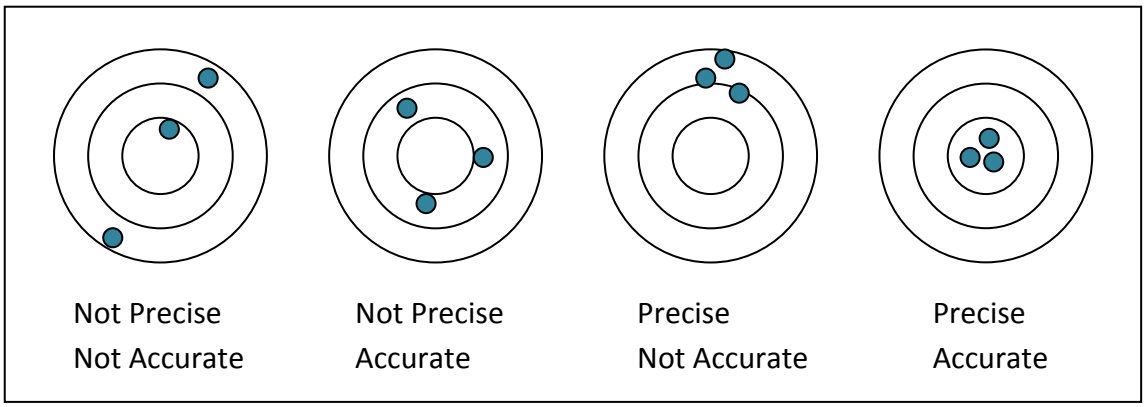

Figure 6.8 - Precision and Accuracy

An ideal experiment would involve no uncertainty, however as this is not possible, the aim is to keep uncertainties to a minimum and record them so a value for δX can be reached. As δX is an estimation of error, experimental uncertainties should be rounded to one significant figure (Taylor, 1997). A list of additional uncertainties

encountered in LIF measurement of lubricant thicknesses is given in Table 6-3. The uncertainties listed are based on the tools used to measure each quantity. Although the distance from the laser to the crown wheel was also measured using a millimetre scale, additional uncertainty has been added to this quantity as the distortion from the housing made it more difficult to be certain of the exact distance. The uncertainty given to the beam diameter is based on the machining tolerance of the diameter of the beam restrictor.

Table 6-3- Table of uncertainties and errors

Location of Uncertainty	**Uncertainty ±**
Lab-jack scale (millimetre scale)	0.5mm
Distance from laser to wedge (millimetre scale)	0.5mm
Distance from laser to crown wheel	1mm
Laser power (As stated by manufacturer (Rev.D 02/05))	6%
Beam diameter 3mm	0.025mm
Laser mode noise	0.03mm

The combination of the wedge dimensions and beam diameter bring out an additional uncertainty. By using a restricted 3mm diameter beam, the fluorescence measurement is not actually a point measurement, but a volume irradiated with the laser. This means there was a change in the thickness under the beam as shown diagrammatically in Figure 6.9.

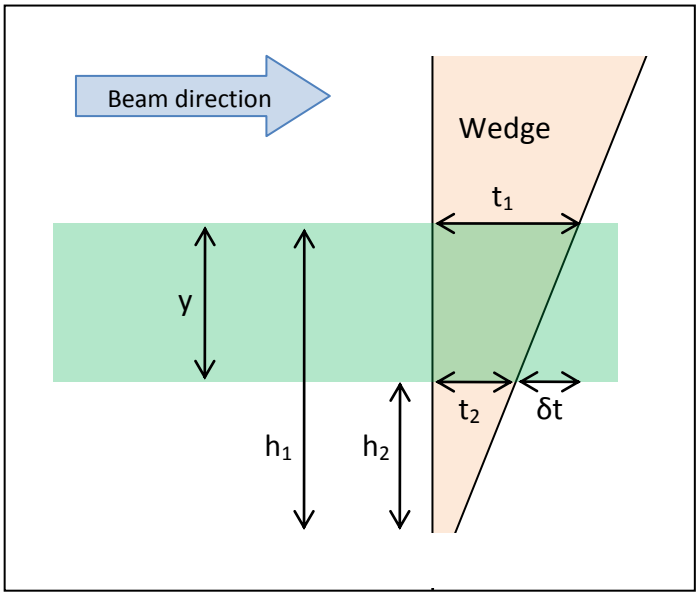

Figure 6.9 - Lubricant thickness variation across laser diameter

$$t = 2\left(\frac{h}{181.2} \times 2.45\right) + 0.35 \tag{6.4}$$

$$\delta t = t_1 - t_2 \tag{6.5}$$

If y is equal to 1mm, equations (**6.4** and (**6.5** can be used to show that the change in lubricant thickness is 0.027mm, so over the diameter of the laser (3mm), the change in lubricant thickness is 0.081mm across the laser contact area (derivation in Appendix 2).

The laser mode noise can be calculated using the calibration curve at the end of Chapter 5 as follows, where y is lubricant thickness, x is normalised fluorescence (0.2758 mean and 0.0037 standard deviation) and a and b are constants:

$$\begin{gathered} y = ax^b \\ y_1 = 4.17 \times (0.2758 - 0.0037)^{1.65} = 0.487 \\ y_2 = 4.17 \times (0.2758 + 0.0037)^{1.65} = 0.517 \\ y_2 - y_1 = 0.03 \end{gathered} \tag{6.6}$$

6.2.3 Statistical Confidence

Identification and calculation of all possible uncertainties and errors within a system is complex, as discussed in sections 0 and 6.2.2. The complete list of uncertainties associated with this technique is given in Equation (6.8, with δF_{wedge} encompassing the uncertainties listed in Table 6-3.

$$\begin{aligned} \delta F_{total} &= \delta F_{laser} + \delta F_{background} + \delta F_{PM} + \delta F_{wedge} \\ \delta F_{total} &= 6 + 1 + 0.78 \\ \delta F_{total} &= 7.8\% \end{aligned} \tag{6.7}$$

If these uncertainties were to be combined to create a single value for δF_{total}, and applied to the measurement data, the outcome would be a conservative estimate of the true fluorescence. Fortunately, Taylor (Taylor, 1997)(Taylor, 1997; Mendenhall and Sincich, 2007) has shown that it is feasible to account for the majority of errors by simply considering the mean, $\bar{X}$, and standard deviation, σ, as shown in Equation (6.8. Essentially all the errors listed can be captured by Equation (6.8) with a 95% confidence level.

$$X = \bar{X} \pm 2\sigma \tag{6.8}$$

It is important to note that this relationship can only be used when multiple sets of data are acquired, so in the case of fluorescence, there are 60 sets of data for the 60 measured pulses.

6.3 FDU Lubricant Thickness Measurement

For FDU measurement collection, the equipment set-up was as previously described, but with the wedge set-up in front of the replica FDU. After calibration was complete, the wedge was lowered beneath the laser path, allowing optical access to the replica FDU. To maintain equal distance between the lubricant and optics the same for both calibration and FDU measurements, the optics were mounted onto a plate, that was repositioned to allow fast and simple adjustment between calibration wedge and FDU measurements.

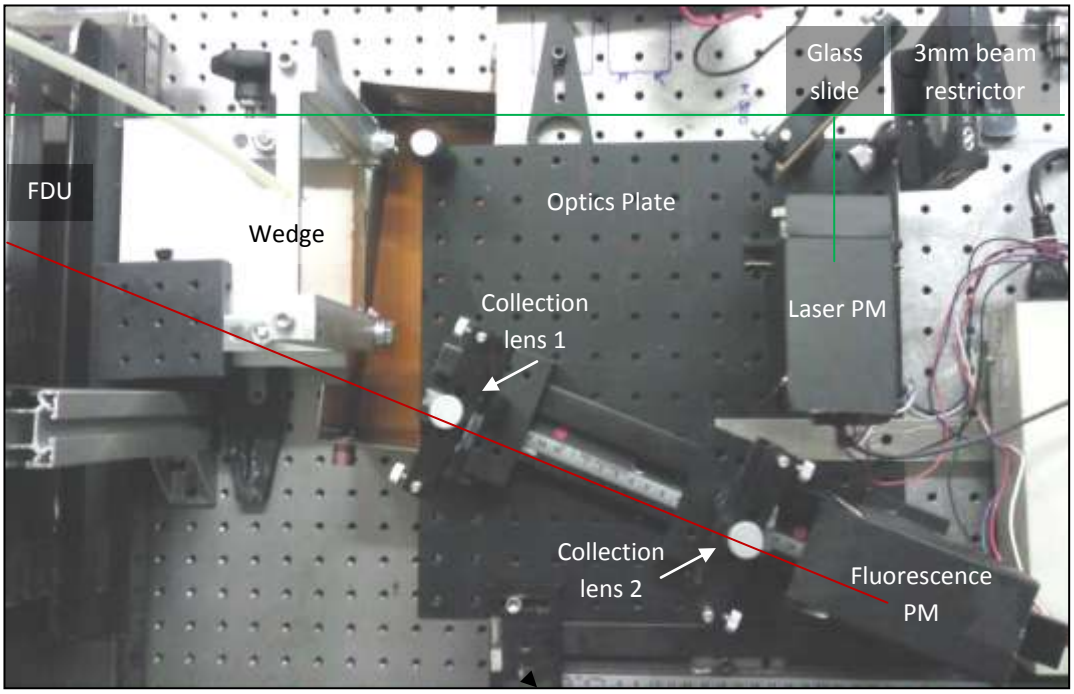

Figure 6.10 - Optics set-up for FDU measurements

The optical layout is shown in Figure 6.10, with a green line to show the path of the laser beam and a red line to show the collection path for the fluorescence. A 532nm filter and a 600nm long-pass filter covered the entrances to the laser monitoring and fluorescence photomultipliers respectively.

6.3.1 Laser Triggering

Timing of the laser pulses, with respect to position on the crown wheel, was carried out initially by fixing a mirror to the pinion input shaft and reflecting light from a He-Ne laser off the mirror once per shaft rotation. The light from the He-Ne was reflected from the mirror and into a photomultiplier connected to an oscilloscope. The signal spikes generated at each rotation together with the gear ratio were used to calculate the number of crown wheel rotations per minute and then the equivalent road speed. The signal from the photomultiplier however was not able to trigger the Surelite laser, so a rotary encoder was introduced.

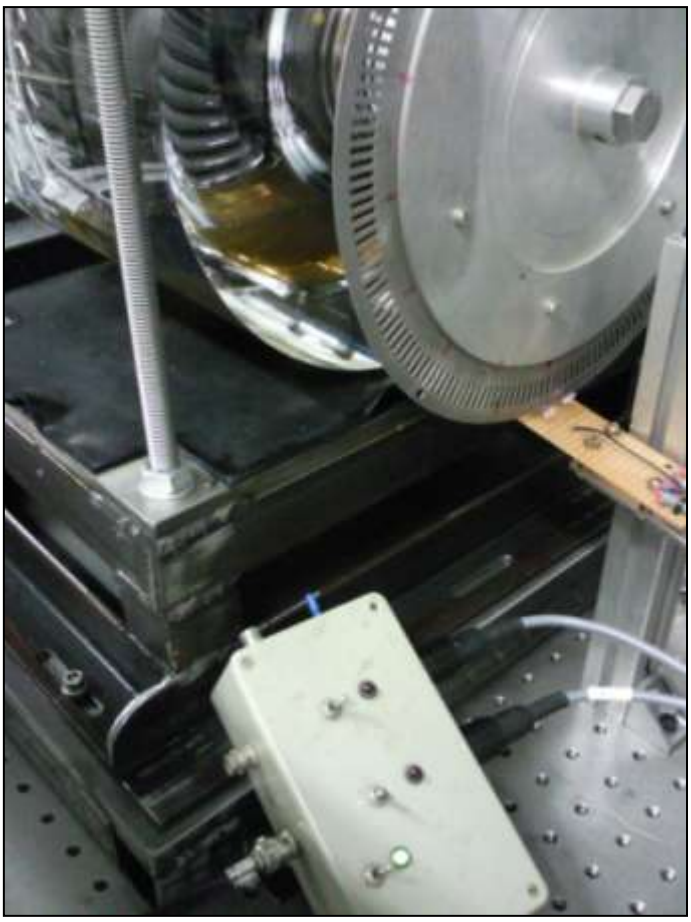

Figure 6.11 - Rotary encoder set-up

The rotary encoder system comprised a disc with a hole, a transmitter and a sensor, which triggered when the hole and sensor were aligned once per rotation (Figure 6.11). The encoder disc was mounted on a splined shaft that was fitted directly to the crown wheel spline, removing the need for conversion from pinion rotation speed. The signal from the encoder was used successfully to trigger the Surelite laser. The corresponding laser pulse rates and equivalent road speeds to the crown wheel rotation speeds can be found in Appendix 3.

6.3.2 Crown Wheel Measurements - Calibration

The measurements taken from the FDU fall into two main categories: data from the rear of the crown wheel (cover side) and data from the front or tooth side (carrier side). Within these two categories, a further two areas are investigated: firstly, the effect of rotational speed on lubricant thickness and secondly, the effect of fill volume on lubricant thickness. The aim of this data is to add numerical values to the visualisation and qualitative data. The gathered data was processed using National Instruments DIAdem, which is capable of dealing with greater volumes of data than Excel. The data was post processed within DIAdem using scripts to make processing quicker. The scripts used can be found in Appendix 4.

Calibration was carried out using the wedge with average fluorescence measurements taken in 10mm increments up to 150mm. The fluorescence data were used to create a calibration curve, which was in turn used to calculate the thickness of the lubricant on the crown wheel. A best-fit curve of the form $y = ax^b$, shown in Figure 6.12, was found to closely follow the averaged wedge measurements, and so was used for all calibration. The red line shows the measurements from the wedge while the blue shows the best-fit curve, which follows the wedge data closely.

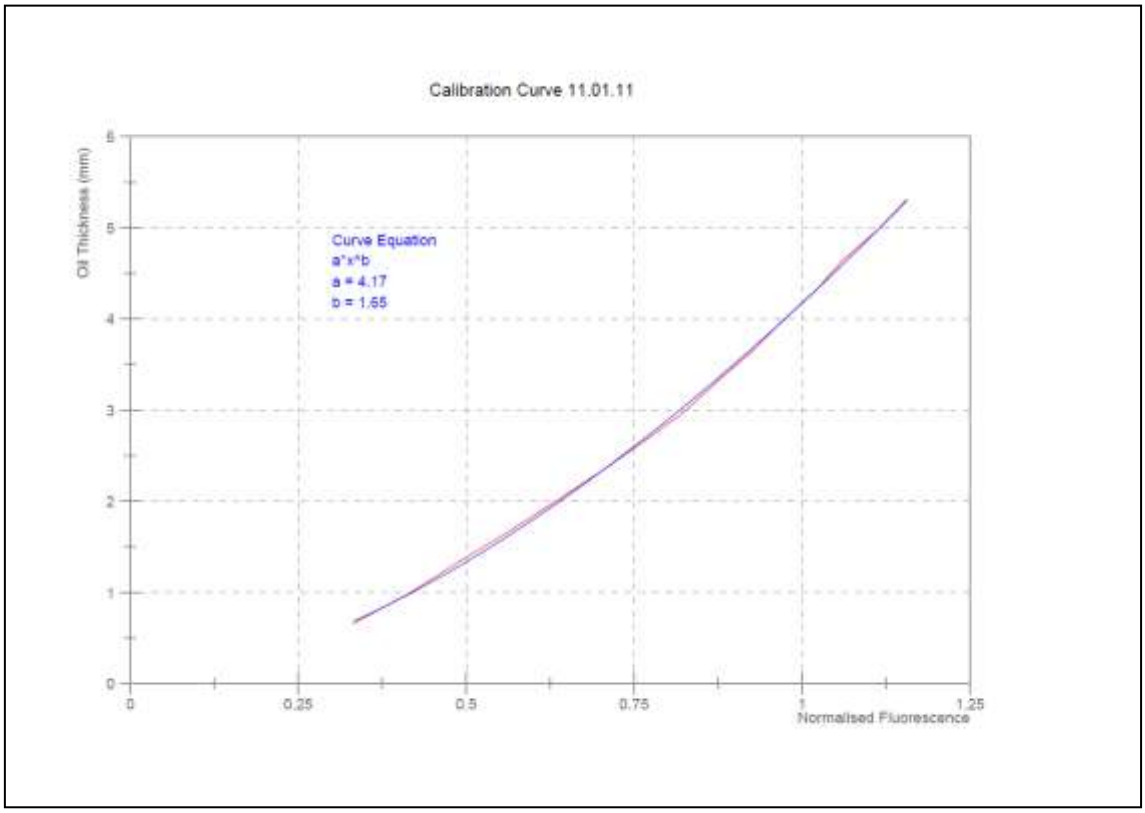

Figure 6.12 - Calibration curve example

Calibration was also carried out after FDU measurements had been taken to check for any changes. Frequently, a shift in the calibration curves was noted, so both calibration curves were used to analyse the FDU data, resulting in upper and lower bands for the measured thicknesses. An example of the shift in calibration curves can be found in Figure 6.13.

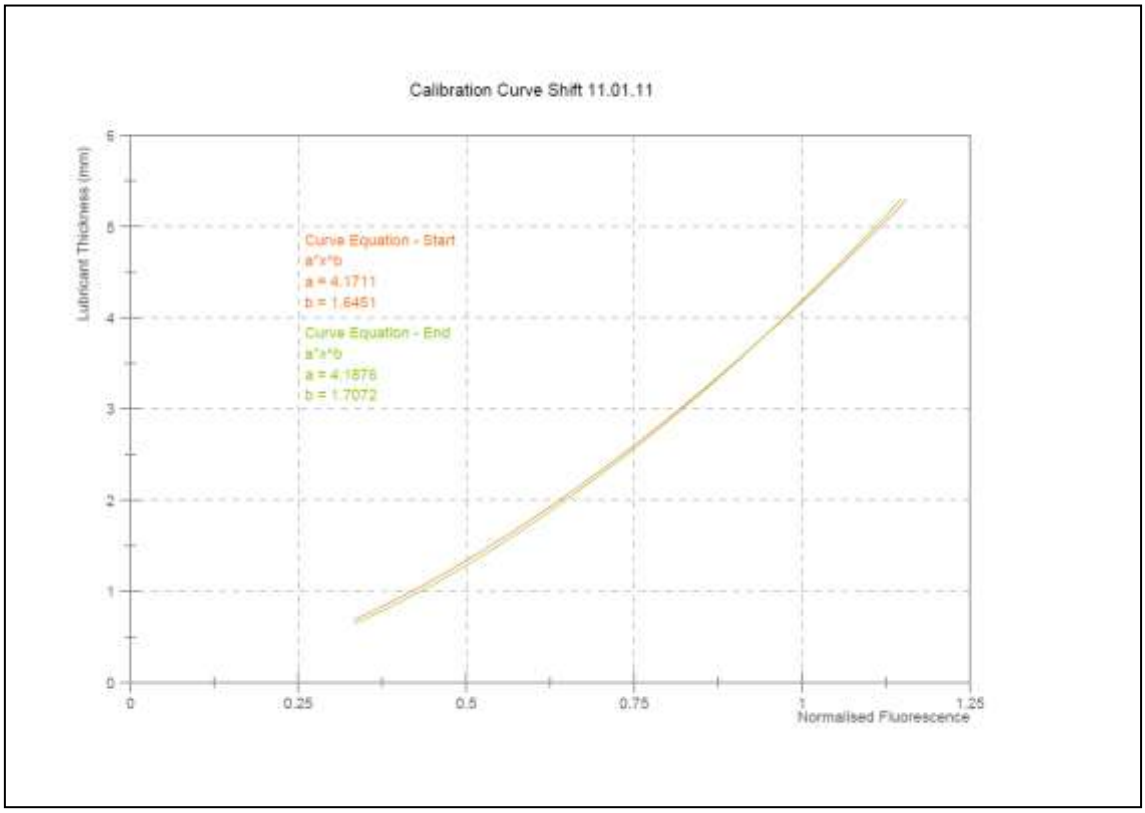

Figure 6.13 - Calibration curve shift example

The possible reasons for the difference between the calibration curves from before and after measurements were taken in the replica FDU are discussed in Section 6.2.

6.3.3 Hypothesis Testing

In Section 0, it was shown that we can calculate the true value of a quantity using the mean and standard deviation. Here we will use this to show that the first and second calibrations are statistically equivalent. The intention is to show that while it is good practice to calibrate systems before and after experimentation, the second calibration data can be used to simply check that no significant changes occurred during experimentation.

Consider the data from Figure 6.13. If Equation (6.8) is applied to the data acquired from the initial pre-experiment calibration, an upper and lower boundary for the true value is generated. That is to say that the true value of fluorescence lies between the two boundaries. When compared with the fluorescence data from the post-experiment calibration (Table 6-4), it can be show that for 13 out of 15 points, the measurement falls within the same true value boundaries.

Table 6-4 - Pre- and post-experiment calibration data

Lubricant Thickness (mm)	Fluorescence Mean Before Experiment $\bar{X}$	Standard Deviation σ	"True Value" Upper Boundary	"True Value" Lower Boundary	Fluorescence Mean After Experiment
0.66	0.33	0.01	0.34	0.32	0.33
0.99	0.42	0.01	0.43	0.40	0.42
1.33	0.49	0.01	0.50	0.48	0.49
1.66	0.56	0.01	0.57	0.55	0.58
1.99	0.63	0.01	0.64	0.62	0.65
2.32	0.70	0.01	0.72	0.68	0.71
2.65	0.76	0.01	0.78	0.75	0.76
2.98	0.83	0.01	0.85	0.80	0.82
3.32	0.87	0.02	0.91	0.84	0.87
3.65	0.93	0.02	0.96	0.89	0.93
3.98	0.97	0.02	1.01	0.93	0.98
4.31	1.02	0.02	1.07	0.97	1.02
4.64	1.06	0.02	1.10	1.02	1.06
4.97	1.11	0.02	1.16	1.06	1.09
5.31	1.16	0.03	1.21	1.10	1.15

The initial and post-experiment calibration data have been compared and found to overlap. This indicates that it may be possible to consider these calibration data as statistically having no significant difference between them (Taylor, 1997). A hypothesis test can be carried out to prove this.

To begin the hypothesis test, a number of hypotheses, including a null hypothesis, are required: Null hypothesis H_N states that there will be no change between the initial and post-experiment calibration data.

$H_N: \bar{X}_1 = \bar{X}_2$

The alternate hypotheses state that the initial calibration is either greater or smaller than the post-experiment calibration.

$H_A: \bar{X}_1 > \bar{X}_2$
$H_A: \bar{X}_1 < \bar{X}_2$

As there is the possibility for the initial data to be higher or lower than the post-experiment data, this requires a two-tail test. For a 95% confidence level, a 0.025 value of t_{stat} is required, which represents 2.5% either side of mean. Similarly, for 99% confidence, a 0.005 value of t_{stat} is required. The statistical t_{stat} value is a function of the number of data sets available. Values from the Biometrika Tables for Statisticians (Pearson and Hartley, 1954) state that the t_{stat} values are 2.00 and 2.66 for 0.025 and 0.005 respectively, when there are 60 degrees of freedom (60 data sets).

The confidence interval is given by:

$$\bar{X} \pm t_{stat} s_{\bar{X}} \tag{6.9}$$

$$s_{\bar{X}} = \frac{\sigma}{\sqrt{n}} \tag{6.10}$$

Where $\bar{X}$ is the mean, $s_{\bar{X}}$ is the standard error, σ is standard deviation and n is the number of data sets. Applying these equations gives the following:

Table 6-5- Hypothesis testing confidence interval

Lubricant thickness (mm)	Fluorescence Mean Before Testing	Fluorescence Mean After Testing	Standard Deviation σ	95% confidence upper boundary	95% confidence lower boundary	99% confidence upper boundary	99% confidence lower boundary
0.66	0.332	0.334	0.01	0.336	0.332	0.336	0.331
2.65	0.764	0.763	0.01	0.765	0.762	0.766	0.761
5.31	1.156	1.149	0.02	1.154	1.144	1.156	1.143

Table 6-5 shows the mean fluorescence from the initial calibration, and both the 95% and 99% upper and lower boundaries. The three sets of data given are representative

of top, middle and bottom wedge thicknesses, and therefore cover the measured range.

As the initial mean falls within the upper and lower confidence boundaries, there is insufficient evidence to reject the null hypothesis, so it can be concluded that the pre- and post- experimental fluorescence data are statistically equivalent. Therefore, thickness measurement data will be carried out using only the first calibration data. Checking calibration after measurements is good practice, and should continue to be carried out.

6.4 Crown Wheel Results – Cover Side

Presented here are the lubricant thickness data collected from the rear surface of the crown wheel at different fill volumes and rotational speeds. The fill volume of the FDU is of interest for a number of reasons. Firstly, removing some of the lubricant could reduce churning losses and secondly, removing lubricant would result in a cost saving. There may also be a small weight saving associated.

The cover side of the crown wheel was selected for the first measurements in the replica FDU because the housing at this point was level both internally and externally, allowing optical access with minimal distortion. The approximate position of the laser contact with the crown wheel is marked with a yellow cross in Figure 6.14. The laser pulses were timed to take place between the bolt heads.

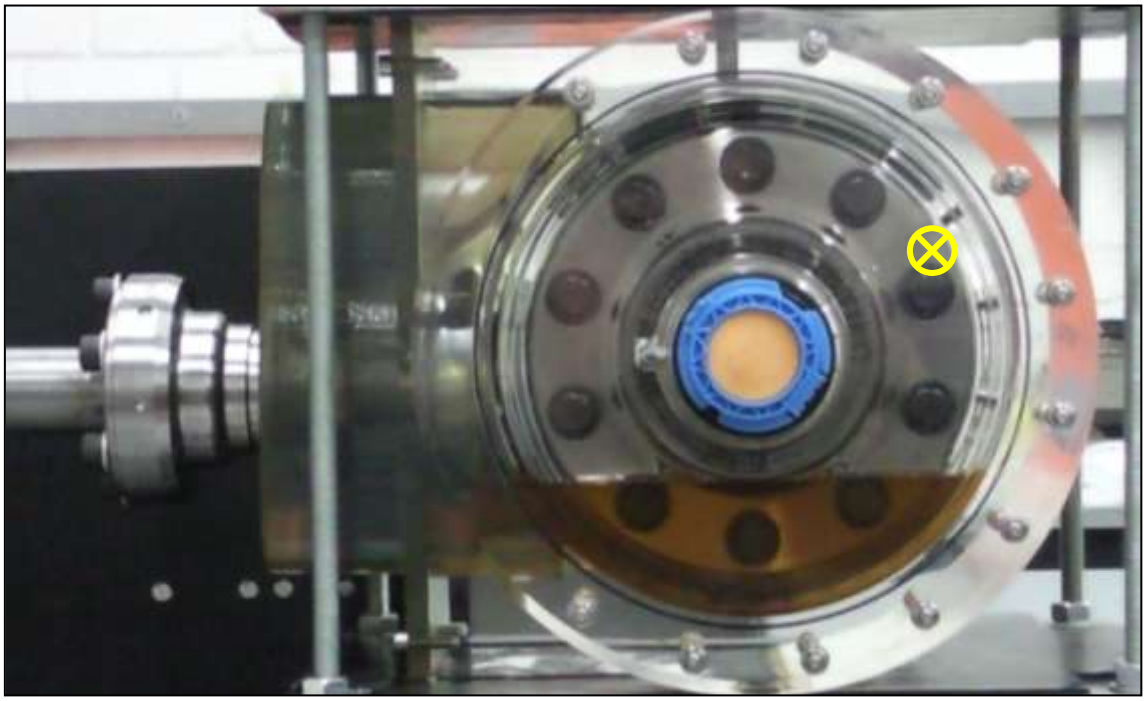

Figure 6.14 - Laser contact position on crown cover side

6.4.1 Speed Study

FDU thickness measurements from the crown wheel were taken in the same way as from the wedge, with the addition of taking background fluorescence readings. Background fluorescence measurements were taken as the housing was found to fluoresce with 532nm light. Due to the off axis optical set-up, the contribution of the housing fluorescence was minimal and easily corrected for. A background reading was taken at 0mph road speed and this was taken away from the fluorescence data from the rotating crown wheel.

Average fluorescence of 60 pulses were taken at equivalent road speeds from approximately 5mph up to 25mph. The speed of slowest rotation was limited by the laser triggering, as the laser would cut out below 1Hz. At speeds higher than 25mph, the lubricant splashing within the housing prevented clear access to the rear of the crown wheel.

The averages from each of the rotational speeds were combined to produce a graph showing the change in lubricant thickness with road speed, as shown in Figure 6.15. The two lines on the graph correspond to the start and end calibration data taken. The calibration curves for this and the following data can be found in Appendix 5.

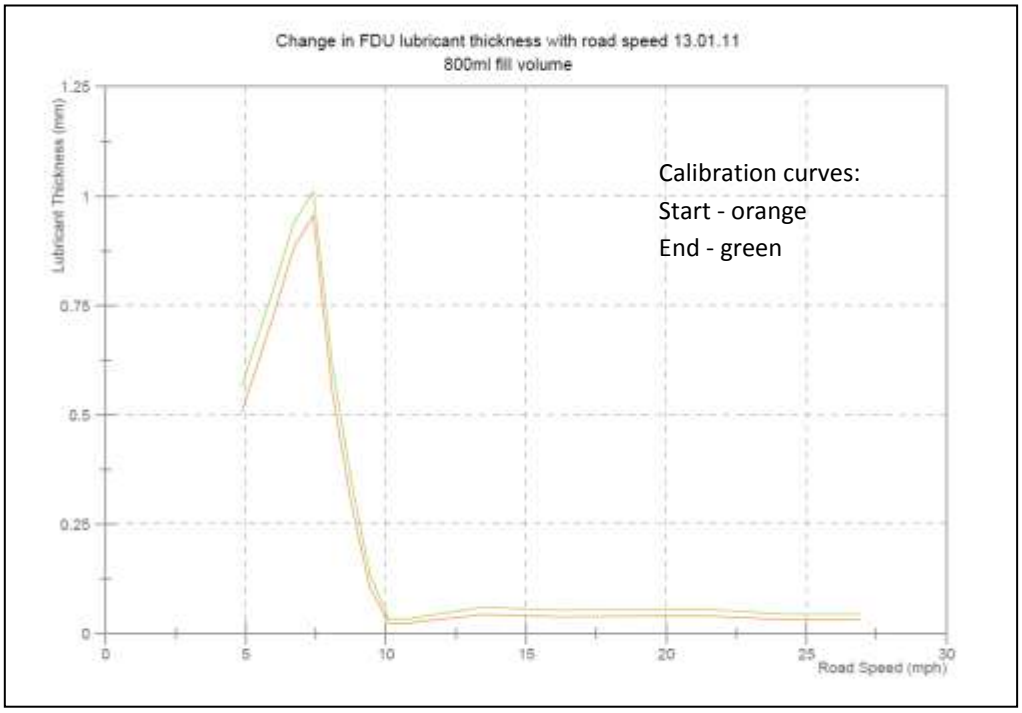

Figure 6.15 - Change in lubricant thickness with road speed

The first thing to note from Figure 6.15 is the peak in lubricant thickness that occurs around 7mph. The graph shows that as the road speed increases from 5 to 7mph, the

lubricant thickness increases up to 1mm. As the road speed increases beyond 7mph up to 25mph, the measured lubricant thickness on the crown wheel decreases rapidly before maintaining an almost constant lubricant thickness of less than 0.05mm. This peak at around 7 to 8mph suggests that an equilibrium is reached between the weight of the lubricant, adhesion of the lubricant to the crown wheel and the rotational speed of the crown wheel. Below 7mph, the lubricant runs off the gear surface back to the sump at the bottom of the housing, and above, the lubricant is pulled around with the gear and flung off onto the housing.

At this stage it is important to point out that any measurements from the crown wheel that are less than 0.3mm fall outside the minimum calibration thickness, and are therefore calculated from extrapolated data. In order to gain calibration data for thicknesses below 0.3mm, a stationary calibration system would have to be set up as the viscosity of SAF-XO at room temperature would be too great to allow the lubricant to flow through a smaller wedge. If the calibration lubricant was stationary, one of the shared similarities between the FDU and calibration set-up would be lost and bleaching may become a problem as there is no way to replenish the lubricant if there is no flow. As a result, extrapolated data has been used.

6.4.2 Fill Volume Study

The lubricant fill volume of a FDU or any geared system is important due to the impact on wear, cooling and churning as previously discussed. In this section, three lubricant volumes were assessed; 700ml, 800ml and 900ml, which is the recommended fill volume for this FDU.

As with the speed study, data was collected in increments from approximately 5mph up to 25mph, and repeated for each of the fill volumes stated. The results for the 700ml, 800ml and 900ml fill volumes are shown in Figure 6.16, Figure 6.17 and Figure 6.18 respectively. At 900ml and above 13mph, the splashing lubricant coated the surface of the housing, making it impossible to get a clear line of sight to and from the gear surface, so measurements were stopped at this point.

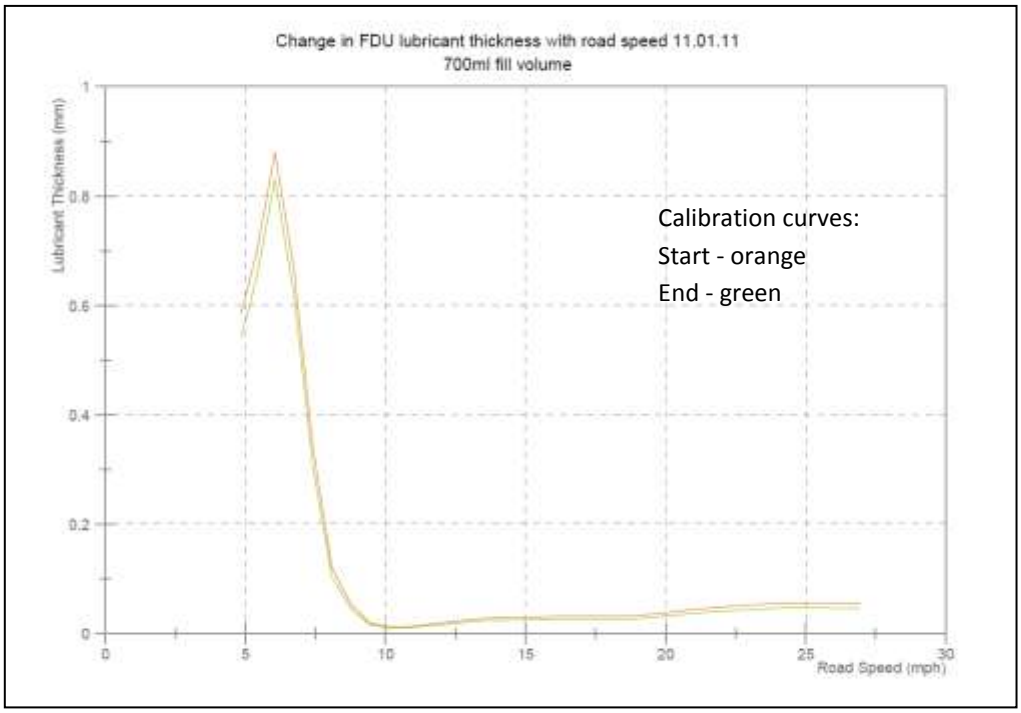

Figure 6.16 - Crown wheel cover side thickness measurements 700ml

Table 6-6 - Peak film thickness - Cover side

Fill Volume (ml)	Peak Film Thickness (mm)	Road Speed (mph)
700	0.80	6
800	0.95	7.4
900	1.75	8

Results from Table 6-6 clearly show that there is a proportional relationship between the fill volume and vehicle speed; increasing the fill volume of the FDU increases the road speed at which the peak lubricant thickness occurs.

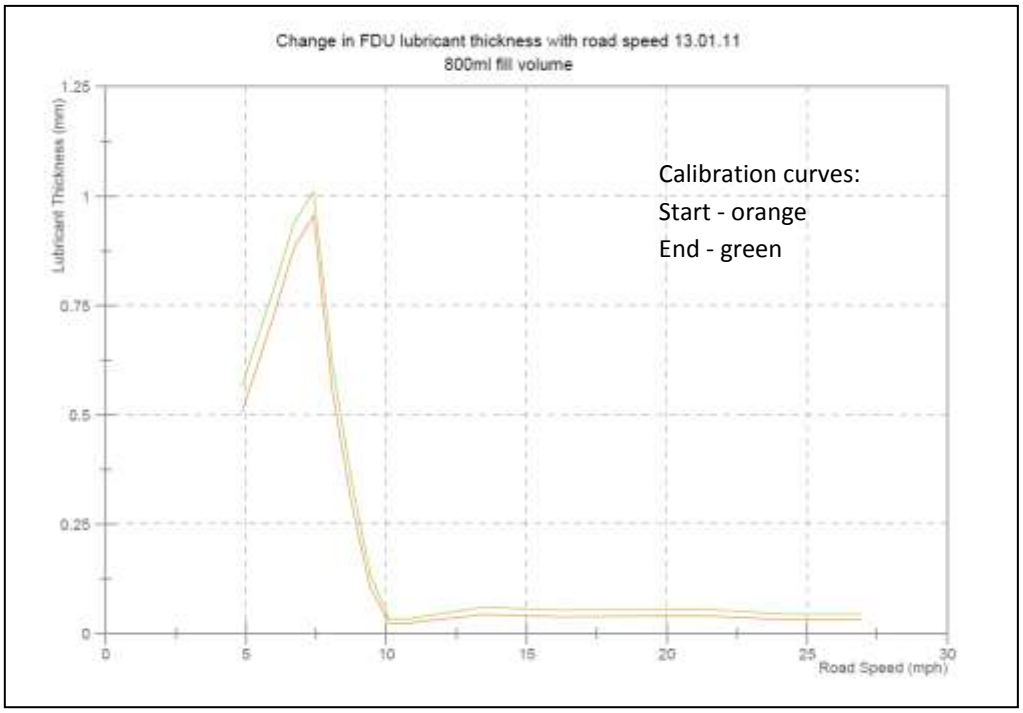

Figure 6.17 - Crown wheel cover side thickness measurements 800ml

In Figure 6.16, the lubricant thickness appears to increase again above 10mph, and is a repeating trend. Although less obvious in Figure 6.17, the trend is visible in other data taken with the 800ml lubricant volume.

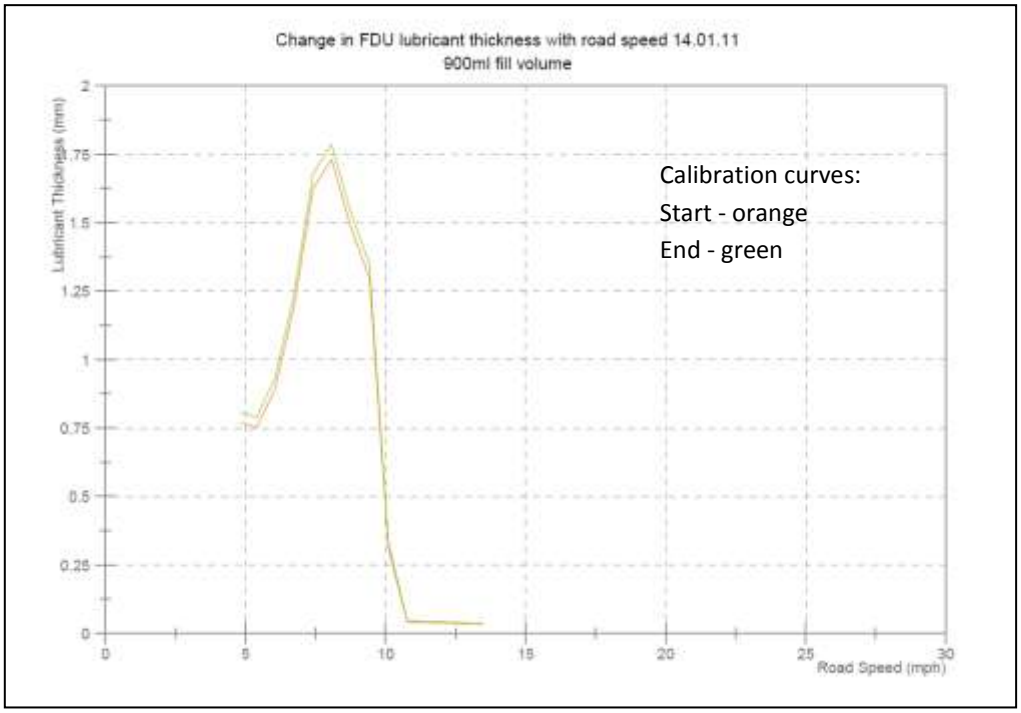

Figure 6.18 - Crown wheel cover side thickness measurements 900ml

By combining the data from the three fill volumes, the relationship between the increase in fill volume and increase in vehicle speed to reach maximum lubricant thickness is clear Figure 6.19.

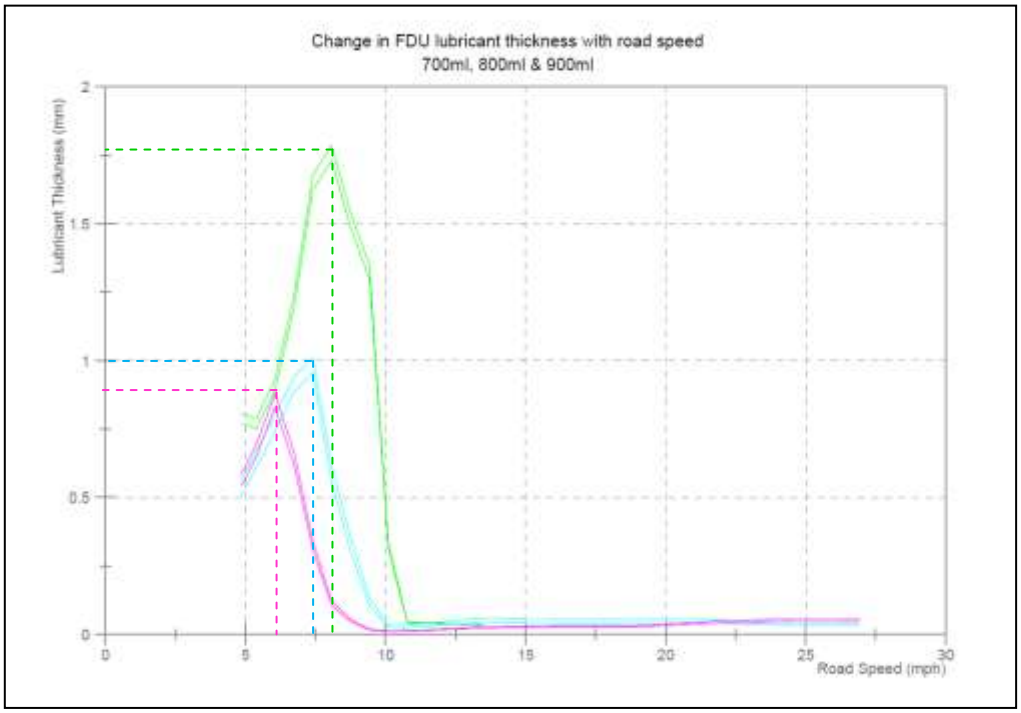

Figure 6.19 - Combined fill volume data - Cover side

6.5 Crown Wheel Results – Carrier side

The breather recess was selected as the best entry point for the laser to reach the front of the crown wheel, Figure 6.20. This was the only point on the front-side of the housing where the wall was not curved. An additional benefit of the recess was that it prevented the lubricant from obstructing the view by lapping on to the housing surface due to it being set-back from the rest of the casing. The gears were visible up until approximately 20-25mph when the splashing oil began to obstruct the laser path. The laser pulses were timed again with the rotary encoder to ensure data was collected from the same point on the crown wheel.

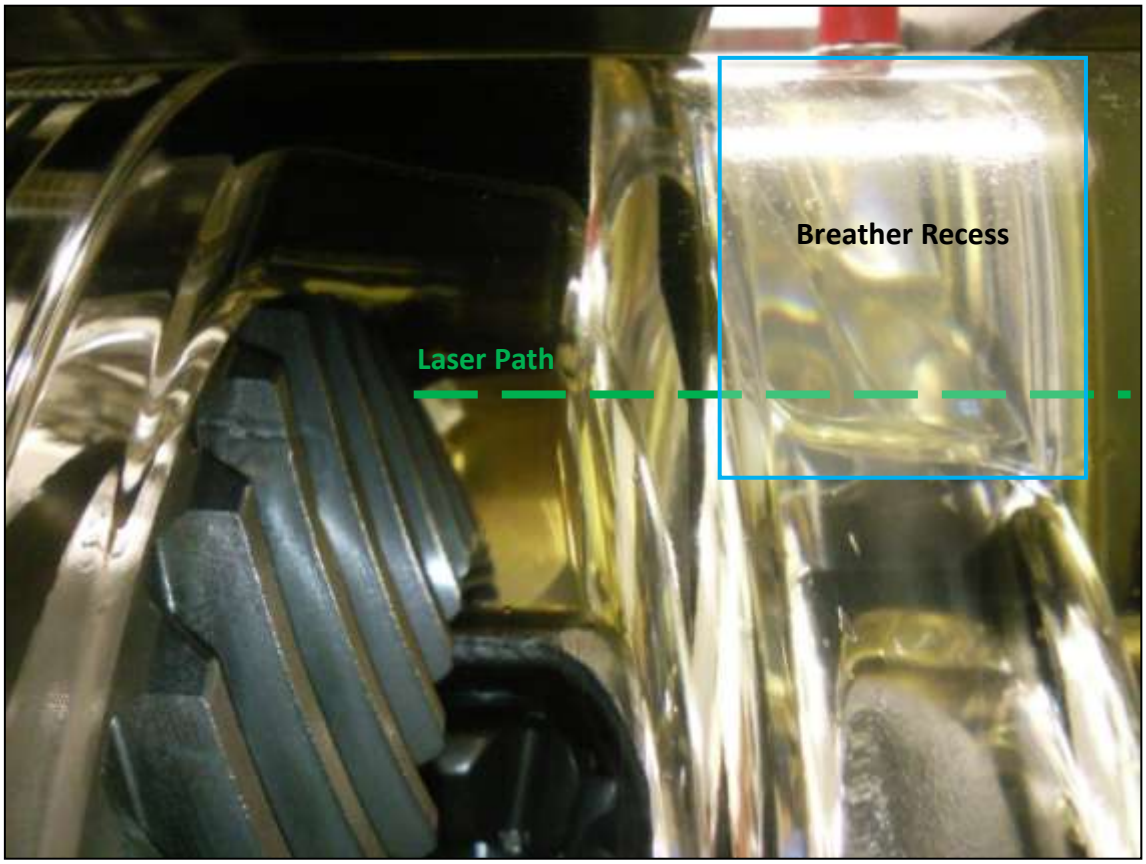

Figure 6.20 - View of crown wheel teeth and breather recess

6.5.1 Speed Study

As with the rear of the crown wheel, the lubricant thickness increased with speed to a peak of approximately 1.7mm at 8mph for a fill volume of 900ml (Figure 6.21). Between 10 and 20mph, the lubricant thickness settled to an almost constant thickness before a sharp increase in thickness at approximately 24mph. At this point, the splashing lubricant between the casing and the gears caused a higher fluorescence reading, making it appear as though the lubricant thickness on the gears themselves was increasing.

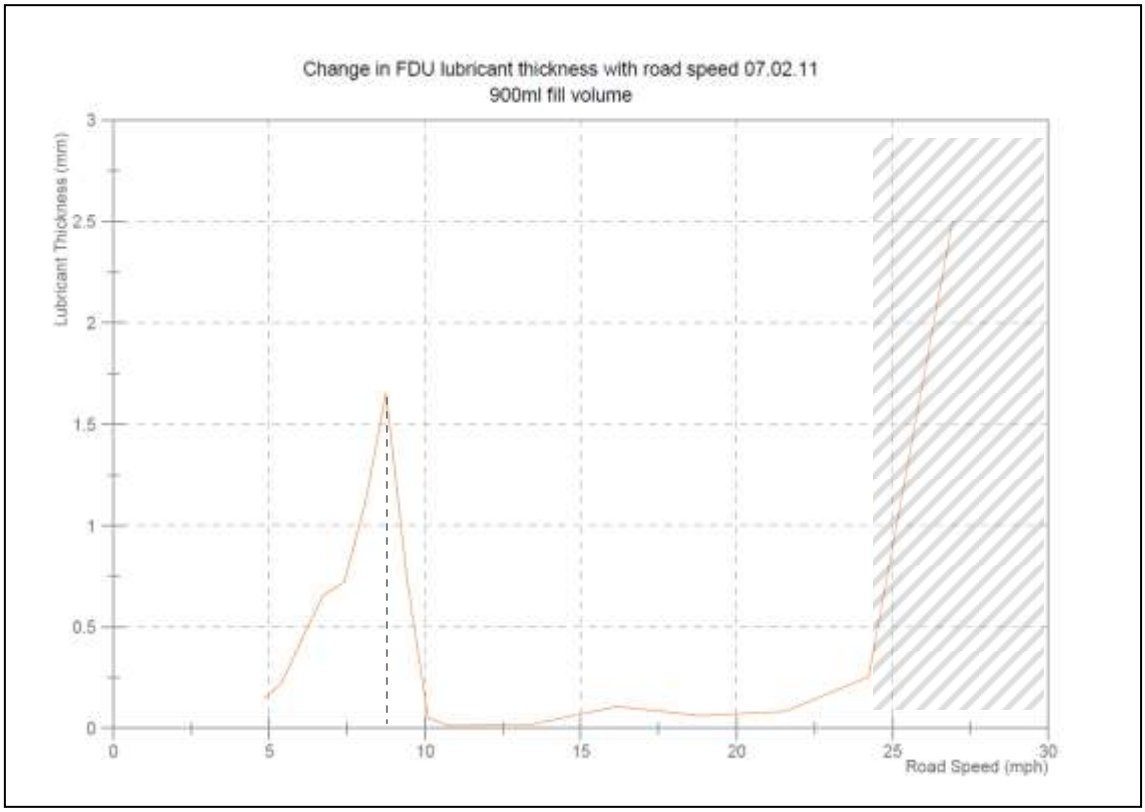

Figure 6.21 - Crown wheel tooth thickness measurements 900ml

One difference between the rear and front thicknesses is the shape of the curve of peak thickness around 8mph. For the rear of the crown wheel, the thickness started at 0.75mm and increased to 1.75mm via a smooth curve. On the front, the lubricant thickness began at less than 0.25mm before increasing to 1.75mm via a jagged curve. This jagged curve is present for all three fill volumes.

6.5.2 Fill Volume Study

The same three lubricant fill volumes were used for the front side of the crown wheel; 700ml (Figure 6.22), 800ml (Figure 6.23) and 900ml (Figure 6.21). The jagged increase in lubricant thickness is visible in all three data sets, and the peak thickness increases with fill volume as with the rear of the crown wheel; approximately 0.9mm for 700ml, 1.1mm for 800ml and 1.75mm for 900ml.

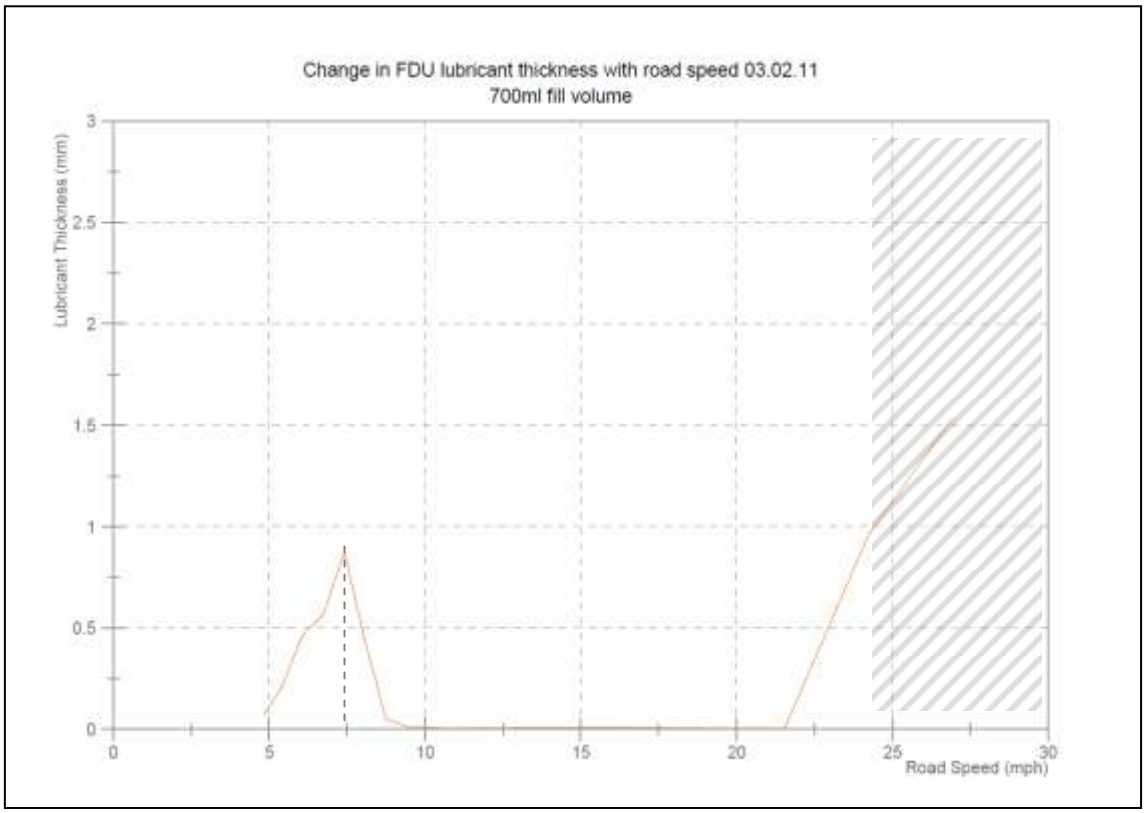

Figure 6.22- Crown wheel tooth thickness measurements 700ml

Table 6-7 - Peak film thickness - Carrier side

Fill Volume (ml)	Peak Film Thickness (mm)	Road Speed (mph)
700	0.8	7
800	1.0	8
900	1.6	9

The speed at which the peak occurs shifts with fill volume also; 7.4mph for 700ml, 8mph for 800ml and 9mph for 900ml. To find the exact speed for the peak, additional measurements would be required between 7mph and 10mph.

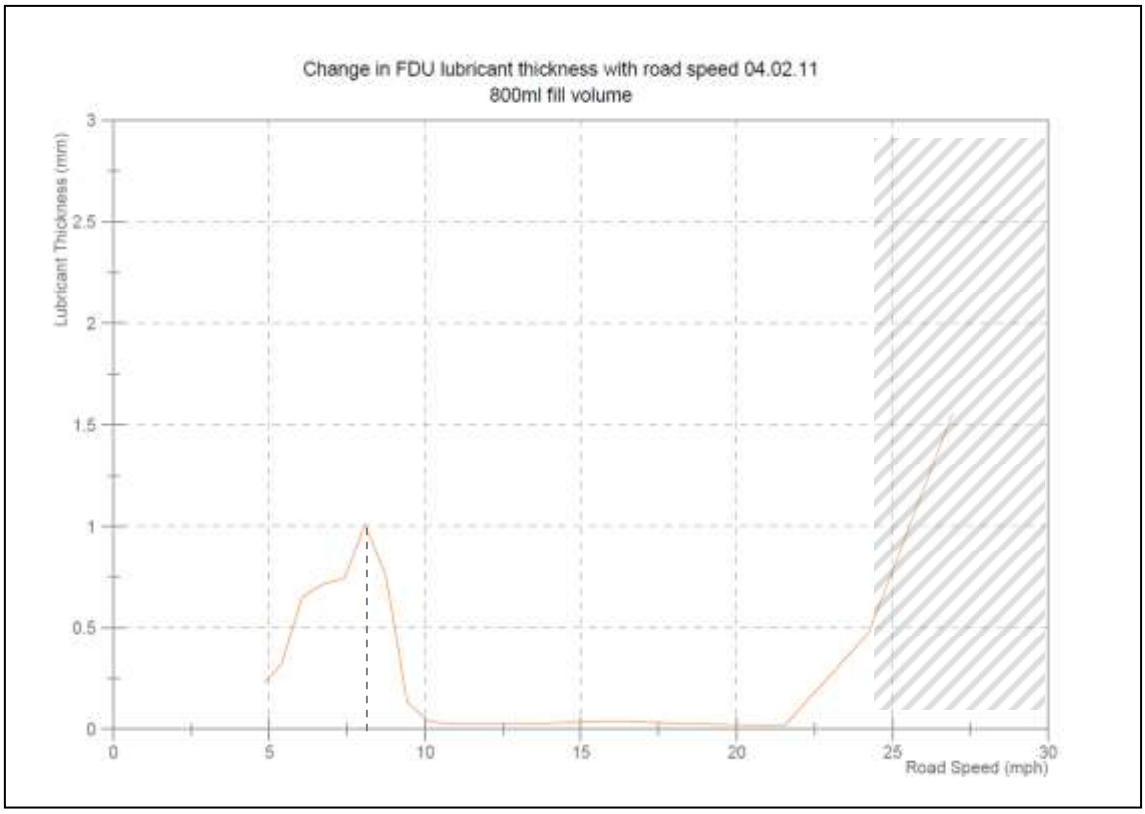

Figure 6.23- Crown wheel tooth thickness measurements 800ml

6.5.3 Temperature Observations

During the speed and fill volume studies, it was noted that the lubricant thickness changed during repeats. On closer inspection, the temperature of the lubricant was found to increase over the course of the data collection. Figure 6.24 and Figure 6.25 show the measurements taken from the gear teeth with a fill volume of 900ml at 20°C and 33°C respectively.

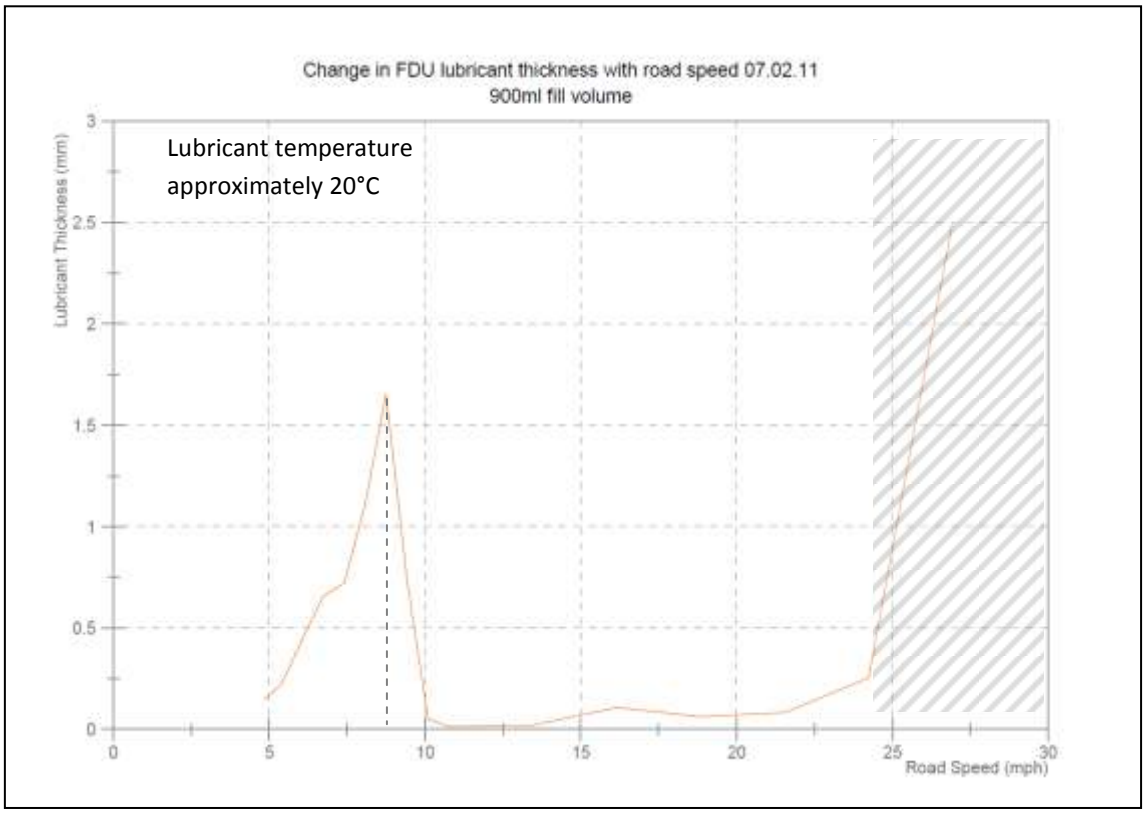

Figure 6.24 - Crown wheel tooth thickness measurements 20°C

The first thing to note is that the peak lubricant thickness decreases as the temperature increases, in this case by a third. This is not surprising as the lubricant viscosity decreases with increasing temperature, but it shows that the LIF technique is able to capture this change. The second point to note is that the point at which the internal lubricant splash begins to interfere with the data acquisition moves to a slower road speed, from 24mph at 20°C to 22mph at 33°C.

While this behaviour occurs for all fill volumes, it is more noticeable at 900ml. Another point of interest is that the speed at which the peak lubricant thickness occurs does not change with temperature. This suggests that the speed of maximum lubricant entrainment is not dependent on lubricant temperature and therefore viscosity.

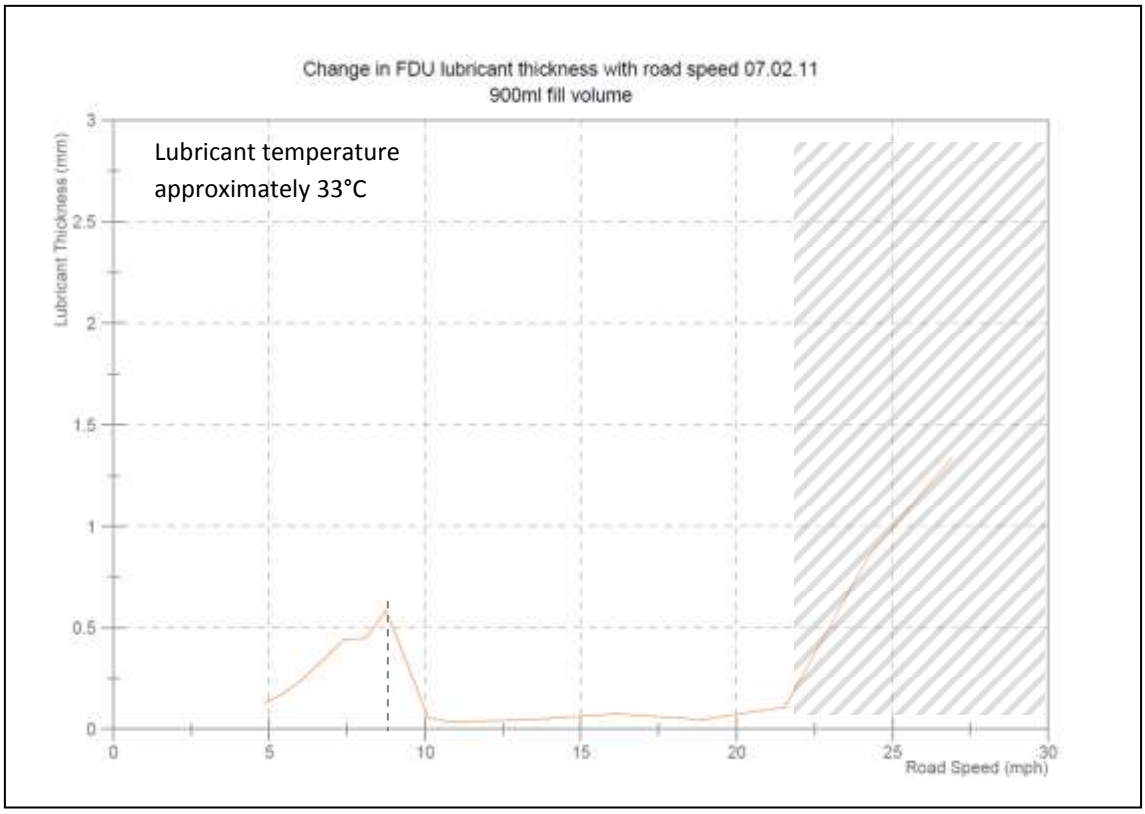

Figure 6.25 - Crown wheel tooth thickness measurements 33°C

6.6 Summary of Chapter 6

Through flow visualisation, lubricant flow patterns over a range of rotational speeds have been observed. At speeds below 30mph equivalent road speed, the lubricant movement was mostly around the crown wheel and pinion with low levels of splash. Above 30mp, the lubricant behaviour was found to be chaotic, with lubricant splashing onto the housing, preventing optical access. The cover-side of the crown wheel and the breather recess were noted to be suitable for lubricant thickness measurement due to the level housing profile at these positions.

The uncertainties of the LIF based lubricant thickness measurement technique have been discussed. Calibration data from before and after data collection were assessed and, the calibration curves were found to be statistically equivalent. This is significant as it shows that the technique is repeatable and reliable.

Lubricant thickness measurements have been successfully obtained from both a flat surface on the rear of the crown wheel and also from gear teeth. The measurement technique was employed effectively to calibrate via the wedge and take fluorescence measurements from the replica FDU housing.

Lubricant thickness measurements from the cover and carrier side of a rotating crown wheel have exposed a trend that shows that peak lubricant thickness occurs between 7 and 10 mph for the three lubricant fill volumes studied. The speed at which peak lubricant thickness occurs on the crown wheel increases with fill volume. This is valuable information that has not been formally recorded before now.

CHAPTER 7
CONCLUSIONS AND FURTHER WORK

7 Conclusions and Further Work

7.1 Achievements and Conclusions

The aim of this research was to successfully implement a lubricant thickness measurement technique, including quantitative calibration, in order to increase understanding of lubricant behaviour within a final drive unit (FDU).

Through research of existing liquid film thickness measurements, laser induced fluorescence (LIF) was identified as being a suitable technique for application in a clear-housed replica FDU. LIF was successfully adopted as part of the crucial wedge calibration technique, which allowed lubricant fluorescence to be converted into a lubricant thickness value. Use of Hamamatsu photomultipliers and National Instruments data acquisition hardware PXI5152, proved to be effective for measurement of lubricant fluorescence.

Lubricant flow visualisation within the replica FDU provided important qualitative data, which increased existing understanding of the complex lubricant behaviour present within a working FDU, fulfilling one of the objectives of this research. The flow patterns showed lubricant waves lapping across the inside of the housing and into the breather recess. This behaviour has only been realised due to the clear nature of the housing and has been documented for the first time in this thesis.

Visualisation was also instrumental in allowing suitable areas for optical access to the gears to be identified. The cover-side of the crown wheel and the breather were found to be suitable access points as a result of the flat housing profile.

Once the calibration and visualisation were completed, LIF was successfully employed to take lubricant thickness measurements from the cover-side and carrier-side of the crown wheel within the FDU. While LIF has been used to measure liquid film thicknesses by a number of authors in literature, its application to a geared system, and more specifically the FDU is original, enabling accurate determination of lubricant thickness.

The results show lubricant thickness trends are dependent on the fill volume and rotational speed of the gear. The measured peak lubricant thickness on the carrier- and cover-side of the crown wheel increased with fill volume. An increase in fill volume from 700ml to 900ml resulted in a lubricant thickness increase of 0.95mm (from 0.80 to 1.75mm) on the cover side of the crown wheel, and 0.80mm (from 0.80 to 1.60mm) on the carrier side.

The same increase in fill volume, from 700ml to 900ml, resulted in the occurrence of peak lubricant thickness shifting by 2mph from 6mph (75rpm crown wheel) to 8mph (100 rpm) at the cover side and 7mph (86.7rpm) to 9mph (111.7rpm) at the carrier side.

At constant fill, the relationship between thickness and rotational speed is perhaps even more interesting. For a fill volume of 900ml, as the equivalent road speed increased to approximately 8 mph the measured lubricant thickness increased to its maximum value of 1.75mm. From 8mph onwards, the lubricant thickness was found to decrease again to less than 0.1mm at around 10mph. The lubricant thickness increase to a peak and subsequent decrease is thought to be the result of the rival forces acting upon the lubricant and crown wheel. Gravity will naturally act to pull the lubricant down from the gear, the lubricant will have a weak adhesion force to the gear and the rotating gear will be forcing the lubricant outward towards the housing (centrifugal force). Up to a vehicle speed of 8 mph, gravity appeared to be the overriding influence, pulling the lubricant from the crown wheel. Above 8 mph, the force from the gear rotation ejected lubricant from the crown wheel. At 8 mph, these forces seemed to be in balance, resulting in the greatest measured lubricant thickness. This is a relationship that has not been identified in a FDU by other authors and shows effective implementation of the LIF technique.

For a geared system, a balance must be found between the amount of lubricant used for wear prevention and cooling, and churning losses. Not enough lubricant leads to shortened system life span, whereas too much increases churning resulting in reduced efficiency. The LIF technique described in this thesis proves suitable for use to add real FDU thickness measurements to in-depth investigations into the optimum fill volumes, fill levels and internal housing profiles. Furthermore, an optimised version of this LIF technique could be used to gather data from various points from within any geared system, provided there is optical access.

This research establishes a new experimental approach for measuring lubricant thicknesses. The tool developed is suitable for application during the design phase of new final drive units, and other geared systems, in an industrial environment.

7.2 Further Work

This thesis presents the early stages in visualising and measuring lubricant thicknesses within final drive units. By establishing effective measurement and calibration procedures, further work can be concentrated on in the future.

Assessment of lubricant fluorescence using an injection seeded laser may help to reduce fluorescence variability. If the fluorophore is sensitive to only a narrow band of wavelengths then the Nd:YAG used may not have been exciting the fluorophore at exactly the correct wavelength each time. A seeded laser emits a much narrower band of wavelengths and would show if the fluorophore within the lubricant is as sensitive to wavelength as suspected.

Investigation of the lubrication at different tilt angles could be considered, which would represent cornering or driving on an incline. It would be possible to monitor lubricant thickness behaviour during a simulated drive cycle where lubricant distribution changes due to high acceleration.

Combination of the LIF technique with fibre optics could allow analysis of a real working FDU. The temperatures experienced would be higher and it would be necessary to keep the fibre optic tip clear of splashing lubricant to allow continuous data collection.

CFD is becoming a powerful modelling and development tool. The research conducted in this thesis provides vital information which can be used for validation and improvement of models, modelling techniques and algorithms. Ultimately, the combination of modelling and experimental techniques will provide most advances in FDU design.

References

Amsoil (2006), *Don't forget the gear oil*, available at: http://www.amsoil.com/news/gearoil_3_06.aspx (accessed 11/28).

Bowen, E. J. (1959), "Viscosity and temperature effects in fluorescence", *Discussions of the Faraday Society,* vol. 27, pp. 40-42.

Brahic, C. (2007), *Climate myths: Human CO_2 emissions are too tiny to matter*, available at: http://www.newscientist.com/article/dn11638-climate-myths-human-co2-emissions-are-too-tiny-to-matter.html.

Bryant (2005), *Lubrication*, available at: http://www.me.utexas.edu/~bryant/courses/me383s/DownloadFiles/LectureNotes/Lubrication.pdf (accessed 2013).

Burlison, M. and Sherwood, G. (2010), *Particle image velocimetry of lubricant flow in a rear differential.*Cranfield University.

Castberg, P. (2010), *Heat dissipation from a rear drive unit* (MSc thesis), Cranfield University, Cranfield University.

Chartier, G. (2005), *Introduction to optics,* Springer.

Cho, H. and Min, K. (2003), "Measurement of liquid fuel film distribution on the cylinder liner of a spark ignition engine using the laser-induced fluorescence technique", *Measurement Science and Technology,* vol. 14, no. 7, pp. 975-982.

Ciulli, E., Draexl, T. and Stadler, K. "Film Thickness Analysis for EHL Contacts under Steady-State and Transient Conditions by Automatic Digital Image Processing", *Advances in Tribology,* .

Continuum, (2002), *Operation and Maintenance Manual for Surelite Lasers*, Rev. J ed., Continuum.

Continuum (2010), *Surelite*, available at: http://www.continuumlasers.com/products/pdfs/Surelite%20Rev%20F%20LR.pdf.

Crook, A. W. (1958), "The Lubrication of Rollers", *Philosophical Transactions of the Royal Society of London.Series A, Mathematical and Physical Sciences (1934-1990),* vol. 250, no. 981, pp. 387-409.

Crosby, G. A. and Demas, J. N. (1971), "Measurement of photoluminescence quantum yields. Review", *The Journal of physical chemistry,* vol. 75, no. 8, pp. 991-1024.

Das, P. (c1991.), *Lasers and optical engineering,* Springer-Verlag, New York ; London.

Dawson, P. H. (1984), "Windage loss in larger high-speed gears", *ARCHIVE: Proceedings of the Institution of Mechanical Engineers, Part A: Power and Process Engineering 1983-1988 (vols 197-202),* vol. 198, no. 1, pp. 51-59.

Degarmo, E. P. (2003), *Materials and processes in manufacturing,* 9th ed, Wiley, New York ; Chichester.

Dowson, D. and Ehret, P. (1999), "Past, present and future studies in elastohydrodynamics", *Proceedings of the Institution of Mechanical Engineers, Part J: Journal of Engineering Tribology,* vol. 213, no. 5, pp. 317-333.

Dowson, D. and Higginson, G. R. (1977), *Elasto-hydrodynamic lubrication,* SI ed, Pergamon Press, Oxford Eng. ; New York.

Driscoll, D. I., Schmitt, R. L. and Stevenson, W. H. (1992), "Thin Flowing Liquid Film Thickness Measurement by Laser Induced Fluorescence", *Journal of Fluids Engineering,* vol. 114, no. 1, pp. 107-112.

Dwyer-Joyce, R. S., Drinkwater, B. W. and Donohoe, C. J. (2003), "The measurement of lubricant-film thickness using ultrasound", *Proceedings of the Royal Society - Mathematical, Physical and Engineering Sciences (Series A),* vol. 459, no. 2032, pp. 957-976.

Dwyer-Joyce, R. S., Harper, P. and Drinkwater, B. W. (2004), "A method for the measurement of hydrodynamic oil films using ultrasonic reflection", *Tribology Letters,* vol. 17, no. 2, pp. 337-348.

Eckbreth, A. C. (1988), *Laser diagnostics for combustion temperature and species,* Abacus, Tunbridge Wells.

Edwards,R. Larivé,J.F. Beziat,J.C. (2011), *Well-to-wheels Analysis of Future Automotive Fuels and Powertrains in the European Contect. WELL-to-WHEELS Report Version*

3c, July 2011, EUR 24952 EN - 2011, Publications Office of the European Union, Luxembourg.

Engineers Edge (2010), *Viscosity Index*, available at: http://www.engineersedge.com/lubrication/viscosity_index.htm (accessed 01/19).

European Commission (30/07/2012), *Road transport: Reducing CO_2 emissions from vehicles*, available at: http://ec.europa.eu/clima/policies/transport/vehicles/index_en.htm (accessed 27/01/2013).

European Parliament (2007), *Euro 5 and Euro 6 standards: reduction of pollutant emissions from light vehicles*, available at: http://europa.eu/legislation_summaries/transport/transport_energy_environment/l28186_en.htm (accessed 01.12.2009).

Ford, R. A. J. and Foord, C. A. (1978), "Laser-based fluorescence techniques for measuring thin liquid films", *Wear,* vol. 51, no. 2, pp. 289-297.

Fusco, L., Hallam, B., Sherwood, G. and Vaughan, N. D. (2009), "Understanding lubricant behaviour in geared systems and housings", 16-17 April 2009, .

Gleason. *Fundamentals of Bevel Gear Design Training Rev 1.1 Customer & Dealer Training Center* .

Gleason Works (Rochester, N. Y.). (1947), *Gleason Bevel and Hypoid Gear Design,* Gleason Works.

Habchi, W., Eyheramendy, D., Bair, S., Vergne, P. and Morales-Espejel, G. (2008), "Thermal Elastohydrodynamic Lubrication of Point Contacts Using a Newtonian/Generalized Newtonian Lubricant", *Tribology Letters,* vol. 30, no. 1, pp. 41-52.

Hamamatsu Photonics (2007), *Photomultiplier Tubes - Basics and Applications Edition 3a*, available at: http://sales.hamamatsu.com/assets/pdf/catsandguides/PMT_handbook_v3aE.pdf .

Hamrock, B. J., Schmid, S. R. and Jacobson, B. O. (2004), *Fundamentals of fluid film lubrication,* 2nd ed, Dekker, New York.

Hatton. (2008), *A short course in gear design* .

Herschel, W. H. (1922), "The Change in Viscosity of Oils with the Temperature", *Journal of Industrial & Engineering Chemistry,* vol. 14, no. 8, pp. 715-722.

Hidrovo, C. H. and Hart, D. P. (2000), "Dual Emission Laser Induced Fluorescence technique (DELIF) for oil film thickness and temperature measurement", *American Society of Mechanical Engineers, Fluids Engineering Division (Publication) FED,* vol. 253, pp. 175-182.

Hidrovo, C. H. and Hart, D. P. (2001), "Emission reabsorption laser induced fluorescence (ERLIF) film thickness measurement", *Measurement Science and Technology,* vol. 12, no. 4, pp. 467-477.

Hillier, V. A. W. (1991), *Fundamentals of motor vehicle technology,* 4th ed, Stanley Thornes Publishers.

Hosten, B. (1991), "Bulk heterogeneous plane waves propagation through viscoelastic plates and stratified media with large values of frequency domain", *Ultrasonics,* vol. 29, no. 6, pp. 445-450.

Hoult, D. P., Lux, J. P., Wong, V. W. and Billian, S. A. (1988), "Calibration of laser fluorescence of film thickness in engines.", *SAE Technical Paper Series,* vol. 881587, pp. 1-2, 3, 4, 5, 6, 7, 8, 9.

IMechE (2009), *Low Carbon Vehicles - Driving the UK's Transport Revolution*, available at: http://www.imeche.org/Libraries/Key_Themes/The_Low_Carbon_Vehicle_Report_IMechE.sflb.ashx.

Invitrogen (2010), *Introduction to fluorescence*, available at: http://probes.invitrogen.com/resources/education/tutorials/1Intro/player.html (accessed 01/11).

Iritani, M., Aoki, H. and Suzuki, K. (1999), "Prediction Technique for the Lubricating Oil Temperature in Manual Transaxle", Society of Automotive Engineers, 400 Commonwealth Dr , Warrendale, PA, 15096, USA, [URL:http://DRL:http://www.sae.org/servlets/productDetail?PROD_TYP=PAPER&PROD_CD=1999-01-0747http://www.sae.org], .

Jacobson, B. O. and Vinet, P. (1987), "A Model for the influence of pressure on the bulk modulus and the influence of temperature on the solidification pressure for liquid lubricants", *Journal of Tribology,* vol. 109, no. 4, pp. 709-714.

Jeon, S. I. (2010), *Improving efficiency in drive lines: an experimental study on churning losses in hypoid axle,* , Imperial College London.

Jermy, M. C., Noel, T. and Doherty, W. G. (2004), "Laser induced fluorescence measurements of the thickness of fuel films on the combustion chamber surface of a gasoline SI engine", *12th International Symposium of Applications of Laser Techniques to Fluid Mechanics,* 12 - 15 July, 2004, Lisbon, Portugal, Springer-Verlag, .

Johnston, G. J., Wayte, R. and Spikes, H. A. (1991), "Measurement and study of very thin lubricant films in concentrated contacts", *Tribology Transactions,* vol. 34, no. 2, pp. 187-194.

Kariyasaki, A., Yamasaki, Y., Kagawa, M., Nagashima, T., Ousaka, A. and Morooka, S. (2009), "Measurement of Liquid Film Thickness by a Fringe Method", *Heat Transfer Engineering,* vol. 30, no. 1-2, pp. 28-36.

Kasolang, S. and Dwyer-Joyce, R. S. (2008), "Observations of Film Thickness Profile and Cavitation Around a Journal Bearing Circumference", *Tribology Transactions,* vol. 51, no. 2, pp. 231.

King, J. (2007), *The King Review of Low Carbon Cars,* , HM Treasury.

Kolivand, M., (2009), *Development of tooth contact and mechanical efficiency models for face-milled and face-hobbed hypoid and spiral bevel gears*, Ohio State University, Columbus, Ohio.

Kollewin Technology (2003), available at: http://www.kollewin.com/EX/09-15-03/em_spectrum.jpg.

Kopeliovich, D. (2009), *Additives in lubricating oils*, available at: http://www.substech.com/dokuwiki/doku.php?id=additives_in_lubricating_oils (accessed 21.12.2009).

Lakowicz, J. R. (2006), *Principles of fluorescence spectroscopy,* 3rd ed, Springer, New York.

Lane, T. B. and Hughes, J. R. (1952), "A study of the oil-film formation in gears by electrical resistance measurements", *British Journal of Applied Physics,* vol. 3, no. 10, pp. 315-318.

Lange, N. A. (2005), *Lange's handbook of chemistry,* 16th ed, McGraw-Hill, New York, N.Y. ; London.

Lilleleht, L. U. and Hanratty, T. J. (1961), "Measurement of interfacial structure for co-current air–water flow", *Journal of Fluid Mechanics Digital Archive,* vol. 11, no. 01, pp. 65.

Luke, P. and Olver, A. (1999), "A study of churning losses in dip-lubricated spur gears", *Proceedings of the Institution of Mechanical Engineers, Part G: Journal of Aerospace Engineering,* vol. 213, no. 5, pp. 337-346.

Mendenhall, W. and Sincich, T. (2007), *Statistics for engineering and the sciences,* 5th ed, Pearson Prentice-Hall, Upper Saddle River, N.J.

Middleman, S. (1998), *An introduction to fluid dynamics : principles of analysis and design,* Wiley.

Moffat, R. J. (1988), "Describing the uncertainties in experimental results", *Experimental Thermal and Fluid Science,* vol. 1, no. 1, pp. 3-17.

Mouza, A. A., Vlachos, N. A., Paras, S. V. and Karabelas, A. J. (2000), "Measurement of liquid film thickness using a laser light absorption method", *Experiments in Fluids,* vol. 28, no. 4, pp. 355-359.

Myant, C., Reddyhoff, T. and Spikes, H. A. (2010), "Laser-induced fluorescence for film thickness mapping in pure sliding lubricated, compliant, contacts", *Tribology International,* vol. 43, no. 11, pp. 1960-1969.

NHTSA *, NHTSA & EPA propose new national program to improve fuel economy and reduce greenhouse gas emission for passenger cars and light trucks*, available at: http://www.nhtsa.dot.gov/portal/nhtsa_static_file_downloader.jsp?file=/staticfiles/DOT/NHTSA/Rulemaking/Rules/Associated Files/MY2012-2016CAFEPRMfactsheet.pdf (accessed 12/11).

Olver, A. V. (2002), "Gear lubrication - a review", *Proceedings of the Institution of Mechanical Engineers, Part J: Journal of Engineering Tribology,* vol. 216, no. 5, pp. 255-267.

Paschotta, R. (10/12), *RP Photonics*, available at: http://www.rp-photonics.com/.

Pearson, E. S. and Hartley, H. O. (1954), *Biometrika tables for statisticians,* University Press for the Biometrika Trustees, Cambridge.

Pengra, D. B. (2009), *Notes on Data Analysis and Experimental Uncertainty*, available at: http://courses.washington.edu/phys431/uncertainty_notes.pdf (accessed 2012).

Pialucha, T., Guyott, C. C. H. and Cawley, P. (1989), "Amplitude spectrum method for the measurement of phase velocity", *Ultrasonics,* vol. 27, no. 5, pp. 270-279.

Pigenel, B. (2009), *Study of fluid motion in a rear differential unit* (MSc thesis), Cranfield University, Cranfield University. School of Engineering;.

Portalski, S. and Clegg, A. J. (1972), "An experimental study of wave inception on falling liquid films", *Chemical Engineering Science,* vol. 27, no. 6, pp. 1257-1265.

Reddyhoff, T., Dwyer-Joyce, R. S., Zhang, J. and Drinkwater, B. W. (2008), "Auto-calibration of ultrasonic lubricant-film thickness measurements", *Measurement Science and Technology,* vol. 19, no. 4.

Richardson, D. E. and Borman, G. L. (1991), "Using fiber optics and laser fluorescence for measuring thin oil films with application to engines", *International Fuels and Lubricants Meeting and Exposition,* 7 October 1991 through 10 October 1991, Toronto, Ont, Can, Publ by SAE, Warrendale, PA, United States, pp. 1.

Ryk, G. and Etsion, I. (2006), "Testing piston rings with partial laser surface texturing for friction reduction", *Wear,* vol. 261, no. 7–8, pp. 792-796.

Schomacker, K. T., Frisoli, J. K. and Deutsch, T. F. (1992), "Medical applications of laser-induced fluorescence", *Recent Advances in the Uses of Light in Physics, Chemistry, Engineering, and Medicine,* Vol. 1599, 19 June 1991 through 21 June 1991, New York, NY, USA, Publ by Int Soc for Optical Engineering, Bellingham, WA, United States, pp. 296.

Shaw, B., Hoult, D. and Wong, V. (1992), "Development of engine lubricant film thickness diagnostics using fiber optics and laser fluorescence", *International Congress and Exposition,* 24 February 1992 through 28 February 1992, Detroit, MI, USA, Publ by SAE, Warrendale, PA, United States, pp. 1.

Silfvast, W. T. (2004.), *Laser fundamentals,* 2nd ed, Cambridge University Press, Cambridge.

Simon, V. (1981), "Elastohydrodynamic lubrication of hypoid gears", *Journal of mechanical design,* vol. 103, no. 4, pp. 195-203.

Smart, A. E. and Ford, R. A. J. (1974), "Measurement of thin liquid films by a fluorescence technique", *Wear,* vol. 29, no. 1, pp. 41-47.

Spectra-Physics, (2002), *Quanta-Ray PRO-Series Pulsed Nd:YAG Lasers User's Manual*.

Stadtfeld, H., (2011),
Tribology Aspects
in Angular
Transmission Systems
Part VII:
Hypoid Gears , June/July 2011 ed., www.geartechnology.com, www.geartechnology.com.

Stadtfeld, H. J. (1993), *Handbook of bevel and hypoid gears: calculation, manufacturing, optimization,* 1st ed, Rochester Institute of Technology, Rochester, N.Y.

Tateishi, Y. (1994), "Tribological issues in reducing piston ring friction losses", *Tribology International,* vol. 27, no. 1, pp. 17-23.

Taylor, J. R. (1997), *An introduction to error analysis: the study of uncertainties in physical measurements,* 2nd ed, University Science Books, Sausalito.

Wakuri, Y., Hamatake, T., Soejima, M. and Kitahara, T. (1992), "Piston ring friction in internal combustion engines", *Tribology International,* vol. 25, no. 5, pp. 299-308.

Wang, K. L. and Cheng, H. S. (1981), "Numerical solution to the dynamic load, film thickness, and surface temperatures in spur gears - 1. Analysis", *Journal of Mechanical Design,* vol. 103, no. 4, pp. 177-187.

Wang, X. C. (1994), *Advanced theories of hypoid gears,* Elsevier, Amsterdam ; London.

Wang, Y., Li, H., Tong, J. and Yang, P. (2004), "Transient thermoelastohydrodynamic lubrication analysis of an involute spur gear", *Tribology International,* vol. 37, no. 10, pp. 773-782.

Wayne, R. P. (1988), *Principles and applications of photochemistry,* Oxford University Press, Oxford.

Weber, M. J. (1999), *Handbook of laser wavelengths,* CRC Press, Boca Raton ; London.

White, J. S., Laplant, F. P., Dixon, J. and Emch, D. J. (1998), "Non-Contact Real-Time Film Thickness Gage for Automotive Body Painting Applications", Society of Automotive Engineers, 400 Commonwealth Dr , Warrendale, PA, 15096, USA, [URL:http://DRL:http://www.sae.org/servlets/productDetail?PROD_TYP=PAPER&PROD_CD=982313http://www.sae.org], .

Willingale, R. (2007)*, Lasers and Quantum Optics*, available at: http://www.star.le.ac.uk/~rw/courses/lect4313.html#tth_sEc3.6.

Wilson, J. and Hawkes, J. F. B. (1987), *Lasers : principles and applications,* Prentice Hall, New York ; London.

Yariv, A. (1989), *Quantum electronics,* 3rd ed, John Wiley & Sons, New York.

Appendix 1

Surelite Specifications

Description	SL I-10	SL I-20	SL I-30	SL II-10	SL II-20	SL III-10
Repetition Rate (Hz)	10	20	30	10	20	10
Energy (mJ)						
1064 nm	450	420	380	650	550	850
532[1] nm	200	160	130	300	250	425
355 nm	65/100[2]	60/100[2]	25/70[2]	100/160[2]	70/120[2]	165/225[2]
266 nm	60	45	30	80	60	100
Pulsewidth[3] (nsec)						
1064 nm	5-7	5-7	5-7	5-7	5-7	4-6
532 nm	4-6	4-6	4-6	4-6	4-6	3-5
355 nm	4-6	4-6	4-6	4-6	4-6	3-5
266 nm	4-6	4-6	4-6	4-6	4-6	3-5
Linewidth (cm^{-1})						
Standard	1	1	1	1	1	1
Divergence[4] (mrad)	0.5	0.5	0.5	0.5	0.5	0.5
Beam Pointing Stability (±µrad)	30	50	70	30	50	50
Beam Diameter (mm)	6	6	6	7	7	9.5
Jitter[5] (±ns)	0.5	0.5	0.5	0.5	0.5	0.5
Energy Stability[6] (±%)						
1064 nm	2.0;0.7	2.0;0.7	2.0;0.7	2.5;0.8	2.5;0.8	2.5;0.8
532 nm	3.5;1.2	3.5;1.2	3.5;1.2	3.5;1.2	3.5;1.2	3.5;1.2
355 nm	4.0;1.3	4.0;1.3	4.0;1.3	4.0;1.3	4.0;1.3	4.0;1.3
266 nm	7.0;2.3	7.0;2.3	7.0;2.3	7.0;2.3	7.0;2.3	7.0;2.3
Power Drift[7] (±%)						
1064 nm	3.0	3.0	3.0	3.0	3.0	3.0
532 nm	3.0	3.0	3.0	6.0	6.0	5.0
355 nm	3.0	3.0	3.0	6.0	6.0	5.0
266 nm	6.0	6.0	6.0	8.0	8.0	8.0
Beam Spatial Profile[8]						
Near Field (<1M)	0.70	0.70	0.65	0.70	0.65	0.70
Far Field (∞)	0.95	0.95	0.90	0.95	0.90	0.95
Deviation from Gaussian[9]						
Near Field (<1M)	30	30	35	30	35	30
Polarization						
1064, 355, 266 nm	---------- Horizontal ----------					
532 nm	---------- Vertical ----------					

Notes

1. With Type II doubler
2. High Energy UV option with Type I doubler
3. Full width, half maximum
4. Full angle for 86% of energy
5. With respect to external trigger
6. The first value represents shot-to-shot for 99.9% of pulses, the second value represents RMS.
7. Average for 8 hours with ΔT_{max} <±3 °C
8. A least squares fit to a Gaussian profile. A perfect fit would have a coefficient of 1
9. Maximum deviation at beam center (±%)

All specifications at 1064 nm unless otherwise noted.
As a part of our continuous improvement program, all specifications are subject to change without notice.

Continuum®
The High Energy Laser Company™

992-0012, Rev. F 10/10

Appendix 2

Wedge Film Thickness Calculations

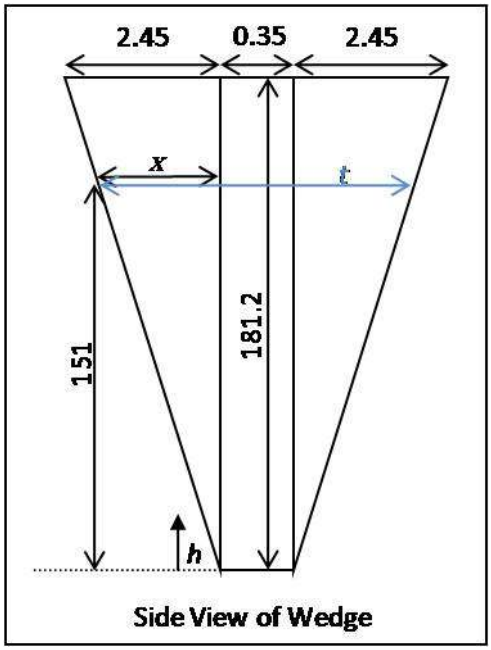

Wedge dimensions: -

Bottom spacer	0.35mm
Top spacer	5.25mm
Width of channel	100.8mm
Length of channel	181.2mm

Film thickness, $t = 2x + 0.35$

Find x using similar triangles ratio:

$$\frac{151}{181.2} = \frac{x}{2.45}$$
$$x = 2.04$$

And so:

$$t = 2(2.04) + 0.35$$
$$t = 4.4333$$

$$t = 2\left(\frac{h}{181.2} \times 2.45\right) + 0.35$$

Wedge dimensions table

h (mm)	ratio	t (mm)
0	0	0.35
1	0.013520971	0.38
5	0.067604857	0.49
10	0.135209713	0.62
15	0.20281457	0.76
20	0.270419426	0.89
25	0.338024283	1.03
50	0.676048565	1.70
60	0.811258278	1.97
70	0.946467991	2.24
80	1.081677704	2.51
90	1.216887417	2.78
100	1.35209713	3.05
120	1.622516556	3.60
140	1.892935982	4.14
160	2.163355408	4.68
180	2.433774834	5.22
181.2	2.45	5.25

Appendix 3

Power/Speed/Pulse rate conversion table:

Motor Power (%)	Crown Wheel Speed (rpm)	Equivalent Road Speed (mph)	Laser pulse rate (Hz)
3.6	60.00	4.85	1.00
4.0	66.67	5.39	1.11
4.5	75.00	6.06	1.25
5.0	83.33	6.73	1.39
5.5	91.67	7.41	1.53
6.0	100.00	8.08	1.67
6.5	108.33	8.75	1.81
7.0	116.67	9.43	1.94
7.5	125.00	10.10	2.08
8.0	133.33	10.77	2.22
9.0	150.00	12.12	2.50
10.0	166.67	13.47	2.78
12.0	200.00	16.16	3.33
14.0	233.33	18.85	3.89
16.0	266.67	21.55	4.44
18.0	300.00	24.24	5.00
20.0	333.33	26.93	5.56
25.0	416.67	33.67	6.94

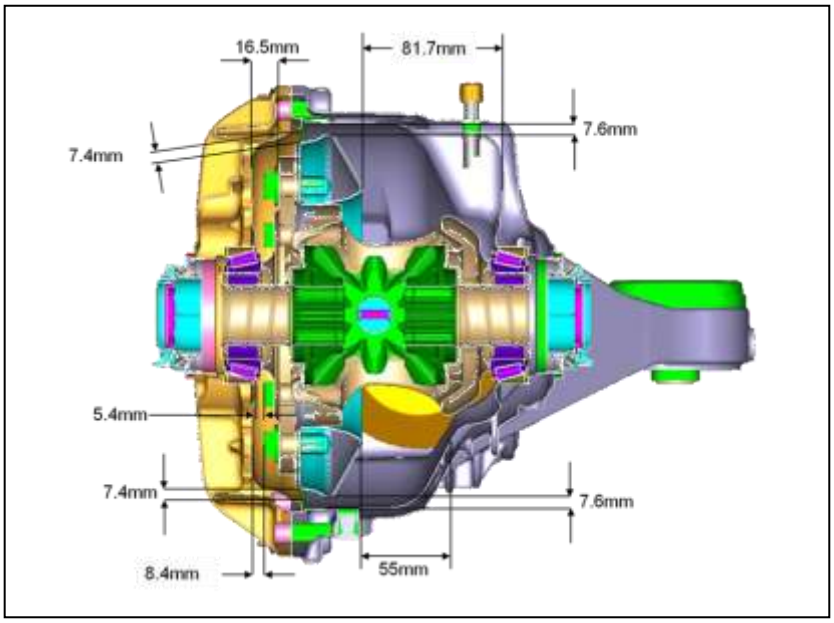

FDU internal dimensions

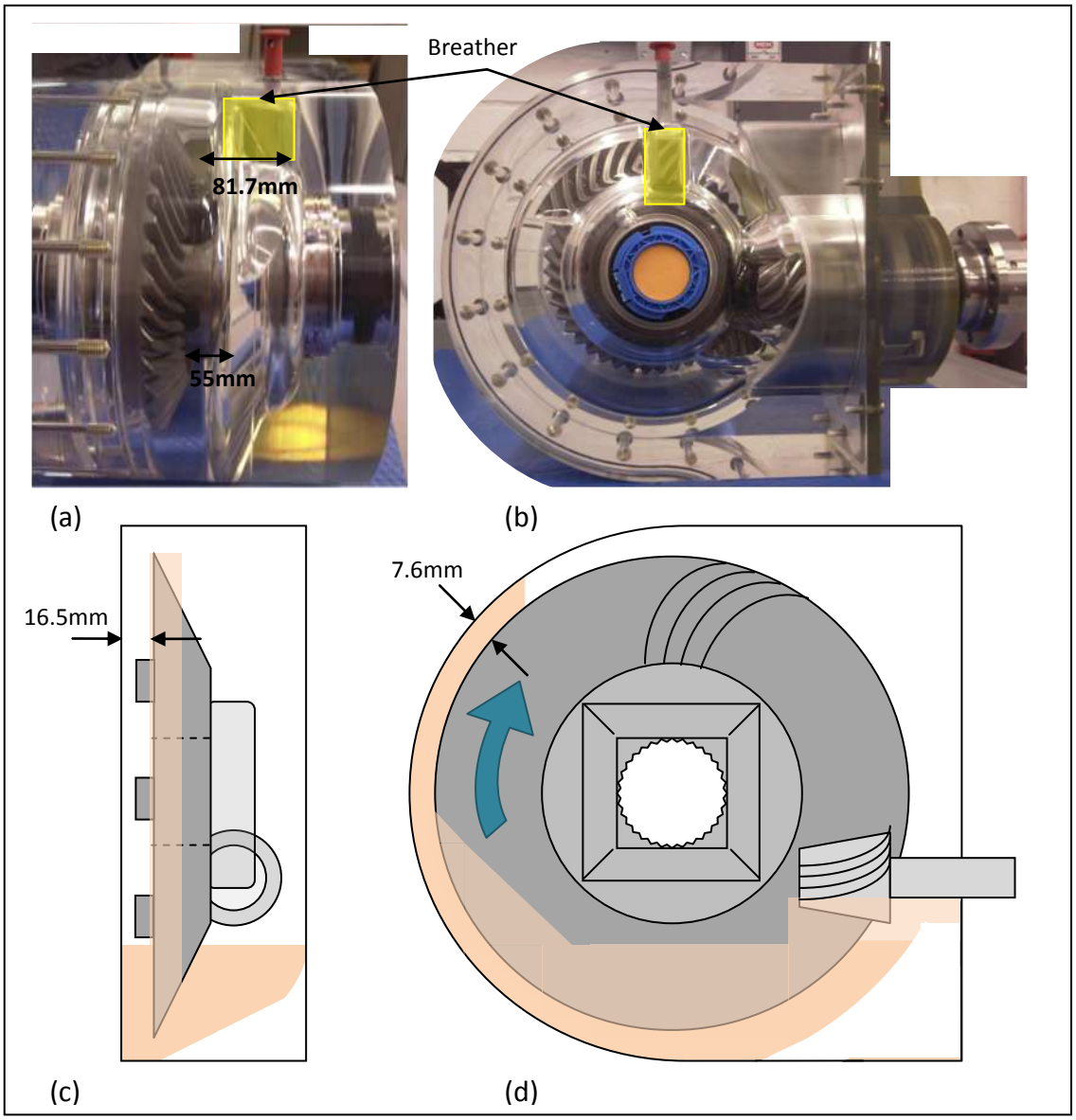
Breather
81.7mm
55mm
(a)
(b)
16.5mm
7.6mm
(c)
(d)

Appendix 4

DIAdem Scripts - Calibration

1st Peak Finding

```
'-------------------------------------------------------------------------
--
'-- VBS script file
'-- Created on 05/03/2011 15:45:48
'-- Author: ---
'-- Comment: ---
'-------------------------------------------------------------------------
--
Option Explicit  'Forces the explicit declaration of all the variables in a
script.

Dim MyFolders()
Call InitMyFolders
'-------------------------------------------------------------------------
--
Sub InitMyFolders
  ReDim MyFolders(1)
  MyFolders(0)="C:\Documents and Settings\c109859\My Documents\- PhD -\-
Lubricant Dynamics -\LabVIEW\FDU data 2011\110111 Calibration & 700ml FDU
data\Calibration\"
End Sub
'-------------------------------------------------------------------------
--
''''''''''Oscillation 1 Peak Finding

''''''''''Pulse 1

Call Data.Root.ChannelGroups(1).Activate()
Call
ChnPeakFind("","[1]/Untitled","/PeakX","/PeakY",2,"Min.Peaks","Amplitude")
'... XW,Y,E,E,PeakNo,PeakType,PeakSort
Call Data.Root.ChannelGroups.Add("10mm Wedge", 2).Activate()
Call Data.Root.ChannelGroups(2).Channels.Add("pulse",DataTypeFloat64,1)
Call ChnGenVal("[2]/pulse",1,60,1,1,0)'...
ChnArg1,ChnRow,ValNo,ChnBegin,ChnStep,ValueOverwrite
CHD(1,63)=CHD(1,62)
Call Data.Root.ChannelGroups(1).Channels.Remove("PeakX")
Call Data.Root.ChannelGroups(1).Channels.Remove("PeakY")

''''''''''Pulse 2

Call Data.Root.ChannelGroups(1).Activate()
Call ChnPeakFind("","[1]/Untitled
1","/PeakX","/PeakY",2,"Min.Peaks","Amplitude") '...
XW,Y,E,E,PeakNo,PeakType,PeakSort
CHD(2,61)=CHD(1,63)
Call Data.Root.ChannelGroups(1).Channels.Remove("PeakX")
Call Data.Root.ChannelGroups(1).Channels.Remove("PeakY")

''''''''''Pulse 3
.
.
.
''''''''''Pulse 59

Call Data.Root.ChannelGroups(1).Activate()
```

```
Call ChnPeakFind("","[1]/Untitled
58","/PeakX","/PeakY",2,"Min.Peaks","Amplitude") '...
XW,Y,E,E,PeakNo,PeakType,PeakSort
CHD(59,61)=CHD(1,63)
Call Data.Root.ChannelGroups(1).Channels.Remove("PeakX")
Call Data.Root.ChannelGroups(1).Channels.Remove("PeakY")

''''''''''Pulse 60

Call Data.Root.ChannelGroups(1).Activate()
Call ChnPeakFind("","[1]/Untitled
59","/PeakX","/PeakY",2,"Min.Peaks","Amplitude") '...
XW,Y,E,E,PeakNo,PeakType,PeakSort
CHD(60,61)=CHD(1,63)
Call Data.Root.ChannelGroups(1).Channels.Remove("PeakX")
Call Data.Root.ChannelGroups(1).Channels.Remove("PeakY")
```

All 1st Peak Finding

```
'--------------------------------------------------------------------------
--
'-- VBS script file
'-- Created on 05/03/2011 15:45:48
'-- Author: ---
'-- Comment: ---
'--------------------------------------------------------------------------
--
Option Explicit  'Forces the explicit declaration of all the variables in a
script.

Dim MyFolders()
Call InitMyFolders
'--------------------------------------------------------------------------
--
Sub InitMyFolders
  ReDim MyFolders(1)
  MyFolders(0)="C:\Documents and Settings\c109859\My Documents\- PhD -\-
Lubricant Dynamics -\LabVIEW\FDU data 2011\110111 Calibration & 700ml FDU
data\Calibration\"
End Sub
'--------------------------------------------------------------------------
--

'''''''''' 10mm ''''''''''
Call Data.Root.Clear()
Call DataFileLoad(MyFolders(0)&"10mm Wedge 110111 1GSs 5Hz 1.12kV Fluo Curve
Data.lvm","LVM","") '... DataFilename,FileImportFilter,ImportAction
call ScriptStart(MyFolders(0)&"SCRIPT - 1st Peak Finding")
Call DataFileSave(MyFolders(0)&"10mm Wedge 110111 1GSs 5Hz 1.12kV Fluo Curve
Data Modified.TDM","TDM") '... DataFilename,FileExportFilter

Call Data.Root.Clear()
Call DataFileLoad(MyFolders(0)&"10mm Wedge 110111 1GSs 5Hz 1.12kV Laser Pwr
Curve Data.lvm","LVM","") '... DataFilename,FileImportFilter,ImportAction
call ScriptStart(MyFolders(0)&"SCRIPT - 1st Peak Finding")
Call DataFileSave(MyFolders(0)&"10mm Wedge 110111 1GSs 5Hz 1.12kV Laser Pwr
Curve Data Modified.TDM","TDM") '... DataFilename,FileExportFilter

'''''''''' 20mm ''''''''''
Call Data.Root.Clear()
Call DataFileLoad(MyFolders(0)&"20mm Wedge 110111 1GSs 5Hz 1.12kV Fluo Curve
Data.lvm","LVM","") '... DataFilename,FileImportFilter,ImportAction
call ScriptStart(MyFolders(0)&"SCRIPT - 1st Peak Finding")
Call DataFileSave(MyFolders(0)&"20mm Wedge 110111 1GSs 5Hz 1.12kV Fluo Curve
Data Modified.TDM","TDM") '... DataFilename,FileExportFilter

Call Data.Root.Clear()
Call DataFileLoad(MyFolders(0)&"20mm Wedge 110111 1GSs 5Hz 1.12kV Laser Pwr
Curve Data.lvm","LVM","") '... DataFilename,FileImportFilter,ImportAction
call ScriptStart(MyFolders(0)&"SCRIPT - 1st Peak Finding")
Call DataFileSave(MyFolders(0)&"20mm Wedge 110111 1GSs 5Hz 1.12kV Laser Pwr
Curve Data Modified.TDM","TDM") '... DataFilename,FileExportFilter

'''''''''' 30mm ''''''''''
.
.
.
'''''''''' 140mm ''''''''''
Call Data.Root.Clear()
Call DataFileLoad(MyFolders(0)&"140mm Wedge 110111 1GSs 5Hz 1.12kV Fluo Curve
Data.lvm","LVM","") '... DataFilename,FileImportFilter,ImportAction
```

```
call ScriptStart(MyFolders(0)&"SCRIPT - 1st Peak Finding")
Call DataFileSave(MyFolders(0)&"140mm Wedge 110111 1GSs 5Hz 1.12kV Fluo Curve
Data Modified.TDM","TDM") '... DataFilename,FileExportFilter

Call Data.Root.Clear()
Call DataFileLoad(MyFolders(0)&"140mm Wedge 110111 1GSs 5Hz 1.12kV Laser Pwr
Curve Data.lvm","LVM","") '... DataFilename,FileImportFilter,ImportAction
call ScriptStart(MyFolders(0)&"SCRIPT - 1st Peak Finding")
Call DataFileSave(MyFolders(0)&"140mm Wedge 110111 1GSs 5Hz 1.12kV Laser Pwr
Curve Data Modified.TDM","TDM") '... DataFilename,FileExportFilter

'''''''''' 150mm ''''''''''
Call Data.Root.Clear()
Call DataFileLoad(MyFolders(0)&"150mm Wedge 110111 1GSs 5Hz 1.12kV Fluo Curve
Data.lvm","LVM","") '... DataFilename,FileImportFilter,ImportAction
call ScriptStart(MyFolders(0)&"SCRIPT - 1st Peak Finding")
Call DataFileSave(MyFolders(0)&"150mm Wedge 110111 1GSs 5Hz 1.12kV Fluo Curve
Data Modified.TDM","TDM") '... DataFilename,FileExportFilter

Call Data.Root.Clear()
Call DataFileLoad(MyFolders(0)&"150mm Wedge 110111 1GSs 5Hz 1.12kV Laser Pwr
Curve Data.lvm","LVM","") '... DataFilename,FileImportFilter,ImportAction
call ScriptStart(MyFolders(0)&"SCRIPT - 1st Peak Finding")
Call DataFileSave(MyFolders(0)&"150mm Wedge 110111 1GSs 5Hz 1.12kV Laser Pwr
Curve Data Modified.TDM","TDM") '... DataFilename,FileExportFilter
```

Run All Averaging

```
'----------------------------------------------------------------------------
--
'-- VBS script file
'-- Created on 05/03/2011 18:22:02
'-- Author: ---
'-- Comment: ---
'----------------------------------------------------------------------------
--
Option Explicit  'Forces the explicit declaration of all the variables in a
script.

Dim MyFolders()
Call InitMyFolders
'----------------------------------------------------------------------------
--
Sub InitMyFolders
  ReDim MyFolders(1)
  MyFolders(0)="C:\Documents and Settings\c109859\My Documents\- PhD -\-
Lubricant Dynamics -\LabVIEW\FDU data 2011\110111 Calibration & 700ml FDU
data\Calibration\"
End Sub
'----------------------------------------------------------------------------
--

'''''''''' 10mm ''''''''''
Call Data.Root.Clear()

Call Data.Root.ChannelGroups.Add("10mm", 1).Activate()
Call DataFileLoadSel(MyFolders(0)&"10mm Wedge 110111 1GSs 5Hz 1.12kV Fluo
Curve Data Modified.TDM","TDM","10mm Wedge/pulse","") '...
DataFilename,FileImportFilter,ImportSelection,ImportAction
Data.Root.ChannelGroups(1).Channels("pulse").Name = "Fluo"

Call DataFileLoadSel(MyFolders(0)&"10mm Wedge 110111 1GSs 5Hz 1.12kV Laser Pwr
Curve Data Modified.TDM","TDM","10mm Wedge/pulse","") '...
DataFilename,FileImportFilter,ImportSelection,ImportAction
Data.Root.ChannelGroups(1).Channels("pulse").Name = "Lasor"

Call Calculate("Ch(""[1]/Normalised
Fluo"")=Ch(""[1]/Fluo"")/Ch(""[1]/Lasor"")",NULL,NULL,"") '...
CalculateFormula,CalculateSymbols,CalculateValues,CalculateTargetUnit
StatSel(1)        = "No"
StatSel(2)        = "No"
StatSel(3)        = "No"
StatSel(4)        = "No"
StatSel(5)        = "No"
StatSel(6)        = "Yes"
StatSel(7)        = "No"
StatSel(8)        = "No"
StatSel(9)        = "No"
StatSel(10)       = "No"
StatSel(11)       = "No"
StatSel(12)       = "No"
StatSel(13)       = "No"
StatSel(14)       = "Yes"
StatSel(15)       = "Yes"
StatSel(16)       = "No"
StatSel(17)       = "No"
StatSel(18)       = "No"
StatSel(19)       = "No"
StatSel(20)       = "No"
StatSel(21)       = "No"
```

```
StatSel(22)       = "No"
StatSel(23)       = "Yes"
StatClipCopy      = 0
StatClipValue     = 0
StatFormat        = ""
StatResChn        = 1
StatResChnNames   = 0
StatResChnNameFormat= "NameName"
Call StatBlockCalc("Channel","1-","[1]/Normalised Fluo") '...
StatDirec,RowNoStr,ChnNoStr
Data.Root.ChannelGroups(1).Channels("ArithmeticMean").Name = "10mm"

Call DataFileSave(MyFolders(0)&"10mm Wedge 110111 1GSs 5Hz 1.12kV Fluo Curve
Data Normalised & Averaged.TDM","TDM") '... DataFilename,FileExportFilter

''''''''' 20mm '''''''''
Call Data.Root.Clear()

Call Data.Root.ChannelGroups.Add("20mm", 1).Activate()
Call DataFileLoadSel(MyFolders(0)&"20mm Wedge 110111 1GSs 5Hz 1.12kV Fluo
Curve Data Modified.TDM","TDM","10mm Wedge/pulse","") '...
DataFilename,FileImportFilter,ImportSelection,ImportAction
Data.Root.ChannelGroups(1).Channels("pulse").Name = "Fluo"

Call DataFileLoadSel(MyFolders(0)&"20mm Wedge 110111 1GSs 5Hz 1.12kV Laser Pwr
Curve Data Modified.TDM","TDM","10mm Wedge/pulse","") '...
DataFilename,FileImportFilter,ImportSelection,ImportAction
Data.Root.ChannelGroups(1).Channels("pulse").Name = "Lasor"

Call Calculate("Ch(""[1]/Normalised
Fluo"")=Ch(""[1]/Fluo"")/Ch(""[1]/Lasor"")",NULL,NULL,"") '...
CalculateFormula,CalculateSymbols,CalculateValues,CalculateTargetUnit
StatSel(1)        = "No"
StatSel(2)        = "No"
StatSel(3)        = "No"
StatSel(4)        = "No"
StatSel(5)        = "No"
StatSel(6)        = "Yes"
StatSel(7)        = "No"
StatSel(8)        = "No"
StatSel(9)        = "No"
StatSel(10)       = "No"
StatSel(11)       = "No"
StatSel(12)       = "No"
StatSel(13)       = "No"
StatSel(14)       = "Yes"
StatSel(15)       = "Yes"
StatSel(16)       = "No"
StatSel(17)       = "No"
StatSel(18)       = "No"
StatSel(19)       = "No"
StatSel(20)       = "No"
StatSel(21)       = "No"
StatSel(22)       = "No"
StatSel(23)       = "Yes"
StatClipCopy      = 0
StatClipValue     = 0
StatFormat        = ""
StatResChn        = 1
StatResChnNames   = 0
StatResChnNameFormat= "NameName"
Call StatBlockCalc("Channel","1-","[1]/Normalised Fluo") '...
StatDirec,RowNoStr,ChnNoStr
Data.Root.ChannelGroups(1).Channels("ArithmeticMean").Name = "20mm"
```

```
Call DataFileSave(MyFolders(0)&"20mm Wedge 110111 1GSs 5Hz 1.12kV Fluo Curve
Data Normalised & Averaged.TDM","TDM") '... DataFilename,FileExportFilter

''''''''' 30mm '''''''''
.
.
.
''''''''' 140mm '''''''''
Call Data.Root.Clear()

Call Data.Root.ChannelGroups.Add("140mm", 1).Activate()
Call DataFileLoadSel(MyFolders(0)&"140mm Wedge 110111 1GSs 5Hz 1.12kV Fluo
Curve Data Modified.TDM","TDM","10mm Wedge/pulse","") '...
DataFilename,FileImportFilter,ImportSelection,ImportAction
Data.Root.ChannelGroups(1).Channels("pulse").Name = "Fluo"

Call DataFileLoadSel(MyFolders(0)&"140mm Wedge 110111 1GSs 5Hz 1.12kV Laser
Pwr Curve Data Modified.TDM","TDM","10mm Wedge/pulse","") '...
DataFilename,FileImportFilter,ImportSelection,ImportAction
Data.Root.ChannelGroups(1).Channels("pulse").Name = "Lasor"

Call Calculate("Ch(""[1]/Normalised
Fluo"")=Ch(""[1]/Fluo"")/Ch(""[1]/Lasor"")",NULL,NULL,"") '...
CalculateFormula,CalculateSymbols,CalculateValues,CalculateTargetUnit
StatSel(1)        = "No"
StatSel(2)        = "No"
StatSel(3)        = "No"
StatSel(4)        = "No"
StatSel(5)        = "No"
StatSel(6)        = "Yes"
StatSel(7)        = "No"
StatSel(8)        = "No"
StatSel(9)        = "No"
StatSel(10)       = "No"
StatSel(11)       = "No"
StatSel(12)       = "No"
StatSel(13)       = "No"
StatSel(14)       = "Yes"
StatSel(15)       = "Yes"
StatSel(16)       = "No"
StatSel(17)       = "No"
StatSel(18)       = "No"
StatSel(19)       = "No"
StatSel(20)       = "No"
StatSel(21)       = "No"
StatSel(22)       = "No"
StatSel(23)       = "Yes"
StatClipCopy      = 0
StatClipValue     = 0
StatFormat        = ""
StatResChn        = 1
StatResChnNames   = 0
StatResChnNameFormat= "NameName"
Call StatBlockCalc("Channel","1-","[1]/Normalised Fluo") '...
StatDirec,RowNoStr,ChnNoStr
Data.Root.ChannelGroups(1).Channels("ArithmeticMean").Name = "140mm"

Call DataFileSave(MyFolders(0)&"140mm Wedge 110111 1GSs 5Hz 1.12kV Fluo Curve
Data Normalised & Averaged.TDM","TDM") '... DataFilename,FileExportFilter

''''''''' 150mm '''''''''
Call Data.Root.Clear()

Call Data.Root.ChannelGroups.Add("150mm", 1).Activate()
```

```
Call DataFileLoadSel(MyFolders(0)&"150mm Wedge 110111 1GSs 5Hz 1.12kV Fluo
Curve Data Modified.TDM","TDM","10mm Wedge/pulse","") '...
DataFilename,FileImportFilter,ImportSelection,ImportAction
Data.Root.ChannelGroups(1).Channels("pulse").Name = "Fluo"

Call DataFileLoadSel(MyFolders(0)&"150mm Wedge 110111 1GSs 5Hz 1.12kV Laser
Pwr Curve Data Modified.TDM","TDM","10mm Wedge/pulse","") '...
DataFilename,FileImportFilter,ImportSelection,ImportAction
Data.Root.ChannelGroups(1).Channels("pulse").Name = "Lasor"

Call Calculate("Ch(""[1]/Normalised
Fluo"")=Ch(""[1]/Fluo"")/Ch(""[1]/Lasor"")",NULL,NULL,"") '...
CalculateFormula,CalculateSymbols,CalculateValues,CalculateTargetUnit
StatSel(1)        = "No"
StatSel(2)        = "No"
StatSel(3)        = "No"
StatSel(4)        = "No"
StatSel(5)        = "No"
StatSel(6)        = "Yes"
StatSel(7)        = "No"
StatSel(8)        = "No"
StatSel(9)        = "No"
StatSel(10)       = "No"
StatSel(11)       = "No"
StatSel(12)       = "No"
StatSel(13)       = "No"
StatSel(14)       = "Yes"
StatSel(15)       = "Yes"
StatSel(16)       = "No"
StatSel(17)       = "No"
StatSel(18)       = "No"
StatSel(19)       = "No"
StatSel(20)       = "No"
StatSel(21)       = "No"
StatSel(22)       = "No"
StatSel(23)       = "Yes"
StatClipCopy      = 0
StatClipValue     = 0
StatFormat        = ""
StatResChn        = 1
StatResChnNames   = 0
StatResChnNameFormat= "NameName"
Call StatBlockCalc("Channel","1-","[1]/Normalised Fluo") '...
StatDirec,RowNoStr,ChnNoStr
Data.Root.ChannelGroups(1).Channels("ArithmeticMean").Name = "150mm"

Call DataFileSave(MyFolders(0)&"150mm Wedge 110111 1GSs 5Hz 1.12kV Fluo Curve
Data Normalised & Averaged.TDM","TDM") '... DataFilename,FileExportFilter
```

Calibration Curve

```
'-------------------------------------------------------------------------
--
'-- VBS script file
'-- Created on 05/04/2011 15:45:14
'-- Author: ---
'-- Comment: ---
'-------------------------------------------------------------------------
--
Option Explicit  'Forces the explicit declaration of all the variables in a
script.

Dim MyFolders()
Call InitMyFolders
'-------------------------------------------------------------------------
--
Sub InitMyFolders
  ReDim MyFolders(1)
  MyFolders(0)="C:\Documents and Settings\c109859\My Documents\- PhD -\-
Lubricant Dynamics -\LabVIEW\FDU data 2011\110111 Calibration & 700ml FDU
data\Calibration\"
End Sub
'-------------------------------------------------------------------------
--

''''''''''Loading Normalised Fluorescence Wedge values

Call Data.Root.Clear()
Call DataFileLoad(MyFolders(0)&"10mm Wedge 110111 1GSs 5Hz 1.12kV Fluo Curve
Data Normalised & Averaged.TDM","TDM","") '...
DataFilename,FileImportFilter,ImportAction
Call DataFileLoad(MyFolders(0)&"20mm Wedge 110111 1GSs 5Hz 1.12kV Fluo Curve
Data Normalised & Averaged.TDM","TDM","") '...
DataFilename,FileImportFilter,ImportAction
Call DataFileLoad(MyFolders(0)&"30mm Wedge 110111 1GSs 5Hz 1.12kV Fluo Curve
Data Normalised & Averaged.TDM","TDM","") '...
DataFilename,FileImportFilter,ImportAction
Call DataFileLoad(MyFolders(0)&"40mm Wedge 110111 1GSs 5Hz 1.12kV Fluo Curve
Data Normalised & Averaged.TDM","TDM","") '...
DataFilename,FileImportFilter,ImportAction
Call DataFileLoad(MyFolders(0)&"50mm Wedge 110111 1GSs 5Hz 1.12kV Fluo Curve
Data Normalised & Averaged.TDM","TDM","") '...
DataFilename,FileImportFilter,ImportAction
Call DataFileLoad(MyFolders(0)&"60mm Wedge 110111 1GSs 5Hz 1.12kV Fluo Curve
Data Normalised & Averaged.TDM","TDM","") '...
DataFilename,FileImportFilter,ImportAction
Call DataFileLoad(MyFolders(0)&"70mm Wedge 110111 1GSs 5Hz 1.12kV Fluo Curve
Data Normalised & Averaged.TDM","TDM","") '...
DataFilename,FileImportFilter,ImportAction
Call DataFileLoad(MyFolders(0)&"80mm Wedge 110111 1GSs 5Hz 1.12kV Fluo Curve
Data Normalised & Averaged.TDM","TDM","") '...
DataFilename,FileImportFilter,ImportAction
Call DataFileLoad(MyFolders(0)&"90mm Wedge 110111 1GSs 5Hz 1.12kV Fluo Curve
Data Normalised & Averaged.TDM","TDM","") '...
DataFilename,FileImportFilter,ImportAction
Call DataFileLoad(MyFolders(0)&"100mm Wedge 110111 1GSs 5Hz 1.12kV Fluo Curve
Data Normalised & Averaged.TDM","TDM","") '...
DataFilename,FileImportFilter,ImportAction
Call DataFileLoad(MyFolders(0)&"110mm Wedge 110111 1GSs 5Hz 1.12kV Fluo Curve
Data Normalised & Averaged.TDM","TDM","") '...
DataFilename,FileImportFilter,ImportAction
```

```
Call DataFileLoad(MyFolders(0)&"120mm Wedge 110111 1GSs 5Hz 1.12kV Fluo Curve
Data Normalised & Averaged.TDM","TDM","") '...
DataFilename,FileImportFilter,ImportAction
Call DataFileLoad(MyFolders(0)&"130mm Wedge 110111 1GSs 5Hz 1.12kV Fluo Curve
Data Normalised & Averaged.TDM","TDM","") '...
DataFilename,FileImportFilter,ImportAction
Call DataFileLoad(MyFolders(0)&"140mm Wedge 110111 1GSs 5Hz 1.12kV Fluo Curve
Data Normalised & Averaged.TDM","TDM","") '...
DataFilename,FileImportFilter,ImportAction
Call DataFileLoad(MyFolders(0)&"150mm Wedge 110111 1GSs 5Hz 1.12kV Fluo Curve
Data Normalised & Averaged.TDM","TDM","") '...
DataFilename,FileImportFilter,ImportAction

''''''''''Normalised Fluorescence

Call Data.Root.ChannelGroups.Add("Normalised Fluorescence", 16).Activate()
Call Data.Root.ChannelGroups(16).Channels.Add("Normalised
Fluorescence",DataTypeFloat64,1)
Call ChnGenVal("[16]/Normalised Fluorescence",1,15,1,1,0) '...
ChnArg1,ChnRow,ValNo,ChnBegin,ChnStep,ValueOverwrite
CHD(1,106)=CHD(1,4)
CHD(2,106)=CHD(1,11)
CHD(3,106)=CHD(1,18)
CHD(4,106)=CHD(1,25)
CHD(5,106)=CHD(1,32)
CHD(6,106)=CHD(1,39)
CHD(7,106)=CHD(1,46)
CHD(8,106)=CHD(1,53)
CHD(9,106)=CHD(1,60)
CHD(10,106)=CHD(1,67)
CHD(11,106)=CHD(1,74)
CHD(12,106)=CHD(1,81)
CHD(13,106)=CHD(1,88)
CHD(14,106)=CHD(1,95)
CHD(15,106)=CHD(1,102)

''''''''''Wedge Dimensions

Call Data.Root.ChannelGroups(16).Channels.Add("Oil Thickness
(mm)",DataTypeFloat64,2)
Call ChnGenVal("[16]/Oil Thickness (mm)",1,15,1,1,0) '...
ChnArg1,ChnRow,ValNo,ChnBegin,ChnStep,ValueOverwrite
CHD(1,107)=(0.66)
CHD(2,107)=(0.99)
CHD(3,107)=(1.33)
CHD(4,107)=(1.66)
CHD(5,107)=(1.99)
CHD(6,107)=(2.32)
CHD(7,107)=(2.65)
CHD(8,107)=(2.98)
CHD(9,107)=(3.32)
CHD(10,107)=(3.65)
CHD(11,107)=(3.98)
CHD(12,107)=(4.31)
CHD(13,107)=(4.64)
CHD(14,107)=(4.97)
CHD(15,107)=(5.31)

''''''''''Fluo vs Thickness & Line of best fit through the origin

NonLinearFitModelFunction= "a*x^b"
NonLinearFitIndepVariable= "x"
NonLinearFitCoefCount= 2
NonLinearFitCoefName(1)= "a"
NonLinearFitCoefName(2)= "b"
```

```
NonLinearFitInitCoef(1)= 1
NonLinearFitInitCoef(2)= 1
Call ChnNonLinearFitXY("[16]/Normalised Fluorescence","[16]/Oil Thickness
(mm)","/NonLinearFitX","/NonLinearFitY","Partition complete area",100,1,10,0)
'...
XW,Y,E,E,XChnStyle,XNo,XDiv,NonLinearFitMaxIterations,NonLinearFitCovariance

Call DataFileSave(MyFolders(0)&"Wedge 110111 1GSs 5Hz 1.12kV Fluo Curve Data
Normalised & Averaged axb.TDM","TDM") '... DataFilename,FileExportFilter

'Call PicLoad(MyFolders(0)&"Calibration Curve.TDR") '... PicFile
'Call PicUpdate(0)                                  '... PicDoubleBuffer
```

DIAdem Scripts – FDU Data

Run All

```
'-------------------------------------------------------------------------
--
'-- VBS script file
'-- Created on 05/11/2011 11:21:00
'-- Author:
'-- Comment:
'-------------------------------------------------------------------------
--
Option Explicit  'Forces the explicit declaration of all the variables in a
script.

Dim MyFolders()
Call InitMyFolders
'-------------------------------------------------------------------------
--
Sub InitMyFolders
  ReDim MyFolders(1)
  MyFolders(0)="C:\Documents and Settings\c109859\My Documents\- PhD -\-
Lubricant Dynamics -\LabVIEW\FDU data 2011\110203 Cali & 700ml & 800ml CW
tooth tip\700ml tooth tip 19.7-24.2\"
End Sub
'-------------------------------------------------------------------------
--

Call ScriptStart(MyFolders(0)&"SCRIPT - RUN ALL 1st Peak Finding FDU")
Call ScriptStart(MyFolders(0)&"SCRIPT - RUN ALL Averaging FDU")
Call ScriptStart(MyFolders(0)&"SCRIPT - Fluorescence Correction")
Call ScriptStart(MyFolders(0)&"SCRIPT - FDU Oil Thicknesses axb")
Call ScriptStart(MyFolders(0)&"SCRIPT - FDU C-End Oil Thicknesses axb")
```

Run All 1st Peak Finding FDU

```
'-------------------------------------------------------------------------
--
'-- VBS script file
'-- Created on 05/03/2011 15:45:48
'-- Author: ---
'-- Comment: ---
'-------------------------------------------------------------------------
--
Option Explicit  'Forces the explicit declaration of all the variables in a
script.

Dim MyFolders()
Call InitMyFolders
'-------------------------------------------------------------------------
--
Sub InitMyFolders
  ReDim MyFolders(1)
  MyFolders(0)="C:\Documents and Settings\c109859\My Documents\- PhD -\-
Lubricant Dynamics -\LabVIEW\FDU data 2011\110203 Cali & 700ml & 800ml CW
tooth tip\700ml tooth tip 19.7-24.2\"
End Sub
'-------------------------------------------------------------------------
--

'''''''''' 3.6% ''''''''''
Call Data.Root.Clear()
Call DataFileLoad(MyFolders(0)&"3.6% FDU 700ml 110203 1GSs Fluo Curve
Data.lvm","LVM","") '... DataFilename,FileImportFilter,ImportAction
call ScriptStart(MyFolders(0)&"SCRIPT - 1st Peak Finding FDU")
Call DataFileSave(MyFolders(0)&"3.6% 700ml 110203 1GSs 5Hz 1.12kV Fluo Curve
Data Modified.TDM","TDM") '... DataFilename,FileExportFilter

Call Data.Root.Clear()
Call DataFileLoad(MyFolders(0)&"3.6% FDU 700ml 110203 1GSs Laser Pwr Curve
Data.lvm","LVM","") '... DataFilename,FileImportFilter,ImportAction
call ScriptStart(MyFolders(0)&"SCRIPT - 1st Peak Finding FDU")
Call DataFileSave(MyFolders(0)&"3.6% 700ml 110203 1GSs 5Hz 1.12kV Laser Pwr
Curve Data Modified.TDM","TDM") '... DataFilename,FileExportFilter

'''''''''' 4% ''''''''''
Call Data.Root.Clear()
Call DataFileLoad(MyFolders(0)&"4% FDU 700ml 110203 1GSs Fluo Curve
Data.lvm","LVM","") '... DataFilename,FileImportFilter,ImportAction
call ScriptStart(MyFolders(0)&"SCRIPT - 1st Peak Finding FDU")
Call DataFileSave(MyFolders(0)&"4% 700ml 110203 1GSs 5Hz 1.12kV Fluo Curve
Data Modified.TDM","TDM") '... DataFilename,FileExportFilter

Call Data.Root.Clear()
Call DataFileLoad(MyFolders(0)&"4% FDU 700ml 110203 1GSs Laser Pwr Curve
Data.lvm","LVM","") '... DataFilename,FileImportFilter,ImportAction
call ScriptStart(MyFolders(0)&"SCRIPT - 1st Peak Finding FDU")
Call DataFileSave(MyFolders(0)&"4% 700ml 110203 1GSs 5Hz 1.12kV Laser Pwr
Curve Data Modified.TDM","TDM") '... DataFilename,FileExportFilter

'''''''''' 4.5% ''''''''''
.
.
.
'''''''''' 18% ''''''''''
Call Data.Root.Clear()
Call DataFileLoad(MyFolders(0)&"18% FDU 700ml 110203 1GSs Fluo Curve
Data.lvm","LVM","") '... DataFilename,FileImportFilter,ImportAction
```

```
call ScriptStart(MyFolders(0)&"SCRIPT - 1st Peak Finding FDU")
Call DataFileSave(MyFolders(0)&"18% 700ml 110203 1GSs 5Hz 1.12kV Fluo Curve
Data Modified.TDM","TDM") '... DataFilename,FileExportFilter

Call Data.Root.Clear()
Call DataFileLoad(MyFolders(0)&"18% FDU 700ml 110203 1GSs Laser Pwr Curve
Data.lvm","LVM","") '... DataFilename,FileImportFilter,ImportAction
call ScriptStart(MyFolders(0)&"SCRIPT - 1st Peak Finding FDU")
Call DataFileSave(MyFolders(0)&"18% 700ml 110203 1GSs 5Hz 1.12kV Laser Pwr
Curve Data Modified.TDM","TDM") '... DataFilename,FileExportFilter

'''''''''' 20% ''''''''''
Call Data.Root.Clear()
Call DataFileLoad(MyFolders(0)&"20% FDU 700ml 110203 1GSs Fluo Curve
Data.lvm","LVM","") '... DataFilename,FileImportFilter,ImportAction
call ScriptStart(MyFolders(0)&"SCRIPT - 1st Peak Finding FDU")
Call DataFileSave(MyFolders(0)&"20% 700ml 110203 1GSs 5Hz 1.12kV Fluo Curve
Data Modified.TDM","TDM") '... DataFilename,FileExportFilter

Call Data.Root.Clear()
Call DataFileLoad(MyFolders(0)&"20% FDU 700ml 110203 1GSs Laser Pwr Curve
Data.lvm","LVM","") '... DataFilename,FileImportFilter,ImportAction
call ScriptStart(MyFolders(0)&"SCRIPT - 1st Peak Finding FDU")
Call DataFileSave(MyFolders(0)&"20% 700ml 110203 1GSs 5Hz 1.12kV Laser Pwr
Curve Data Modified.TDM","TDM") '... DataFilename,FileExportFilter

'''''''''' BACKGROUND ''''''''''
Call Data.Root.Clear()
Call DataFileLoad(MyFolders(0)&"FDU Bkgd 110203 1GSs 5Hz 1.12kV Fluo Curve
Data.lvm","LVM","") '... DataFilename,FileImportFilter,ImportAction
call ScriptStart(MyFolders(0)&"SCRIPT - 1st Peak Finding FDU")
Call DataFileSave(MyFolders(0)&"FDU Bkgd 110203 1GSs 5Hz 1.12kV Fluo Curve
Data Modified.TDM","TDM") '... DataFilename,FileExportFilter

Call Data.Root.Clear()
Call DataFileLoad(MyFolders(0)&"FDU Background 110203 1GSs 5Hz 1.12kV Laser
Pwr Curve Data.lvm","LVM","") '... DataFilename,FileImportFilter,ImportAction
call ScriptStart(MyFolders(0)&"SCRIPT - 1st Peak Finding FDU")
Call DataFileSave(MyFolders(0)&"FDU Background 110203 1GSs 5Hz 1.12kV Laser
Pwr Curve Data Modified.TDM","TDM") '... DataFilename,FileExportFilter
```

Run All Averaging FDU

```
'-------------------------------------------------------------------------
--
'-- VBS script file
'-- Created on 05/03/2011 18:22:02
'-- Author: ---
'-- Comment: ---
'-------------------------------------------------------------------------
--
Option Explicit  'Forces the explicit declaration of all the variables in a
script.

Dim MyFolders()
Call InitMyFolders
'-------------------------------------------------------------------------
--
Sub InitMyFolders
  ReDim MyFolders(1)
  MyFolders(0)="C:\Documents and Settings\c109859\My Documents\- PhD -\-
Lubricant Dynamics -\LabVIEW\FDU data 2011\110203 Cali & 700ml & 800ml CW
tooth tip\700ml tooth tip 19.7-24.2\"
End Sub
'-------------------------------------------------------------------------
--

''''''''' 3.6% '''''''''

Call Data.Root.Clear()

Call Data.Root.ChannelGroups.Add("3.6%", 1).Activate()
Call DataFileLoadSel(MyFolders(0)&"3.6% 700ml 110203 1GSs 5Hz 1.12kV Fluo
Curve Data Modified.TDM","TDM","3.6%/pulse","") '...
DataFilename,FileImportFilter,ImportSelection,ImportAction
Data.Root.ChannelGroups(1).Channels("pulse").Name = "Fluo"

Call DataFileLoadSel(MyFolders(0)&"3.6% 700ml 110203 1GSs 5Hz 1.12kV Laser Pwr
Curve Data Modified.TDM","TDM","3.6%/pulse","") '...
DataFilename,FileImportFilter,ImportSelection,ImportAction
Data.Root.ChannelGroups(1).Channels("pulse").Name = "Laser"

Call Calculate("Ch(""[1]/Normalised
Fluo"")=Ch(""[1]/Fluo"")/Ch(""[1]/Laser"")",NULL,NULL,"") '...
CalculateFormula,CalculateSymbols,CalculateValues,CalculateTargetUnit
StatSel(1)        = "No"
StatSel(2)        = "No"
StatSel(3)        = "No"
StatSel(4)        = "No"
StatSel(5)        = "No"
StatSel(6)        = "Yes"
StatSel(7)        = "No"
StatSel(8)        = "No"
StatSel(9)        = "No"
StatSel(10)       = "No"
StatSel(11)       = "No"
StatSel(12)       = "No"
StatSel(13)       = "No"
StatSel(14)       = "Yes"
StatSel(15)       = "Yes"
StatSel(16)       = "No"
StatSel(17)       = "No"
StatSel(18)       = "No"
StatSel(19)       = "No"
StatSel(20)       = "No"
StatSel(21)       = "No"
StatSel(22)       = "No"
```

```
StatSel(23)       = "Yes"
StatClipCopy      = 0
StatClipValue     = 0
StatFormat        = ""
StatResChn        = 1
StatResChnNames   = 0
StatResChnNameFormat= "NameName"
Call StatBlockCalc("Channel","1-","[1]/Normalised Fluo") '...
StatDirec,RowNoStr,ChnNoStr
Data.Root.ChannelGroups(1).Channels("ArithmeticMean").Name = "3.6%"

Call DataFileSave(MyFolders(0)&"3.6% 700ml 110203 1GSs 5Hz 1.12kV Fluo Curve
Data Normalised & Averaged.TDM","TDM") '... DataFilename,FileExportFilter

''''''''' 4% ''''''''''

Call Data.Root.Clear()

Call Data.Root.ChannelGroups.Add("4%", 1).Activate()
Call DataFileLoadSel(MyFolders(0)&"4% 700ml 110203 1GSs 5Hz 1.12kV Fluo Curve
Data Modified.TDM","TDM","3.6%/pulse","") '...
DataFilename,FileImportFilter,ImportSelection,ImportAction
Data.Root.ChannelGroups(1).Channels("pulse").Name = "Fluo"

Call DataFileLoadSel(MyFolders(0)&"4% 700ml 110203 1GSs 5Hz 1.12kV Laser Pwr
Curve Data Modified.TDM","TDM","3.6%/pulse","") '...
DataFilename,FileImportFilter,ImportSelection,ImportAction
Data.Root.ChannelGroups(1).Channels("pulse").Name = "laser"

Call Calculate("Ch(""[1]/Normalised
Fluo"")=Ch(""[1]/Fluo"")/Ch(""[1]/laser"")",NULL,NULL,"") '...
CalculateFormula,CalculateSymbols,CalculateValues,CalculateTargetUnit
StatSel(1)        = "No"
StatSel(2)        = "No"
StatSel(3)        = "No"
StatSel(4)        = "No"
StatSel(5)        = "No"
StatSel(6)        = "Yes"
StatSel(7)        = "No"
StatSel(8)        = "No"
StatSel(9)        = "No"
StatSel(10)       = "No"
StatSel(11)       = "No"
StatSel(12)       = "No"
StatSel(13)       = "No"
StatSel(14)       = "Yes"
StatSel(15)       = "Yes"
StatSel(16)       = "No"
StatSel(17)       = "No"
StatSel(18)       = "No"
StatSel(19)       = "No"
StatSel(20)       = "No"
StatSel(21)       = "No"
StatSel(22)       = "No"
StatSel(23)       = "Yes"
StatClipCopy      = 0
StatClipValue     = 0
StatFormat        = ""
StatResChn        = 1
StatResChnNames   = 0
StatResChnNameFormat= "NameName"
Call StatBlockCalc("Channel","1-","[1]/Normalised Fluo") '...
StatDirec,RowNoStr,ChnNoStr
Data.Root.ChannelGroups(1).Channels("ArithmeticMean").Name = "4%"
```

```
Call DataFileSave(MyFolders(0)&"4% 700ml 110203 1GSs 5Hz 1.12kV Fluo Curve
Data Normalised & Averaged.TDM","TDM") '... DataFilename,FileExportFilter

''''''''' 4.5% '''''''''
.
.
.
''''''''' 18% '''''''''
Call Data.Root.Clear()

Call Data.Root.ChannelGroups.Add("18%", 1).Activate()
Call DataFileLoadSel(MyFolders(0)&"18% 700ml 110203 1GSs 5Hz 1.12kV Fluo Curve
Data Modified.TDM","TDM","3.6%/pulse","") '...
DataFilename,FileImportFilter,ImportSelection,ImportAction
Data.Root.ChannelGroups(1).Channels("pulse").Name = "Fluo"

Call DataFileLoadSel(MyFolders(0)&"18% 700ml 110203 1GSs 5Hz 1.12kV Laser Pwr
Curve Data Modified.TDM","TDM","3.6%/pulse","") '...
DataFilename,FileImportFilter,ImportSelection,ImportAction
Data.Root.ChannelGroups(1).Channels("pulse").Name = "laser"

Call Calculate("Ch(""[1]/Normalised
Fluo"")=Ch(""[1]/Fluo"")/Ch(""[1]/laser"")",NULL,NULL,"") '...
CalculateFormula,CalculateSymbols,CalculateValues,CalculateTargetUnit
StatSel(1)        = "No"
StatSel(2)        = "No"
StatSel(3)        = "No"
StatSel(4)        = "No"
StatSel(5)        = "No"
StatSel(6)        = "Yes"
StatSel(7)        = "No"
StatSel(8)        = "No"
StatSel(9)        = "No"
StatSel(10)       = "No"
StatSel(11)       = "No"
StatSel(12)       = "No"
StatSel(13)       = "No"
StatSel(14)       = "Yes"
StatSel(15)       = "Yes"
StatSel(16)       = "No"
StatSel(17)       = "No"
StatSel(18)       = "No"
StatSel(19)       = "No"
StatSel(20)       = "No"
StatSel(21)       = "No"
StatSel(22)       = "No"
StatSel(23)       = "Yes"
StatClipCopy      = 0
StatClipValue     = 0
StatFormat        = ""
StatResChn        = 1
StatResChnNames   = 0
StatResChnNameFormat= "NameName"
Call StatBlockCalc("Channel","1-","[1]/Normalised Fluo") '...
StatDirec,RowNoStr,ChnNoStr
Data.Root.ChannelGroups(1).Channels("ArithmeticMean").Name = "18%"

Call DataFileSave(MyFolders(0)&"18% 700ml 110203 1GSs 5Hz 1.12kV Fluo Curve
Data Normalised & Averaged.TDM","TDM") '... DataFilename,FileExportFilter

''''''''' 20% '''''''''
Call Data.Root.Clear()

Call Data.Root.ChannelGroups.Add("20%", 1).Activate()
```

```
Call DataFileLoadSel(MyFolders(0)&"20% 700ml 110203 1GSs 5Hz 1.12kV Fluo Curve
Data Modified.TDM","TDM","3.6%/pulse","") '...
DataFilename,FileImportFilter,ImportSelection,ImportAction
Data.Root.ChannelGroups(1).Channels("pulse").Name = "Fluo"

Call DataFileLoadSel(MyFolders(0)&"20% 700ml 110203 1GSs 5Hz 1.12kV Laser Pwr
Curve Data Modified.TDM","TDM","3.6%/pulse","") '...
DataFilename,FileImportFilter,ImportSelection,ImportAction
Data.Root.ChannelGroups(1).Channels("pulse").Name = "laser"

Call Calculate("Ch(""[1]/Normalised
Fluo"")=Ch(""[1]/Fluo"")/Ch(""[1]/laser"")",NULL,NULL,"") '...
CalculateFormula,CalculateSymbols,CalculateValues,CalculateTargetUnit
StatSel(1)        = "No"
StatSel(2)        = "No"
StatSel(3)        = "No"
StatSel(4)        = "No"
StatSel(5)        = "No"
StatSel(6)        = "Yes"
StatSel(7)        = "No"
StatSel(8)        = "No"
StatSel(9)        = "No"
StatSel(10)       = "No"
StatSel(11)       = "No"
StatSel(12)       = "No"
StatSel(13)       = "No"
StatSel(14)       = "Yes"
StatSel(15)       = "Yes"
StatSel(16)       = "No"
StatSel(17)       = "No"
StatSel(18)       = "No"
StatSel(19)       = "No"
StatSel(20)       = "No"
StatSel(21)       = "No"
StatSel(22)       = "No"
StatSel(23)       = "Yes"
StatClipCopy      = 0
StatClipValue     = 0
StatFormat        = ""
StatResChn        = 1
StatResChnNames   = 0
StatResChnNameFormat= "NameName"
Call StatBlockCalc("Channel","1-","[1]/Normalised Fluo") '...
StatDirec,RowNoStr,ChnNoStr
Data.Root.ChannelGroups(1).Channels("ArithmeticMean").Name = "20%"

Call DataFileSave(MyFolders(0)&"20% 700ml 110203 1GSs 5Hz 1.12kV Fluo Curve
Data Normalised & Averaged.TDM","TDM") '... DataFilename,FileExportFilter

''''''''' BACKGROUND '''''''''
Call Data.Root.Clear()

Call Data.Root.ChannelGroups.Add("Background", 1).Activate()
Call DataFileLoadSel(MyFolders(0)&"FDU Bkgd 110203 1GSs 5Hz 1.12kV Fluo Curve
Data Modified.TDM","TDM","3.6%/pulse","") '...
DataFilename,FileImportFilter,ImportSelection,ImportAction
Data.Root.ChannelGroups(1).Channels("pulse").Name = "Fluo"

Call DataFileLoadSel(MyFolders(0)&"FDU Background 110203 1GSs 5Hz 1.12kV Laser
Pwr Curve Data Modified.TDM","TDM","3.6%/pulse","") '...
DataFilename,FileImportFilter,ImportSelection,ImportAction
Data.Root.ChannelGroups(1).Channels("pulse").Name = "laser"
```

```
Call Calculate("Ch(""[1]/Normalised
Fluo"")=Ch(""[1]/Fluo"")/Ch(""[1]/laser"")",NULL,NULL,"") '...
CalculateFormula,CalculateSymbols,CalculateValues,CalculateTargetUnit
StatSel(1)        = "No"
StatSel(2)        = "No"
StatSel(3)        = "No"
StatSel(4)        = "No"
StatSel(5)        = "No"
StatSel(6)        = "Yes"
StatSel(7)        = "No"
StatSel(8)        = "No"
StatSel(9)        = "No"
StatSel(10)       = "No"
StatSel(11)       = "No"
StatSel(12)       = "No"
StatSel(13)       = "No"
StatSel(14)       = "Yes"
StatSel(15)       = "Yes"
StatSel(16)       = "No"
StatSel(17)       = "No"
StatSel(18)       = "No"
StatSel(19)       = "No"
StatSel(20)       = "No"
StatSel(21)       = "No"
StatSel(22)       = "No"
StatSel(23)       = "Yes"
StatClipCopy      = 0
StatClipValue     = 0
StatFormat        = ""
StatResChn        = 1
StatResChnNames   = 0
StatResChnNameFormat= "NameName"
Call StatBlockCalc("Channel","1-","[1]/Normalised Fluo") '...
StatDirec,RowNoStr,ChnNoStr
Data.Root.ChannelGroups(1).Channels("ArithmeticMean").Name = "Background"

Call DataFileSave(MyFolders(0)&"FDU Background 110203 1GSs 5Hz 1.12kV Fluo
Curve Data Normalised & Averaged.TDM","TDM") '...
DataFilename,FileExportFilter
```

Fluorescence Correction

```
'-------------------------------------------------------------------------
--
'-- VBS script file
'-- Created on 05/04/2011 15:45:14
'-- Author: ---
'-- Comment: ---
'-------------------------------------------------------------------------
--
Option Explicit  'Forces the explicit declaration of all the variables in a
script.

Dim MyFolders()
Call InitMyFolders
'-------------------------------------------------------------------------
--
Sub InitMyFolders
  ReDim MyFolders(1)
  MyFolders(0)="C:\Documents and Settings\c109859\My Documents\- PhD -\-
Lubricant Dynamics -\LabVIEW\FDU data 2011\110203 Cali & 700ml & 800ml CW
tooth tip\700ml tooth tip 19.7-24.2\"
End Sub
'-------------------------------------------------------------------------
--

''''''''''Loading Normalised Fluorescence FDU values

Call Data.Root.Clear()
Call DataFileLoad(MyFolders(0)&"3.6% 700ml 110203 1GSs 5Hz 1.12kV Fluo Curve
Data Normalised & Averaged.TDM","TDM","") '...
DataFilename,FileImportFilter,ImportAction
Call DataFileLoad(MyFolders(0)&"4% 700ml 110203 1GSs 5Hz 1.12kV Fluo Curve
Data Normalised & Averaged.TDM","TDM","") '...
DataFilename,FileImportFilter,ImportAction
Call DataFileLoad(MyFolders(0)&"4.5% 700ml 110203 1GSs 5Hz 1.12kV Fluo Curve
Data Normalised & Averaged.TDM","TDM","") '...
DataFilename,FileImportFilter,ImportAction
Call DataFileLoad(MyFolders(0)&"5% 700ml 110203 1GSs 5Hz 1.12kV Fluo Curve
Data Normalised & Averaged.TDM","TDM","") '...
DataFilename,FileImportFilter,ImportAction
Call DataFileLoad(MyFolders(0)&"5.5% 700ml 110203 1GSs 5Hz 1.12kV Fluo Curve
Data Normalised & Averaged.TDM","TDM","") '...
DataFilename,FileImportFilter,ImportAction
Call DataFileLoad(MyFolders(0)&"6% 700ml 110203 1GSs 5Hz 1.12kV Fluo Curve
Data Normalised & Averaged.TDM","TDM","") '...
DataFilename,FileImportFilter,ImportAction
Call DataFileLoad(MyFolders(0)&"6.5% 700ml 110203 1GSs 5Hz 1.12kV Fluo Curve
Data Normalised & Averaged.TDM","TDM","") '...
DataFilename,FileImportFilter,ImportAction
Call DataFileLoad(MyFolders(0)&"7% 700ml 110203 1GSs 5Hz 1.12kV Fluo Curve
Data Normalised & Averaged.TDM","TDM","") '...
DataFilename,FileImportFilter,ImportAction
Call DataFileLoad(MyFolders(0)&"7.5% 700ml 110203 1GSs 5Hz 1.12kV Fluo Curve
Data Normalised & Averaged.TDM","TDM","") '...
DataFilename,FileImportFilter,ImportAction
Call DataFileLoad(MyFolders(0)&"8% 700ml 110203 1GSs 5Hz 1.12kV Fluo Curve
Data Normalised & Averaged.TDM","TDM","") '...
DataFilename,FileImportFilter,ImportAction
Call DataFileLoad(MyFolders(0)&"10% 700ml 110203 1GSs 5Hz 1.12kV Fluo Curve
Data Normalised & Averaged.TDM","TDM","") '...
DataFilename,FileImportFilter,ImportAction
Call DataFileLoad(MyFolders(0)&"12% 700ml 110203 1GSs 5Hz 1.12kV Fluo Curve
Data Normalised & Averaged.TDM","TDM","") '...
DataFilename,FileImportFilter,ImportAction
```

```
Call DataFileLoad(MyFolders(0)&"14% 700ml 110203 1GSs 5Hz 1.12kV Fluo Curve
Data Normalised & Averaged.TDM","TDM","") '...
DataFilename,FileImportFilter,ImportAction
Call DataFileLoad(MyFolders(0)&"16% 700ml 110203 1GSs 5Hz 1.12kV Fluo Curve
Data Normalised & Averaged.TDM","TDM","") '...
DataFilename,FileImportFilter,ImportAction
Call DataFileLoad(MyFolders(0)&"18% 700ml 110203 1GSs 5Hz 1.12kV Fluo Curve
Data Normalised & Averaged.TDM","TDM","") '...
DataFilename,FileImportFilter,ImportAction
Call DataFileLoad(MyFolders(0)&"20% 700ml 110203 1GSs 5Hz 1.12kV Fluo Curve
Data Normalised & Averaged.TDM","TDM","") '...
DataFilename,FileImportFilter,ImportAction
Call DataFileLoad(MyFolders(0)&"FDU Background 110203 1GSs 5Hz 1.12kV Fluo
Curve Data Normalised & Averaged.TDM","TDM","") '...
DataFilename,FileImportFilter,ImportAction

''''''''''Normalised Fluorescence

Call Data.Root.ChannelGroups.Add("Normalised FDU Fluorescence", 18).Activate()
Call Data.Root.ChannelGroups(18).Channels.Add("Normalised FDU
Fluorescence",DataTypeFloat64,1)
Call ChnGenVal("[18]/Normalised FDU Fluorescence",1,16,1,1,0) '...
ChnArg1,ChnRow,ValNo,ChnBegin,ChnStep,ValueOverwrite
CHD(1,120)=CHD(1,4)
CHD(2,120)=CHD(1,11)
CHD(3,120)=CHD(1,18)
CHD(4,120)=CHD(1,25)
CHD(5,120)=CHD(1,32)
CHD(6,120)=CHD(1,39)
CHD(7,120)=CHD(1,46)
CHD(8,120)=CHD(1,53)
CHD(9,120)=CHD(1,60)
CHD(10,120)=CHD(1,67)
CHD(11,120)=CHD(1,74)
CHD(12,120)=CHD(1,81)
CHD(13,120)=CHD(1,88)
CHD(14,120)=CHD(1,95)
CHD(15,120)=CHD(1,102)
CHD(16,120)=CHD(1,109)

''''''''''CORRECTED Normalised Fluorescence

Call Data.Root.ChannelGroups(18).Channels.Add("Corrected Normalised FDU
Fluorescence",DataTypeFloat64,2)
Call ChnGenVal("[18]/Corrected Normalised FDU Fluorescence",1,16,1,1,0) '...
ChnArg1,ChnRow,ValNo,ChnBegin,ChnStep,ValueOverwrite
CHD(1,121)=CHD(1,4)-CHD(1,116)
CHD(2,121)=CHD(1,11)-CHD(1,116)
CHD(3,121)=CHD(1,18)-CHD(1,116)
CHD(4,121)=CHD(1,25)-CHD(1,116)
CHD(5,121)=CHD(1,32)-CHD(1,116)
CHD(6,121)=CHD(1,39)-CHD(1,116)
CHD(7,121)=CHD(1,46)-CHD(1,116)
CHD(8,121)=CHD(1,53)-CHD(1,116)
CHD(9,121)=CHD(1,60)-CHD(1,116)
CHD(10,121)=CHD(1,67)-CHD(1,116)
CHD(11,121)=CHD(1,74)-CHD(1,116)
CHD(12,121)=CHD(1,81)-CHD(1,116)
CHD(13,121)=CHD(1,88)-CHD(1,116)
CHD(14,121)=CHD(1,95)-CHD(1,116)
CHD(15,121)=CHD(1,102)-CHD(1,116)
CHD(16,121)=CHD(1,109)-CHD(1,116)

''''''''''Road Speed mph
```

```
Call Data.Root.ChannelGroups(18).Channels.Add("Road Speed
(mph)",DataTypeFloat64,3)
Call ChnGenVal("[18]/Road Speed (mph)",1,16,1,1,0) '...
ChnArg1,ChnRow,ValNo,ChnBegin,ChnStep,ValueOverwrite
CHD(1,122)=(4.85)
CHD(2,122)=(5.39)
CHD(3,122)=(6.06)
CHD(4,122)=(6.73)
CHD(5,122)=(7.41)
CHD(6,122)=(8.08)
CHD(7,122)=(8.75)
CHD(8,122)=(9.43)
CHD(9,122)=(10.10)
CHD(10,122)=(10.77)
CHD(11,122)=(13.47)
CHD(12,122)=(16.16)
CHD(13,122)=(18.85)
CHD(14,122)=(21.55)
CHD(15,122)=(24.24)
CHD(16,122)=(26.93)

Call DataFileSave(MyFolders(0)&"FDU 700ml 110203 1GSs 5Hz 1.12kV Fluo Curve
Data Normalised & Averaged.TDM","TDM") '... DataFilename,FileExportFilter


''''''''''Fluo vs Thickness & Line of best fit through the origin
''
''NonLinearFitModelFunction= "b*x+c*x^2"
''NonLinearFitIndepVariable= "x"
''NonLinearFitCoefCount= 2
''NonLinearFitCoefName(1)= "b"
''NonLinearFitCoefName(2)= "c"
''NonLinearFitInitCoef(1)= 1
''NonLinearFitInitCoef(2)= 1
''Call ChnNonLinearFitXY("[16]/Normalised Fluorescence","[16]/Road Speed
(mph)","/NonLinearFitX","/NonLinearFitY","Partition complete area",100,1,10,0)
'...
XW,Y,E,E,XChnStyle,XNo,XDiv,NonLinearFitMaxIterations,NonLinearFitCovariance
''
''Call PicLoad(MyFolders(0)&"Calibration Curve.TDR") '... PicFile
''Call PicUpdate(0)                          '... PicDoubleBuffer
```

FDU Oil Thickness axb

```
'-------------------------------------------------------------------------
--
'-- VBS script file
'-- Created on 05/12/2011 11:36:43
'-- Author: ---
'-- Comment: ---
'-------------------------------------------------------------------------
--
Option Explicit  'Forces the explicit declaration of all the variables in a
script.

Dim MyFolders()
Call InitMyFolders
'-------------------------------------------------------------------------
--
Sub InitMyFolders
  ReDim MyFolders(2)
  MyFolders(0)="C:\Documents and Settings\c109859\My Documents\- PhD -\-
Lubricant Dynamics -\LabVIEW\FDU data 2011\110203 Cali & 700ml & 800ml CW
tooth tip\Calibration\"
  MyFolders(1)="C:\Documents and Settings\c109859\My Documents\- PhD -\-
Lubricant Dynamics -\LabVIEW\FDU data 2011\110203 Cali & 700ml & 800ml CW
tooth tip\700ml tooth tip 19.7-24.2\"
End Sub
'-------------------------------------------------------------------------
--
Call Data.Root.Clear()
Call DataFileLoad(MyFolders(0)&"Wedge 110203 1GSs 5Hz 1.12kV Fluo Curve Data
Normalised & Averaged axb.TDM","TDM","") '...
DataFilename,FileImportFilter,ImportAction
Call DataFileLoad(MyFolders(1)&"FDU 700ml 110203 1GSs 5Hz 1.12kV Fluo Curve
Data Normalised & Averaged.TDM","TDM","") '...
DataFilename,FileImportFilter,ImportAction
Call Data.Root.ChannelGroups.Add("FDU Oil Thicknesses", 35).Activate()
Call Data.Root.ChannelGroups(35).Channels.Add("FDU Oil Thicknesse
(mm)",DataTypeFloat64,1)
Call ChnGenVal("[35]/FDU Oil Thicknesse (mm)",1,16,1,1,0) '...
ChnArg1,ChnRow,ValNo,ChnBegin,ChnStep,ValueOverwrite
CHD(1,232)=((3.8389)*CHD(1,230)^(2.5389))
CHD(2,232)=((3.8389)*CHD(2,230)^(2.5389))
CHD(3,232)=((3.8389)*CHD(3,230)^(2.5389))
CHD(4,232)=((3.8389)*CHD(4,230)^(2.5389))
CHD(5,232)=((3.8389)*CHD(5,230)^(2.5389))
CHD(6,232)=((3.8389)*CHD(6,230)^(2.5389))
CHD(7,232)=((3.8389)*CHD(7,230)^(2.5389))
CHD(8,232)=((3.8389)*CHD(8,230)^(2.5389))
CHD(9,232)=((3.8389)*CHD(9,230)^(2.5389))
CHD(10,232)=((3.8389)*CHD(10,230)^(2.5389))
CHD(11,232)=((3.8389)*CHD(11,230)^(2.5389))
CHD(12,232)=((3.8389)*CHD(12,230)^(2.5389))
CHD(13,232)=((3.8389)*CHD(13,230)^(2.5389))
CHD(14,232)=((3.8389)*CHD(14,230)^(2.5389))
CHD(15,232)=((3.8389)*CHD(15,230)^(2.5389))
CHD(16,232)=((3.8389)*CHD(16,230)^(2.5389))

Call DataFileSave(MyFolders(1)&"FDU 700ml Oil Thicknesses 110203 1GSs 1.12kV
axb.TDM","TDM") '... DataFilename,FileExportFilter
```

FDU End Oil Thickness axb

```
'--------------------------------------------------------------------------
--
'-- VBS script file
'-- Created on 05/12/2011 11:36:43
'-- Author: ---
'-- Comment: ---
'--------------------------------------------------------------------------
--
Option Explicit  'Forces the explicit declaration of all the variables in a
script.

Dim MyFolders()
Call InitMyFolders
'--------------------------------------------------------------------------
--
Sub InitMyFolders
  ReDim MyFolders(2)
  MyFolders(0)="C:\Documents and Settings\c109859\My Documents\- PhD -\-
Lubricant Dynamics -\LabVIEW\FDU data 2011\110203 Cali & 700ml & 800ml CW
tooth tip\Calibration End\"
  MyFolders(1)="C:\Documents and Settings\c109859\My Documents\- PhD -\-
Lubricant Dynamics -\LabVIEW\FDU data 2011\110203 Cali & 700ml & 800ml CW
tooth tip\700ml tooth tip 19.7-24.2\"
End Sub
'--------------------------------------------------------------------------
--
Call Data.Root.Clear()
Call DataFileLoad(MyFolders(0)&"Wedge 110203 1GSs 5Hz 1.12kV Fluo Curve Data
Normalised & Averaged axb.TDM","TDM","") '...
DataFilename,FileImportFilter,ImportAction
Call DataFileLoad(MyFolders(1)&"FDU 700ml 110203 1GSs 5Hz 1.12kV Fluo Curve
Data Normalised & Averaged.TDM","TDM","") '...
DataFilename,FileImportFilter,ImportAction
Call Data.Root.ChannelGroups.Add("FDU Oil Thicknesses", 35).Activate()
Call Data.Root.ChannelGroups(35).Channels.Add("FDU Oil Thicknesse
(mm)",DataTypeFloat64,1)
Call ChnGenVal("[35]/FDU Oil Thicknesse (mm)",1,16,1,1,0) '...
ChnArg1,ChnRow,ValNo,ChnBegin,ChnStep,ValueOverwrite
CHD(1,232)=((2.8976)*CHD(1,230)^(2.4320))
CHD(2,232)=((2.8976)*CHD(2,230)^(2.4320))
CHD(3,232)=((2.8976)*CHD(3,230)^(2.4320))
CHD(4,232)=((2.8976)*CHD(4,230)^(2.4320))
CHD(5,232)=((2.8976)*CHD(5,230)^(2.4320))
CHD(6,232)=((2.8976)*CHD(6,230)^(2.4320))
CHD(7,232)=((2.8976)*CHD(7,230)^(2.4320))
CHD(8,232)=((2.8976)*CHD(8,230)^(2.4320))
CHD(9,232)=((2.8976)*CHD(9,230)^(2.4320))
CHD(10,232)=((2.8976)*CHD(10,230)^(2.4320))
CHD(11,232)=((2.8976)*CHD(11,230)^(2.4320))
CHD(12,232)=((2.8976)*CHD(12,230)^(2.4320))
CHD(13,232)=((2.8976)*CHD(13,230)^(2.4320))
CHD(14,232)=((2.8976)*CHD(14,230)^(2.4320))
CHD(15,232)=((2.8976)*CHD(15,230)^(2.4320))
CHD(16,232)=((2.8976)*CHD(16,230)^(2.4320))

Call DataFileSave(MyFolders(1)&"FDU C-End 700ml Oil Thicknesses 110203 1GSs
1.12kV axb.TDM","TDM") '... DataFilename,FileExportFilter

Call Data.Root.Clear()
Call DataFileLoadSel(MyFolders(1)&"FDU 700ml Oil Thicknesses 110203 1GSs
1.12kV axb.TDM","TDM","[35]/*","") '...
DataFilename,FileImportFilter,ImportSelection,ImportAction
```

```
Call DataFileLoadSel(MyFolders(1)&"FDU C-End 700ml Oil Thicknesses 110203 1GSs
1.12kV axb.TDM","TDM","[35]/*","") '...
DataFilename,FileImportFilter,ImportSelection,ImportAction
Call DataFileLoadSel(MyFolders(1)&"FDU C-End 700ml Oil Thicknesses 110203 1GSs
1.12kV axb.TDM","TDM","[34]/[3]","") '...
DataFilename,FileImportFilter,ImportSelection,ImportAction
```

Appendix 5

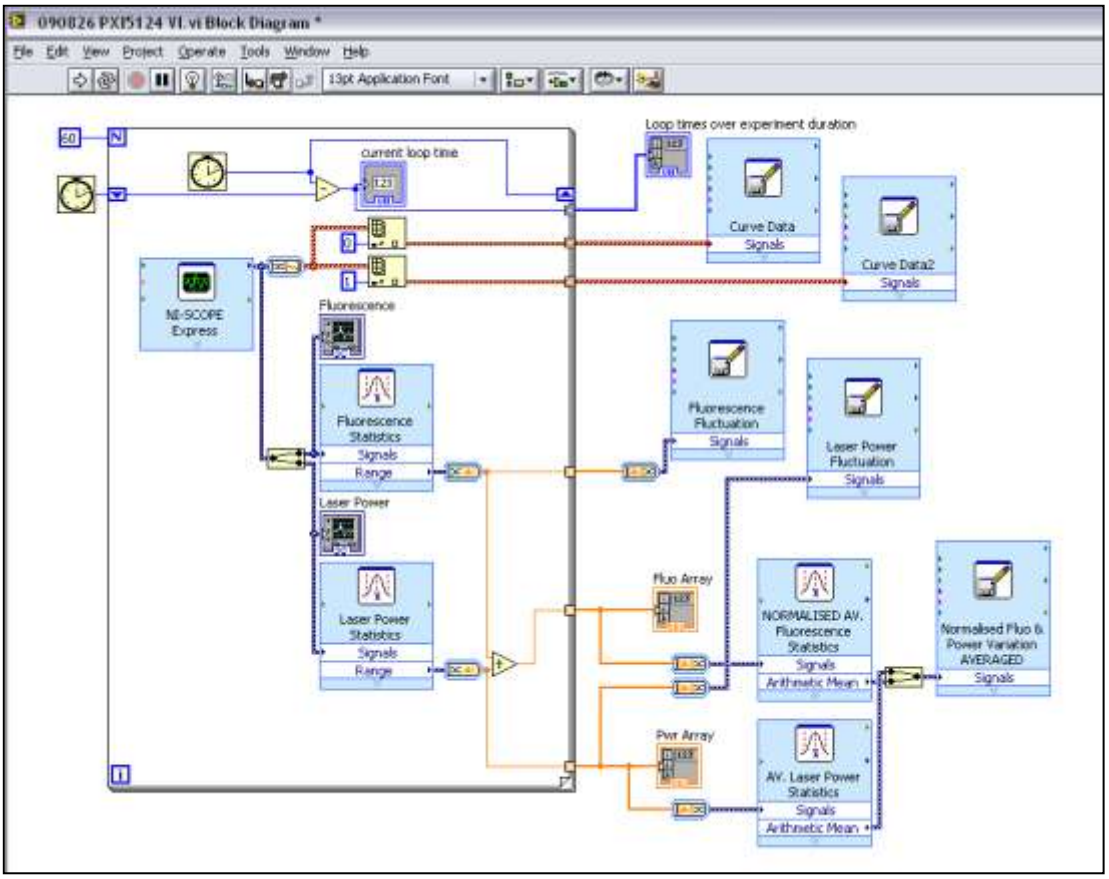

National Instruments LabVIEW Virtual Instrument

Appendix 6

Additional Wedge Calibration Curves

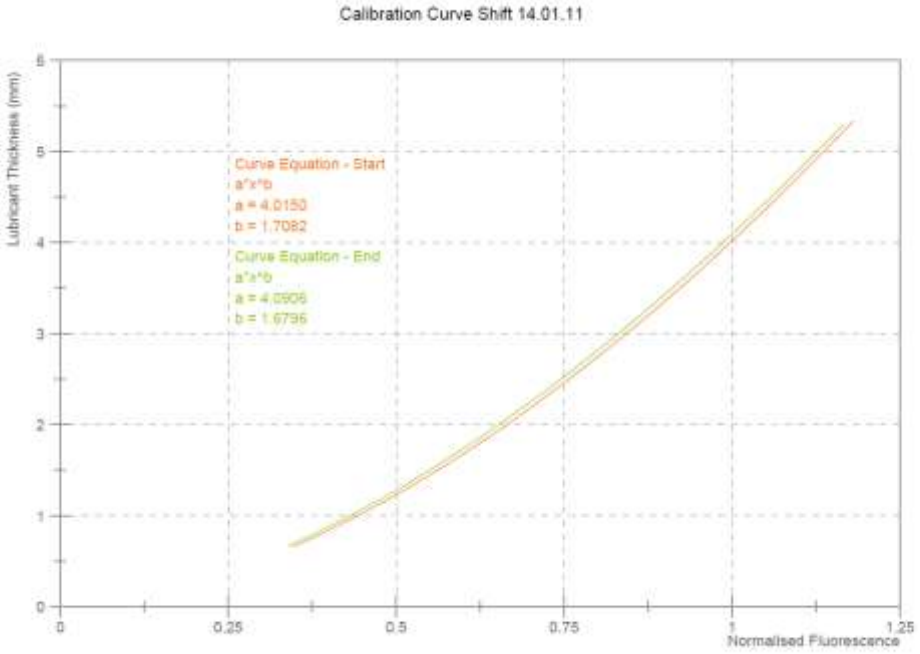

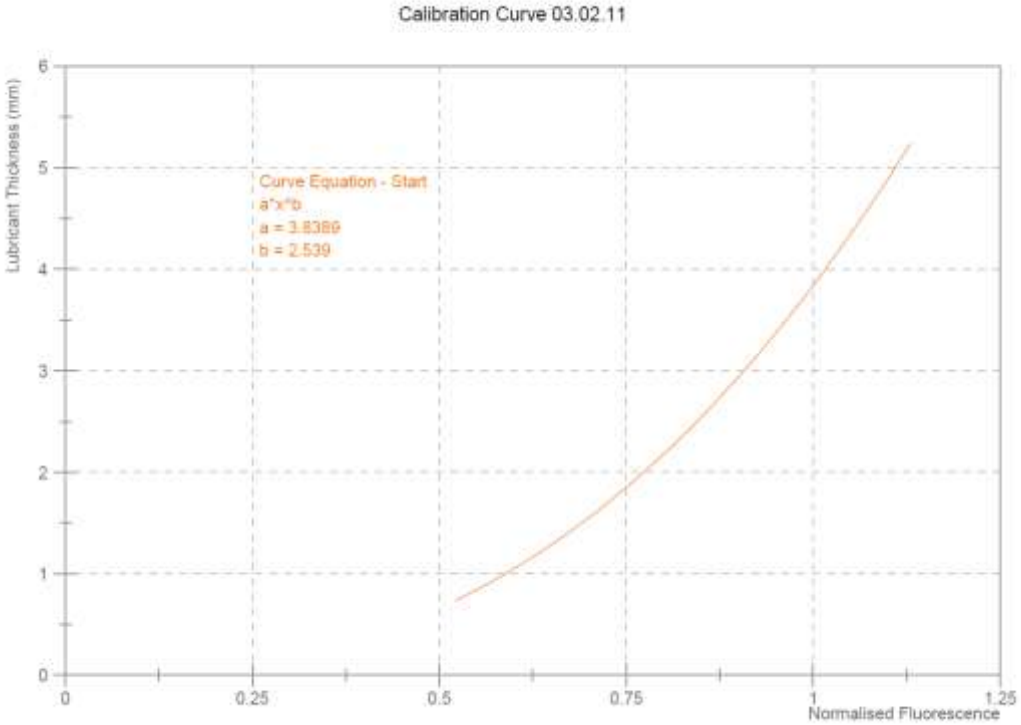
Calibration Curve 03.02.11
Lubricant Thickness (mm)
Curve Equation - Start
a*x^b
a = 3.8389
b = 2.539
0
1
2
3
4
5
6
0
0.25
0.5
0.75
1
1.25
Normalised Fluorescence

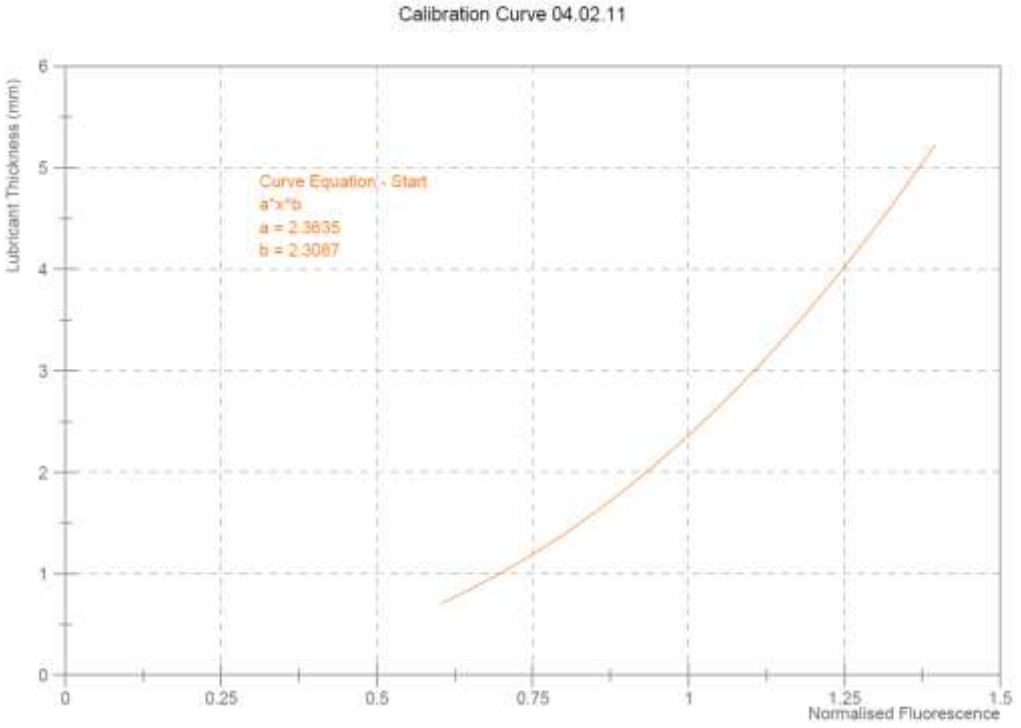
Calibration Curve 04.02.11
Lubricant Thickness (mm)
Curve Equation - Start
a*x^b
a = 2.3635
b = 2.3087
0
1
2
3
4
5
6
0
0.25
0.5
0.75
1
1.25
1.5
Normalised Fluorescence

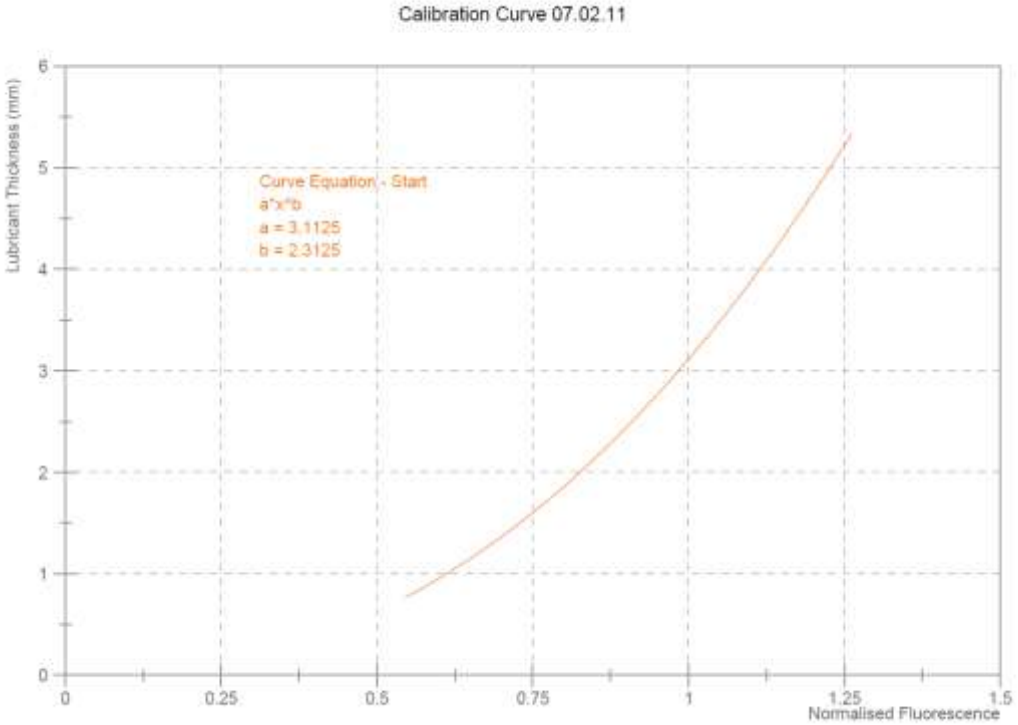
Calibration Curve 07.02.11
Lubricant Thickness (mm)
Curve Equation - Start
a*x^b
a = 3.1125
b = 2.3125
0
1
2
3
4
5
6
0
0.25
0.5
0.75
1
1.25
1.5
Normalised Fluorescence